AD-A194 979 AIRCRAFT BATTERY STATE OF CHARGE AND CHARGE CONTROL SYSTEM(U) ENERGY RESEARCH CORP DANBURY CT S VISWANATHAN ET AL. JAN 88 AFWAL-TR-87-2088 1/2

UNCLASSIFIED F33615-84-C-2435 F/G 10/2 NL

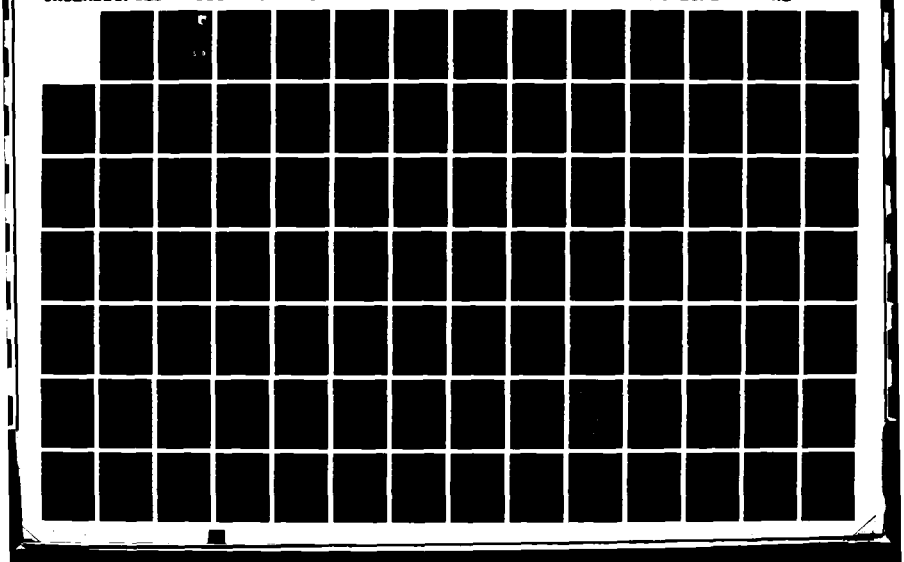

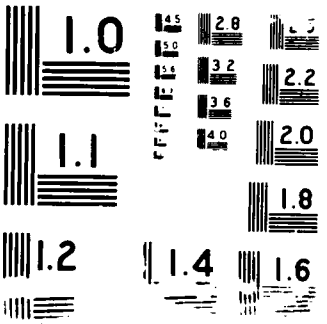
1.0
1.1
1.2
2.8
3.2
3.6
4.0
2.2
2.0
1.8
1.4
1.6

(2)

AFWAL-TR-87-2088

AIRCRAFT BATTERY STATE OF CHARGE AND CHARGE CONTROL SYSTEM

Sivaswamy Viswanathan
Allen Charkey

Energy Research Corporation
3 Great Pasture Road
Danbury, CT. 06813

JANUARY 1988

Final Report for Period July 84 - June 87

Approved for public release; distribution unlimited

AERO PROPULSION LABORATORY
AIR FORCE WRIGHT AERONAUTICAL LABORATORIES
AIR FORCE SYSTEMS COMMAND
WRIGHT-PATTERSON AIR FORCE BASE, OHIO 45433-6563

UNCLASSIFIED
SECURITY CLASSIFICATION OF THIS PAGE

REPORT DOCUMENTATION PAGE

Form Approved OMB No. 0704-0188

1a. REPORT SECURITY CLASSIFICATION UNCLASSIFIED	1b. RESTRICTIVE MARKINGS None
2a. SECURITY CLASSIFICATION AUTHORITY	3. DISTRIBUTION/AVAILABILITY OF REPORT Approved for public release; distribution is unlimited
2b. DECLASSIFICATION/DOWNGRADING SCHEDULE	
4. PERFORMING ORGANIZATION REPORT NUMBER(S)	5. MONITORING ORGANIZATION REPORT NUMBER(S) AFWAL-TR-87-2088
6a. NAME OF PERFORMING ORGANIZATION Energy Research Corporation 6b. OFFICE SYMBOL (If applicable)	7a. NAME OF MONITORING ORGANIZATION Aero Propulsion Laboratory (AFWAL/POOS-2) Air Force Wright Aeronautical Laboratories
6c. ADDRESS (City, State, and ZIP Code) 3 Great Pasture Road Danbury, CT 06813	7b. ADDRESS (City, State, and ZIP Code) Wright-Patterson AFB, OH 45433-6563
8a. NAME OF FUNDING/SPONSORING ORGANIZATION Aero Propulsion Laboratory Air Force Wright Aeronautical 8b. OFFICE SYMBOL (If applicable) AFWAL/POOS-2	9. PROCUREMENT INSTRUMENT IDENTIFICATION NUMBER F33615-84-C-2435
8c. ADDRESS (City, State, and ZIP Code) Wright-Patterson AFB, Ohio 45433-6563	10. SOURCE OF FUNDING NUMBERS PROGRAM ELEMENT NO: 62203F; PROJECT NO: 3145; TASK NO: 22; WORK UNIT ACCESSION NO: 03

11. TITLE (Include Security Classification)
AIRCRAFT BATTERY STATE OF CHARGE AND CHARGE CONTROL

12. PERSONAL AUTHOR(S)
Sivaswamy Viswanathan/Allen Charkey

13a. TYPE OF REPORT	13b. TIME COVERED	14. DATE OF REPORT (Year, Month, Day)	15. PAGE COUNT
FINAL	FROM JUL84 TO JUN87	88 JANUARY	174

16. SUPPLEMENTARY NOTATION

17. COSATI CODES			18. SUBJECT TERMS (Continue on reverse if necessary and identify by block number)
FIELD	GROUP	SUB-GROUP	
09	01		Nickel, Cadmium, State-of-Charge, Battery Charger, Nickel-Oxygen, Charge Controller
10	02		

19. ABSTRACT (Continue on reverse if necessary and identify by block number)

This Final Report describes work done by Energy Research Corporation (ERC) in developing an aircraft battery state-of-charge indicator and charge control system. The basis for this system, developed by ERC, is a nickel-oxygen (NiO_2) "pilot" cell (0.374 Ah). This pilot cell is cycled in tandem with nickel-cadmium battery. The oxygen pressure of the pilot cell is used to determine and control the state-of-charge of the nickel-cadmium battery. Nickel-cadmium batteries from different manufacturers were cycled using this pilot cell charge indication and control system.

20. DISTRIBUTION/AVAILABILITY OF ABSTRACT	21. ABSTRACT SECURITY CLASSIFICATION	
☒ UNCLASSIFIED/UNLIMITED ☐ SAME AS RPT ☐ DTIC USERS	UNCLASSIFIED	
22a. NAME OF RESPONSIBLE INDIVIDUAL Joe Fellner	22b. TELEPHONE (Include Area Code) 513-255-7770	22c. OFFICE SYMBOL AFWAL/POOS-2

DD Form 1473, JUN 86 Previous editions are obsolete

TABLE OF CONTENTS

LIST OF FIGURES

LIST OF FIGURES (Continued)

LIST OF FIGURES (Continued)

LIST OF FIGURES (Continued)

LIST OF FIGURES (Continued)

LIST OF TABLES

LIST OF TABLES (Continued)

SECTION 1
INTRODUCTION

A 3-year research and development program for the Air Force was undertaken to develop a new technique to measure the state-of-charge of nickel-cadmium aircraft batteries.

The objective of this effort was to develop a state-of-charge indicator/charge controller with the following key features:

1. Accurately track the state-of-charge of the main battery.
2. Provide a visual display of the state of charge continuously, similar to the fuel gauge in an automobile.
3. Use an end-point signal to terminate charge and/or discharge at a predetermined level thereby preventing decrease in battery life and increased maintenance.
4. Develop a control pilot cell which remains in tandem with the main battery at all times and at all operating conditions.
5. Develop suitable electronics circuitry for effective tandem operation.

In accordance with the program schedule, the technical efforts were terminated at the end of June 1987. Throughout the duration of the program, detailed data were submitted to WPAFB by means of monthly letter reports.

SECTION 2

EXECUTIVE SUMMARY

As a direct result of the R & D efforts expended, Energy Research Corporation has successfully developed a new charge indicator which functions in the laboratory over a wide range of operating conditions with excellent accuracy. The technique developed at ERC also provides a means for terminating the charge without the addition of complex circuitry since proper charge termination can have a significant effect on improvement of battery life.

This system employs a Ni-O_2 pilot cell containing an electrode type perfectly matched to the main Ni-Cd battery and is charged and discharged in tandem with it. The gas pressure of the pilot cell indicates the capacity of the pilot cell and therefore is an accurate measure of state of charge of the main battery. The unique feature of this concept is that the pilot cell contains the same electrode type and is operated at the same current density as the battery being monitored. The pilot cell exhibits a similar charge/discharge efficiency, the same aging rate and is subjected to the same environmental regimes as the main battery and therefore, remains in phase with it. This concept is uniquely adaptable to any battery chemistry as long as the pilot cell's metal electrode is selected to be the same type of controlling electrode as is used in the battery being monitored. The concept also serves to act as an ideal system for charge control.

When the nickel electrode is charged in a conventional nickel-cadmium battery, oxygen gas is consumed on the surface of the oxygen electrode. During the reverse process, (conventional discharge for the nickel electrode), the nickel electrode is reduced and oxygen gas is evolved on the surface of the gas electrode. The cell is

constructed in a sealed compartment and the oxygen gas pressure is a direct measure of the state of charge or the degree of oxidation of the nickel electrode.

Extensive testing was carried out both with the pilot cell alone and with integrated systems using commercial aircraft batteries. Performance characteristics at different parameters such as current density, temperature and depth of discharge were evaluated. System life and stability were also investigated by means of life cycle tests.

SECTION 3

TECHNICAL BACKGROUND

3.1 NICKEL-CADMIUM ELECTROCHEMISTRY

During the charging process, the nickel hydroxide is oxidized to nickel oxyhydroxide and the negative electrode undergoes a simultaneous reduction according to the following equations:

$$2Ni(OH)_2 + 2OH^- \rightarrow 2NiOOH + 2H_2O + 2E \qquad E_o = -0.48$$

$$Cd(OH)_2 + 2E^- \rightarrow Cd + 2OH^- \qquad E_o = -0.809$$

$$E = -1.289$$

During overcharge in the vented cell, water from the electrolyte is decomposed to form oxygen gas at the nickel electrode and hydrogen at the cadmium electrode according to the equation:

$$2H_2O + 2E^- \rightarrow H_2 + 2OH^- \qquad E_o = -0.829$$

$$2OH^- \rightarrow 1/2O_2 + H_2O + 2E^- \qquad E_o = -0.401$$

$$E = -1.230$$

The charge process of the nickel electrode occurs at a potential which is very close to that of evolution of oxygen gas. Due to the closeness of the potential of oxygen evolution and charging of the nickel, both processes go on during the charging of the nickel electrode. Figure 3.1 shows a typical distribution of the current that contributes to charging a nickel electrode and the fraction of current that results in oxygen evolution. When all the active nickel is fully charged, subsequent charging results in 100 percent of the current contributing to oxygen evolution. It is therefore necessary, due to the competing processes, to recharge more than 100 percent of removed capacity from the previous discharge to fully charge the nickel electrode. The amount of overcharge that is required is a function of electrode construction, operating

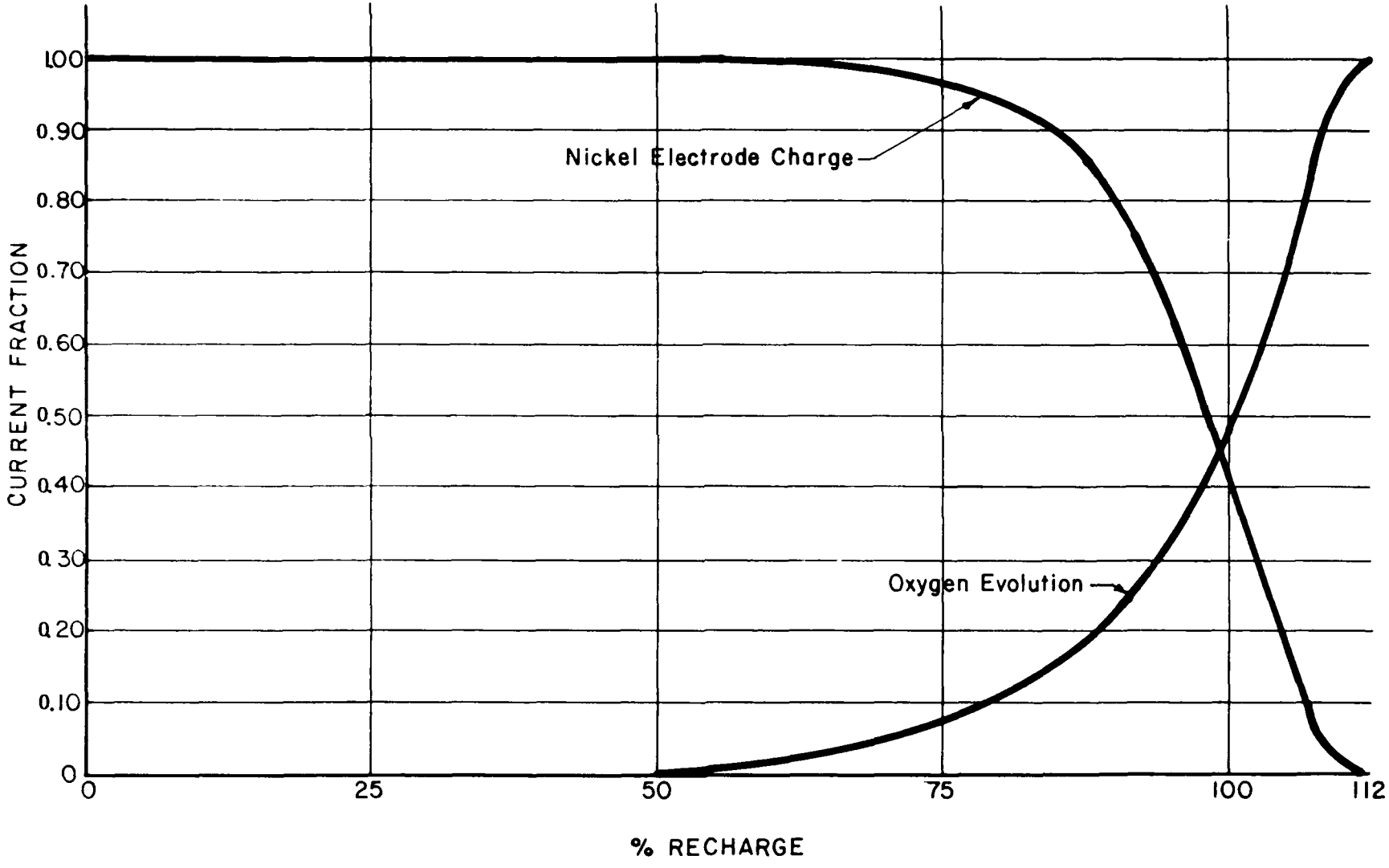

FIGURE 3.1 TYPICAL NICKEL ELECTRODE CHARGE ACCEPTANCE

current density, temperature, electrode history and state-of-charge.

Unlike the nickel electrode, the cadmium electrode normally accepts charge at 100 - percent efficiency until all active material is fully charged and then makes a sharp transition to hydrogen evolution.

Figure 3.2 shows a typical constant current charge/discharge voltage trace of nickel-cadmium vented cells. In vented batteries, the sharp voltage shift near the end of charge represents hydrogen evolution at the cadmium electrode. This occurs at 100 percent replacement of ampere hours from the previous discharge and is not suited as a means of determining state-of-charge. In addition, the Cd voltage is unsuitable as a means of charge termination since it does not allow for the required overcharge of the nickel electrode.

From an understanding of the chemistry, it is clear that the best measure of state-of-charge of a nickel battery is the degree of oxidation of the nickel electrode i.e., how much active material has been converted to the higher oxide state.

3.2 NICKEL-OXYGEN CELL THEORY

The state of oxidation of a nickel electrode can be readily and accurately monitored in a nickel-oxygen cell. The construction of such a cell consists of a nickel electrode of the type used in the battery to be monitored, a separator, alkaline electrolyte and gas electrode of the type utilized in fuel cells. When the nickel electrode is charged as in a conventional nickel-cadmium battery, oxygen gas is consumed on the surface of the oxygen electrode. (Table 3.1)

During the reverse process, (conventional discharge for the nickel electrode), the nickel electrode is reduced and oxygen gas

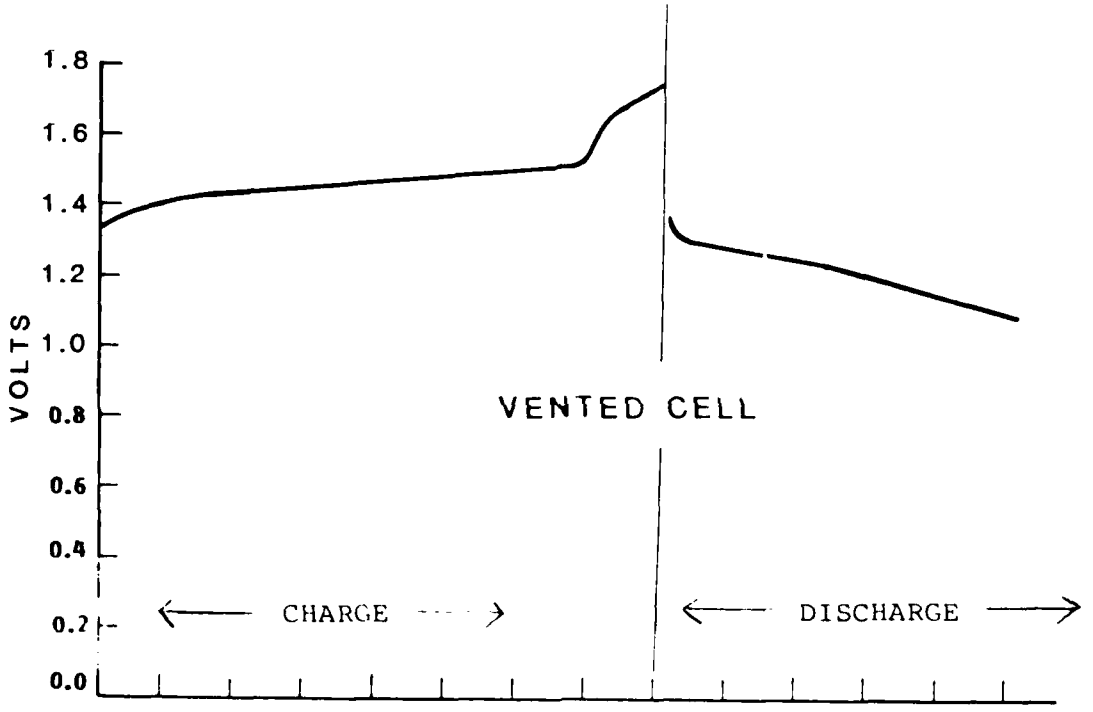

FIGURE 3.2. TYPICAL NICKEL-CADMIUM VOLTAGE CHARACTERISTICS

TABLE 3.1

CHEMISTRY OF NICKEL-OXYGEN CELLS

CHARGE - DISCHARGE	E_O
$2Ni(OH)_2 + 2OH^- \underset{D}{\overset{C}{\rightleftharpoons}} 2Ni\,OOH + 2H_2O + 2E^-$	0.49
$1/2\ O_2 + H_2O + 2E^- \underset{D}{\overset{C}{\rightleftharpoons}} 2OH^-$	0.401
$2Ni(OH)_2 + 1/2\ O_2 \underset{D}{\overset{C}{\rightleftharpoons}} 2Ni\,OOH + H_2O$	0.089

is evolved on the surface of the gas electrode. If the cell is constructed in a sealed compartment, the surrounding oxygen gas pressure is a direct measure of the state-of-charge or the degree of oxidation of the nickel electrode.

The top portion of Figure 3.3 shows a typical pressure profile of a nickel oxygen cell during charge and discharge. The lower curve shows the voltage of the pilot cell during normal operation on the same time scale. If the cell is continuously charged to the point where all the nickel active material has been fully oxidized, subsequent charging will cause the evolution of oxygen gas on the surface of the nickel electrode and simultaneous consumption of oxygen gas on the oxygen electrode, this results in a leveling off of pressure.

Similarly, any inefficiency in the charge of the nickel electrode resulting in oxygen gas evolution during charge, has no effect on the change in oxygen pressure of the pilot cell. It is this phenomenon that allows the pilot cell's pressure to accurately reflect the state-of-charge and oxidation of the nickel electrode regardelss of the electrode's charge acceptance efficiency.

3.3 CIRCUIT OVERVIEW

Figure 3.4 shows the overall block diagram circuit for the metal gas cell and main battery. A shunt is placed into the normal charge/discharge circuit of the main battery to be monitored to give a millivolt signal output proportional to the current flowing in and out of the main battery circuit. The metal gas pilot cell is charged and discharged by means of an amplifier power supply which can be powered from the main battery, an auxiliary battery, or any other power source.

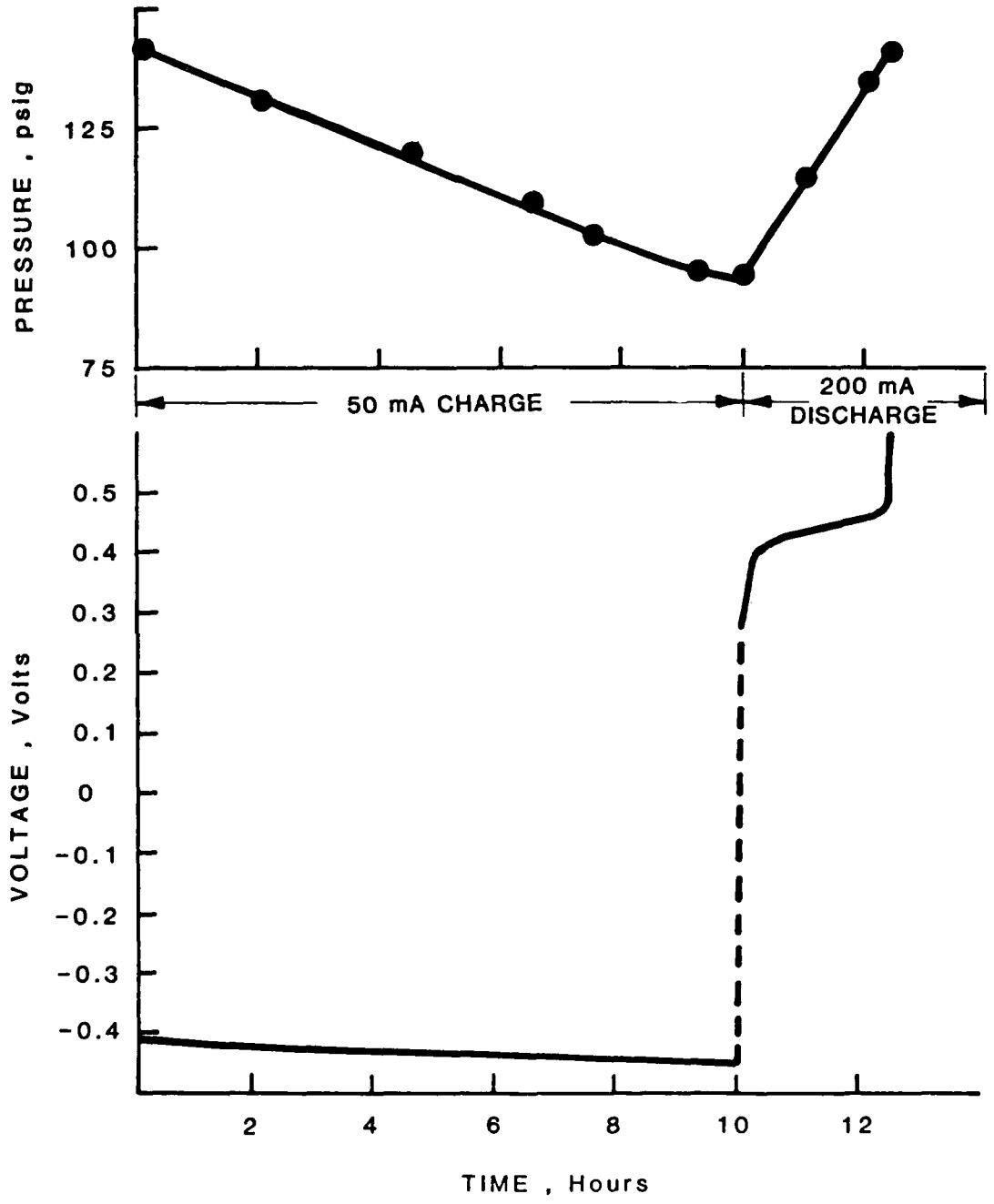

FIGURE 3.3. PERFORMANCE OF ERC Ni-O_2 COULOMETER

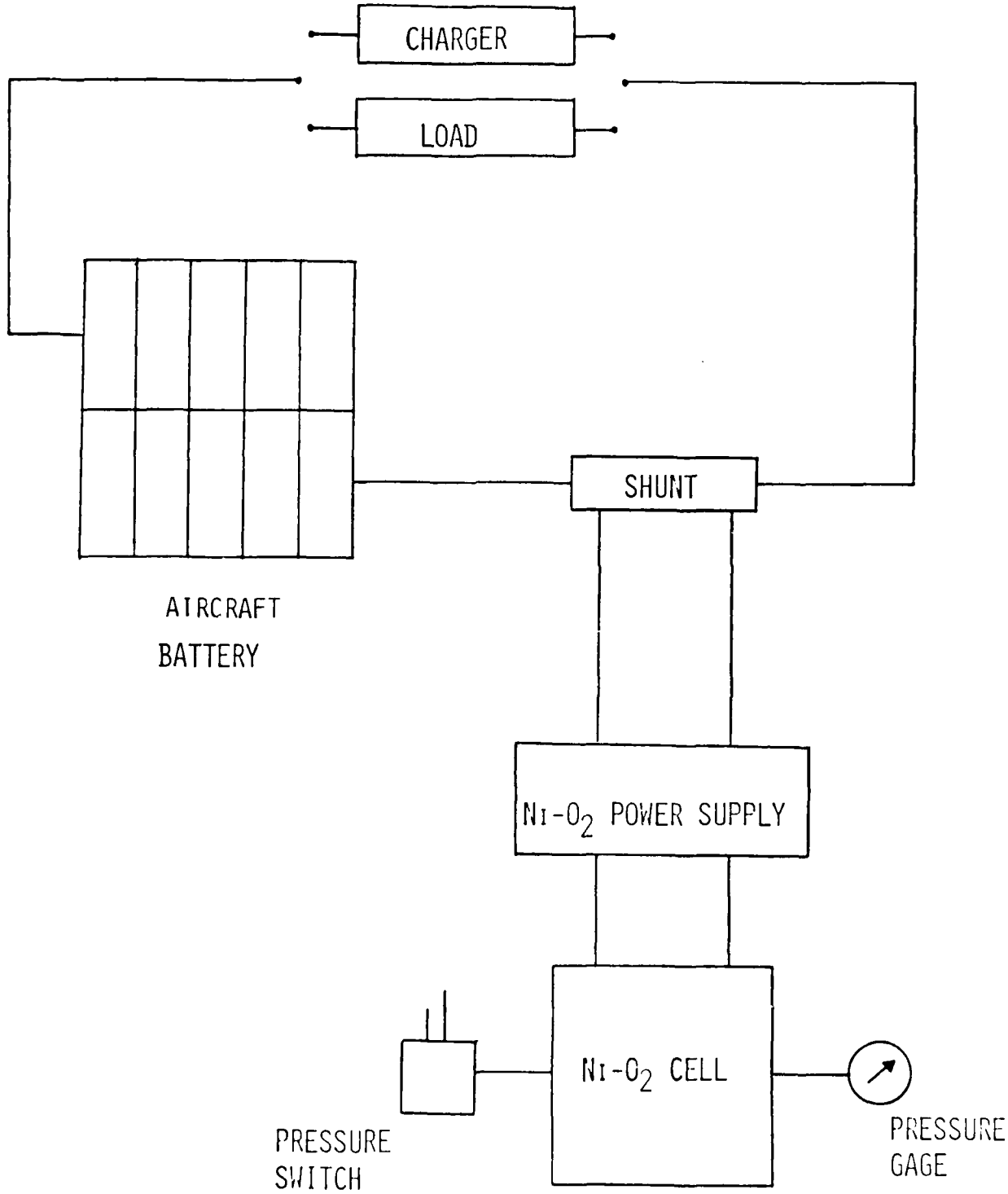

CHARGE CONTROLLER CONCEPT
FIGURE 3.4 ERC METAL-GAS COULOMETER CIRCUIT

The power supply's function is to charge and discharge the metal gas pilot cell at a current proportional to the current flowing in the main circuit. The proportioning factor is selected for the pilot cell so that its active electrode is run at the same current density as the electrodes in the main battery. For example, if the main battery consisted of 250 ampere-hour cells and the pilot cell electrode is 1/500 of the main battery, the power supply circuitry would be calibrated to run the pilot cell at 1/500 of the current of the main battery.

Since the gas pressure in the pilot cell is a direct measure of its state-of-charge and the main battery, the pressure can be read visually or via a transducer to give the state-of-charge of the main battery. Furthermore, a pressure switch can be set at a predetermined pressure point to indicate a fully charged state and thereby, terminate the charge when the appropriate level is reached. This method of charge control should also prevent thermal runaway as the EMF of the main battery will not control the on-board charger. Further, by preselecting pressure set points stepped charging can be programed and/or discharge can be terminated to prevent battery damage.

3.4 PILOT CELL

For the pilot cell to give stable results, the oxygen electrode must electrochemically consume and evolve oxygen. This type of operation, which has been studied for rechargeable batteries i.e., H_2-O_2, Zn-Air, Fe-Air, etc., is not readily obtainable. Problems encountered have been that catalysts that function for oxygen consumption tend to oxidize or dissolve when subjected to oxygen evolution.

To overcome this problem, ERC has developed a three-electrode configuration that utilizes one electrode for oxygen evolution and a separate electrode for oxygen consumption. This concept divides the functions and may result in the most stable system.

Figure 3.5 shows the results of a three-electrode cell when run in conjunction with a 200-Ah, 6-Volt Ni-Cd Electric Vehicle module in a simulate EV pulse discharge profile. The linear pressure profiled accurately reflects the capacity removed from the battery. The sloping pressure profile during charge accurately reflects the charge acceptance efficiency during contact current charge.

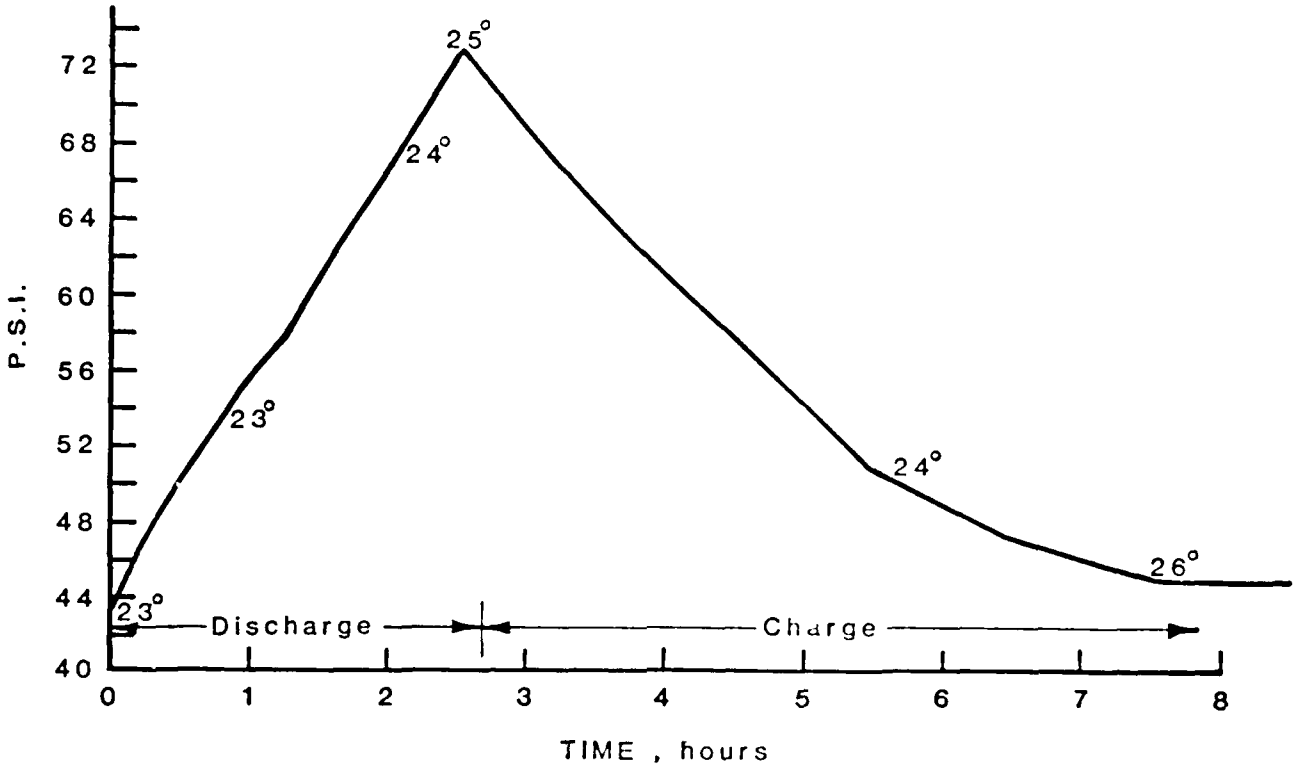

TABLE

PT#	TIME (Hours)	P.S.I.	TEMPERATURE
1	0	43	23
2	0.25	47	
3	0.5	50	
4	0.75	53	23
5	1	56	
6	1.25	58	
7	1.5	61	
8	1.75	64	
9	2	67	24
10	2.25	70	
11	2.5	73	25
12	2.5	73	
13	3.5	64.5	
14	5.5	50.5	24
15	6.5	47	
16	7.5	45	26

FIGURE 3.5 COULOMETER 75-MILE RUN

SECTION 4

EXPERIMENTAL RESULTS

The program was divided into the following major tasks in a logical sequence:

1. Baseline Characteristics
2. Electronics Test Unit
3. Life, stability and performance testing of the integrated system

4.1 BASELINE CHARACTERISTICS

First, commercial aircraft batteries were tested both as single cells and as battery stack to evaluate their performance characteristics. In parallel, design, fabrication and testing of $Ni-O_2$ pilot cells were started. A number of cells were built and extensive testing under various regimens were performed to insure reliability and reproducibility. It was also established through life cycle tests that the life of the $Ni-O_2$ cells was well in excess of that of the battery, ensuring that the pilot cells will not deteriorate during the life of the main battery.

4.1.1 $Ni-O_2$ Cell Design and Fabrication

The nickel-oxygen test cells employed a three-electrode configuration utilizing one electrode for oxygen evolution and a different electrode for oxygen consumption. This concept divides the functions and eliminates problems encountered in conventional two-electrode systems, in which catalysts that function well during oxygen consumption tend to oxidize or dissolve when subjected to evolution.

The normal specifications for the nickel electrodes are as follows:

Electrode Size	1.26 x 1.00 x 0.070 inch
Active Material	2.53 gms
Theoretical Capacity	0.440 Ah
Normal Capacity	0.374 Ah

Depending on the active material content, the area of the electrode is varied to obtain the required capacity. The cell can be designed to any capacity as long as the proportionality of current to the main battery is maintained. A sketch of the cell is shown in Figure 4.1.

The electrodes are first housed in a test fixture and fully charged, the end of charge being indicated by the leveling out of the pressure profile. The cell is then discharged to 100-percent depth and the delivered capacity calculated. The procedure is repeated until the nickel electrode is stabilized and reproducible results are obtained. This procedure qualifies the system, after which the electrode assembly is removed from the test fixture and assembled in a stainless steel can. Ziegler seals and welding of the cover ensure a leak-proof construction; then a pressure gauge is screwed into the top. The cell is now ready to undergo characterization tests.

Using the three-electrode concept, the nickel electrode of the pilot cell is charged against the platinum gas electrode and discharged against the nickel screen. The potentials and pressures are monitored during the tests.

4.1.2 Cell Characterization

The test matrix for characterization of cells is shown in Table 4.1. The cell was charged and is charged at different C-rates and different depths of discharge. Table 4.2 shows the test results of Cell 1.

Some problems were encountered with the first cell fabricated after 22 cycles. This cell was cycled manually to evaluate the relationship among charge, discharge and depth of discharge.

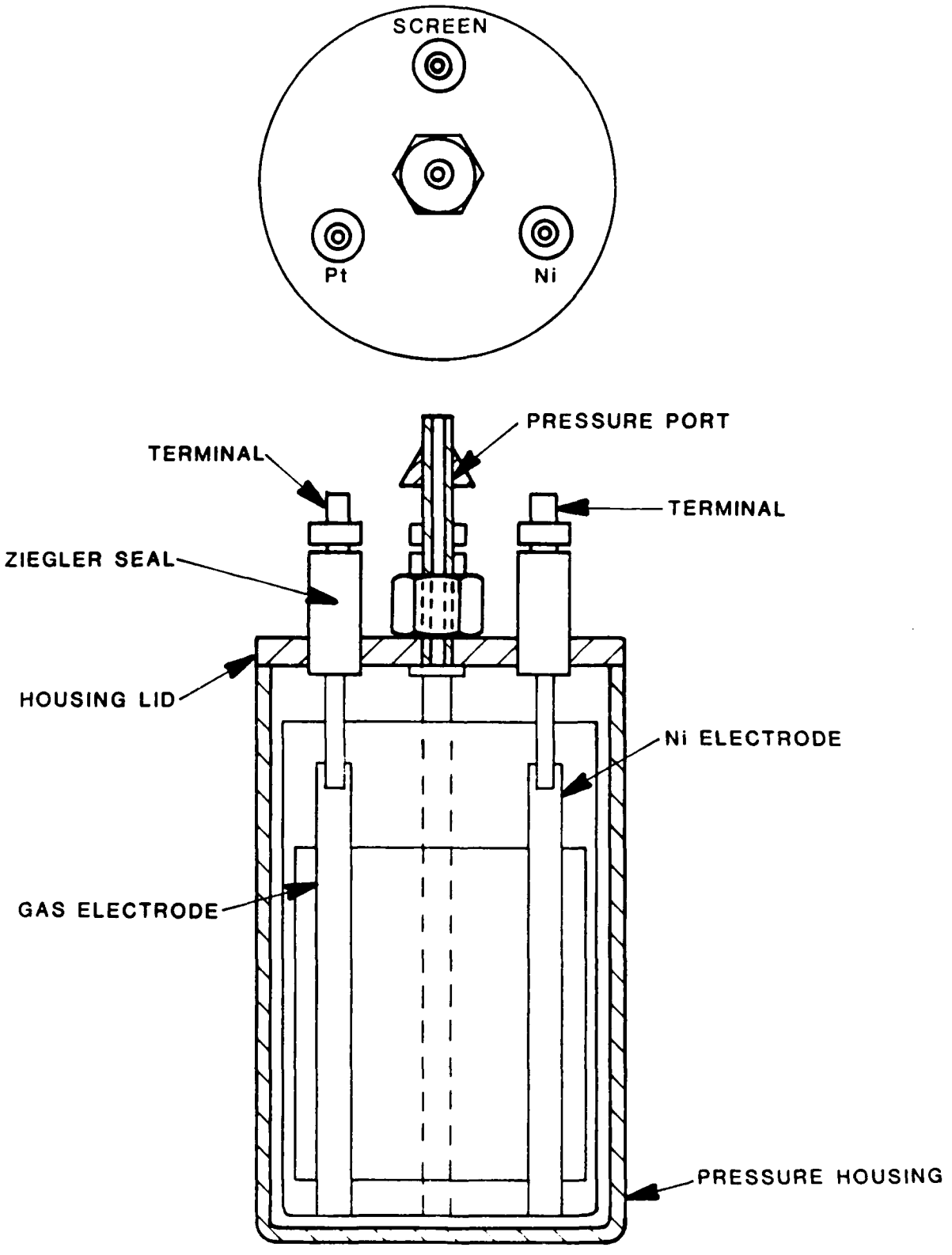

Figure 4.1. Ni_1-O_2 PILOT CELL SCHEMATIC

TABLE 4.1

CELL TEST MATRIX

Cell No.	1	2
Test Temperature	Ambient	Ambient
Test Mode	Manual	Automatic
Charge Current, mA	50, 100, 150	100
Time	Current Dependent	4 hours
Overcharge	25 to 67%	10%
Discharge Current	50, 100, 150, 200	100
Time	Current Dependent	3½ hours
Depth	100%	94%

TABLE 4.2

CELL PERFORMANCE AT DIFFERENT DEPTHS OF DISCHARGES

CYCLE	CHARGE				DISCHARGE				
No.	I	AH	V	P	I	AH	V	P	DOD
	(mA)		(volts)	(psig)	(mA)		(volts)	(psig)	(%)
1	100	0.450	0.617	60	100	0.358	- 0.915	88	100
2	100	0.400	0.617	56	200	0.367	- 0.100	87	100
3	100	0.625	0.615	50	200	0.383	- 1.035	82	100
4	100	0.376	0.599	50	200	0.376	- 1.000	80	100
5	100	0.475	0.599	50	200	0.383	- 1.000	82	100
6	50	0.488	0.525	50	100	0.405	- 0.965	85	100
7	150	0.487	0.642	50	150	0.375	- 0.954	84	100
8	150	0.450	0.652	50	100	0.400	- 0.950	85	100
9	150	0.450	0.646	50	200	0.400	-	87	100
10	50	0.500	0.544	51	50	0.413	- 1.050	84	100
11	50	0.325	0.514	60	50	0.280	- 0.826	82	75
12	50	0.342	0.526	59	100	0.280	- 1.061	82	75
* 13	50	0.308	-	59	200	0.823	- 1.440	84	75
14	50	0.310	0.511	63	200	0.240	- 1.540	82	75

* Excessive discharge by mistake.

TABLE 4.2

CELL PERFORMANCE AT DIFFERENT DEPTHS OF DISCHARGE (continued)

	CHARGE				DISCHARGE				
CYCLE NO.	I (mA)	AH	V	P (psig)	I (mA)	AH	V	P (psig)	DOD %
15	100	0.195	0.595	56	50	0.168	- 0.780	78	45
16	100	0.176	0.608	54	100	0.163	- 0.909	76	44
17	100	0.185	-	53	200	0.170	- 1.090	78	45
18	150	0.180	0.620	54	50	0.185	-	76	49
19	150	0.188	-	52	100	0.175	-	74	47
20	150	0.180	-	64	200	0.170	-	84	45

TABLE 4.2

CELL PERFORMANCE AT DIFFERENT DOD (continued)

CYCLE NO.	MODE	I (mA)	AH	V	P (psig)	DOD (%)
21	Charge	100	0.300	+ 0.550	58	-
	Discharge	50	0.283	- 0.820	80	75%
22	Charge	100	0.300	+ 0.584	50	-
	Discharge	100	0.283	- 0.801	72	75%
23	Charge	100	0.300	+ 0.558	50	-
	Discharge	200	0.234	- 1.051	68	63%
24	Charge	100	0.317	+ 0.588	50	-
	Discharge	200	0.200	- 0.948	63	53%

The charging of the cell on cycle 23 was normal, but when the cell was discharged at 200 mA, the actual delivered capacity of the cell was 0.232 Ah, less than the expected value of 0.280 Ah. The cycle was repeated, and the capacity delivered was only 0.200 Ah. The loss in capacity could be due to a leak in the system and/or shorting of the cell. The cell was dissected and a postmortem examination was carried out. The cell case was carefully cut open and the cell components examined.

The electrode assembly looked clean, and no evidence of shorts was noticeable. The electrodes and separator did not exhibit any damage, defects or discoloration, and the current lead welds were clean.

The only abnormality was the accumulation of a few cc's of brown liquid in the bottom of the cell. We theorized that if a recombination of gases had taken place resulting in the production of water, the water could have leached out some of the active materials from the positive electrode and settled at the bottom of the cell.

To investigate the performance of the electrodes, the same electrode assembly from the cell was housed in a test fixture and fully charged. It was then discharged at 200 mA and a delivered capacity of 0.350 Ah was obtained, indicating that the electrodes were still capable of delivering 94 percent of the original capacity.

Cell 26 was built using ERC rolled nickel. The nominal capacity of the cell is 450 mAh. The first series of tests were directed towards investigating the dependence of charge efficiency on the amount of overcharge. Both charge and discharge currents

were kept constant at 100 mA and the cell was charged between 0 and 100 percent over its nominal capacity. For each overcharge, the cell was discharged to 100 percent depth and the delivered capacity was calculated. As to be expected, the delivered capacities increased with the amount of overcharge but at a lower magnitude. Next, the cell was charged at 200 mA and the amount of charge was varied between 0 and 100% over the nominal capacity. Again, the cell was discharged to 100% depth and the delivered capacities were calculated. Test results for currents of 100 and 200 mA are summarized in Table 4.3a.

The second part of the tests consisted of evaluating the dependency of the delivered capacity on the rate of discharge. For each charge cycle, the current and the amount of overcharge were maintained constant at 100 mA and 20% over nominal, respectively. The discharge currents were varied between 50 and 900 mA (0.1 C to 2.0 C rates) and delivered capacities were calculated. The ratio of delivered to nominal capacity was 1.28 at 50 mA and 0.84 at 900 mA. The other parameters are summarized in Table 4.3b.

The voltage profiles on discharge at the different rates are shown in Figures 4.2, 4.3 and 4.4. Figure 4.5 shows the variations in delivered capacities with discharge currents.

Having completed characterization of ERC roll-bonded nickel electrodes, work was started in evaluating the performance of a nickel-oxygen cell containing sintered nickel electrode. Small sections were cut from the positive plate of a commercial Saft aircraft cell and assembled with counter electrodes in a test fixture. After confirming performance in the fixture, the electrode assembly was transferred to the standard container and the cell sealed to

TABLE 4.3a

DISCHARGE PERFORMANCE - DISCHARGE CURRENT VS. DELIVERED CAPACITY

CYCLE NO.	RATE	I mA	t hrs	VOLTS		END P	CUTOFF VOLTS	CAP. AH	EFF. %
				END	PLATEAU				
15	0.1C	50	11.58	-1.056	-0.745	64	-1.0	0.576	128
3	0.2C	100	4.58	-1.000	-0.819	61	-1.1	0.470	104
20	0.3C	150	3.50	-1.280	-0.835	68	-1.2	0.468	104
6	0.4C	200	2.25	-1.000	-0.937	59	-1.1	0.470	104
19	0.6C	250	2.07	-2.000	-1.080	68	-1.2	0.454	101
14	0.8C	350	1.33	-1.232	-1.060	59	-1.2	0.455	101
18	1.0C	450	1.20	-1.600	-1.096	68	-1.4	0.420	93
16	1.5C	675	0.67	-1.654	-1.281	64	-1.4	0.420	93
17	2.0C	900	0.58	-2.000	-1.294	64	-1.6	0.378	84

CELL 26 - NOMINAL CAPACITY 0.450 Ah - DOD 100%

CHARGE PER CYCLE - 5.4 hrs at 100 mA, 0.54 Ah, 20% OVERCHARGE

TABLE 43b

EFFECT OF OVERCHARGE ON DELIVERED CAPACITY

		CHARGE						DISCHARGE					
S.NO.	CYCLE NO.	t Hrs.	I mA	Ah	END V	END P	OVER-CHARGE %	t hrs	I mA	Ah	END V	END P	DEL'D/ NOM. %
1	8	4.50	100	0.450	0.562	23	0	4.50	100	0.450	-1.000	63	100
2	2	4.75	"	0.475	0.611	20	6	"	"	"	-1.010	60	"
3	3	5.30	"	0.530	0.611	19	18	4.58	"	0.458	-1.000	61	102
4	5	6.40	"	0.640	0.605	19¼	42	5.00	"	0.500	-1.000	62	111
5	10	7.90	"	0.790	0.595	16½	76	5.33	"	0.533	-1.000	64	118
6	11	9.00	"	0.900	0.594	16	100	5.50	"	0.550	-1.000	65½	122
7	9	2.33	200	0.466	0.605	23	4	2.00	200	0.400	-1.000	60	89
8	4	2.40	"	0.480	0.653	20	7	"	"	"	-1.000	56	"
9	6	2.75	"	0.550	0.657	19¼	22	2.25	"	0.450	-1.000	59	100
10	7	3.20	"	0.640	0.670	17	42	2.42	"	0.484	-1.070	62	108
11	12	3.95	"	0.790	0.680	16	76	2.50	"	0.500	-1.090	61½	111
12	13	4.50	"	0.900	0.670	14	100	2.58	"	0.516	-1.090	62½	115

CELL 26 - NOMINAL CAPACITY 0.450 Ah - 100% DOD

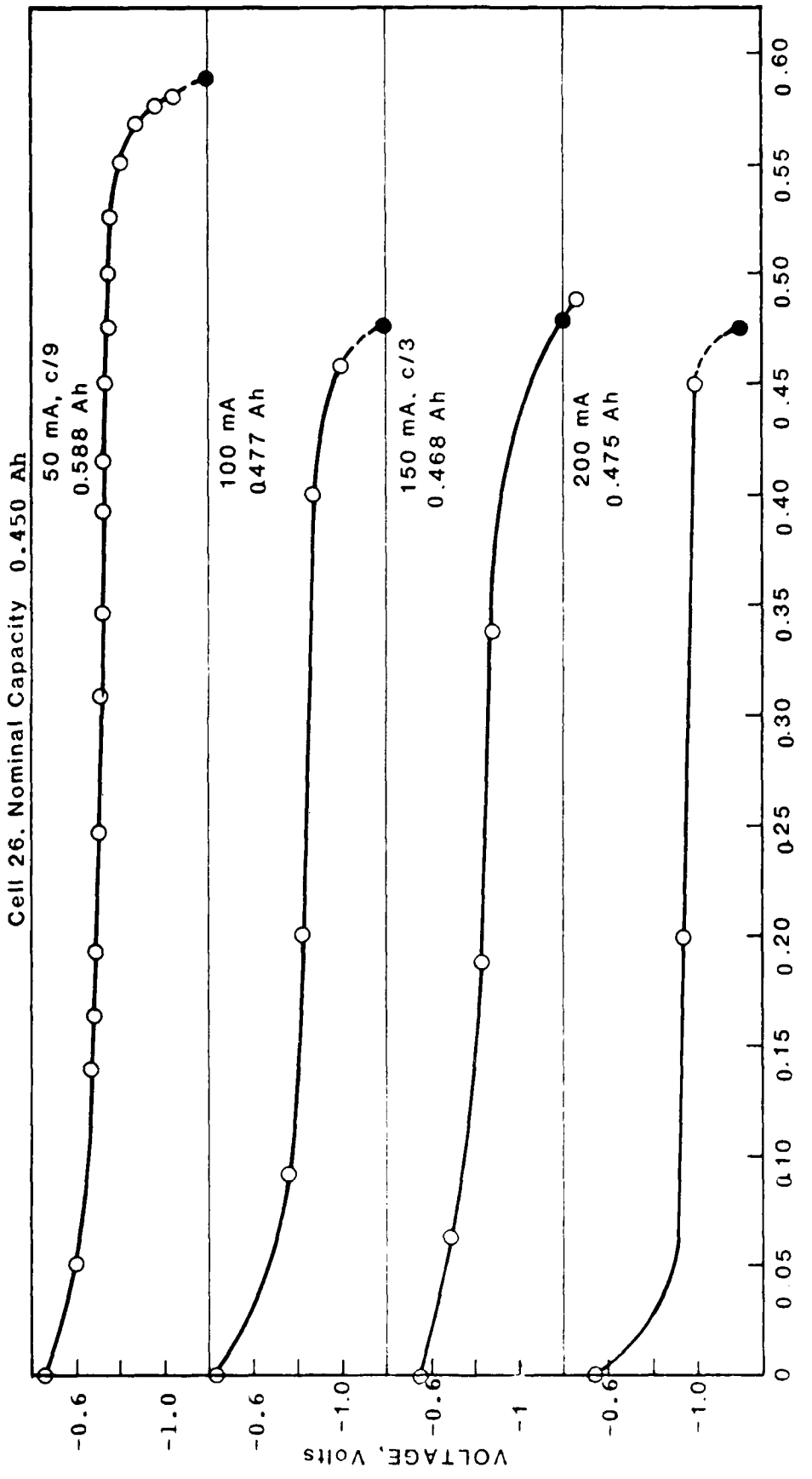

FIGURE 4.2 DISCHARGE PERFORMANCE OF CELL 26-50, 100, 150, 200 mA

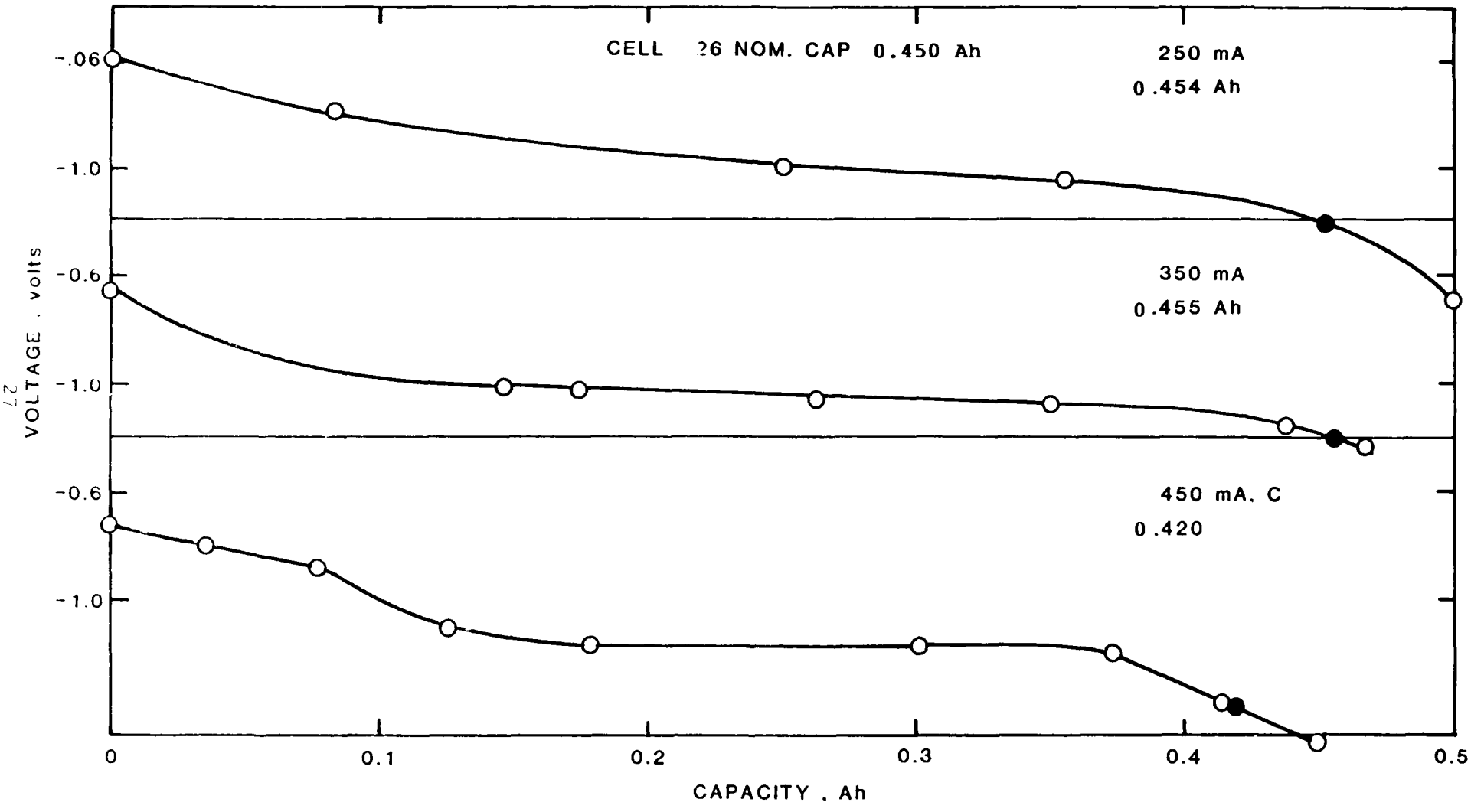

FIGURE 4.3 DISCHARGE PERFORMANCE OF CELL 26 - 250, 350, 450 mA

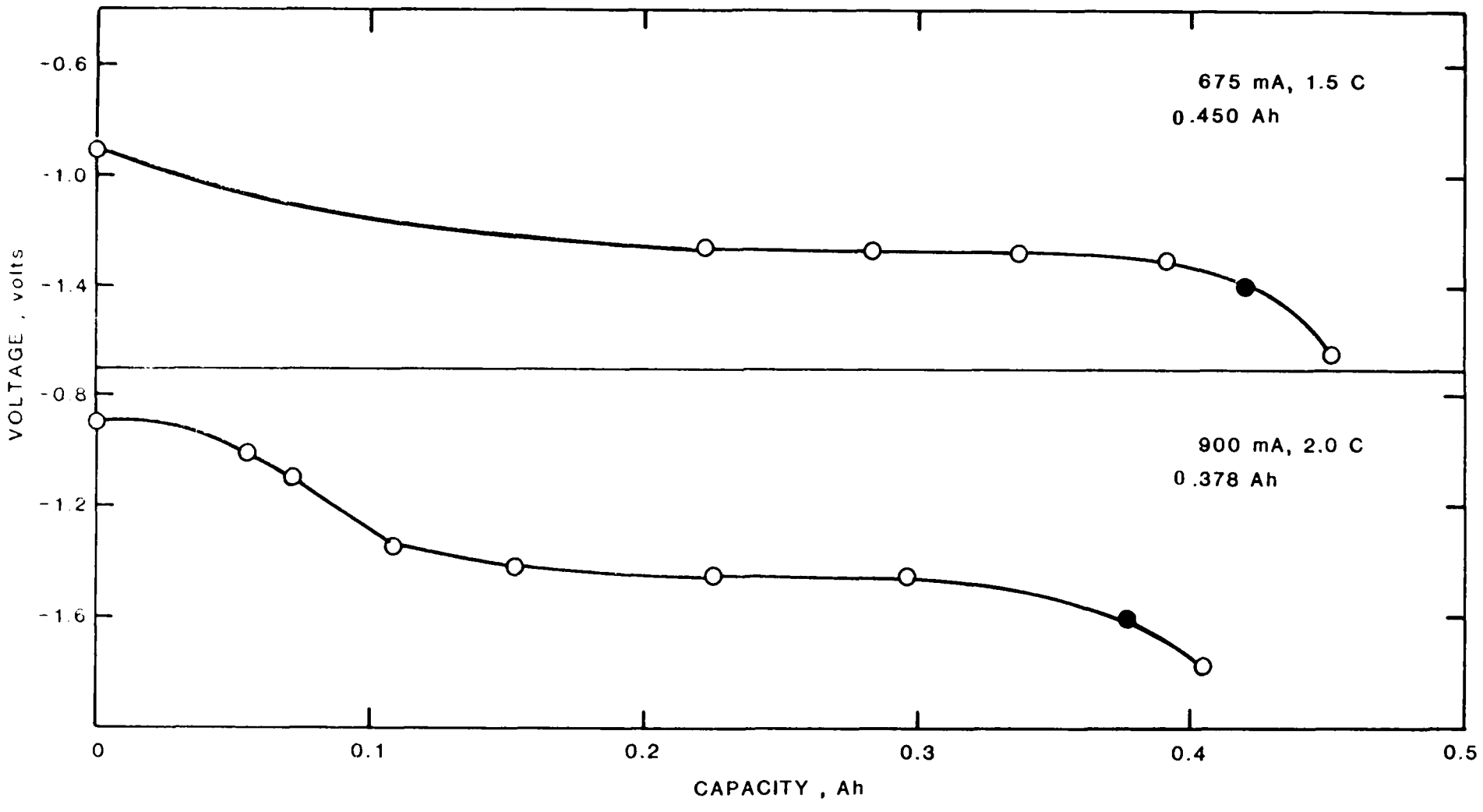

FIGURE 4.4 DISCHARGE PERFORMANCE OF CELL 26, 675, 900 mA

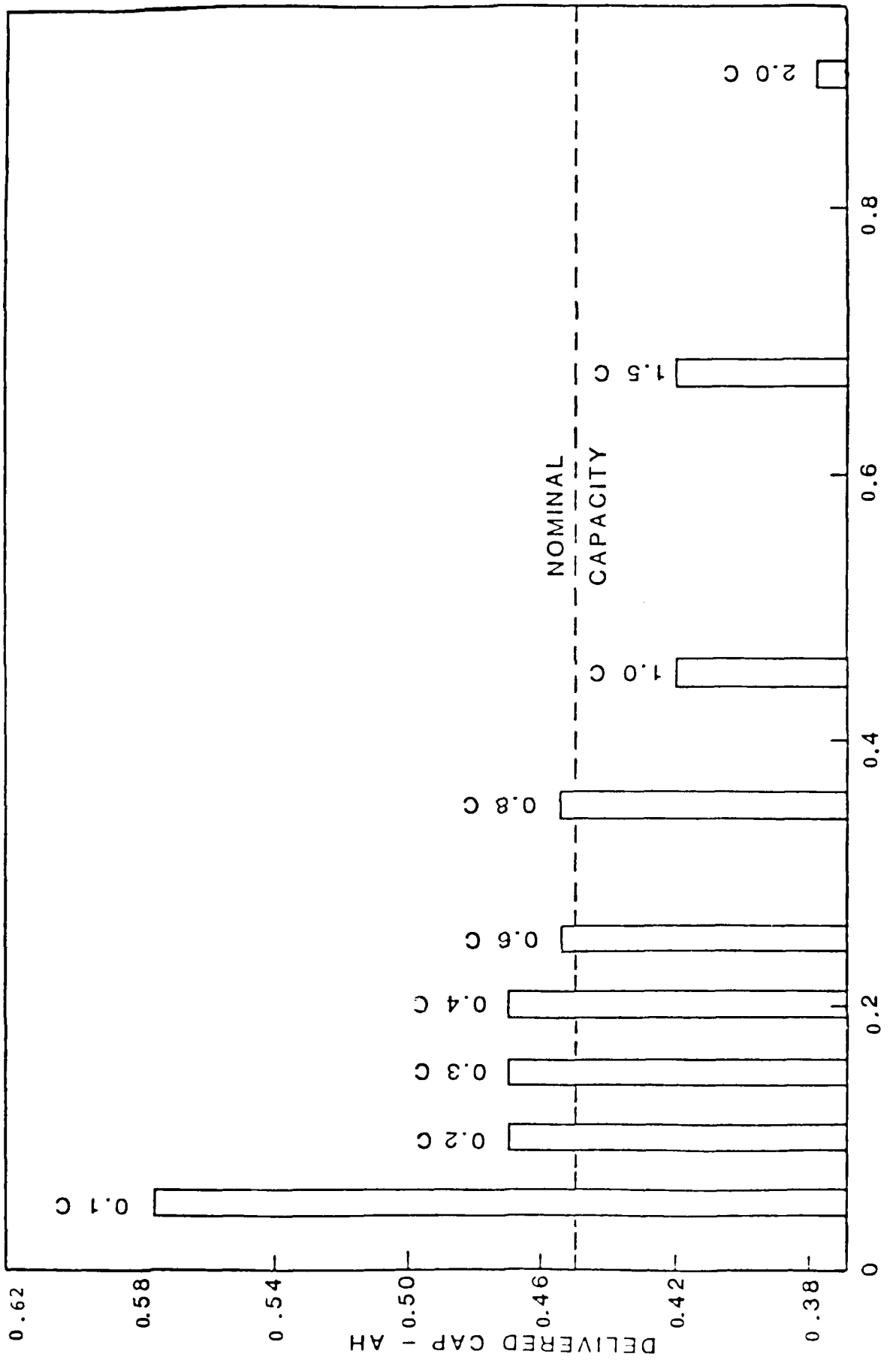

FIGURE 4.5 EFFECT OF DISCHARGE CURRENT ON DELIVERED CAPACITY - CELL 26

form a leak-proof system. The cell design was the same as before, employing a three-electrode configuration.

Prior to starting life cycle tests, characterization and performance verification of this cell was carried out. The procedure was the same as that used to verify the performance of Cell 26 containing ERC roll-bonded nickel. From the test data, summarized in Tables 4.4 and 4.5, it can readily be seen that the cell's performance was excellent and it satisfied the requirements for monitoring and controlling the main battery.

The cell was tested manually 10 times before starting routine life cycle tests. The test regime is given below.

Charge	3-½ hours at 100 mA
Discharge	2-½ hours at 100 mA
DOD	83%
Overcharge	40%

4.1.3 Cell Characterization with Respect to Temperature

This phase of the program was originally scheduled to commence during the first year. But characterization at room temperature took longer than planned and therefore the study of temperature effects was delayed. However, this delay did not have an impact on the overall program objectives and schedule.

The first series of tests were done on nickel-oxygen pilot cell 30, fabricated with a sintered (Marathon) electrode. The cell was first charged and discharged at 100 mA at room temperature and a capacity of 0.5 Ah was delivered. To accelerate testing, the current was increased to 150 mA and the test was repeated. Keeping the test current the same, the tests were done at different temperatures in the range between 0 and 140 °F. The temperature characteristics are shown in Figures 4.6 to 4.12 for each

TABLE 4.4

EFFECT OF OVERCHARGE ON DELIVERED CAPACITY - CELL NO. 27

CELL 27 - SAFT SINTERED Ni - NOM CAP **0.360 AH**

Overcharge vs. Delivered Capacity @ 100% DOD, c/3 rate

CYCLE #	MODE	I mA	t hours	AH	VOLTS end	VOLTS plateau	P start	P end	ΔP	OVERCHARGE %	%DELIVERED/NOMINAL
3-14-85	Chg	120	3.00	.360	0.589	0.512	60	30	30	0	-
2	Dischg	120	2.69	.323	1.000	0.782	30	60	30	-	89
3-18-85	C	120	3.75	.450	0.680	0.584	44	13	31	25	-
4	D	120	2.75	.330	1.005	0.826	13	43	30	-	92
3-19-85	C	120	4.50	.540	0.688	0.651	43	10	33	50	-
5	D	120	2.92	.350	1.000	0.839	10	43	33	-	97
3-20-85	C	120	5.25	.630	0.690	0.660	43	9	34	75	-
6	D	120	3.00	.360	1.036	0.893	9	45	36	-	100
3-21-85	C	120	6.00	.720	0.709	0.680	45	11	34	100	-
7	D	120	3.00	.360	0.814	0.814	11	45	34	-	100

TABLE 4.5

EFFECT OF DISCHARGE CURRENT ON DELIVERED CAPACITY - CELL NO. 27

CELL NO 27 - SAFT SINTERED Ni - NOM CAP : 0.360 AH

Discharge Performance - 100% DOD

Charge Per Cycle - 3.75 hours at 120 mA, 0.450 AH, 25% Overcharge

CYCLE NO	RATE	I mA	t Hours	VOLTS		P		ΔP	VOLTS Cut-Off	CAP AH	EFF %
				END	Plateau	Start	End				
3-26-85 10	c/9	40	9.81	1.000	0.684	13	48	35	1.000	0.392	109
3-22-85 8	c/6	60	6.38	1.000	0.733	12	46	34	1.000	0.382	106
3-18-85 4	c/3	120	2.75	1.005	0.826	13	43	30	1.000	0.330	92 *
3-28-85 12	c/2	180	2.00	1.144	0.848	13	47	34	1.000	0.360	100
3-29-85 13	c	360	0.94	1.238	0.913	13	47	34	1.000	0.338	94
3-27-85 11	1.5c	540	0.59	1.290	0.963	14	47	33	1.100	0.321	89
3-25-85 9	2.0c	720	0.44	1.400	0.986	12	46	34	1.100	0.315	88

*CYCLE 4, c/3 rate, not fully discharged as indicated by ΔP

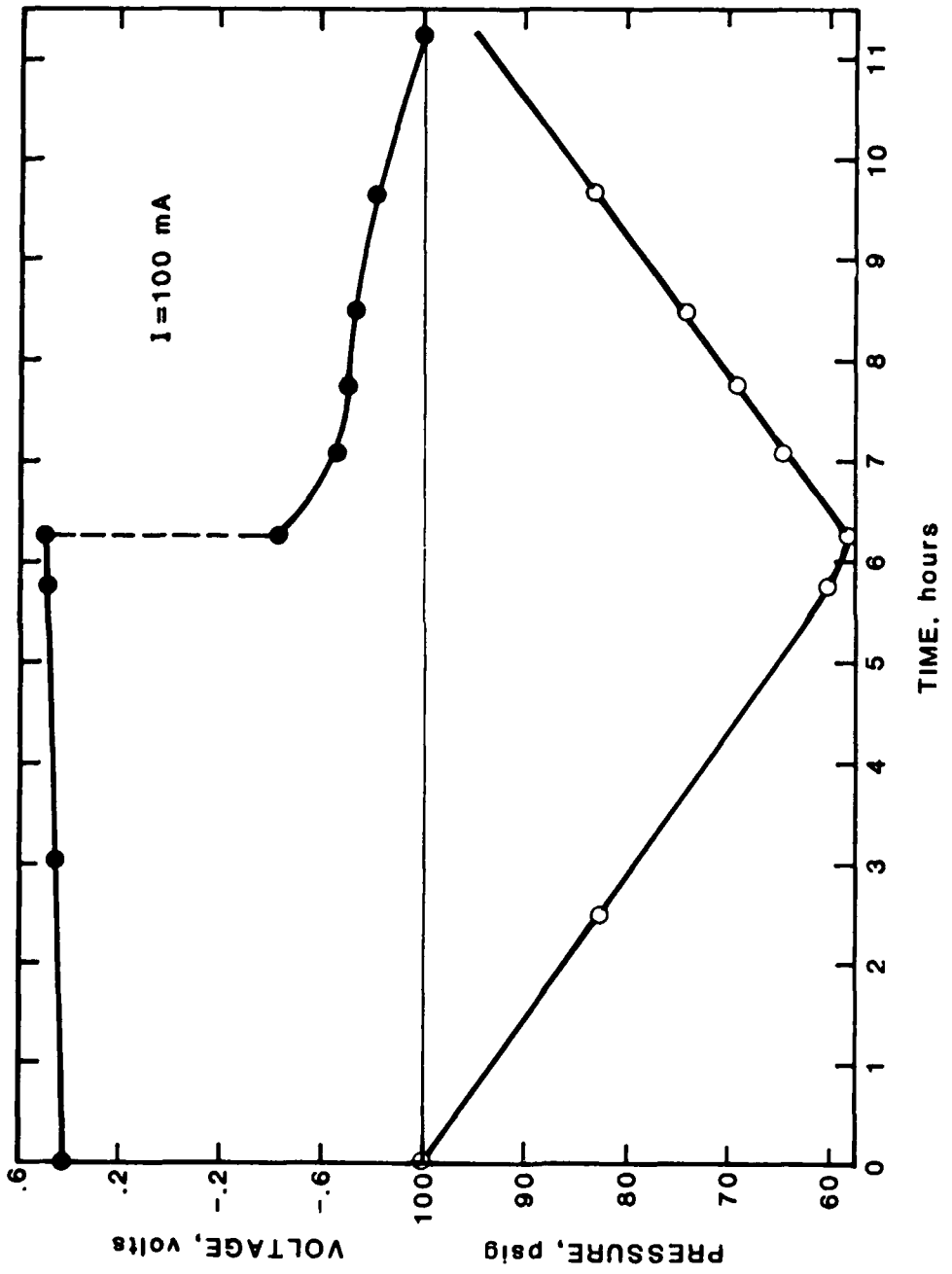

FIGURE 4.6 PERFORMANCE CHARACTERISTICS-Ni-O_2
CELL 30 AT ROOM TEMPERATURE, 100 mA

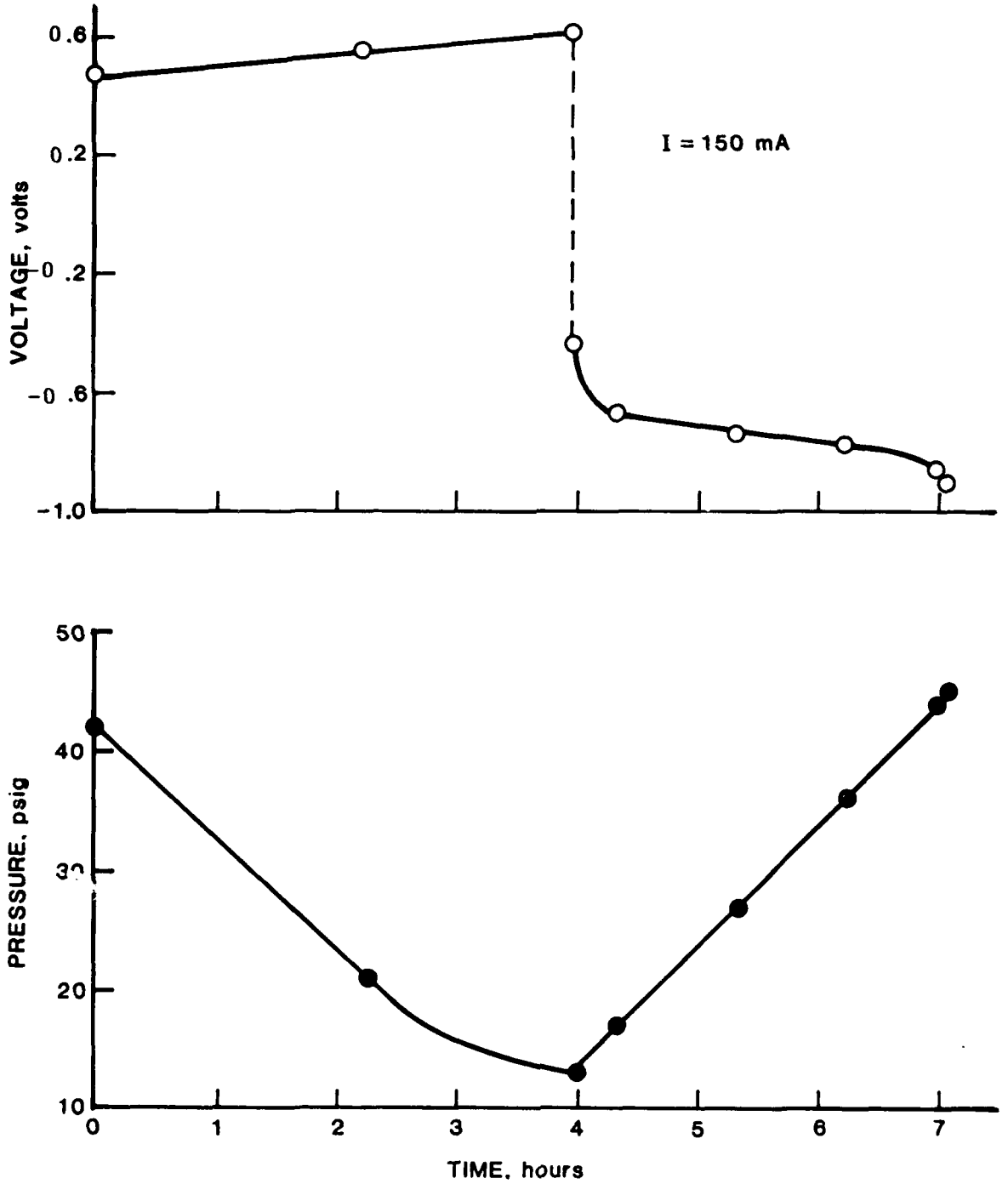

FIGURE 4.7 PERFORMANCE CHARACTERISTICS-Ni-O_2 CELL 30 AT ROOM TEMPERATURE, 150 mA

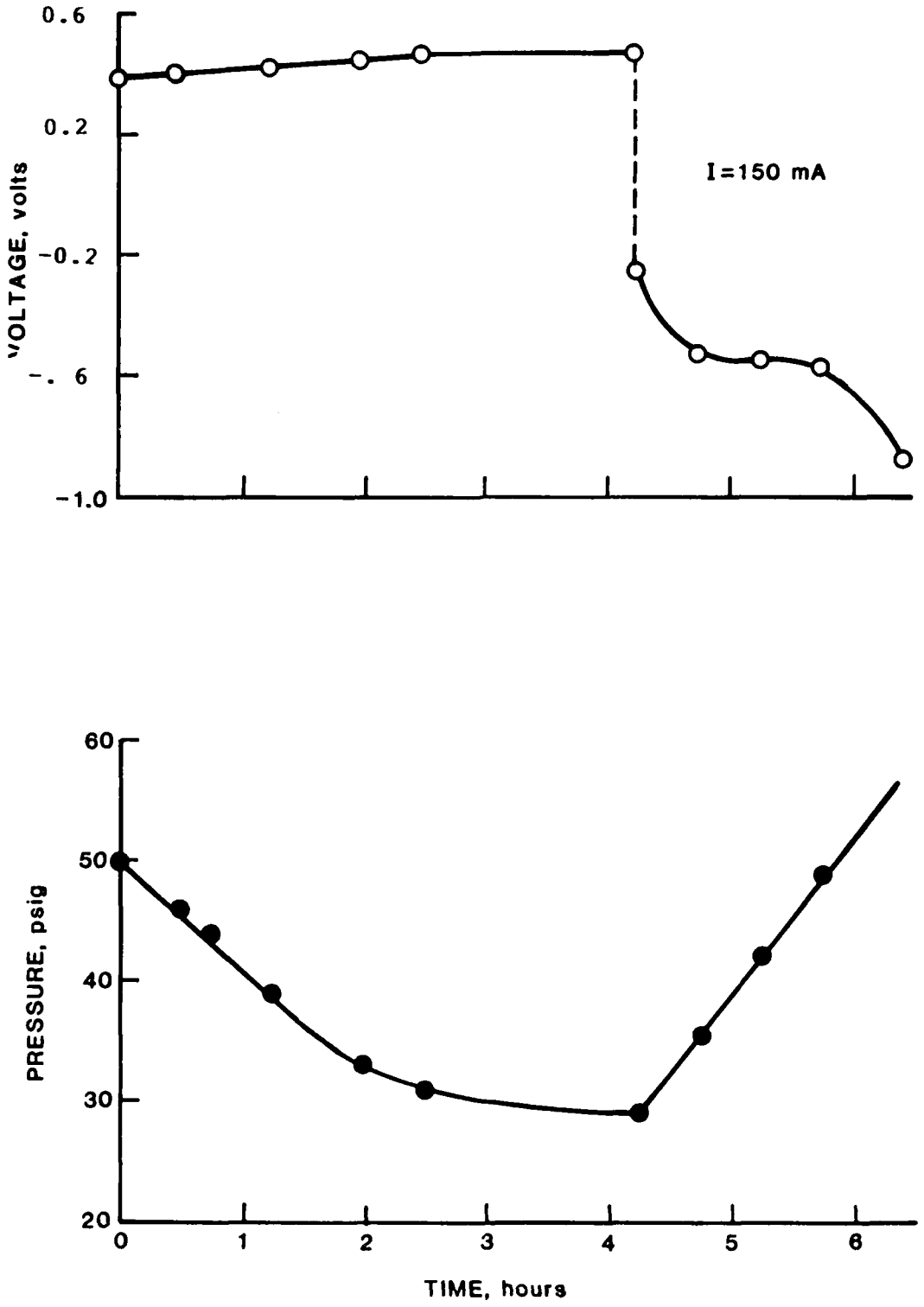

FIGURE 4.8 PERFORMANCE CHARACTERISTIC-Ni-O_2 CELL 30 AT 140°F

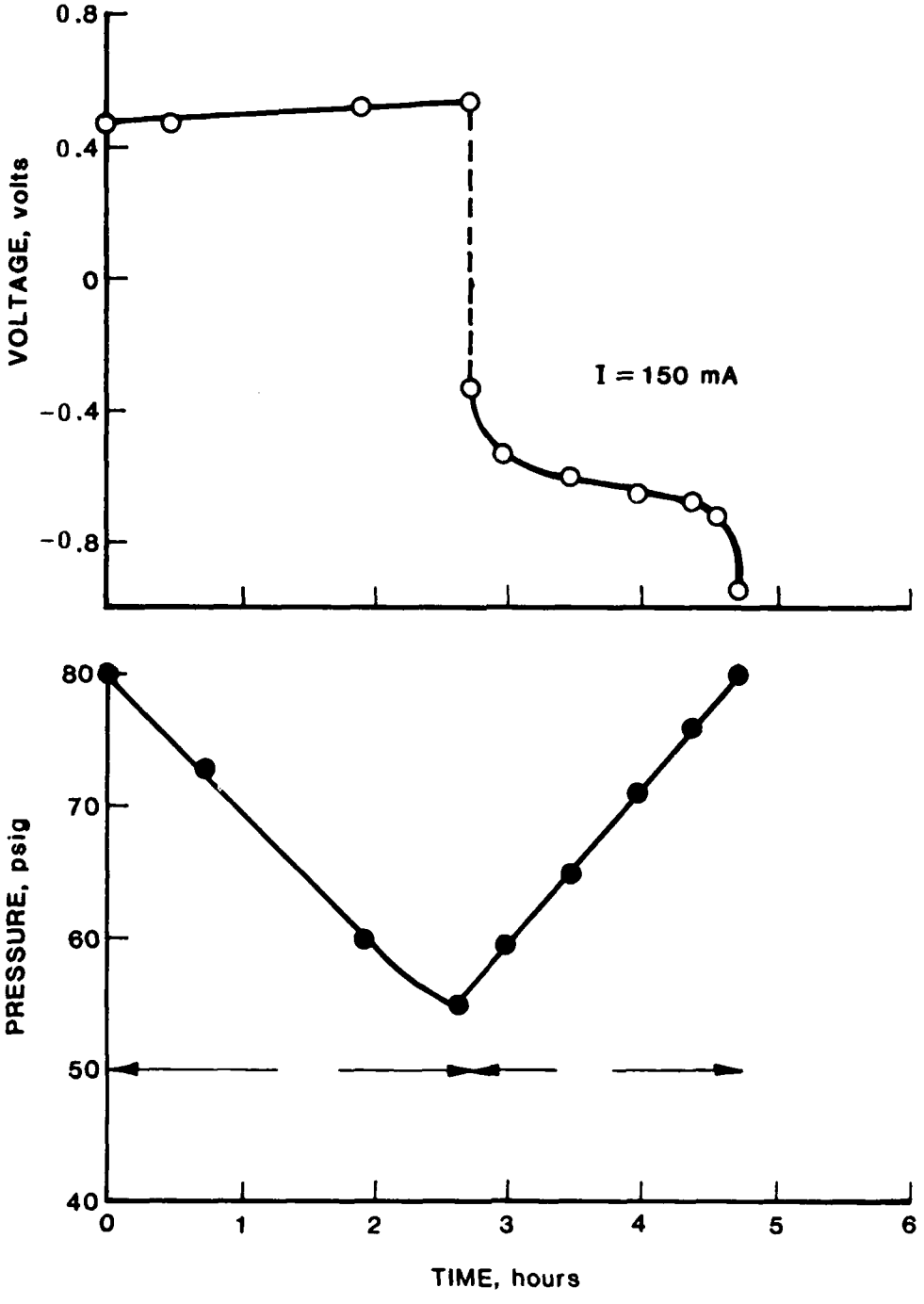

FIGURE 4.9 PERFORMANCE CHARACTERISTICS--Ni-O_2 CELL 30 AT 100°F

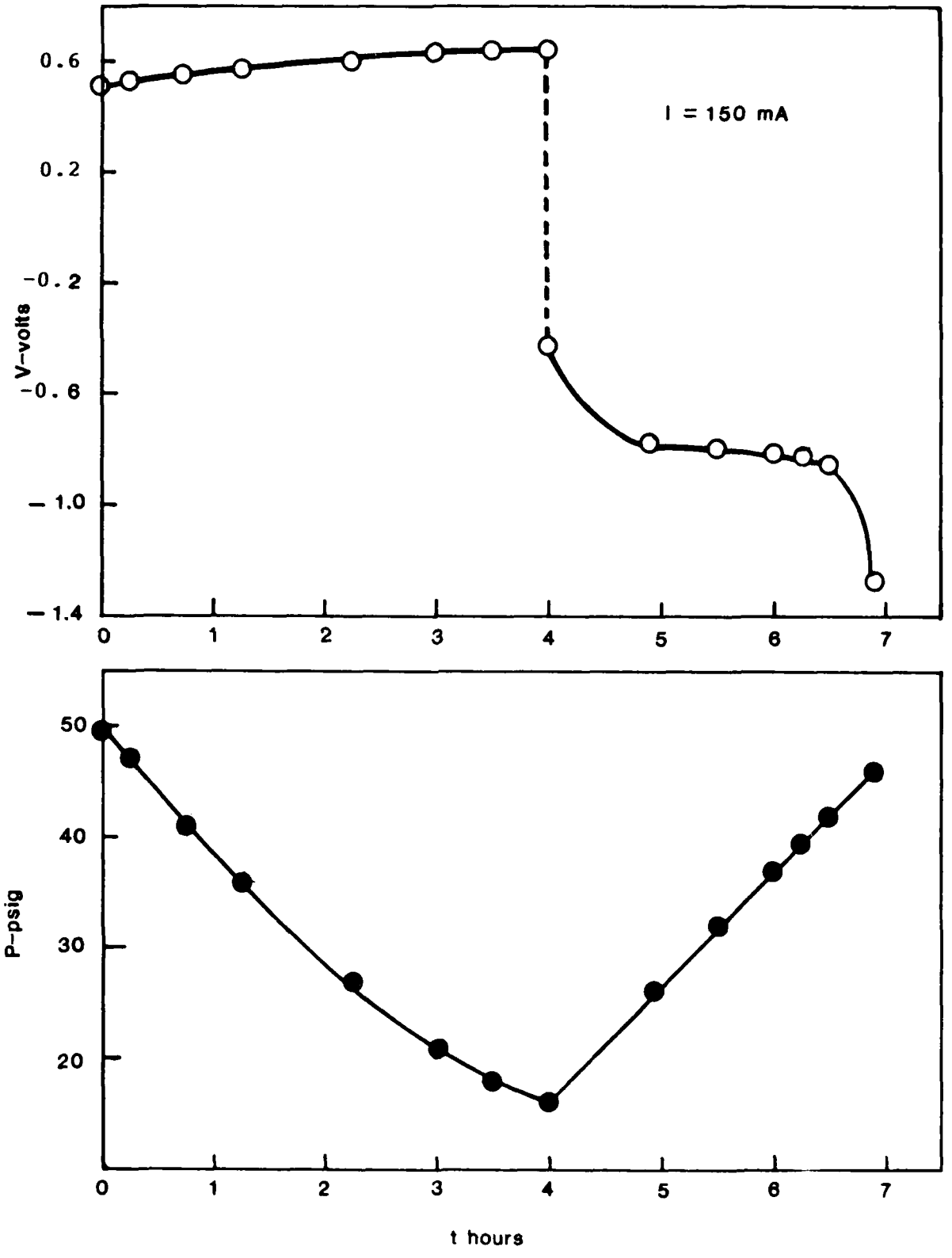

FIGURE 4.10 PERFORMANCE CHARACTERISTICS-Ni-O_2 CELL 30 AT 0°F

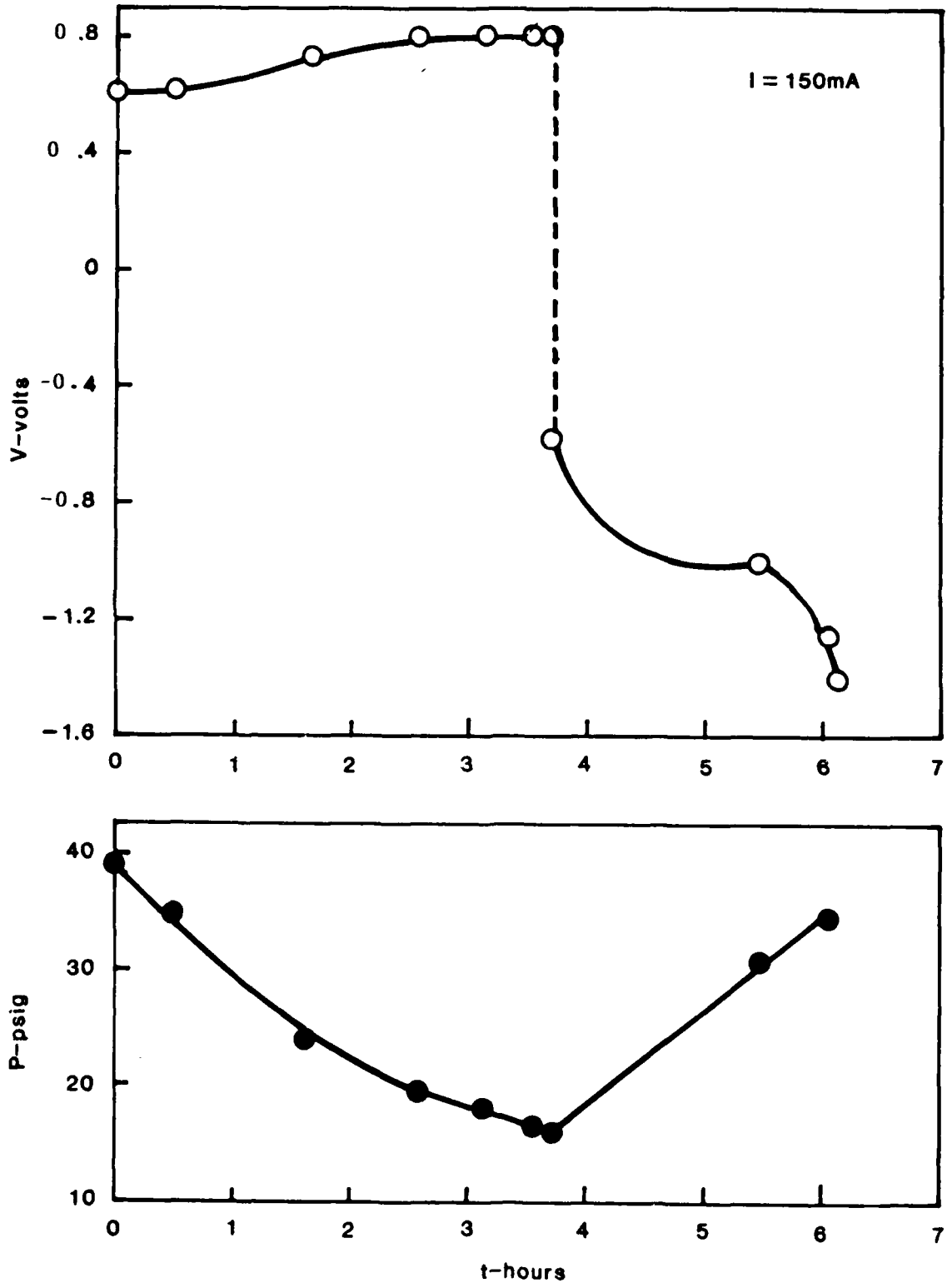

FIGURE 4.11 PERFORMACE CHARACTERISTICS-Ni-O_2 CELL 30 AT 60°F

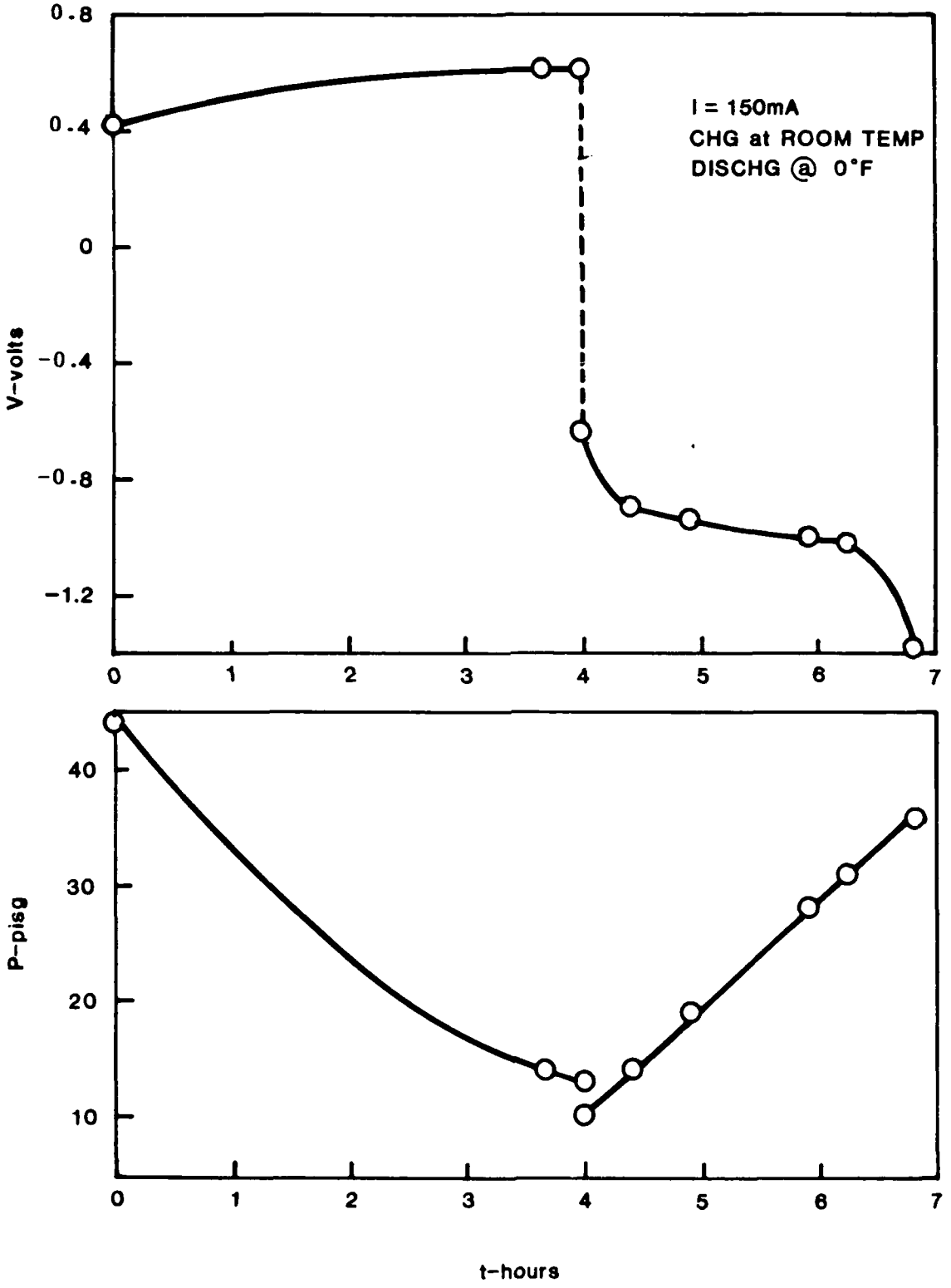

FIGURE 4.12 PERFORMANCE CHARACTERISTICS-Ni-O_2 CELL 30 AT 0°F

of the temperatures.

The results are summarized in Table 4.6 and the discharge performance at different temperatures are compared in Figure 4.13. The data indicate that

- Best delivered capacity is obtained at room temperature.
- Average discharge voltage is inversely proportional to test temperature.
- As evidenced by discharge at 0°F, charge acceptance is better at room temperature than at 0°F.

4.1.4 Linearity of Pressure

The cells that were cycled were monitored at regular intervals and the pressure profiles analyzed. To investigate the stability of the linear relationship with time, from the data of Cell 25 (ERC nickel), a plot of pressure against time was made. This is shown in Figure 4.14 (the top portion for cycles 1 through 260) after which the pressure at the end of discharge was reduced.

The bottom portion of Figure 4.14 shows the pressure profile for cycles 261 through 460. The results show that the values of ΔP and slope are independent of the absolute values of pressure and that the linearity does not change with time. The minor fluctuations are attributable to variations in the temperature of the surroundings. A similar plot for Cell 21 containing sintered nickel electrode is shown in Figure 4.15.

The effect of variations in ambient temperature on cell pressure during open circuit stand was also measured. Life tests of Cells 21(sintered Ni), 25 and 26 (roll-bonded Ni) were stopped after they had undergone 1,026, 766 and 795 cycles,

TABLE 4.6

CELL PERFORMANCE AT DIFFERENT TEMPERATURES

$Ni-O_2$ Cell 30

Ni Electrode: Sintered, Marathon

	Charge			Discharge		
Cycle No.	T°F	Ah	ΔP	T°F	Ah	ΔP
1	Room	0.625	42	Room	0.500	45
2	100	0.413	25	100	0.300	24
3	140	0.638	21	140	0.326	26
4	60	0.600	34	60	0.432	30
5	0	0.558	23	0	0.362	21
6	Room	0.600	31	0	0.425	26
7	Room	0.600	29	Room	0.458	32

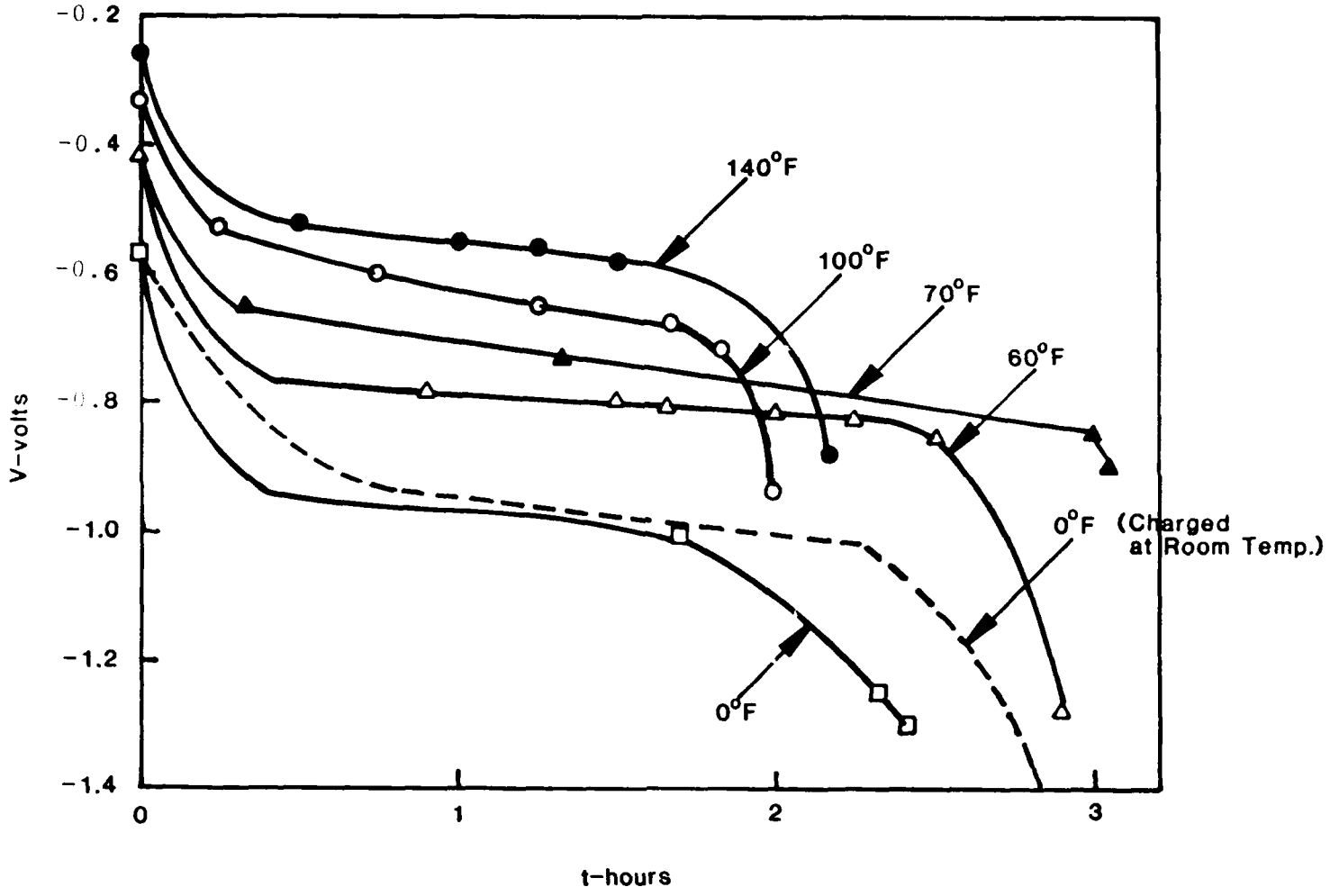

FIGURE 4.13 DISCHARGE PERFORMANCE OF Ni-O_2 CELL 30 AT DIFFERENT TEMPERATURES

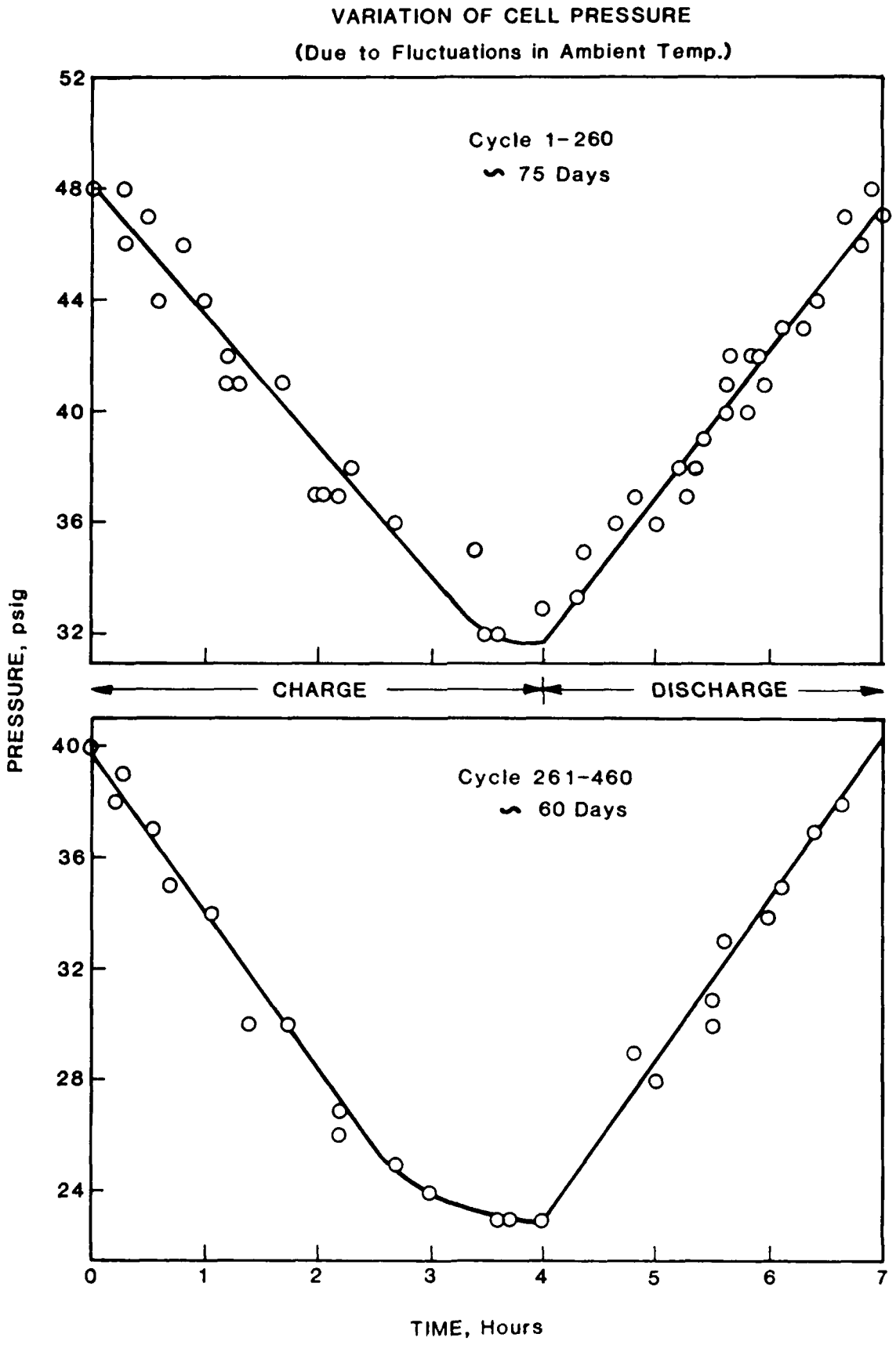

FIGURE 4.14 OVERALL PRESSURE PROFILE-ERC Ni

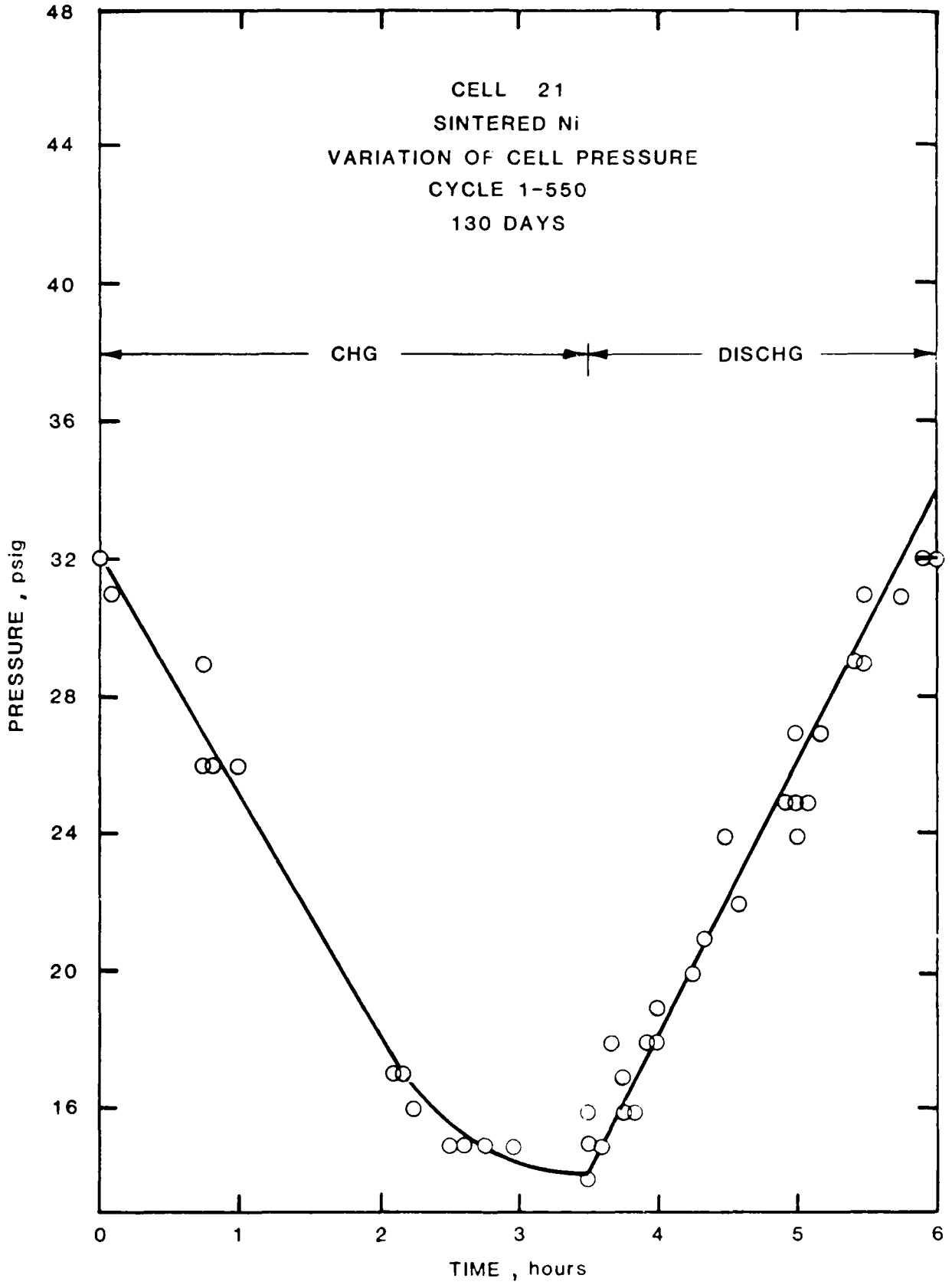

FIGURE 4.15 OVERALL PRESSURE PROFILE - SINTERED Ni

respectively. To compare the variation in pressure under identical environmental and state of charge conditions, all three cells were fully charged. The pressure at the end of charge was set at 10 psig for each cell.

The cells were next allowed to stand on open circuit and the room temperature and cell pressure were monitored daily.

The initial preset value of 10 psig increased slightly in the first 2 days, after which it remained constant. In the temperature range of 19 to 26°C, all three cells exhibited very little change in pressure. The results, plotted in Figure 4.16 show that over the temperature range investigated, the values of pressure of all three cells remain steady with very little fluctuations on open circuit stand. However, we should point out that during charge and discharge at high rates, temperature excursions could become significant.

The tests were repeated with Cells 41 and 45 after completion of life cycle tests. The data over a 5-month period are shown in Table 4.7 and Figure 4.17. Again it appears that in the temperature range of 18 to 28°C variation in cell pressure is minimal as exhibited by Cell 45. Cell 41 shows a continuous decline in pressure which can be attributed to a slow leak in the system.

4.1.5 Single Electrode Potentials

To monitor the potentials of individual electrodes and identify the electrode responsible for cell failure, at test fixture was designed and built. In addition to the three electrodes, the assembly was designed to accommodate a cadmium wire to be used as a reference to monitor the potential of each working electrode.

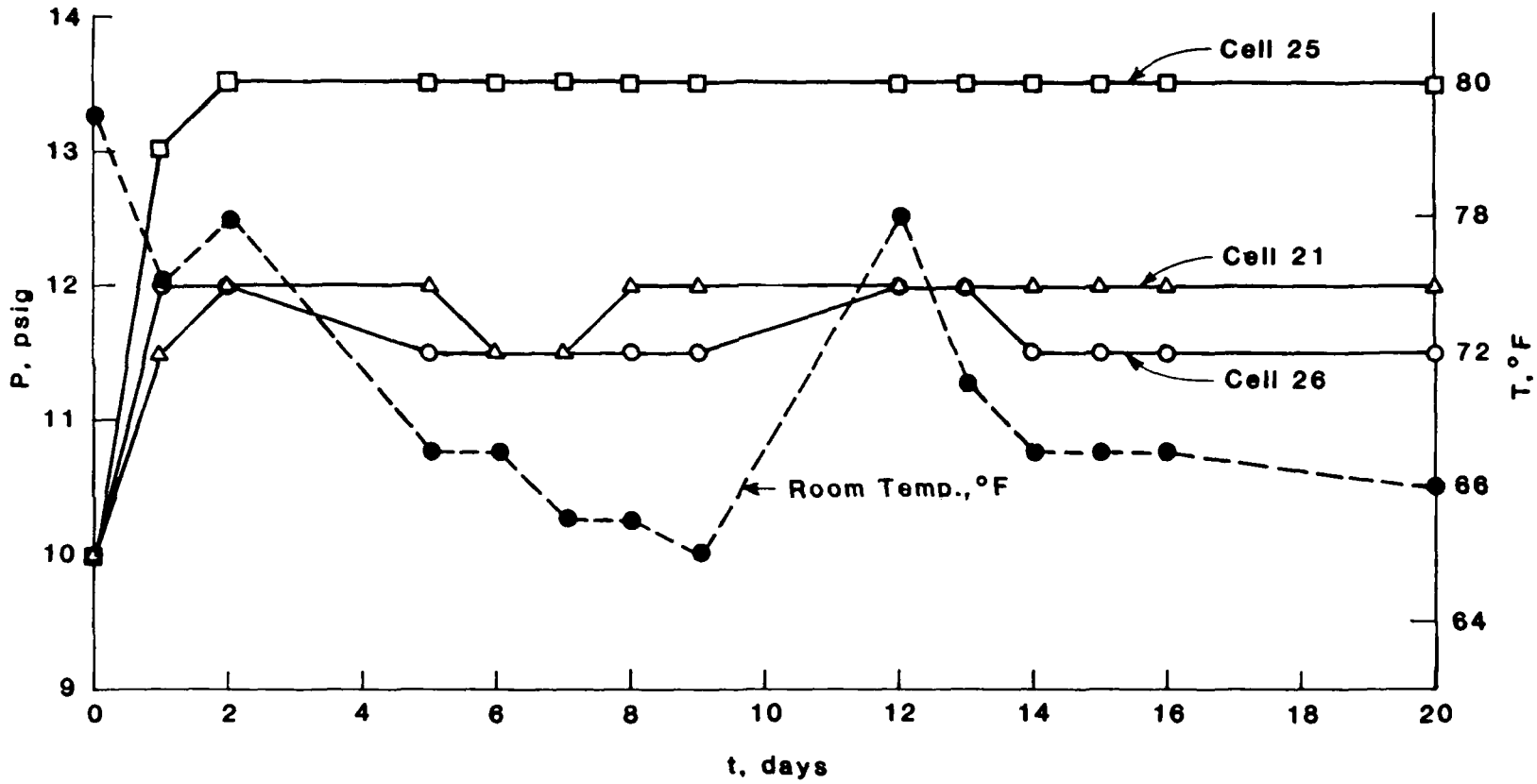

FIGURE 4.16 VARIATION OF CELL PRESSURE WITH AMBIENT TEMPERATURE ON OPEN CIRCUIT STAND

No. of Days	Room Temp. (°C)	Cell Pressure (PSIG) #41	#45
		filled with O_2 to 25 psig	
0	-		
2	13	24½	24
3	21	25	25
9	20	24½	24
14	18	24	24
16	22	24½	24½
19	22	24	24½
21	19	24	24
25	20	24	24
27	20	23½	24
32	13	22½	23½
33	24	23½	24½
36	24	23½	24
48	25	23	24
54	17½	22	23½
60	17½	22	23½
63	22½	22½	24½
70	22½	22	24
78	21	21½	23½
84	21	21½	24
85	19½	21	23½
92	22	21	24
103	19	20	23
118	22	19½	23½
124	22	19	23½
134	27	19	23½
145	28	18	23
n	26	26	26
$\bar{x}$	21.25	22.29	23.88
S.D.$_n$	2.7148	1.9274	0.4663
S.D.$_{n-1}$	2.7686	1.9656	0.4756
High	28	25	25
Low	17½	18	23

TABLE 4.7 Variation of cell pressure during open circuit stand.

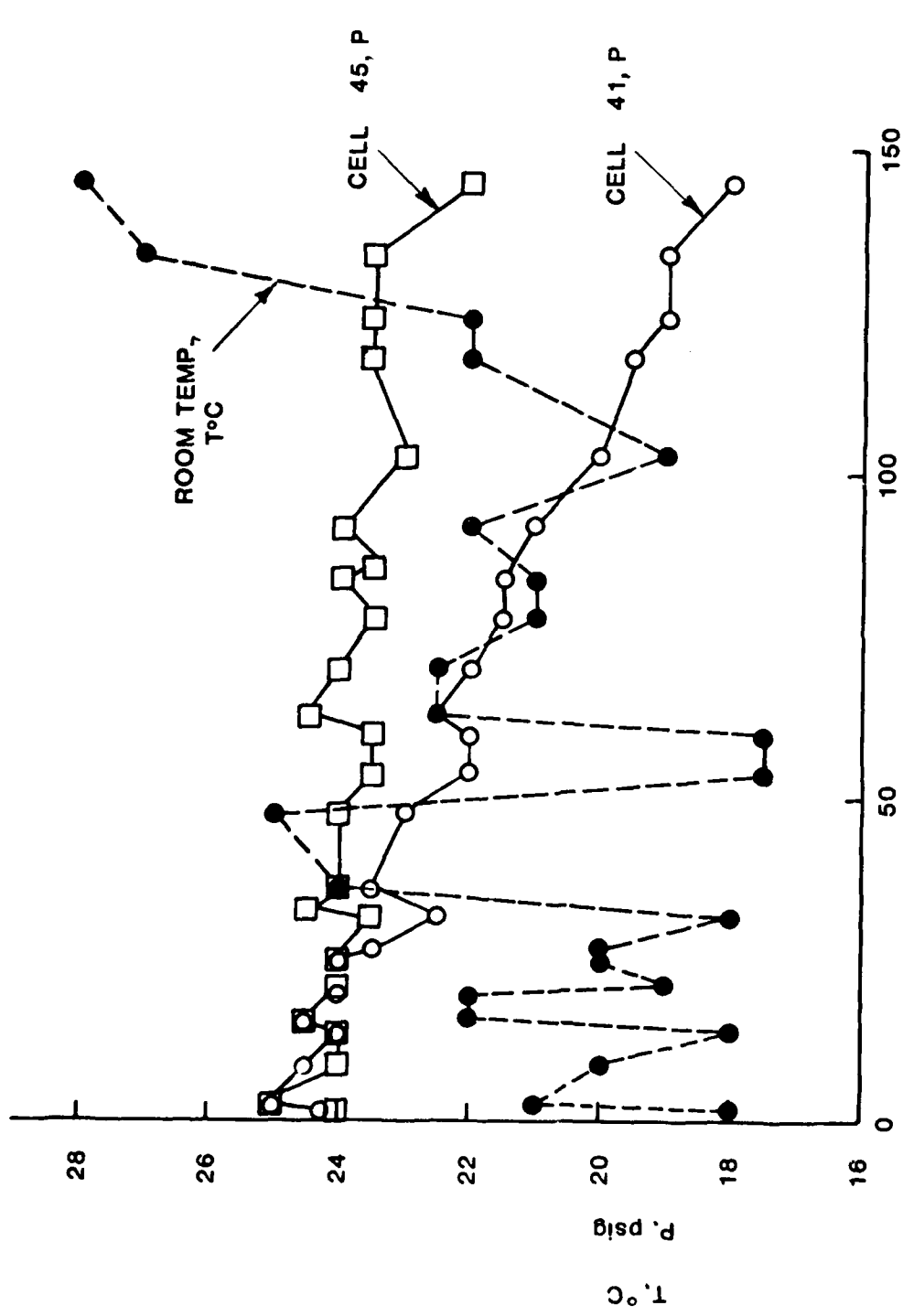

FIGURE 4.17 VARIATION OF CELL PRESSURE WITH AMBIENT TEMPERATURE ON OPEN CIRCUIT STAND

Cell 25, built with ERC roll-bonded nickel was assembled in a test fixture. After undergoing a conditioning cycle, the cell was charged for 5 hours at a current of 100 mA followed by discharge at the same current and a capacity of 0.292 Ah was delivered. The potentials of nickel and platinum electrodes were monitored against each other and also against screen and the cadmium reference wire.

The values of the cell voltage and the single electrode potentials of the fresh cell are shown in Figure 4.18. The test plan was to subject the cell to continuous charge/discharge cycles and monitor the potentials of individual electrodes at regular intervals. Abnormal changes in voltage would indicate cell failure and also identify which of the electrode(s) exhibit a deterioration with time.

The cell completed over 650 charge/discharge cycles and except for a slight increase in the nickel electrode potential over a period of 6 months, performance characteristics were very similar to that at the beginning of life tests. The voltage and pressure profiles for cycle 624 are shown in Figure 4.19 and the performance characteristics during cycling are summarized in Table 4.8.

Life cycle tests were continued and a change in performance was first noticed during cycle 730. The performance started to deteriorate with high values of polarization and lowered values of capacity. From the single electrode potentials in Figure 4.20, the gas electrode is still performing well, and the mechanism of failure is attributed to the high polarization of the nickel electrode. For purposes of comparison, similar values for

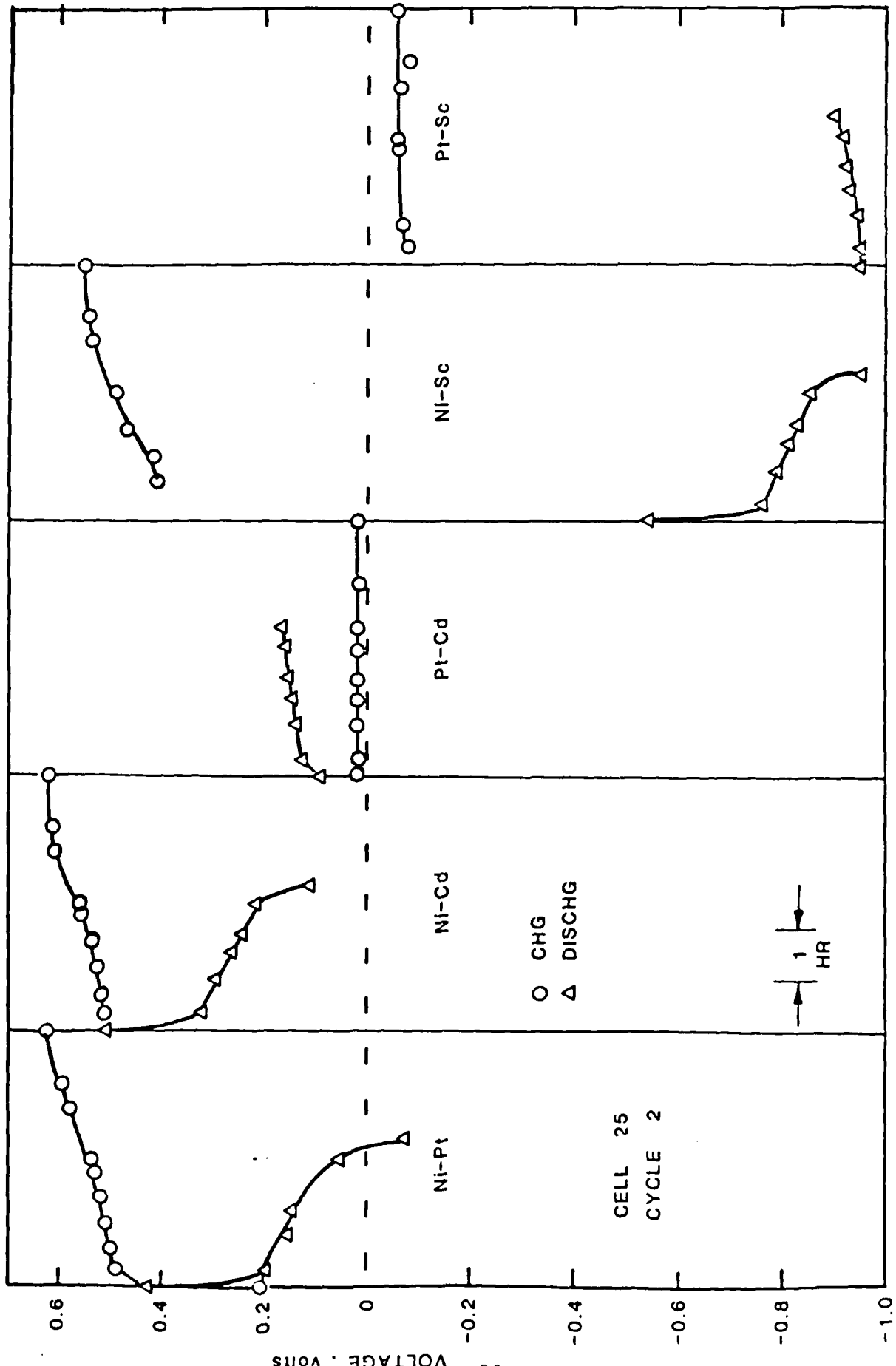

FIGURE 4.18 SINGLE ELECTRODE POTENTIALS

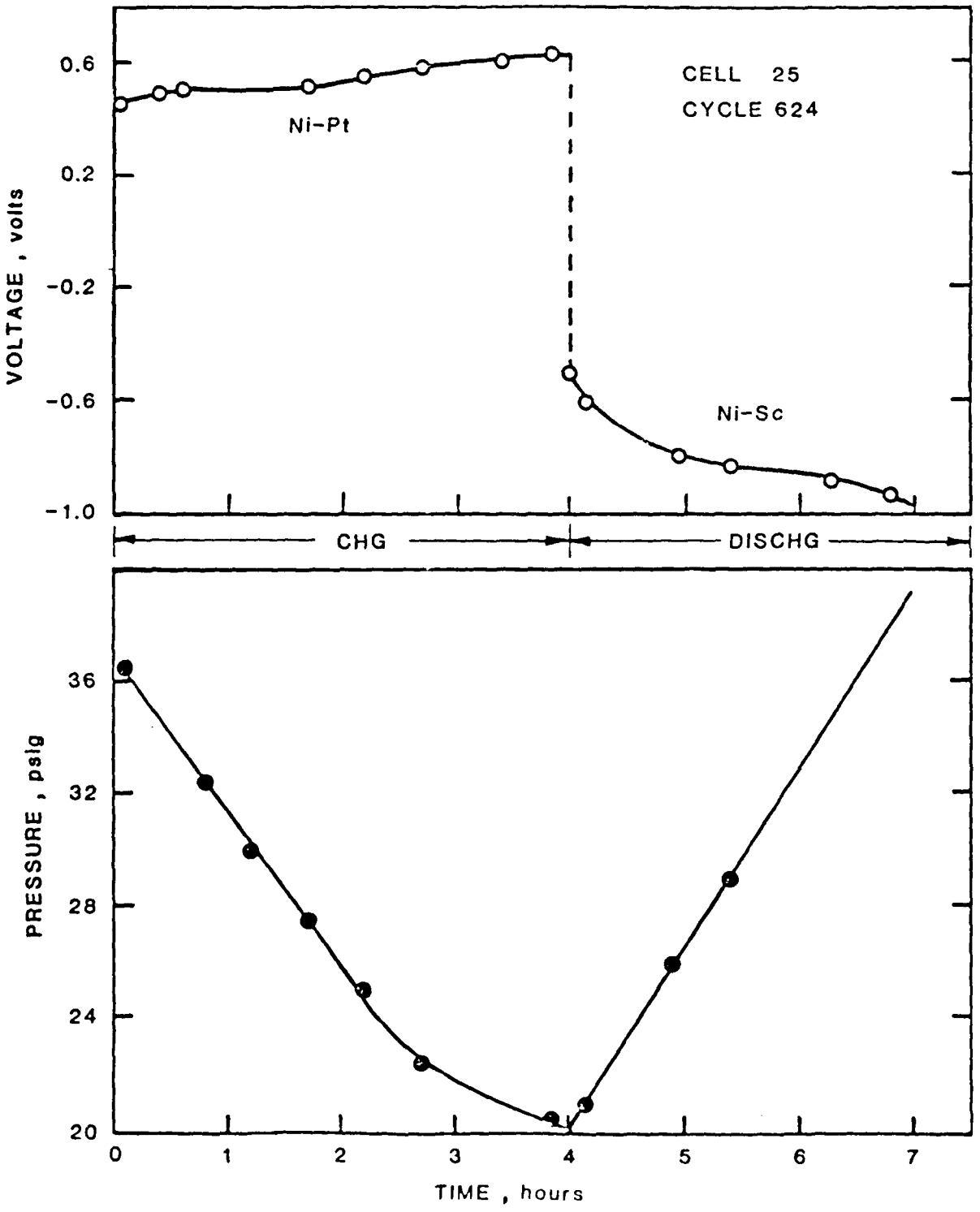

FIGURE 4.19 PRESSURE PROFILE - CELL 25, CYCLE 624

TABLE 4.8

CELL PARAMETERS ON LIFE CYCLE

Cell No.: 25 (with reference electrode)
Ni Positive: ERC roll-bonded

Cycle Time: 7.0 hours
Charge: 4.0 hours
Discharge: 3.0 hours
Current: 100 mA

CYCLE NO.	CHARGE Average Voltage Ni-Pt	Ni-Cd	Pt-Cd	ΔP	DISCHARGE Average Voltage Ni-Sc	Ni-Cd	ΔP	END VOLTS Charge D'chrge Ni-Pt	Ni-Sc
2	0.542	0.565	0.022	20	-0.831	0.246	23	0.601	-0.954
50	0.518	0.532	0.021	16	-0.766	0.278	18	0.614	-0.800
113	0.516	0.554	0.037	16	-0.789	0.287	16	0.640	-0.890
175	0.520	0.551	0.030	15	-0.790	0.305	15	0.635	-0.901
234	0.540	0.568	0.029	16	-0.736	0.347	16	0.618	-0.835
273	0.523	0.547	0.024	18	-0.732	0.335	18	0.618	-0.807
381	0.483	0.533	0.025	-	-0.794	0.298	-	0.610	-0.823
457	0.564	-		-	-	-	-	0.625	-0.850
500	0.501	0.517	0.014	16	-0.790	0.282	17	0.620	-0.885
548	0.511	0.554	0.017	17	-0.774	0.290	17	0.610	-0.910
623	0.547	0.557	0.012	18	-0.804	0.254	19	0.620	-0.960
$\bar{x}$	0.524	0.548	0.023	16.9	-0.781	0.292	17.7	0.619	-0.874
σ	0.0228	0.0160	7.6659	1.5366	0.0300	0.0316	2.3452	0.0112	0.0556

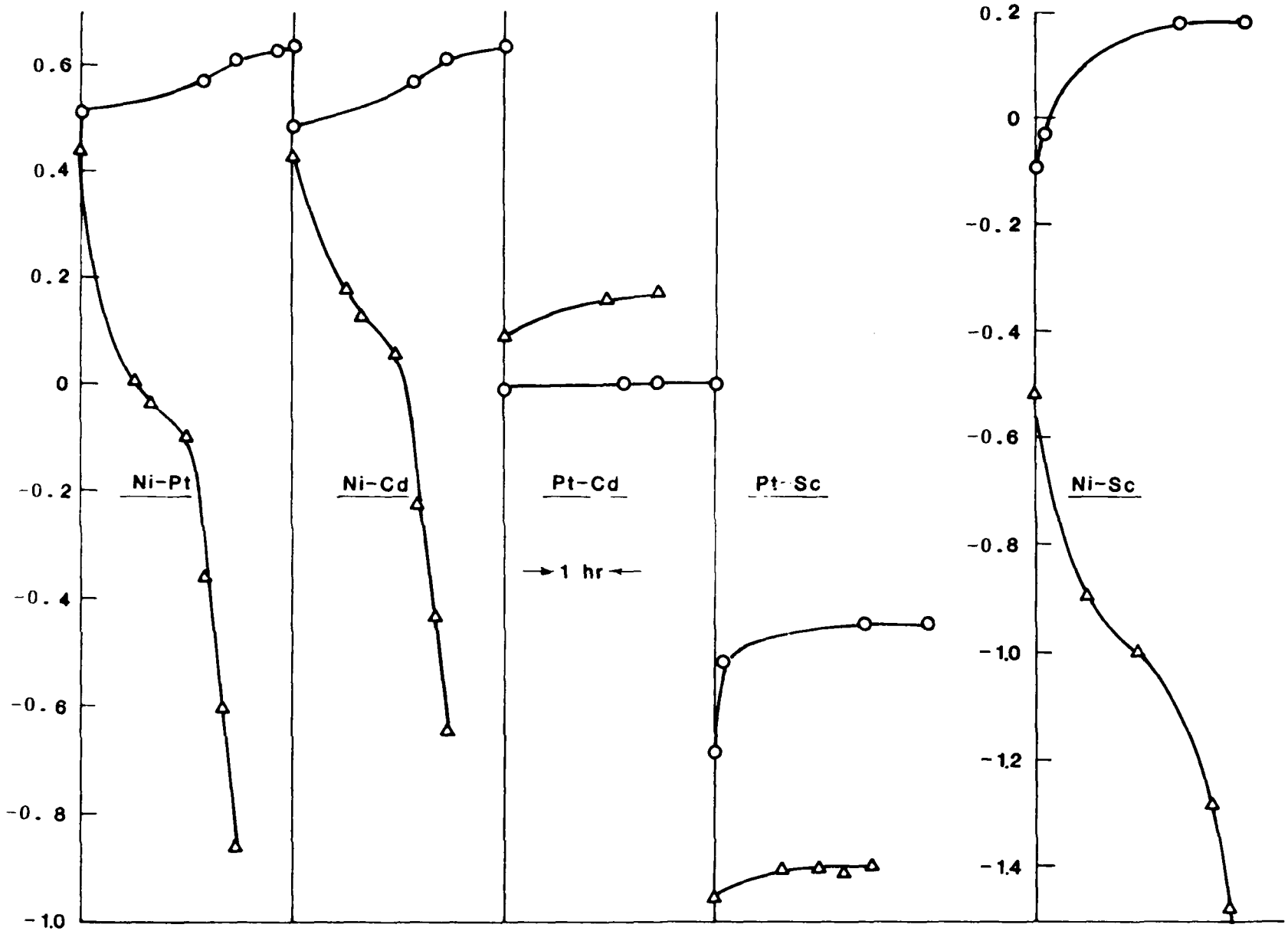

FIGURE 4.20 SINGLE ELECTRODE POTENTIALS-CELL 25, CYCLE 730

cycle 624 are shown in Figure 4.21.

Despite the increased polarization of the nickel electrode, the Ni-O_2 cell continued to exhibit linearity of pressure with time and tapering of pressure at the conclusion of charge (Figure 4.22).

Test results of Cell 25 further confirm the excellent suitability of the nickel-oxygen cell to function as an indicator of the stare of charge of the main battery. The analysis of the data from this series of tests shows that

(1) Since the main battery and pilot cell are run in tandem and since the failure of the pilot cell is caused by the decay of the nickel electrode, the positive plate of the main battery would also fail at the same time. This would result in the usefulness of the main battery being terminated, and as such no further monitoring would be required.

(2) Even if the main battery does not fail at the same time, the pilot cell would still have the capability to track the pressure, despite the deterioration of the nickel electrode.

Life cycle tests were discontinued and Cell 25 was used evaluate variations in cell pressure with temperature on open circuit stand (paragraph 4.1.4).

Another experimental Cell (No. 41) was constructed in a test fixture with the cadmium reference electrode. The design of this cell was similar to that of Cell 25, the only difference being the type of nickel electrode. Cell 25 was fabricated with ERC roll-bonded nickel and data on cycle life and single

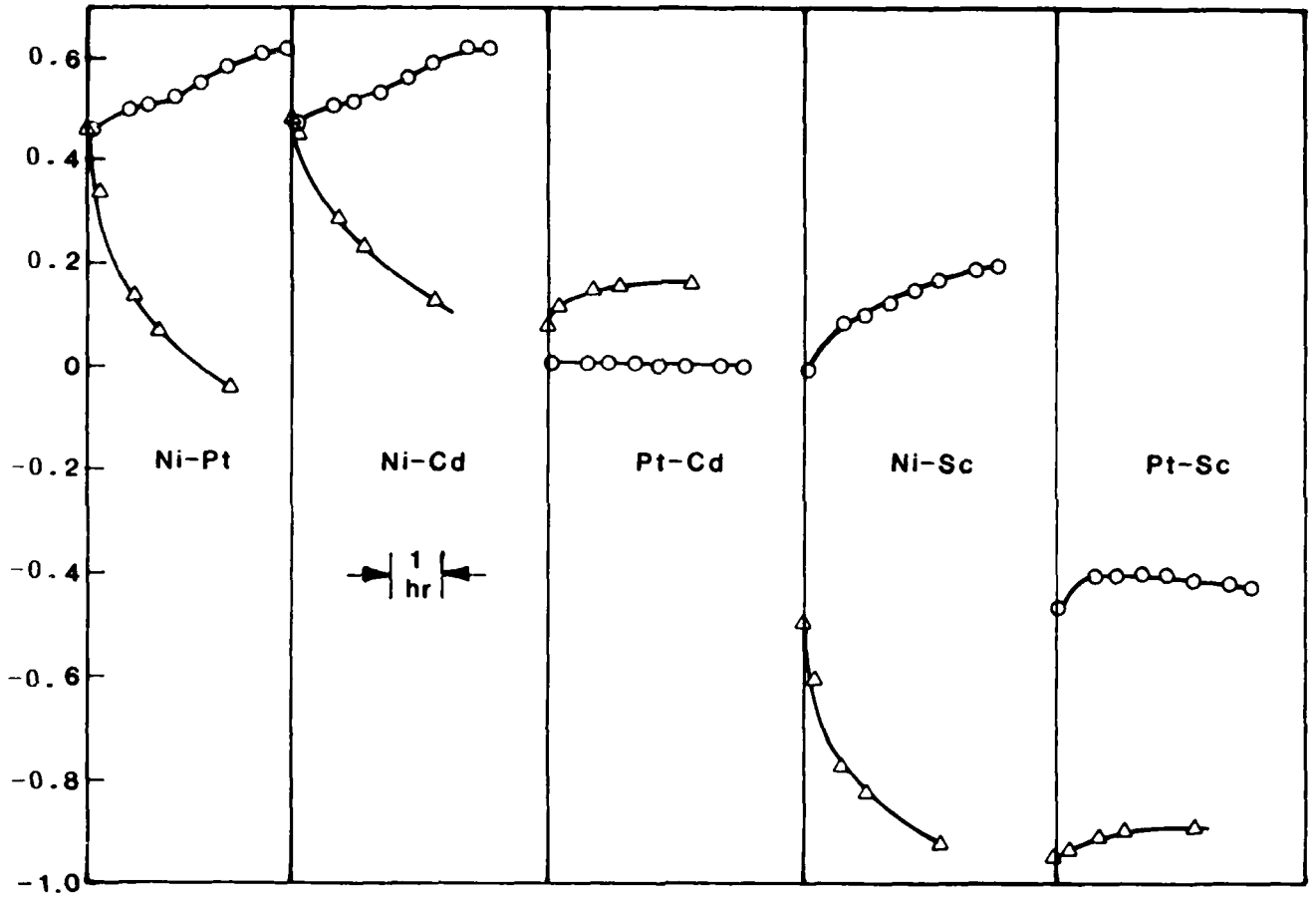

FIGURE 4.21 SINGLE ELECTRODE POTENTIALS-CELL 25, CYCLE 624

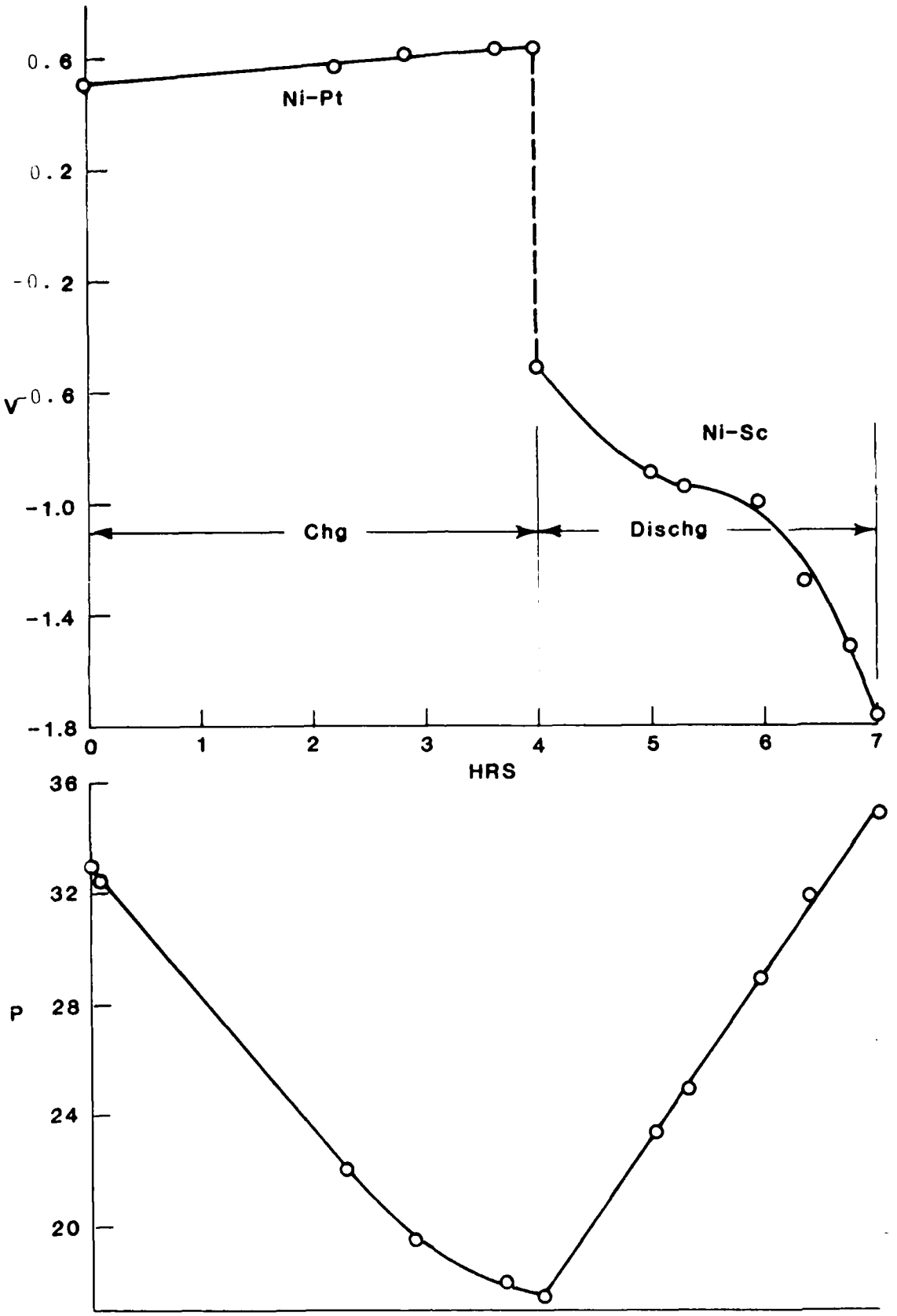

FIGURE 4.22 PRESSURE PROFILE-CELL 25, CYCLE 730

electric potentials were obtained. Cell 41 was built with a sintered nickel electrode from a fresh aircraft cell manufactured by Marathon Battery Company. This cell was tested under the same conditions employed for Cell 25, and since all other parameters remain the same, the test data will provide a means for directly comparing the performance characteristics of the two types of nickel electrodes. Cell 41 exhibited the following parameters when newly built:

Delivered Capacity = 0.46 at 100 mA

	End of Discharge Volts
Ni-Pt	0.020
Ni-Cd	0.299
Ni-Sc	0.841
Pt-Cd	0.319
Pt-Sc	0.822

Cycling of the cell was started at 100 mA with charge and discharge times being 4 and 3 hours respectively-the same parameters used for Cell 25. Single electrode potentials of Cells 41 and 25 for comparable cycles are shown in Figures 4.23 and 4.24. The cell completed 1400 cycles prior to discontinuing tests. The data for cycle 736 are shown in Figure 4.25, and cycle 1257 in Figure 4.26.

4.2 LIFE CYCLE TESTS

Having characterized the performance of the Ni-O_2 cell with respect to current density, temperature, linearity of pressure, single electrode potentials etc., the cells were subjected to long term life cycle tests.

Automatic cyclers with adjustable current and time settings were designed and built. Cycling of the cells commenced, charging,

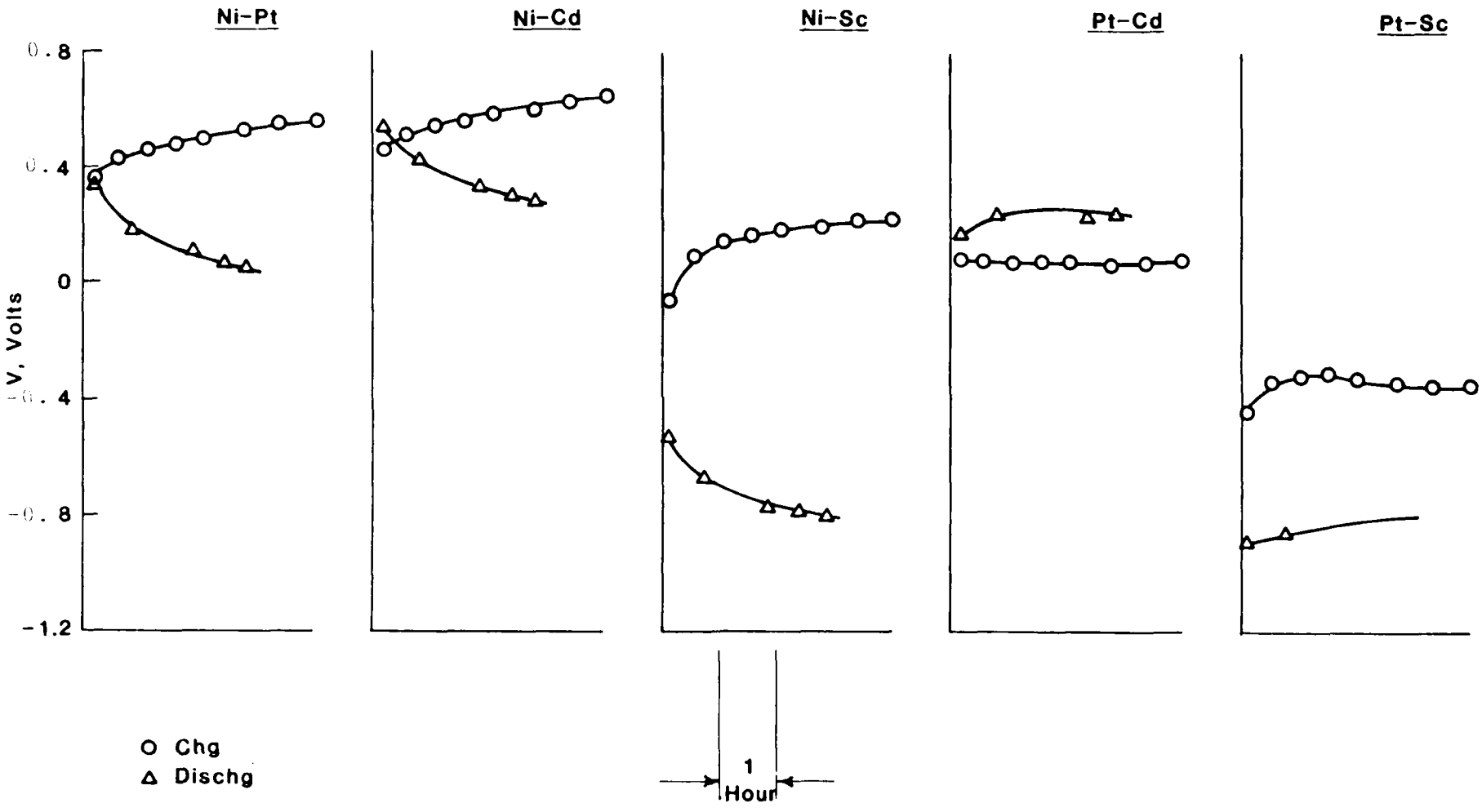

FIGURE 4.23 SINGLE ELECTRODE POTENTIALS-CELL 41, CYCLE 65

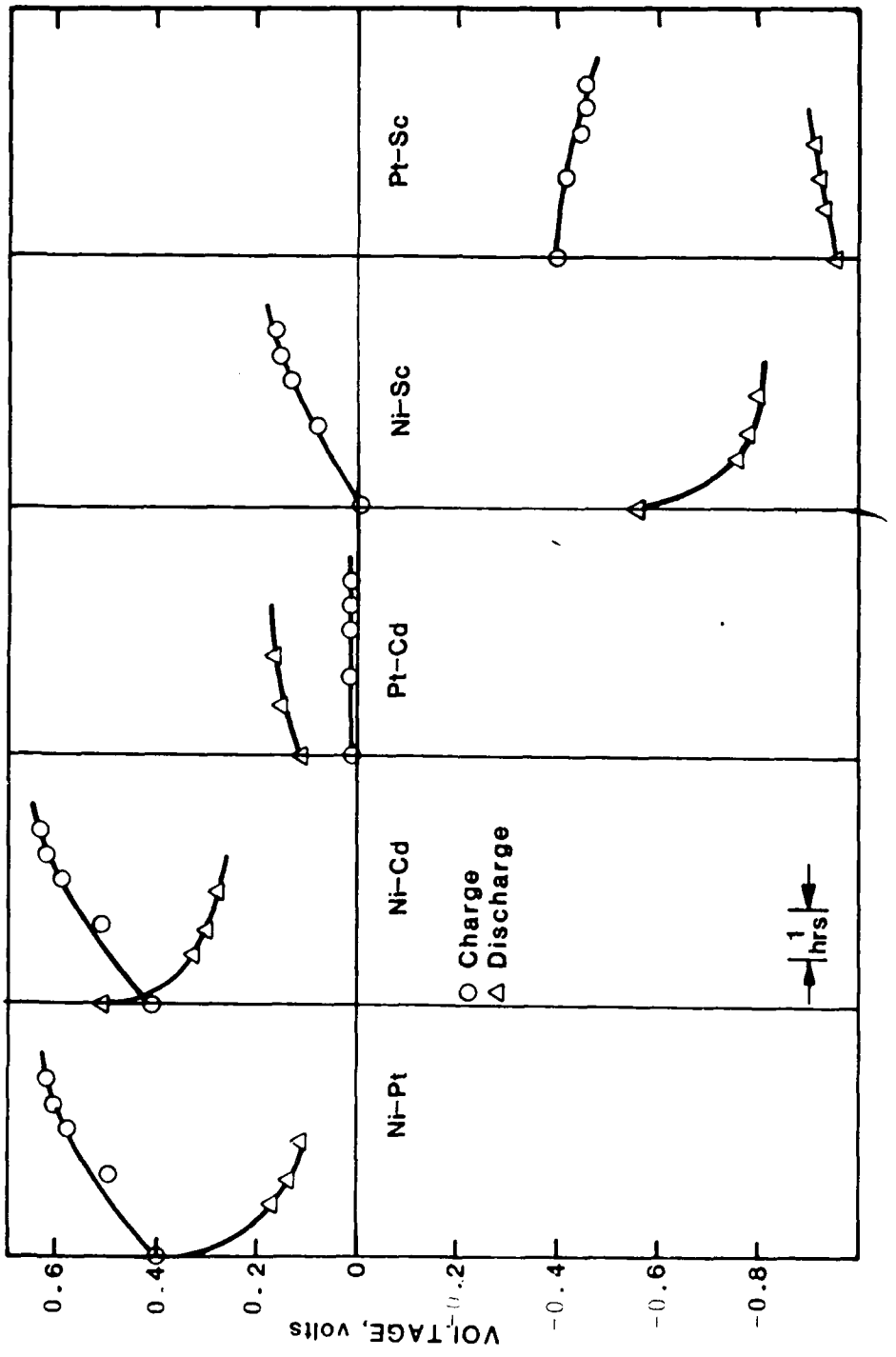

FIGURE 4.24 SINGLE ELECTRODE POTENTIALS-CELL 25, CYCLE 73

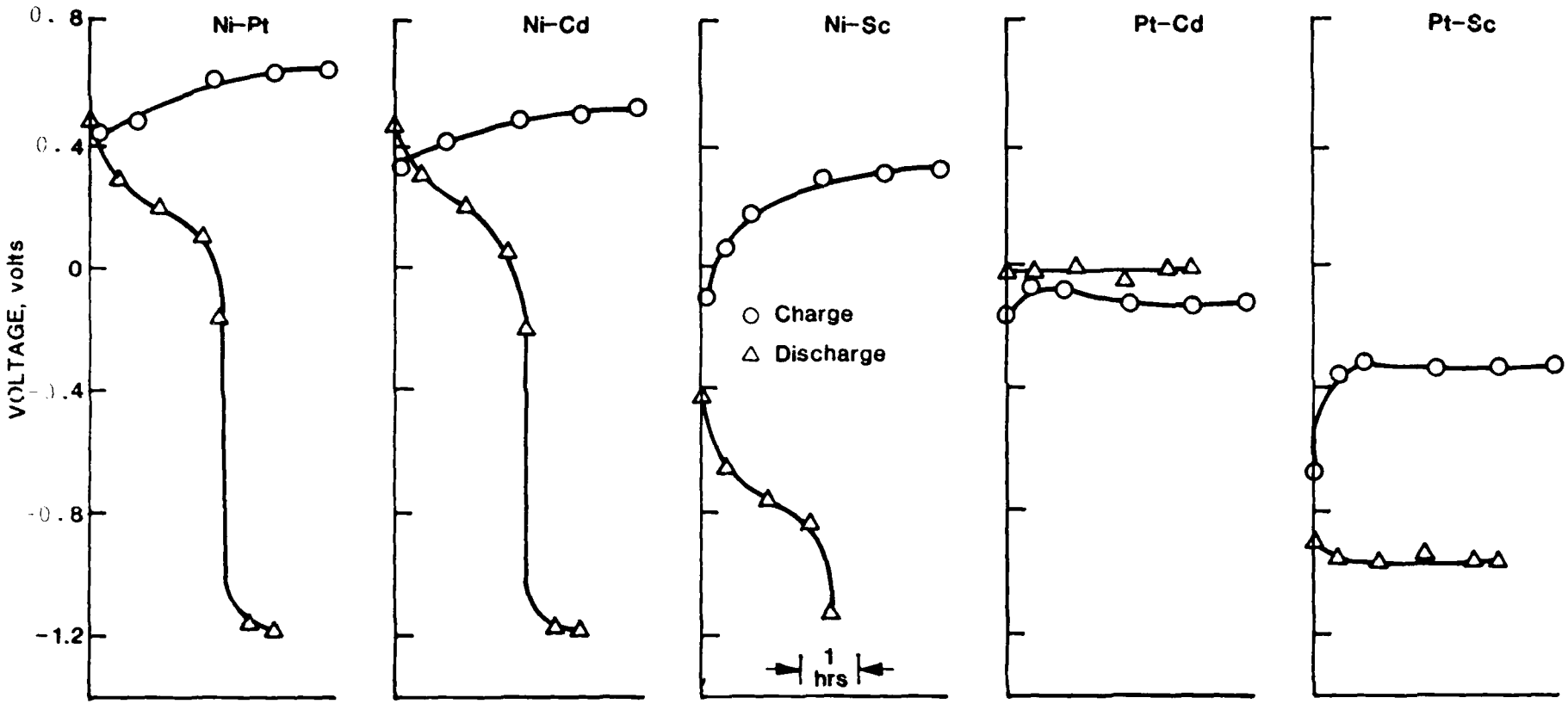

FIGURE 4.25 SINGLE ELETRODE POTENTIALS-CELL 41, CYCLE 736

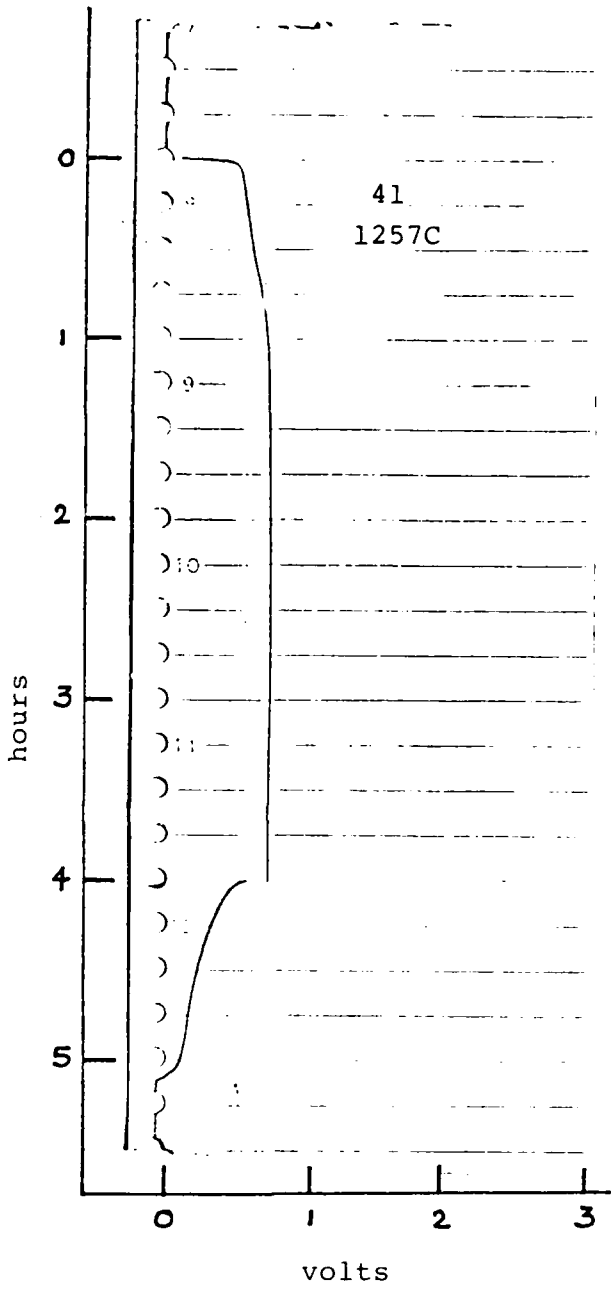

CHARGE, Ni vs Pt

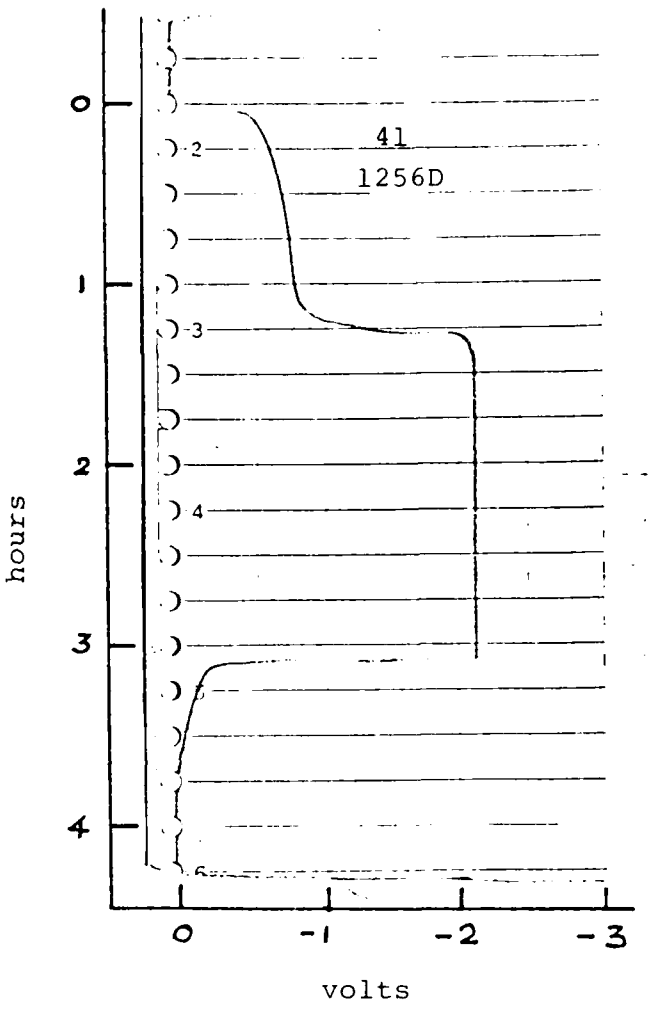

DISCHARGE, Ni vs SCREEN

FIGURE 4.26 Voltage Profile - Cell 41, Cycle 1257

and discharging cells alternately at constant current and fixed times; voltage and pressure profiles were monitored at regular intervals. cycling was interrupted periodically to monitor variations in pressure with changes in ambient temperature on an open-circuit stand. This ensured that the cells did not leak or exhibit electrochemical decay due to self-discharge on stand. Cells fabricated both with ERC roll-bonded and sintered nickel aircraft nickel electrodes were tested.

Cell 2: Life cycle tests commenced with one cell from the first batch. This cell was fabricated with ERC roll-bonded nickel electrode. The cycling regime was set at 4-1/2 and 3-1/2 hours for charge and discharge modes, respectively, and the current was kept constant at 100 mA in both cases. After 677 cycles, the cell did not exhibit any deterioration in performance. To accelerate the testing, the cycling regime was changed from cycle 678 such that the number of cycles per time period was doubled. By increasing the current by a factor of 2 and reducing the cycle time by half, the ampere hours were maintained the same. The old and new regimes were as follows:

Cycle Number	1-677	from 678
Charge - hours	4.50	2.25
mA	100	200
Ah	0.450	0.450
Discharge - hours	3.50	1.75
mA	100	200
Ah	0.350	0.350
Number of cycles/day	3	6

The voltage profiles of the old and new regimes are shown in Figure 4.27. As expected, the potentials increased during the new

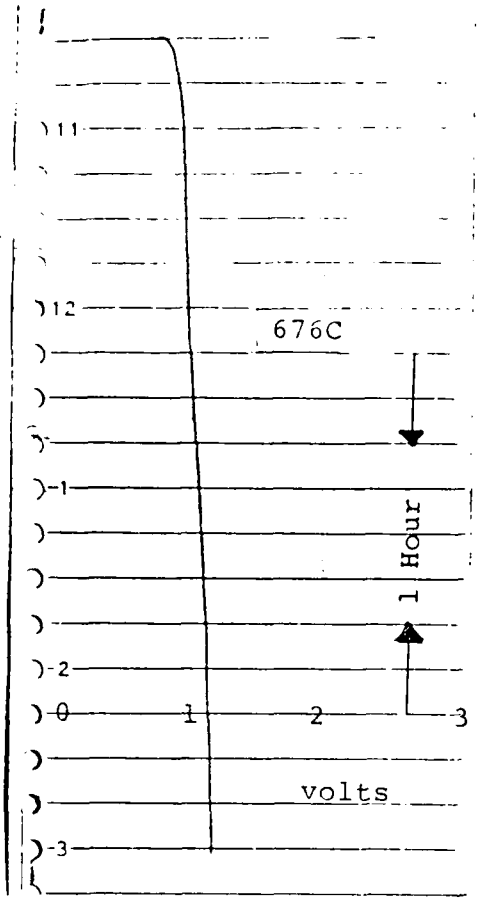

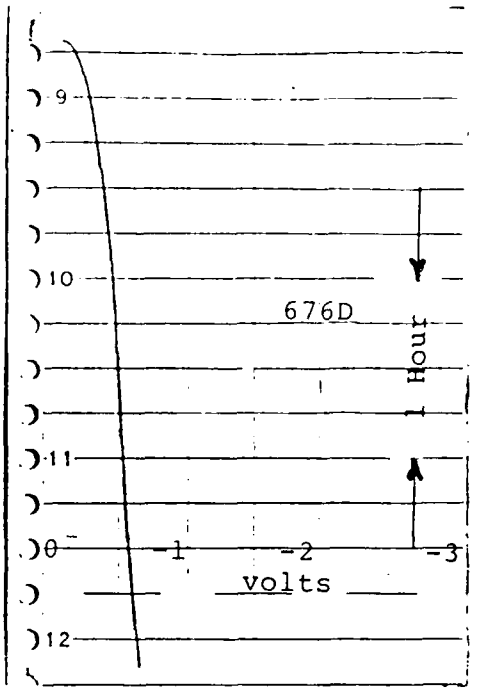

OLD REGIME

Charge: 4½ hrs @ 100 mA
Discharge: 3½ hrs @ 100 mA

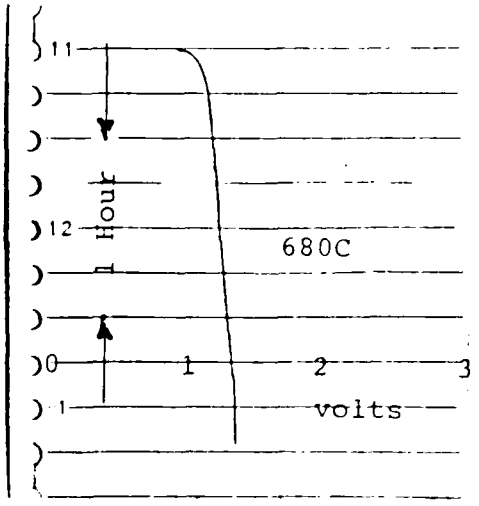

Charge, Ni/Pt

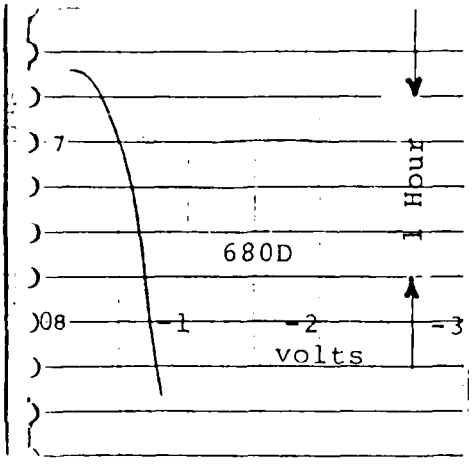

Discharge, Ni/Screen

NEW REGIME

CHARGE: 2¼ hrs @ 200 mA
DISCHARGE: 1-¾ hrs @ 200 mA

Figure 4.27. VOLTAGE PROFILE OF CELL 2

regime, owing to the higher operating current, and the change in pressure was not affected (Figures 4.28 and 4.29).

After the cycling regime was changed, the cell underwent another 200 cycles before failure. The voltage profile for cycle 883 is presented in Figure 4.30. Deterioration in performance is indicated by the erratic profile and the high values of potentials. In spite of this, the cell continued to exhibit excellent linearity in pressure (Figure 4.31).

The test was discontinued and the cell was cut open. Post-mortem showed that the integral structure of the electrode assembly remained intact. However, brownish colored liquid and brown deposits in the case were noticeable. The average values of voltage and pressure on cycling, and the standard deviation, are summarized in Table 4.9.

Initial test results indicated that the cells can be subjected to continuous charge-discharge cycles for extended periods; e.g., Cell 2 was cycled over 800 times over 7 months and was still capable of delivering the required capacity.

Cell 26: After completing cell characterization tests (paragraph 4.1) Cell 26 was next subjected to life cycle tests. Life testing of the cell on alternate charge/discharge modes was started in the following regime:

Charge:	2-1/4 hrs. at 225 mA, 0.506 Ah
Discharge:	1-3/4 hrs. at 225 mA, 0.394 Ah
Nominal Capacity:	0.450 Ah
Overcharge per Cycle:	12% over nominal capacity 28% over delivered capacity
Depth of Discharge:	88% of nominal capacity
Charge/Discharge Rates:	C/2

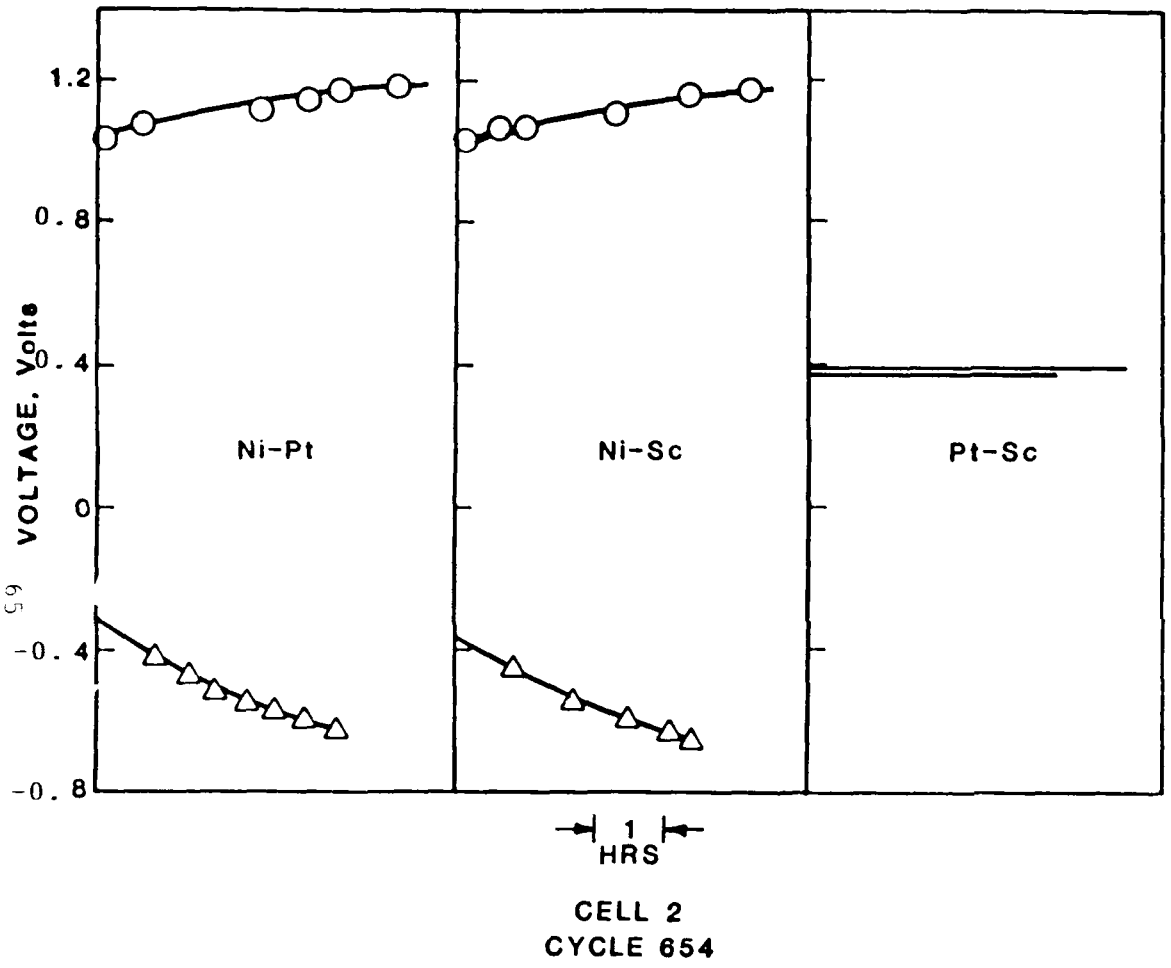

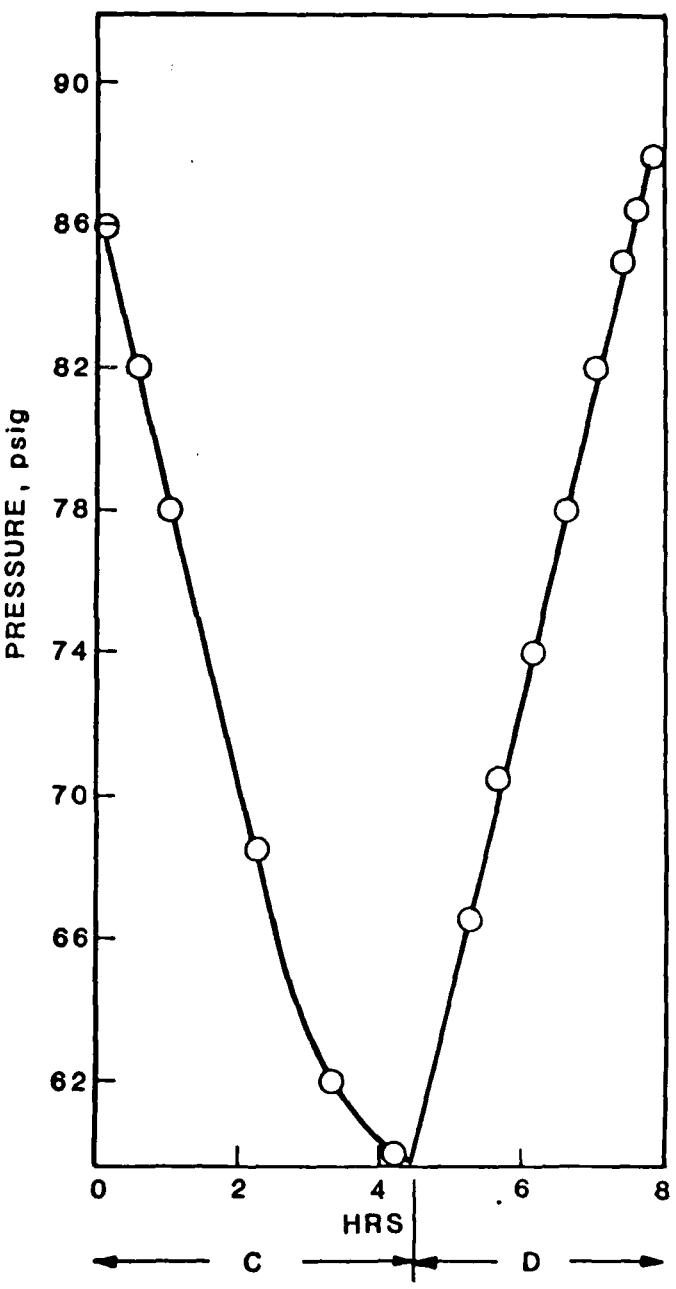

FIGURE 4.28 CELL PERFORMANCE IN OLD CYCLING REGIME

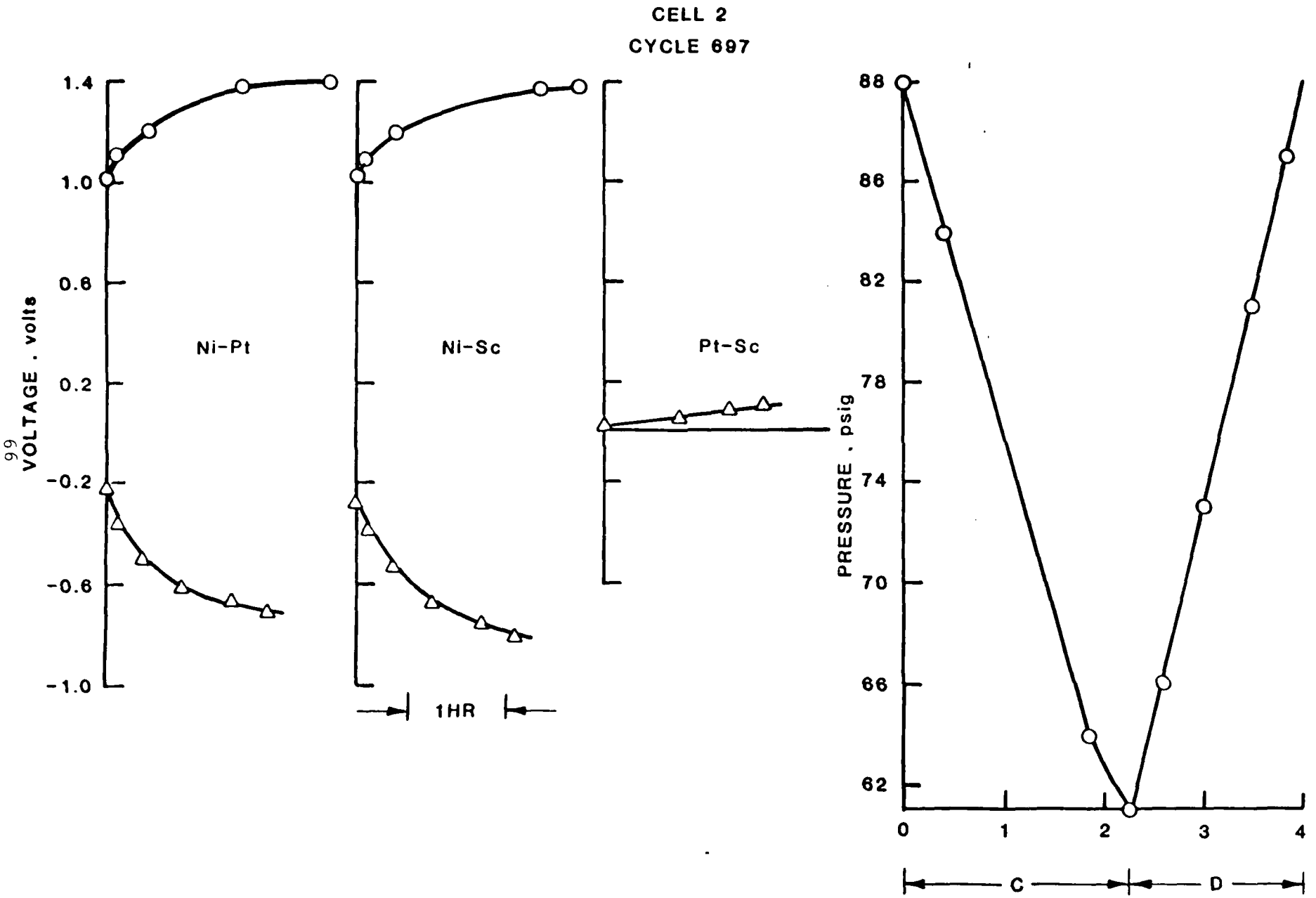

FIGURE 4.29 CELL PERFORMANCE IN THE NEW CYCLING REGIME

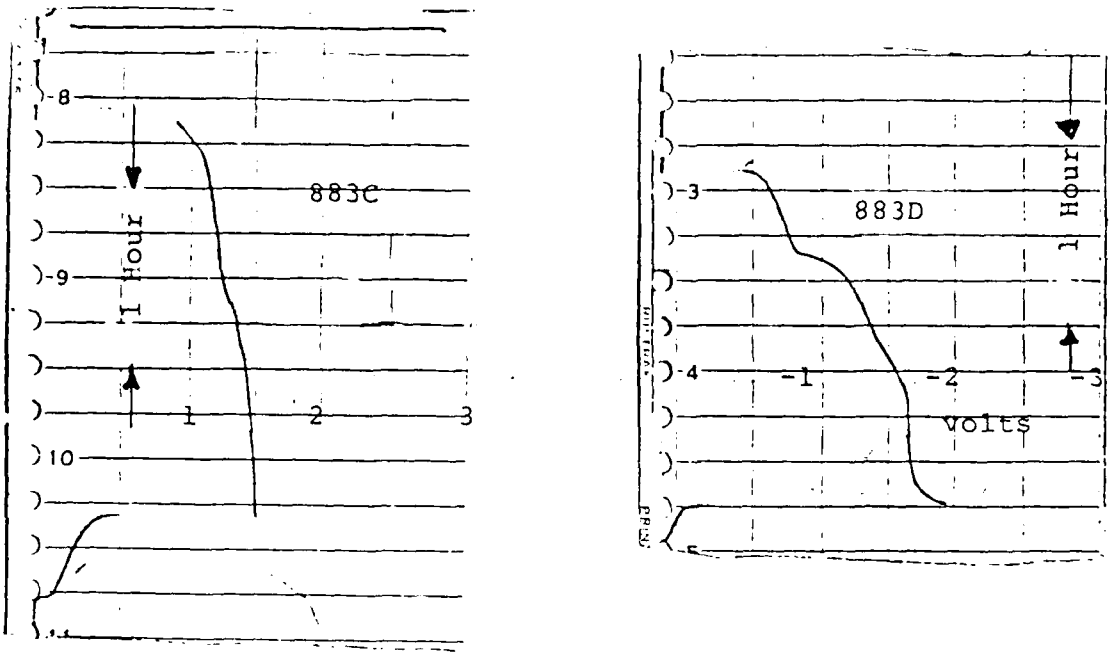

Charge - Ni-Pt

Discharge, Ni-Screen

FIGURE 4.30 VOLTAGE PROFILE - CELL 2, CYCLE 883

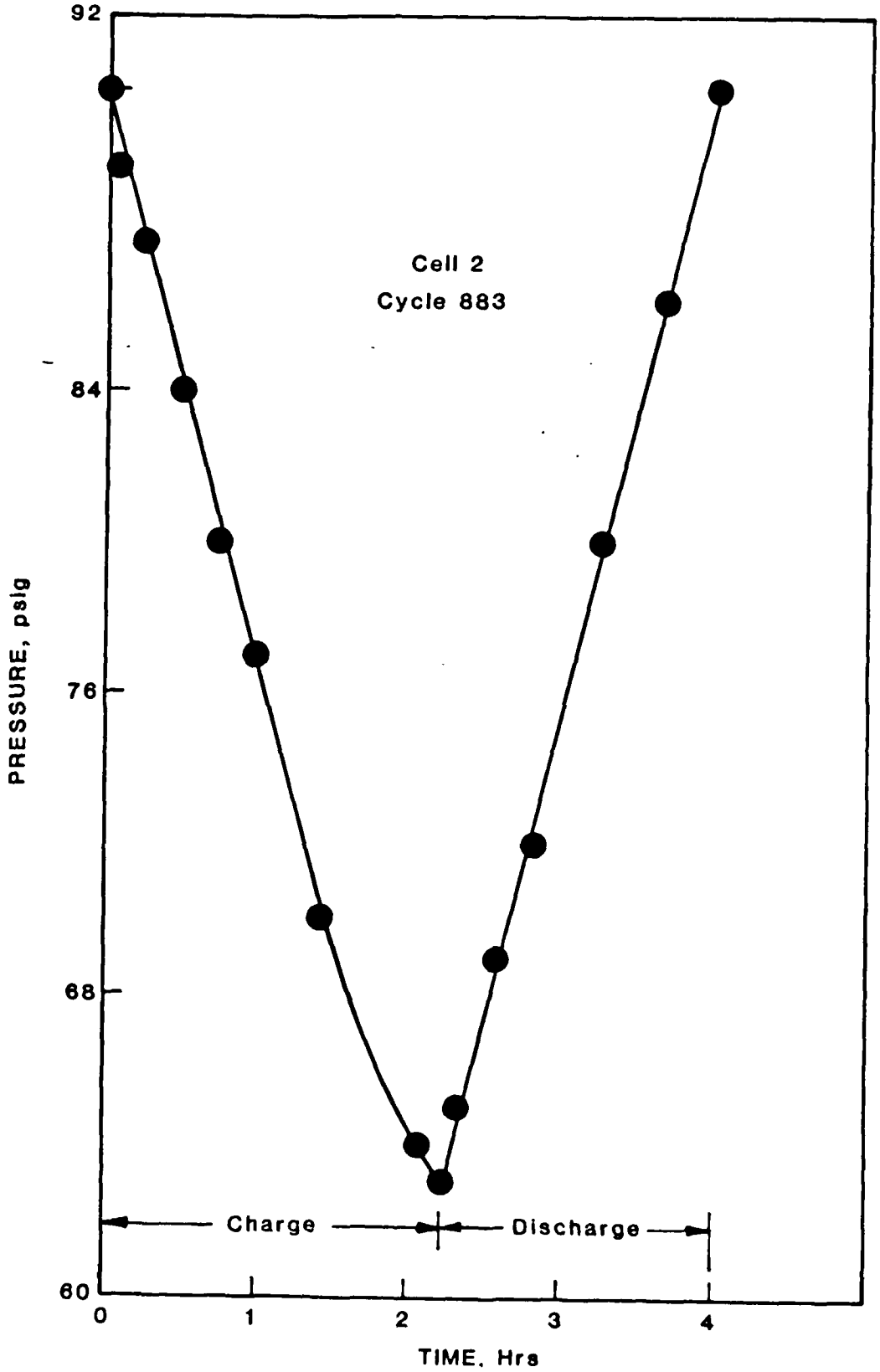

FIGURE 4.31 PRESSURE PROFILE CELL 2, CYCLE 883

TABLE 4.9

CELL PARAMETERS ON LIFE CYCLE

Cell No.: 2
Ni Positive: ERC roll-bonded

Cycle No.: 1-677 from 678
Cycle Time: 6.75 hours 4.00 hours
Charge: 4.50 hours 2.25 hours
Discharge: 2.25 hours 1.75 hours

CYCLE NO.	CHARGE V, Ni-Pt Avg.	End	ΔP	DISCHARGE V, Ni-Sc. Avg.	End	ΔP
342	0.553	-	23	-	-	23
405	0.683	-	25	-0.617	-	24
450	0.939	-	24	-0.616	-	24
545	1.217	1.140	25	-0.576	-0.650	21
597	1.145	1.187	27	-0.625	-0.683	28
654	1.110	1.176	26	-0.565	-0.646	21
$\bar{x}$	0.941	1.1677	24.8	-0.600	-0.660	23.5
σ	0.2696	0.0246	1.4720	0.0273	0.0203	2.5884
697	1.229	1.350	28	-0.609	-0.800	29
883	1.199	1.500	29	-1.296	-1.950	30

This cell was tested for cycle life at a higher operating current of 225 mA. Though the cell functioned normally, the potentials during discharge were high because of the higher current density and depth of discharge. The current was accordingly reduced to 150 mA which resulted in more acceptable values of operating parameters.

The voltage and pressure profiles for cycles 493 are shown in Figure 4.32. The high polarization of nickel on discharge seems to indicate deterioration of the nickel electrode. Currently, cycling is being continued and the cell is being monitored to check for stabilization or failure.

Summary of the life cycle data and statistical analysis for standard deviation are given in Table 4.10.

Though the discharge potential was high, the relationship between state of charge and pressure continued to be good (Figure 4.33, cycle 763). The tests were terminated after 800 cycles.

Cell 21: This cell was built using a sintered nickel electrode from commercial aircraft battery manufactured by SAFT. Life cycle tests were started in November 1984 and terminated in June 1986 when the cell failed. Cell voltages (nickel vs. platinum during charge, nickel vs. screen during discharge) and pressure were monitored at regular intervals. After about 450 cycles the polarization did not affect the relationship between cell pressure and the state of charge of the nickel electrode. The cell continued to exhibit the same characteristics - increased polarization towards end of discharge, levelling of pressure towards the end of charge and a linear relationship between state of charge and cell pressure - for 1,900 cycles.

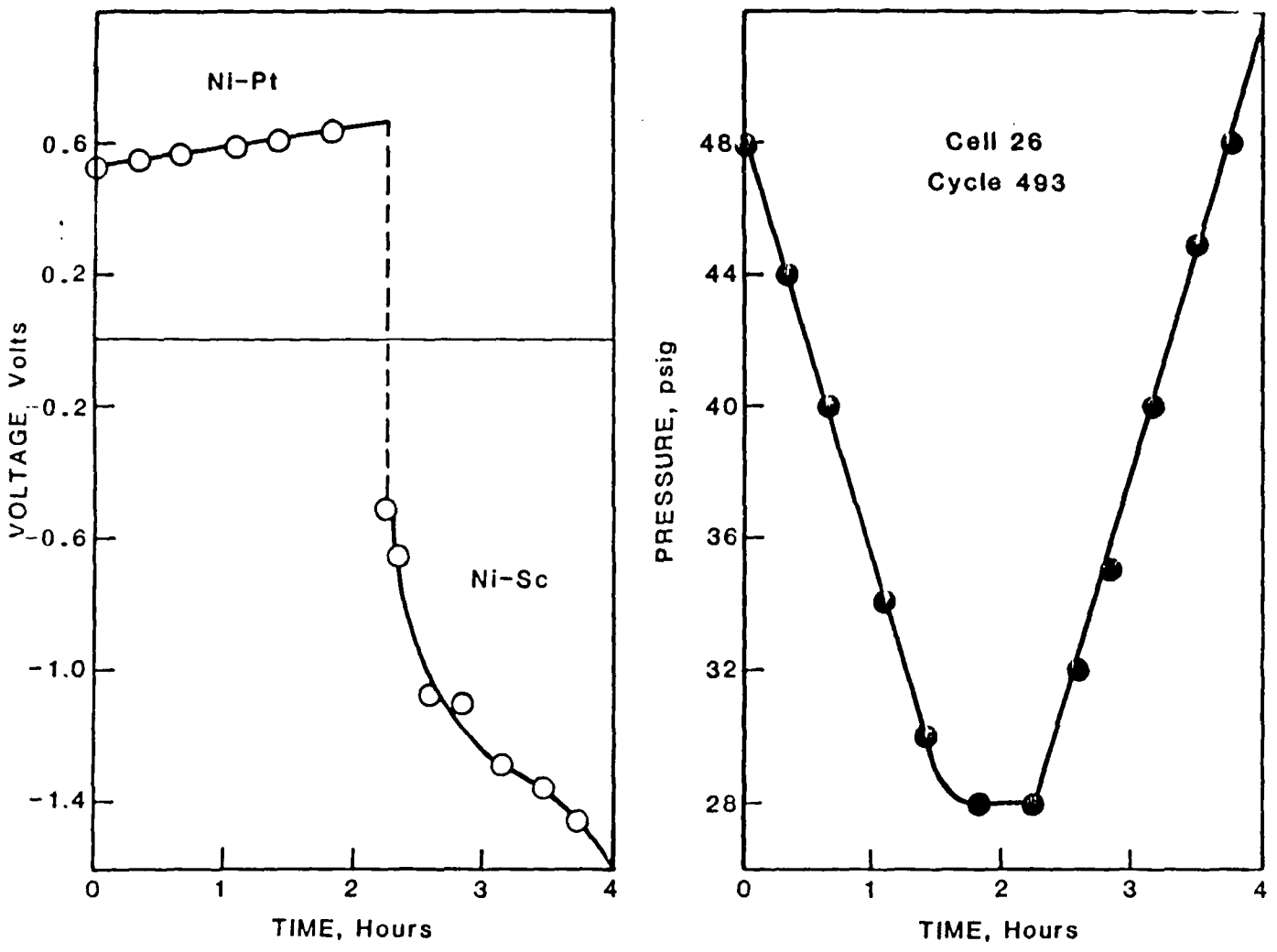

FIGURE 4.32. VOLTAGE AND PRESSURE PROFILES-CELL 26, CYCLE 493

TABLE 4.10

CELL PARAMETERS ON LIFE CYCLE

Cell No.: 26
Ni Positive: ERC roll-bonded

Cycle Time: 4 hours
Charge: 2-1/4 hours
Discharge: 1-3/4 hours

CYCLE NO.	I mA	CHARGE V, Ni-Pt Avg.	End	ΔP	DISCHARGE V, Ni-Sc. Avg.	End	ΔP
5	225	0.614	0.716	34	-0.836	-1.025	35
29	225	0.600	0.700	33	-0.763	-0.985	34
132	225	0.693	0.720	33	-0.872	-1.110	34
$\bar{x}$		0.636	0.712	33.3	-0.824	-1.040	34.3
σ		0.0501	0.0106	0.5774	0.0555	0.0638	0.5774
245	150	0.589	0.660	22	-0.866	-1.150	26
324	150	0.609	0.660	23	-0.862	-1.100	22
493	150	0.606	0.660	22	-1.251	-1.590	22
$\bar{x}$		0.601	0.660	22.3	-0.993	-1.280	23.2
σ		0.0108	0	0.1119	0.2234	0.2696	2.309

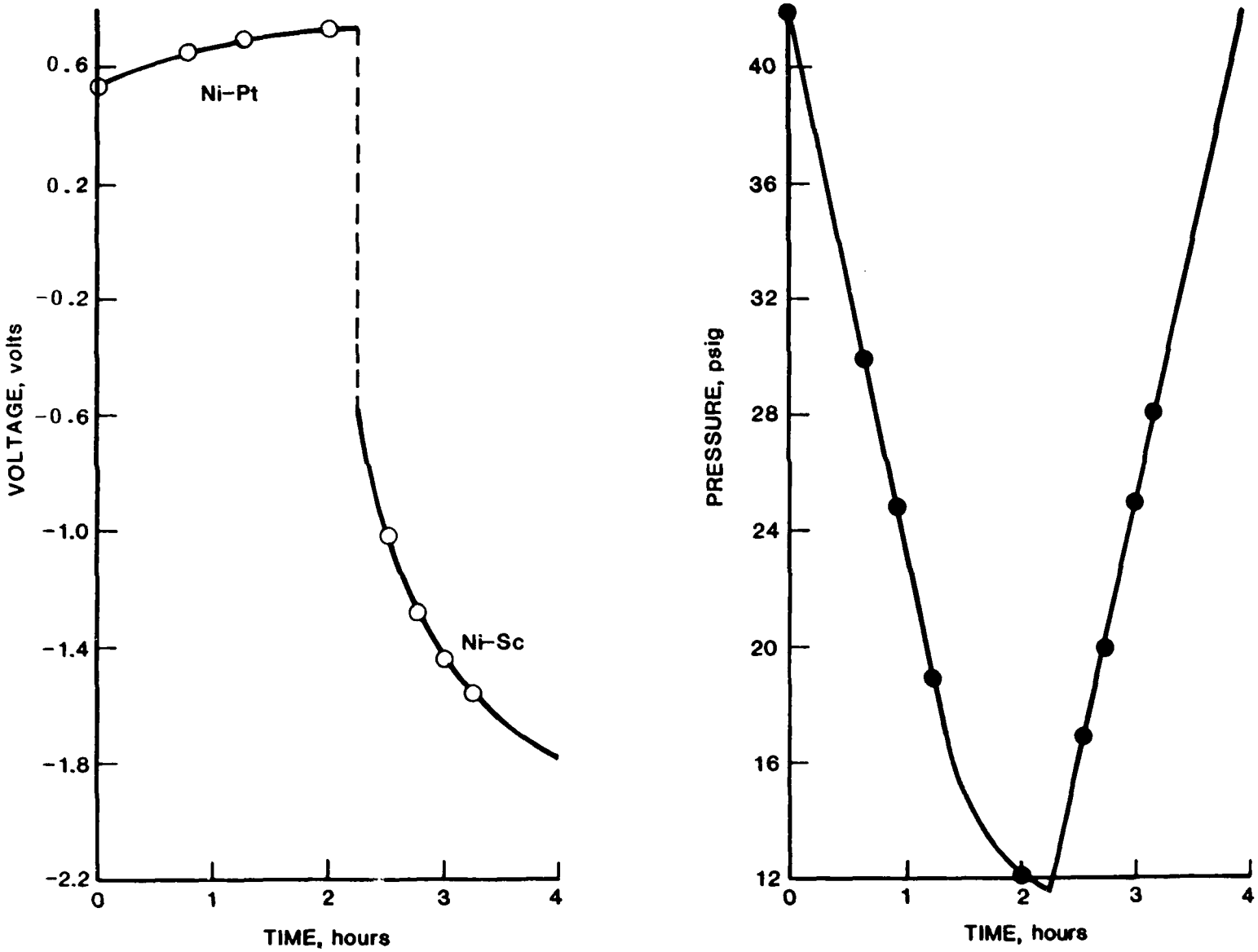

FIGURE 4.33 PERFORMANCE CHARACTERISTIC CELL 26, CYCLE 763

The data on cycling up to cycle 838 are summarized in Table 4.11.

During cycle 1919, a marked change in the voltage profile was noticed; the rapid increase in voltage towards the end of discharge did not occur. In addition, the change in pressure during charge and discharge had dropped to 8 psig from a norm of 20. This indicates that the cell had lost its activity and ability to perform as required. Tests were continued for another 100 cycles to confirm that the cell's loss in activity was irreversible. This was found to be true and the tests were terminated. The changes in the voltage profile during discharge are apparent from Figures 4.34 and 4.35. Figure 4.36 shows the corresponding changes in pressure profile.

Representative data of the performance characteristics of Cell 21 are shown in Figures 4.37 through 4.45.

After terminating the tests, a failure analysis of the cell was performed. Note that these are the longest lifetime tests performed on a single nickel oxygen cell. The cell was cycled over 2,000 times and including shutdown time, the cell was on test for 20 months.

The cell was carefully cut open and no defects such as dry-out, shedding of nickel or corrosion were noticeable. It appears that failure was caused by loss in electrochemical activity of the nickel electrode.

The nickel electrode was carefully removed and SCM photographs were taken. For purposes of comparison, photographs of a fresh electrode were taken at the same magnifications (Figures 4.46

TABLE 4.11

CELL PARAMETERS ON LIFE CYCLE

Cell No. 21
Ni Positive: Sintered, Saft

Cycle Time: 6 Hours
Charge: 3-1/2 hours
Discharge: 2-1/2 hours
Current: 100 mA

CYCLE NO.	CHARGE V, Ni-Pt Avg.	End	ΔP	DISCHARGE V, Ni-Sc. Avg.	End	ΔP
47	0.716	0.853	19	-0.736	-	19
100	0.768	0.850	18	-0.692	-0.825	18
192	0.725	0.850	17	-0.759	-0.900	17
265	0.830	0.935	19	-0.690	-	19
334	0.845	0.960	19	-0.708	-0.880	19
404	0.894	0.970	19	-0.623	-1.480	19
562	0.898	1.025	-	-0.709	-2.050	-
697	0.931	0.900	19	-0.605	-2.050	21
750	0.967	1.050	-	-0.970	-2.050	-
838	0.924	1.000	19	-0.638	-2.050	19
$\bar{x}$	0.850	0.939	18.6	-0.713	-1.535	18.9
	0.0886	0.0742	0.7440	0.1028	0.5856	1.1260

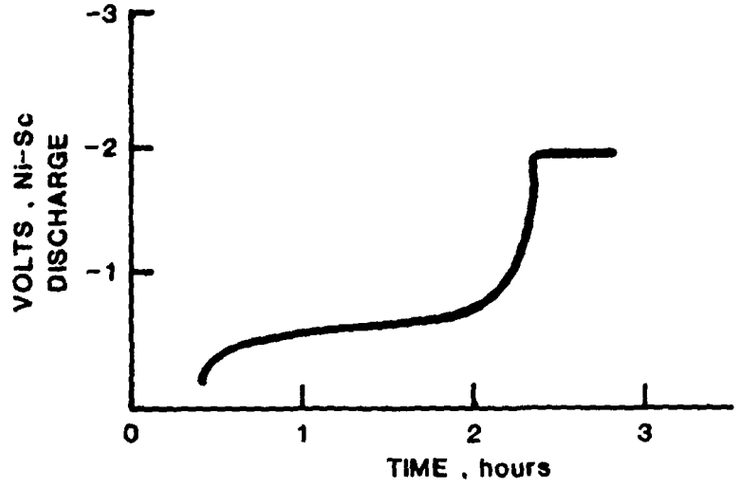

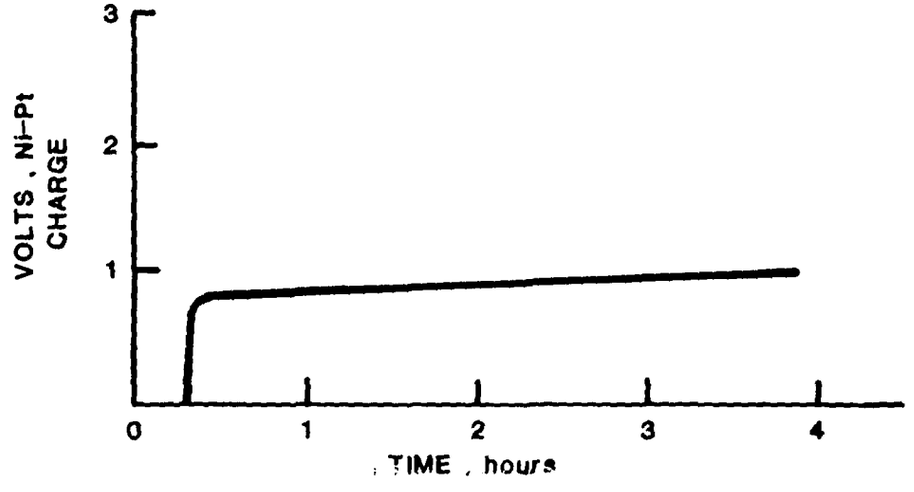

FIGURE 4.34. VOLTAGE PROFILE CELL 21 CYCLE 1766

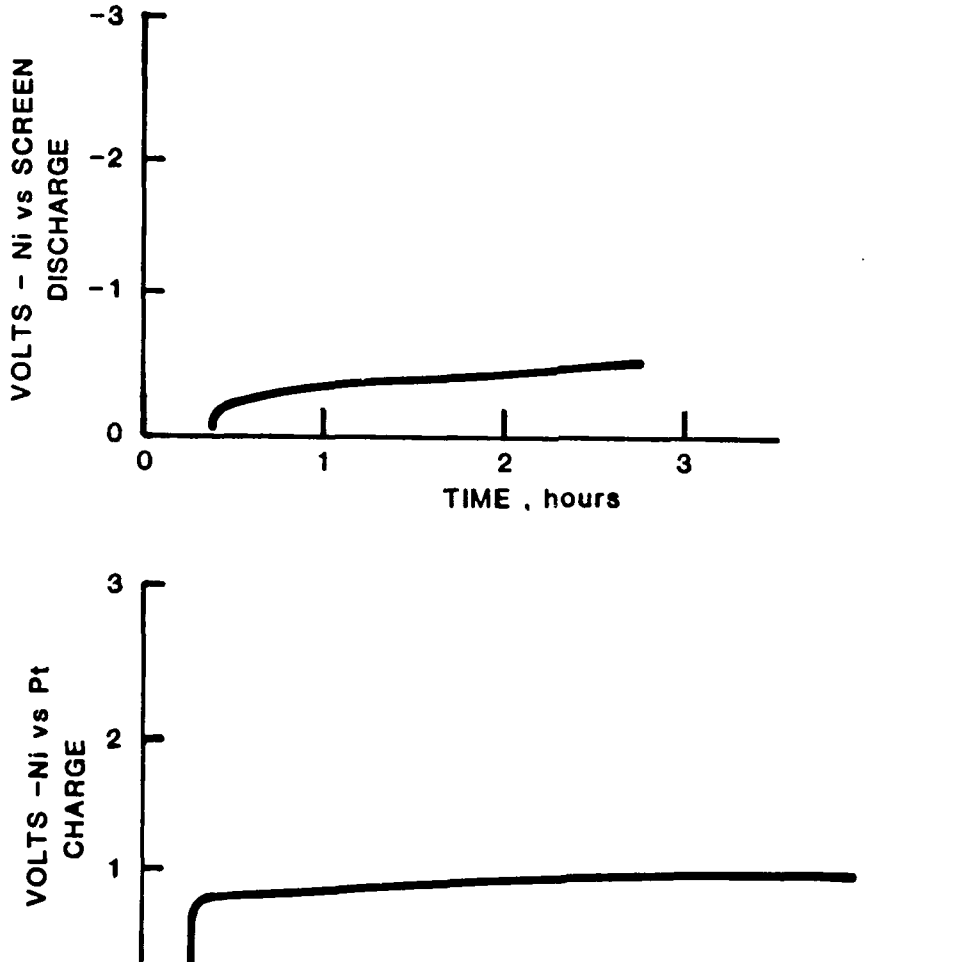

FIGURE 4.35 VOLTAGE PROFILE CELL 21 - CYCLE 1919

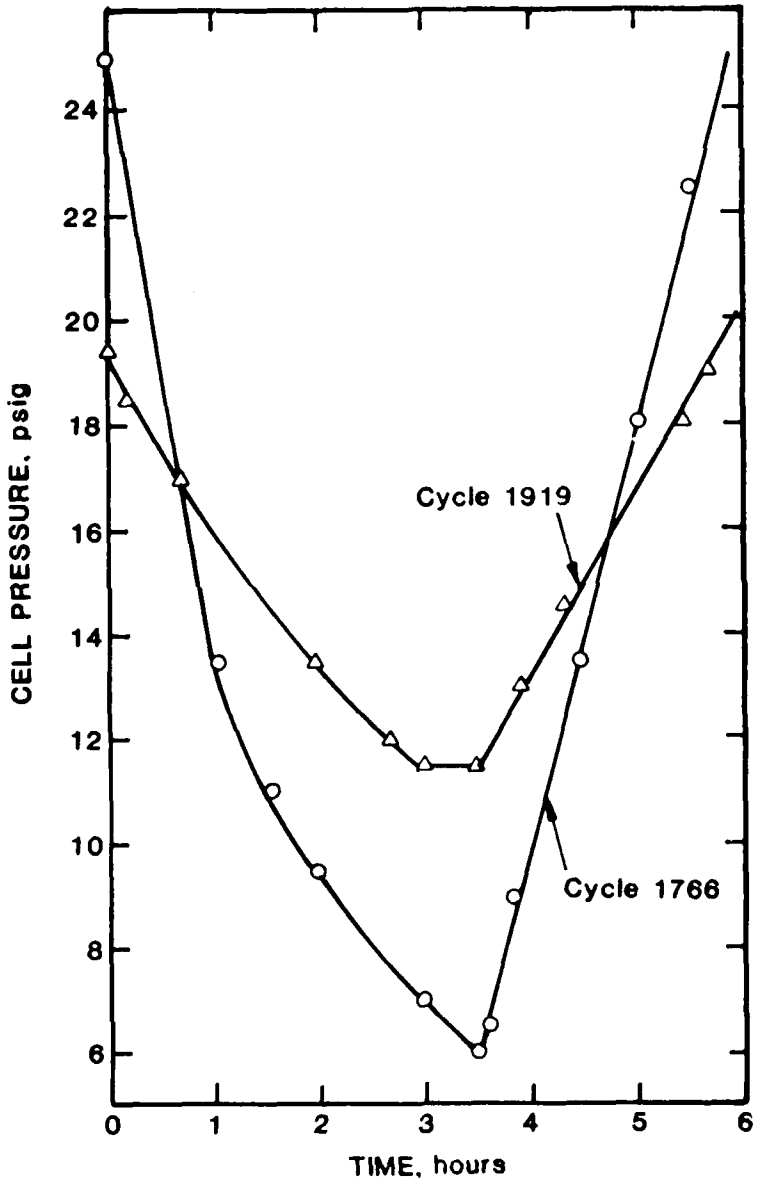

FIGURE 4.36 COMPARISON OF PRESSURE PROFILES-CELL 21

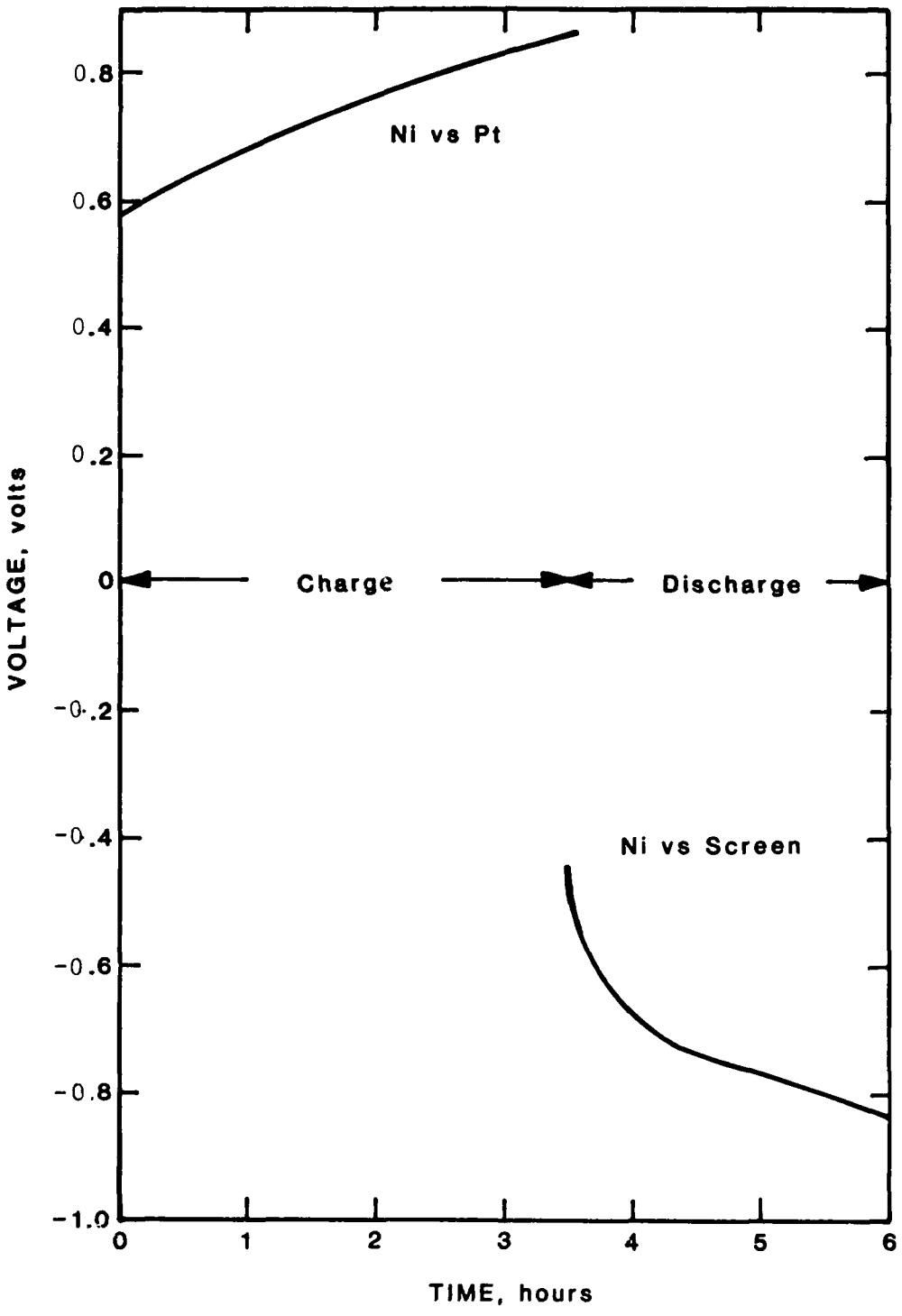

FIGURE 4.37 VOLTAGE PROFILE-CELL 21, CYCLE 100

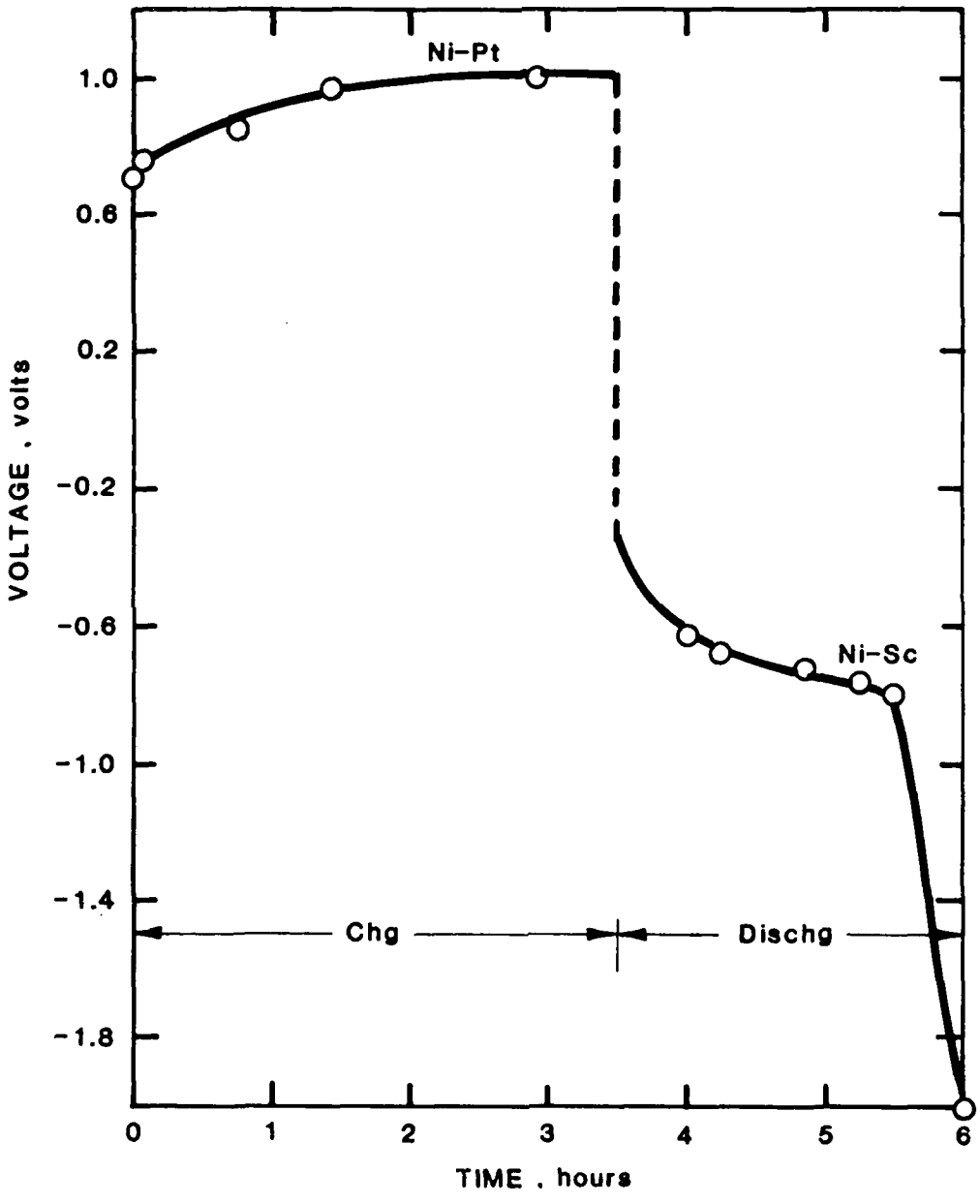

FIGURE 4.38 VOLTAGE PROFILE - CELL 21, CYCLE 562

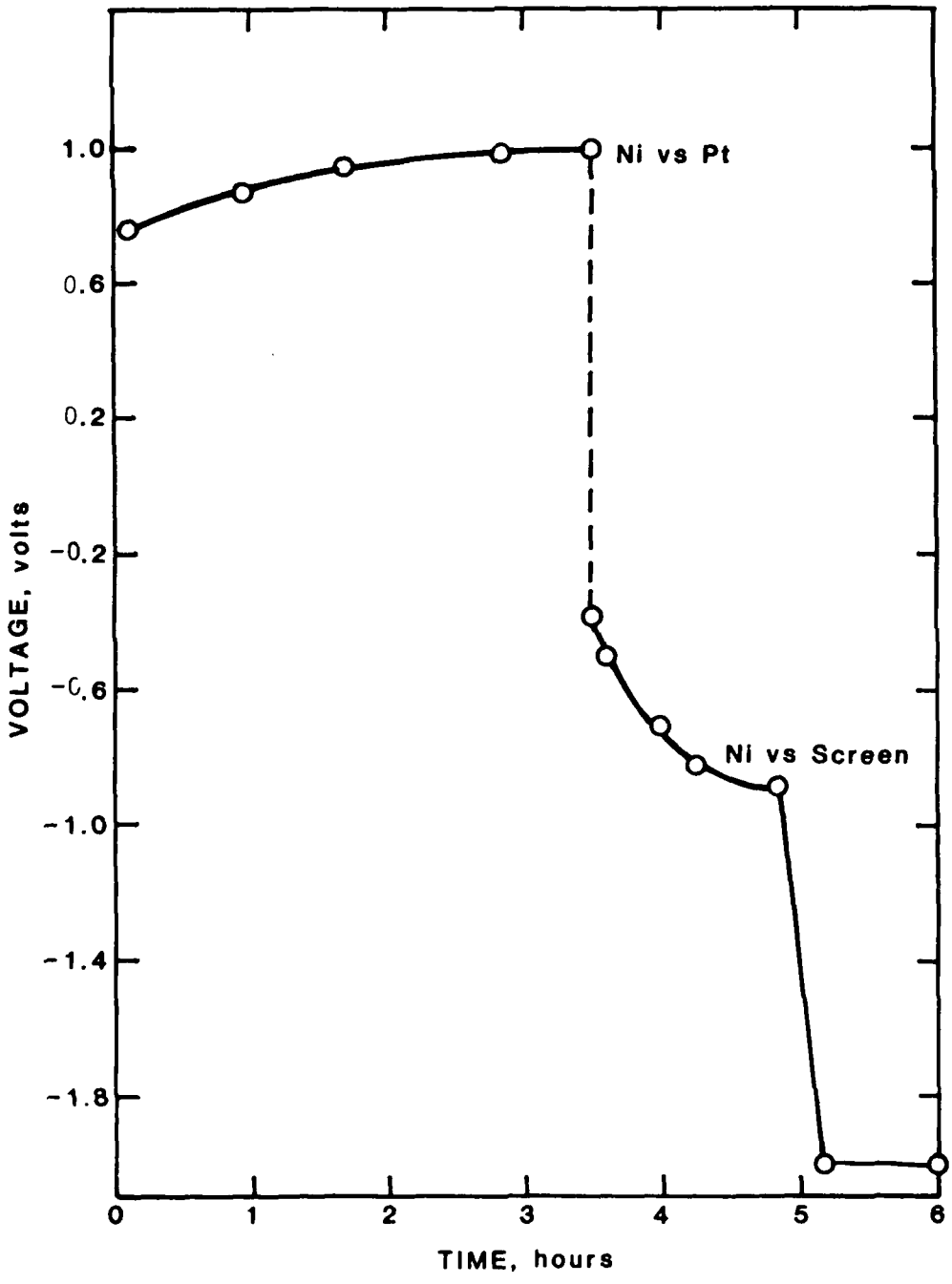

FIGURE 4.39 VOLTAGE PROFILE-CELL 21, CYCLE 1060

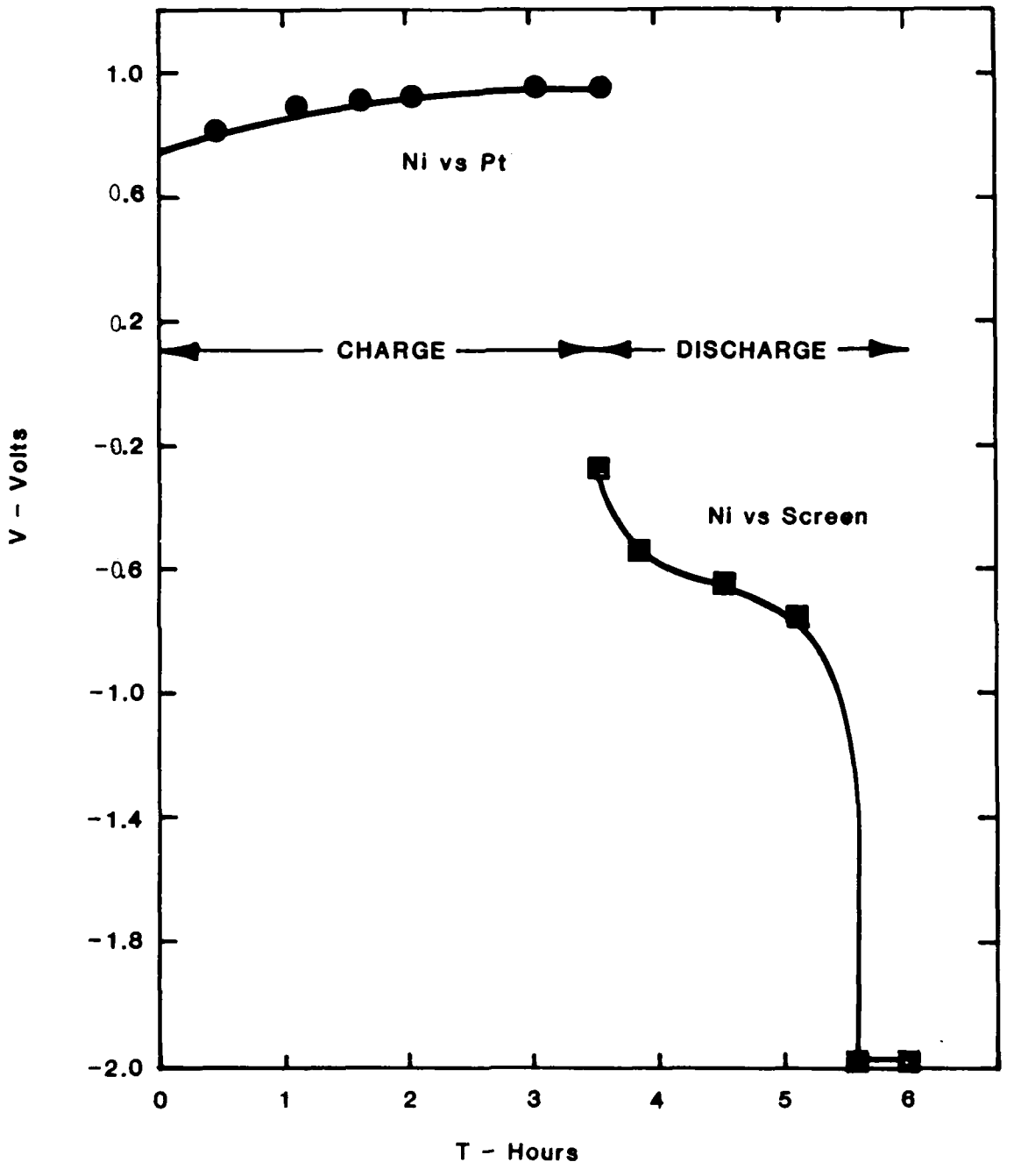

Fig. 4.40 Voltage Profile -Cell 21, Cycle 1764

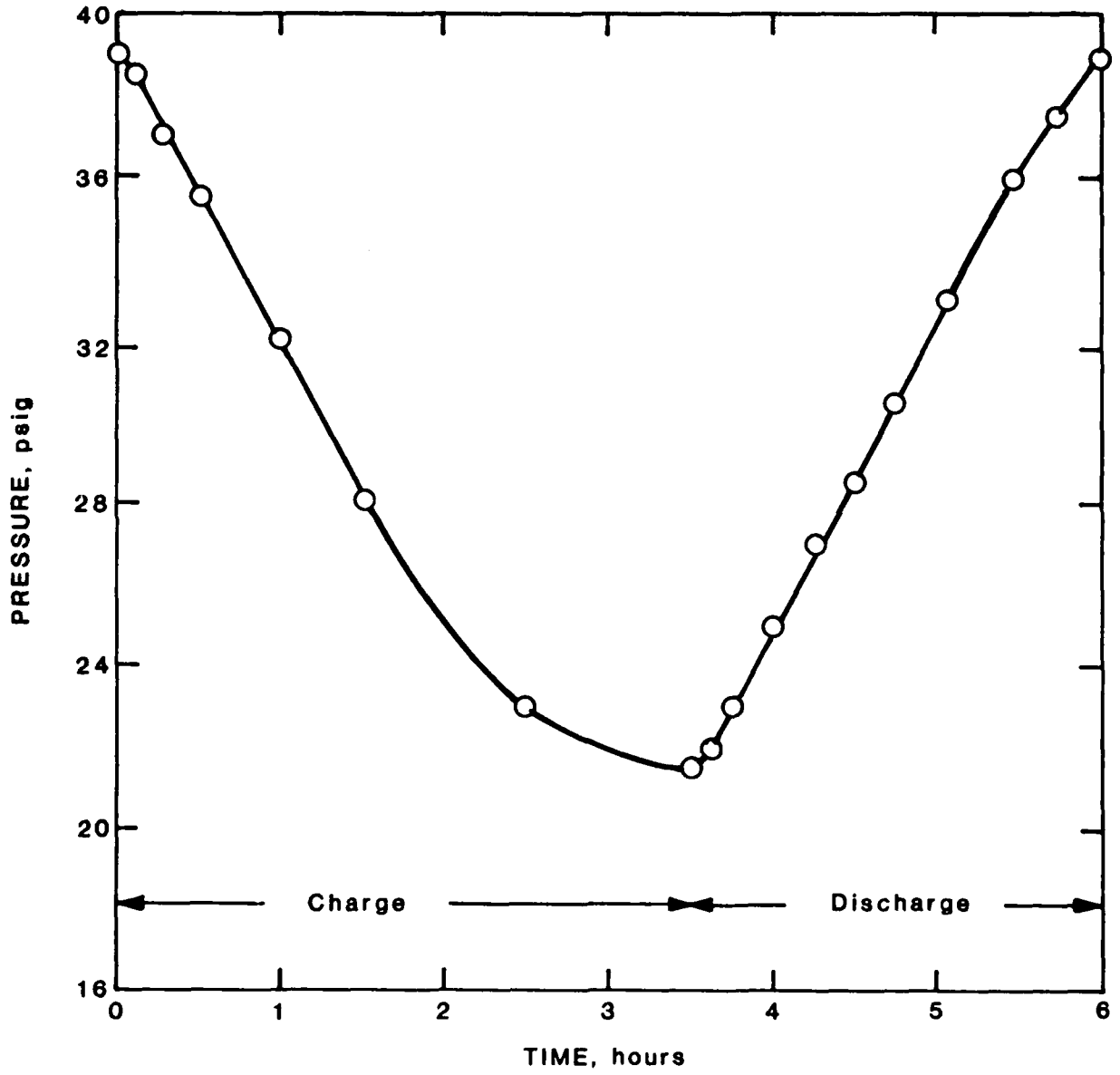

FIGURE 4.41 PRESSURE PROFILE, CELL 21, CYCLE 47

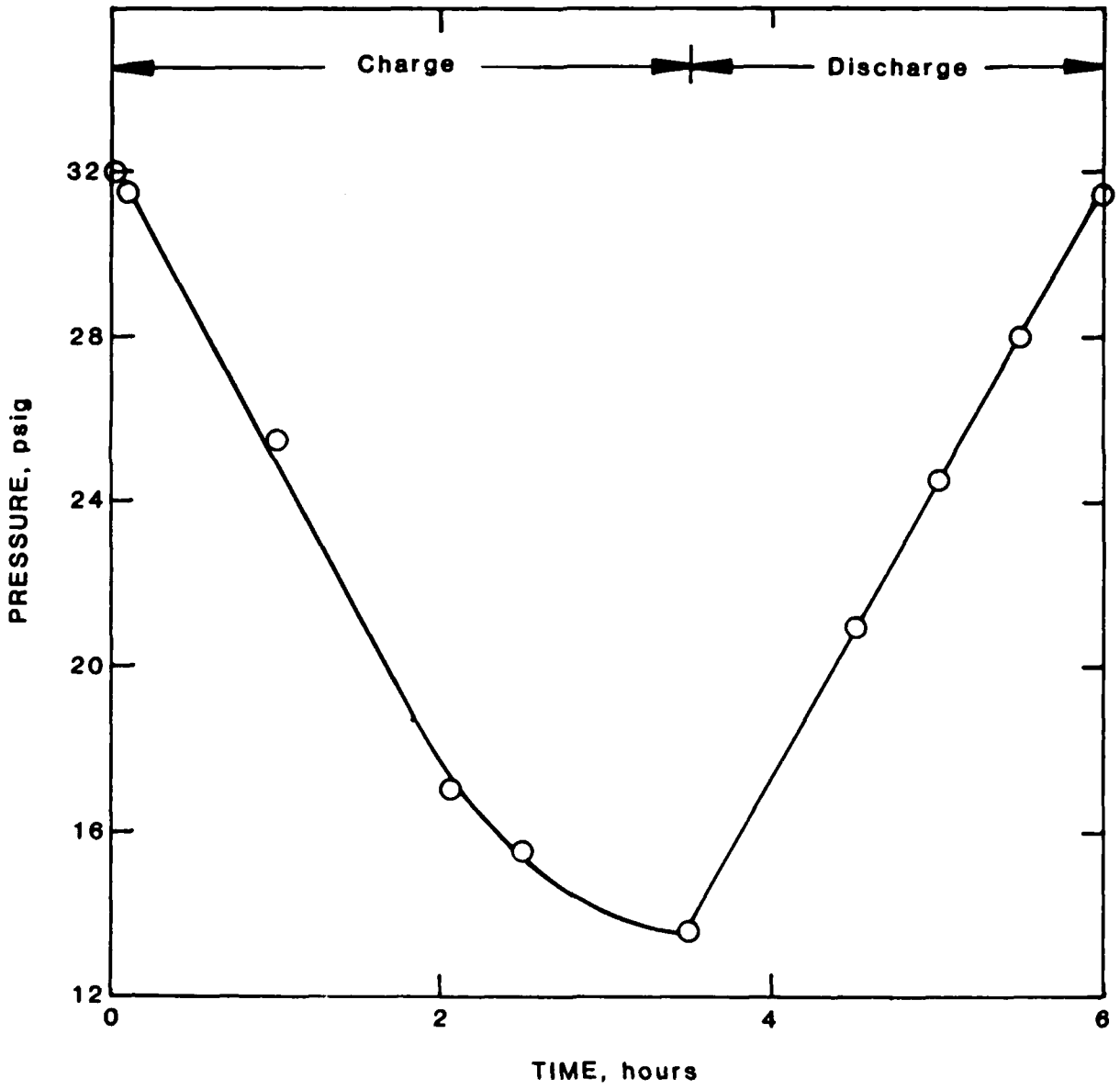

FIGURE 4.42 PRESSURE PROFILE-CELL 21, CYCLE 334

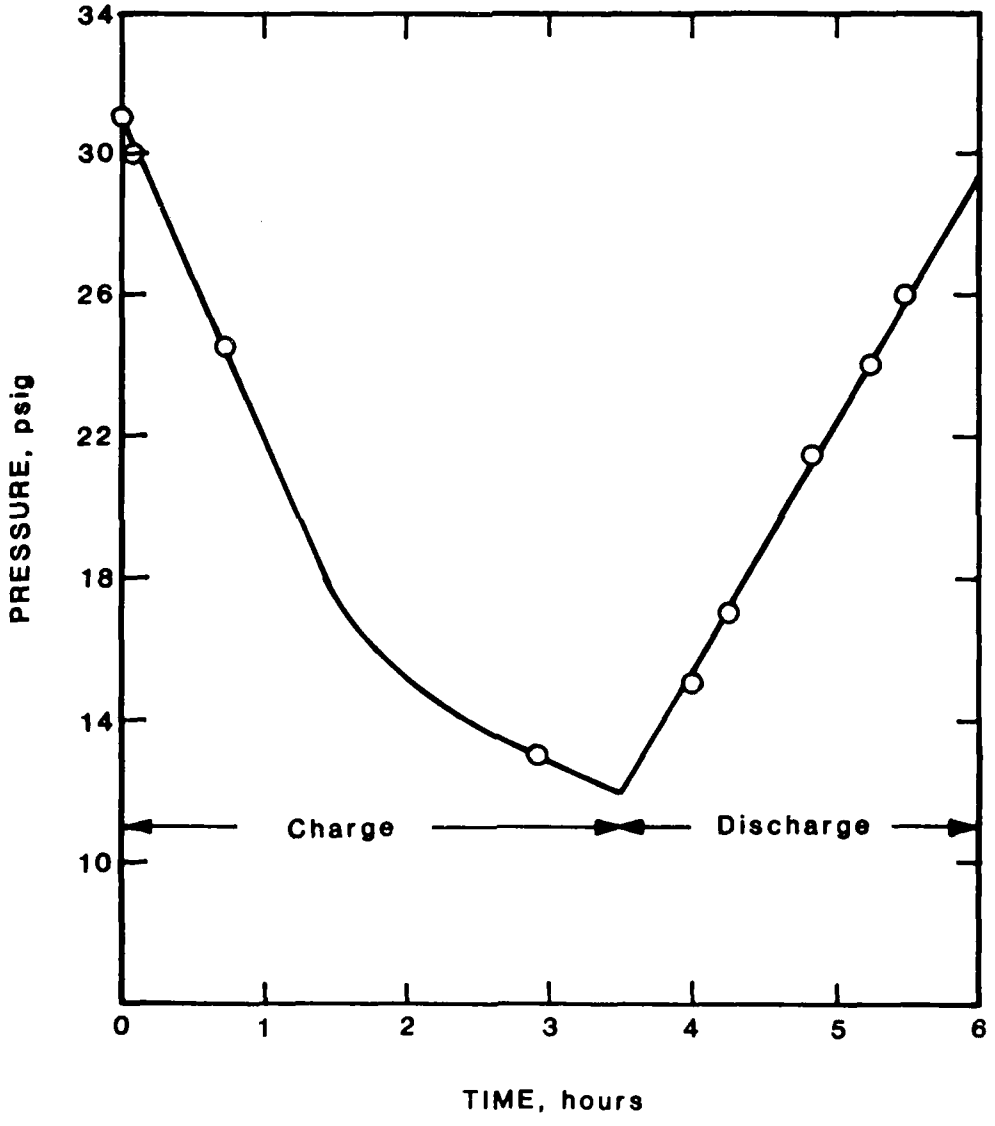

FIGURE 4.43 PRESSURE PROFILE-CELL 21, CYCLE 562

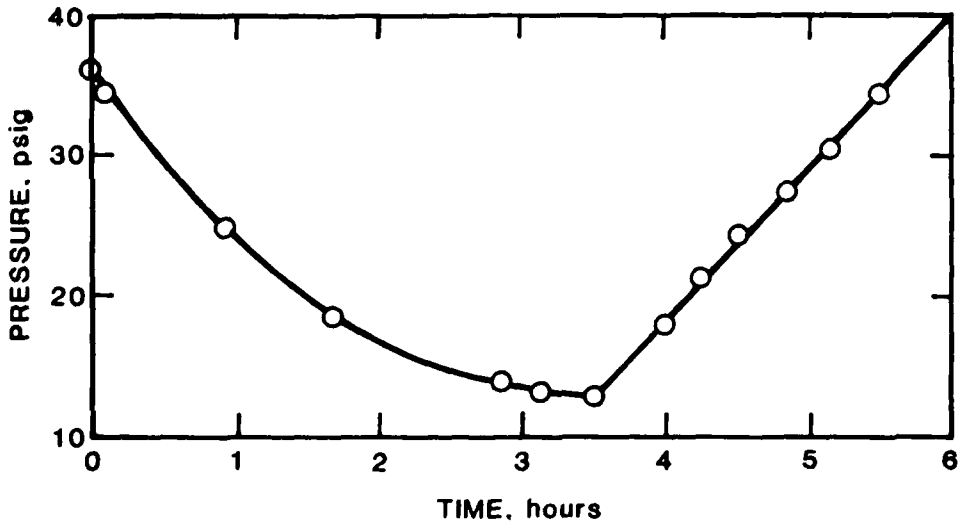

FIGURE 4.44 PRESSURE PROFILE, CELL 21, CYCLE 1060

AD-A194 979 AIRCRAFT BATTERY STATE OF CHARGE AND CHARGE CONTROL SYSTEM(U) ENERGY RESEARCH CORP DANBURY CT S VISWANATHAN ET AL. JAN 88 AFWAL-TR-87-2088 2/2

UNCLASSIFIED F33615-84-C-2435 F/G 10/2 NL

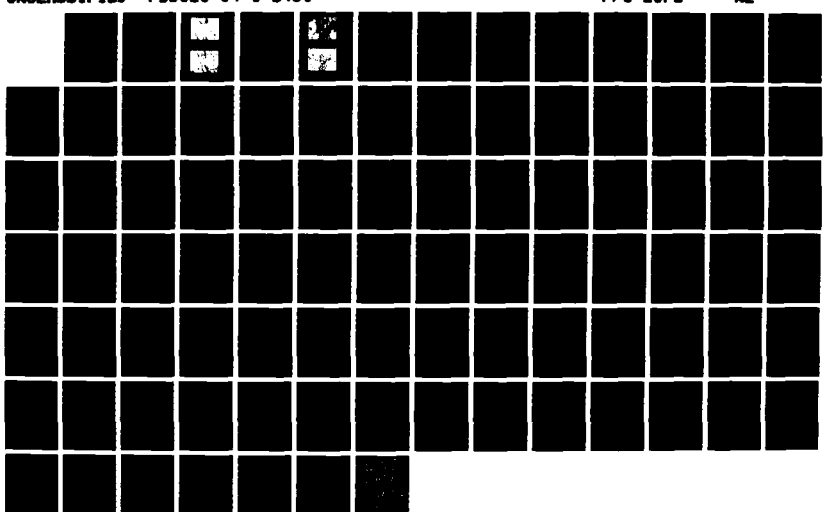

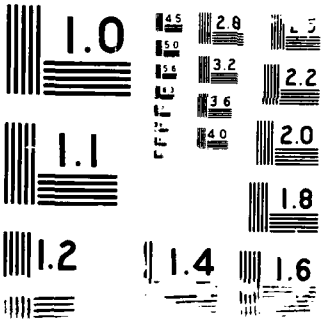
1.0
1.1
1.2
1.4
1.6
2.0
2.2
1.8

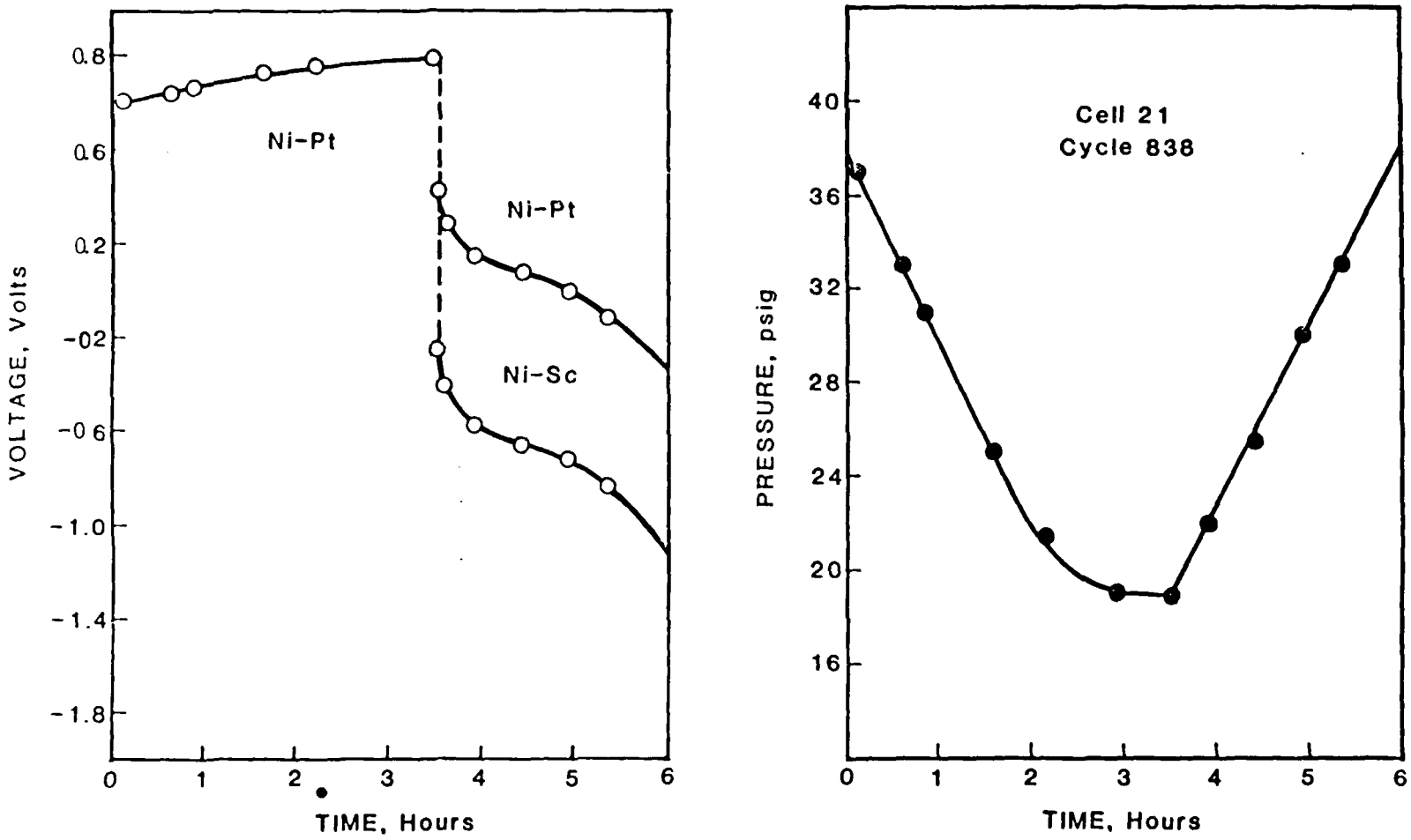

FIGURE 4.45 PRESSURE PROFILE-CELL 21, CYCLE 838

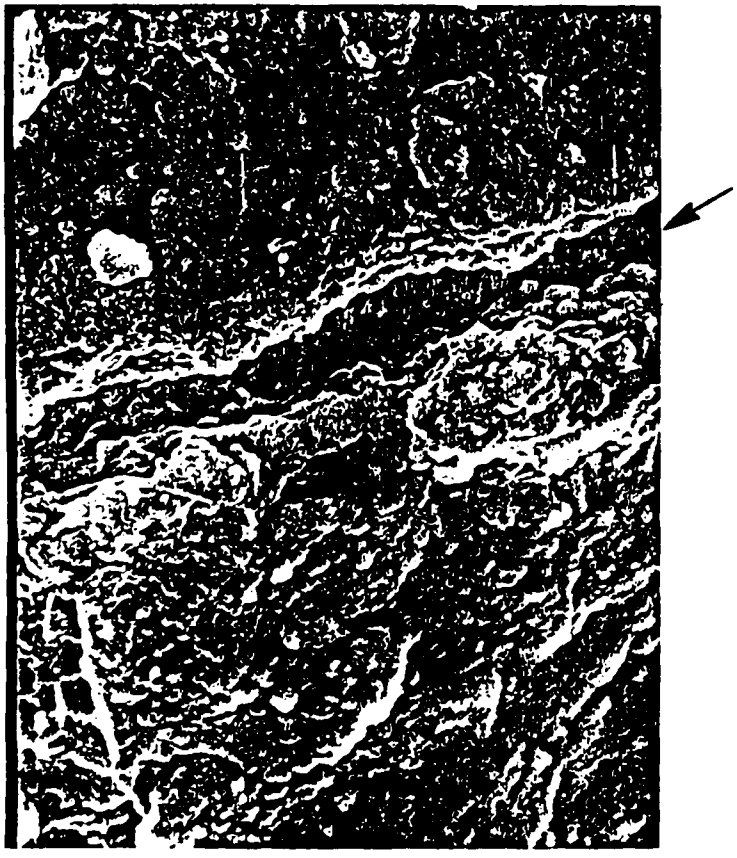

Nickel Plack Electrode 6-26-86
Cell 21 1200X

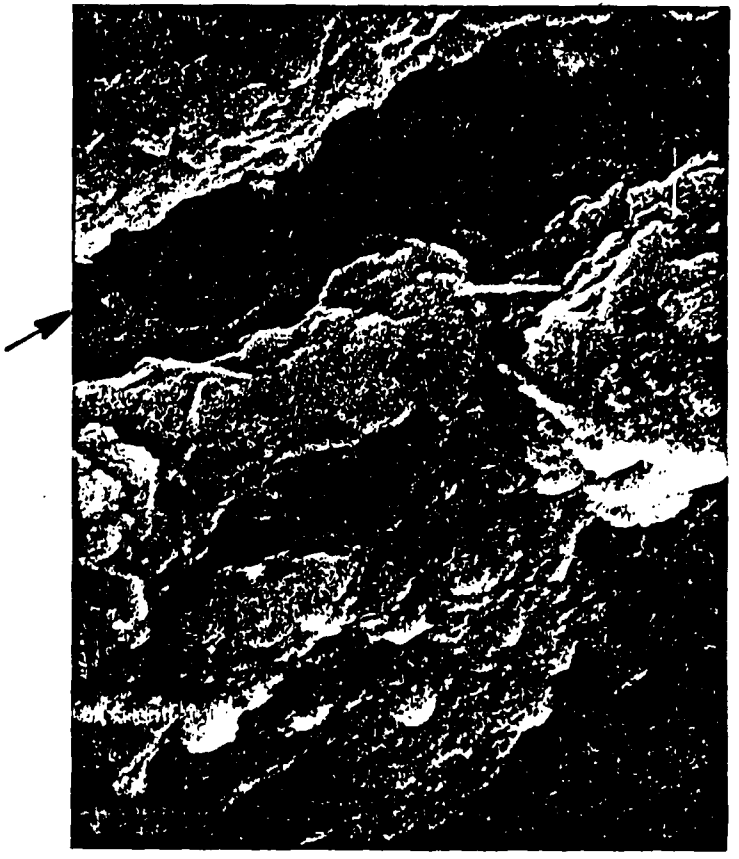

Nickel Plack Electrode 6-26-86
Cell 21 3000X

FIGURE 4.46 ELECTRON MICROGRAPH, USED Ni ELECTRODE, CELL 21

and 4.47). It appears that the particles exhibited low density to begin with, and become denser with use. Conceivable, this has resulted in creating crevices as indicated by the arrow in Figure 4.46. It is not known whether this crevice exists along the entire surface of the electrode or only at certain spots.

The statistical analysis of the data for roll-bonded electrodes are compared with that of sintered electrodes in Table 4.12. With respect to voltage, the roll-bonded electrodes obviously exhibit a better uniformity compared with the sintered electrode. However, the reverse is true in case of change in pressure. Cells using sintered nickel electrodes show a lesser variation of change in pressure than the roll-bonded electrode. Note, however, that the order of magnitude of the differences are small and both types of cells show more than adequate consistency to be used to track the main battery's state of charge.

Cell 30: This cell was fabricated with sintered nickel electrode obtained from Marathon aircraft battery. After performance evaluation at various temperatures, (paragraph 4.1.3) life cycle tests of the cell was started. After 1300 cycles, tests were terminated due to malfunction of the test equipment. Typical performance data are shown in Figures 4.48 through 4.51.

Cell 45: This cell was constructed using the nickel electrode from a General Electric aircraft battery. First, the cell was manually discharged twice to 100% depth and the delivered capacity was 0.325 Ah. After about 1000 cycles, testing was discontinued. This cell also exhibited the normal operating characteristics.

4.3 COMMERCIAL AIRCRAFT BATTERIES

One cell each from Saft and Marathon (nominal capacity 12 Ah)

Nickel Electrode 1200X

Nickel Electrode 3000X

FIGURE 4.47 ELECTRON MICROGRAPH, FRESH Ni ELECTRODE

TABLE 4.12

COMPARISON OF STATISTICAL DATA

TYPE		ROLL-BONDED			SINTERED
CELL NO.		2	26	25	21
CHARGE					
V avg.	$\bar{x}$	0.941	0.601	0.524	0.850
	σ	0.2696	0.0108	0.0228	0.0886
ΔP	$\bar{x}$	24.8	22.3	16.9	18.6
	σ	1.4720	0.5774	1.5366	0.7440
DISCHARGE					
V avg.	$\bar{x}$	-0.600	-0.824	-0.781	-0.713
	σ	0.0273	0.0555	0.0300	0.1028
ΔP	$\bar{x}$	23.5	23.2	17.7	18.9
	σ	2.5884	0.5774	2.3452	1.1260

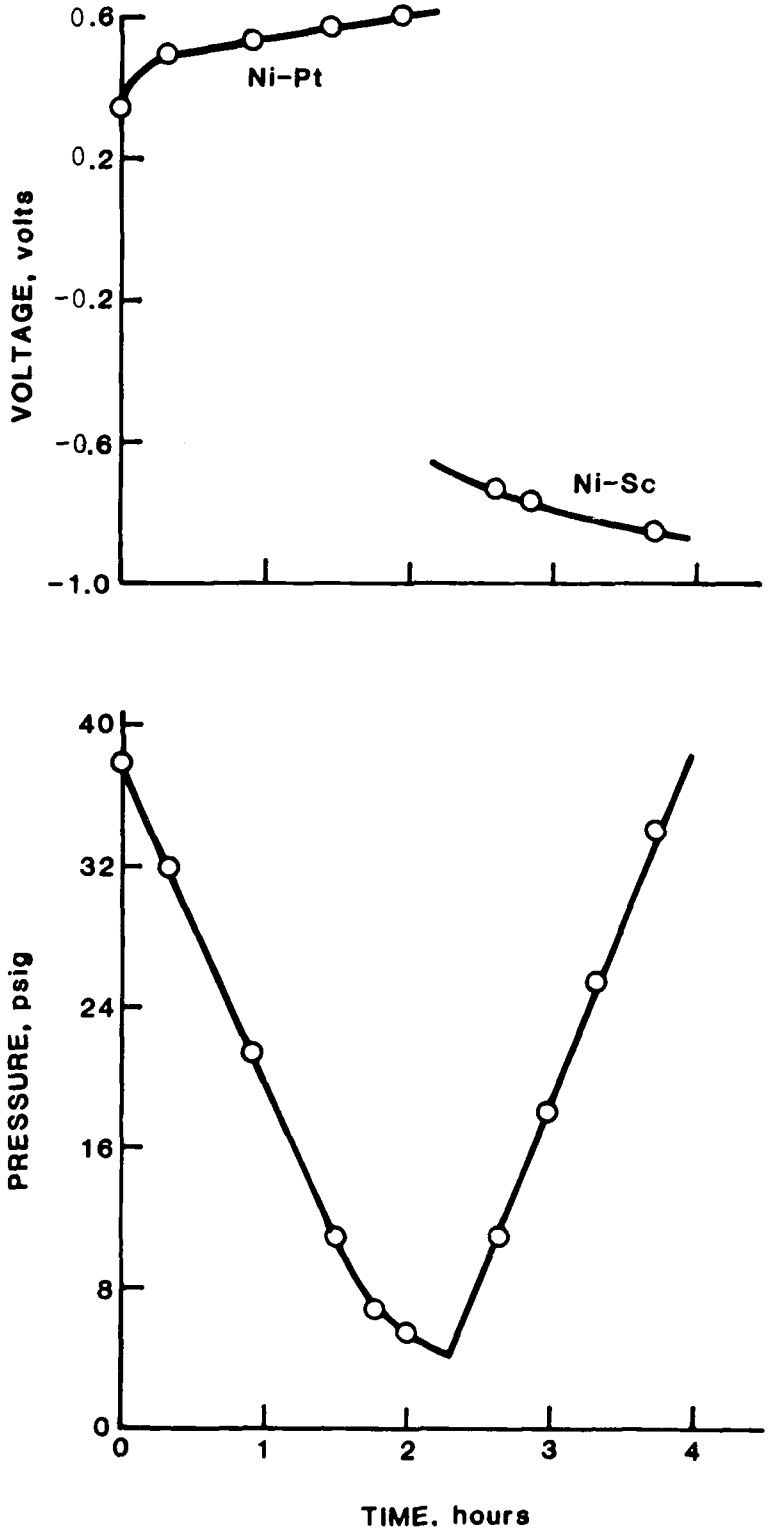

FIGURE 4.48 PERFORMANCE CHARACTERISTICS -CELL 30, CYCLE 597

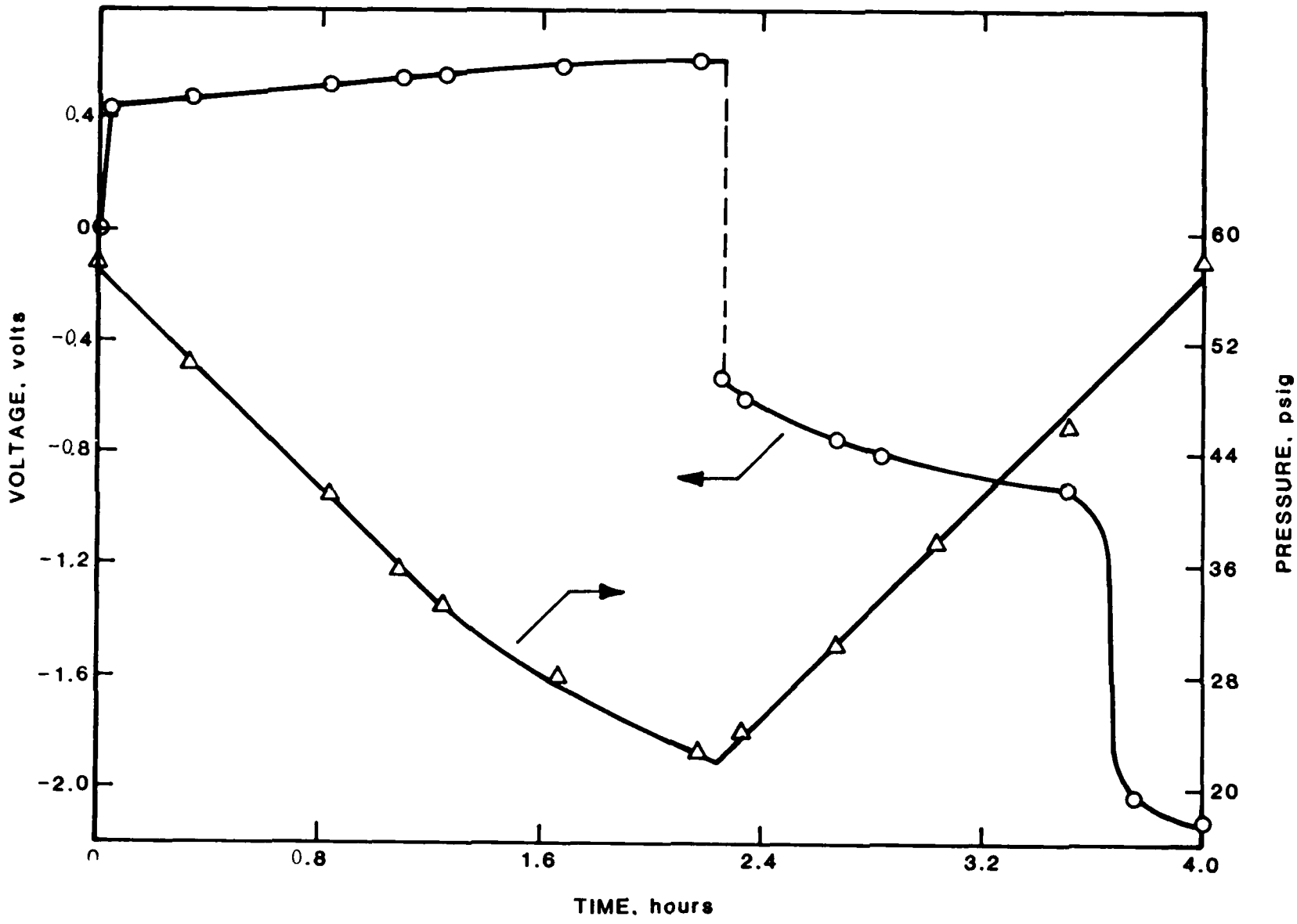

FIGURE 4.49 PERFORMANCE CHARACTERISTICS CELL 30, CYCLE 795

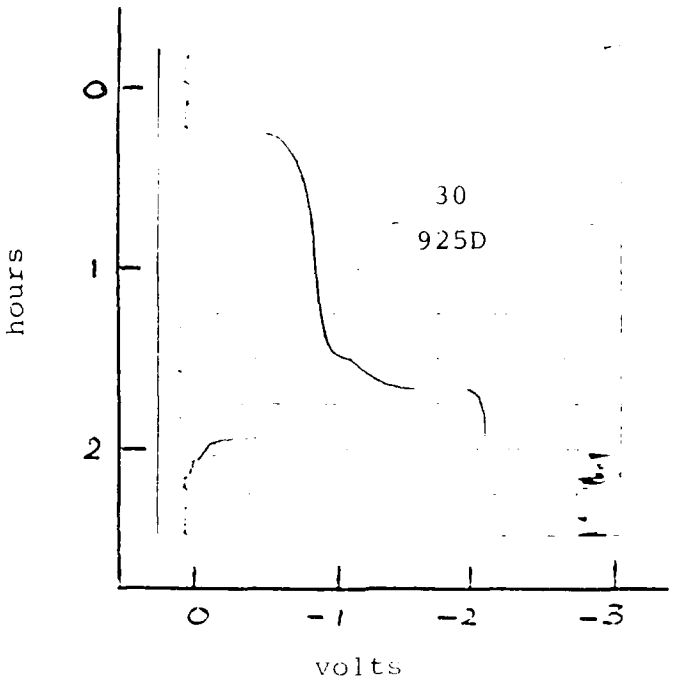

FIGURE 4.50 DISCHARGE VOLTAGE PR
CELL 30, CYCLE 925

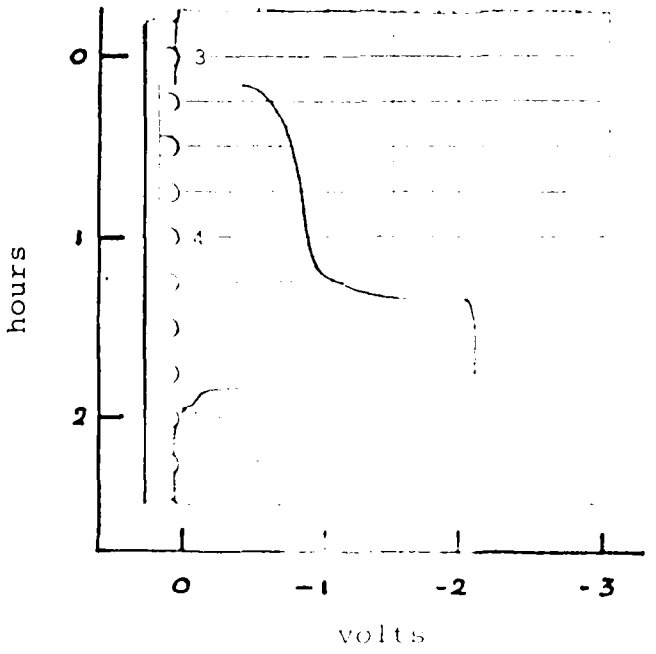

were discharged at 6 Amps (C/2 rate), immediately after charging. The discharge was repeated with the cells allowed to stand overnight after charging. The delivered capacity in the first case was 26.5 and 17.5 Ah for Marathon and Saft respectively. The capacity values were reduced by 15 and 20% when discharged after overnight stand. The discharge characteristics of the cells are shown in Figure 4.52.

The cells were also discharged as per MIL-Spec DOD-C-85050 (AS), 4.7.2.7, duty cycle test. No problems were encountered with the high currents and the test results are summarized in Table 4.13.

After completing tests of single cells, 16 cells each manufactured by Saft and Marathon were assembled to constitute battery stacks. The batteries were also subjected to MIL-Spec-DOD-C-85050 (AS), 4.7.2.7 duty cycle test and the results are shown in Table 4.14.

A carbon pile resistor was used for these tests. Its magnitude, as measured by means of a shunt, was different from that specified in the Mil-Specs and the resistance value of a 16-cell battery was not consistent with that for single cells. Furthermore, as discovered later, some of the aircraft cells were defective and had to be removed. These are the apparent reasons that the voltage values of the batteries (Table 4.14) are not consistent with those of single cells (Table 4.13).

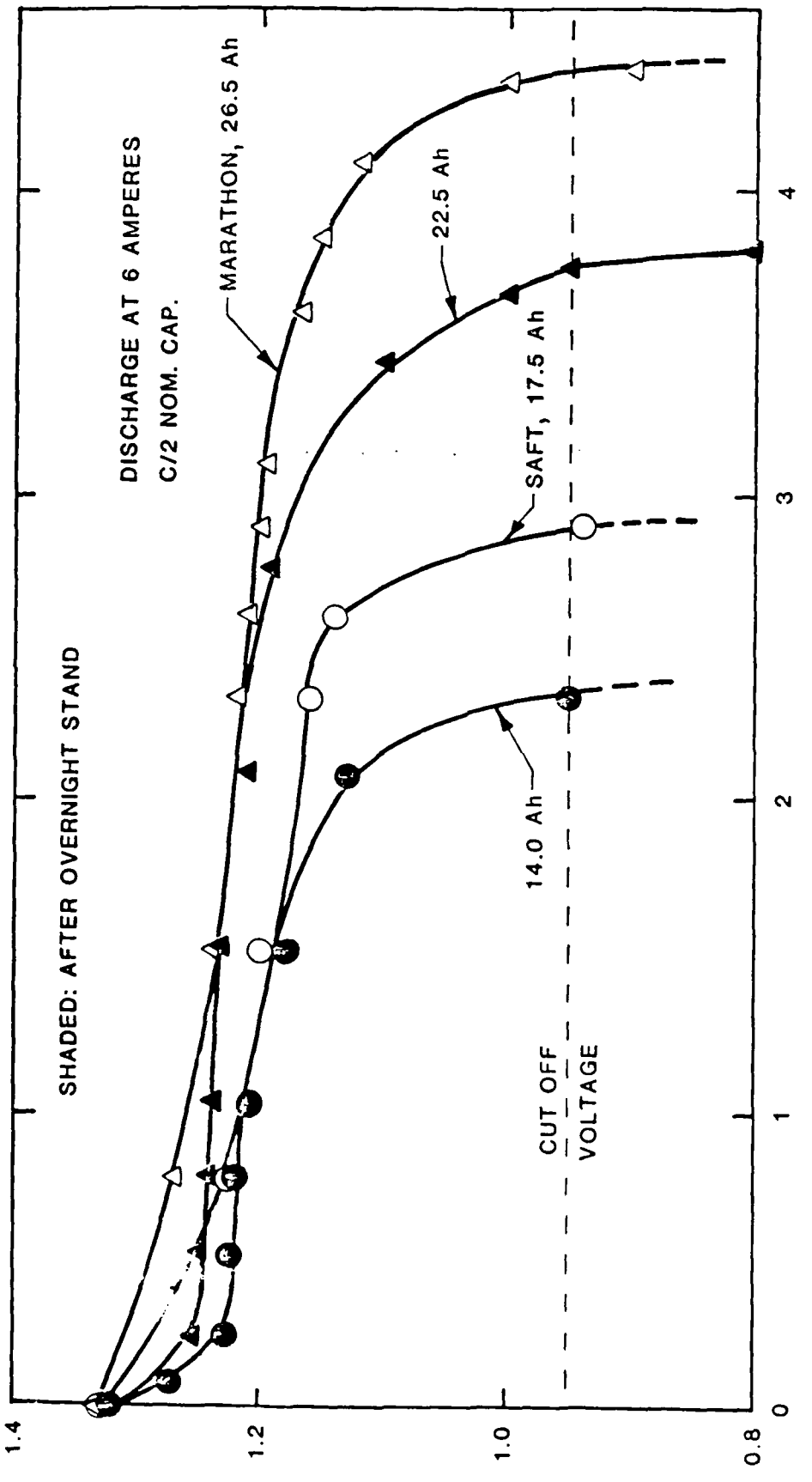

FIGURE 4.52 DISCHARGE PERFORMANCE OF AIRCRAFT CELLS

TABLE 4.13

DUTY CYCLE TEST ON AIRCRAFT CELLS

CELL TYPE	CYCLE NO.	MODE ··· SECS. ···	OCV 0	DISCHG 0	DISCHG 20	OCV 0	OCV 260	DISCHG 0	DISCHG 20
SAFT	1	V(volts)	-	0.62	0.54	1.22	1.27	0.59	0.49
		I(amps)	0	324	282	0	0	318	252
	2	V	1.35	0.67	0.61	1.30	1.32	0.64	0.59
		I	0	378	330	0	0	366	330
MARATHON	1	V	1.34	0.49	0.46	1.33	1.39	0.49	0.45
		I	0	468	420	0	0	468	396

TABLE 4.14

DUTY CYCLE TEST ON AIRCRAFT BATTERIES

BATTERY TYPE	CYCLE NO.	MODE →→→ SECS.→→→	OCV 0	DISCHARGE 0	DISCHARGE 20	OCV 0	OCV 260	DISCHARGE 0	DISCHARGE 20
Marathon	1	V(volts)	22.4	7.5	6.3	20.1	21.0	6.9	6.0
		I(amps)	0	522	462	0	0	522	450
	2	V	21.7	7.7	6.5	20.3	-	6.9	6.1
		I	0	522	466	0	0	528	450
Saft	1	V	22.1	12.7	10.8	20.5	21.1	12.1	10.4
		I	0	360	318	0	0	342	323
	2	V	22.0	13.5	11.6	19.8	20.9	13.2	10.8
		I	0	324	312	0	0	336	312

SECTION 5

DESIGN OF ELECTRONIC TEST UNIT

Efforts during the second phase of the program were directed towards the design and assembly of an electronic package capable of maintaining the main battery and pilot cell in a tandem at all times. A self-contained test system capable of cycling in either a manual or automatic mode was built to evaluate tracking capability.

The current through the main battery is monitored through a precision current shunt (50 amperes - 50 volts) and amplified by an instrumentation amplifier and related circuitry. The purpose of the circuitry is to maintain the precise ratio between the battery and pilot cell as current during either charging or discharging. For example, if the desired ratio is 50 to 1, when the battery current is 25 amperes the current to the pilot cell should be exactly 0.50 amperes through all ranges, both during charge and discharge.

Pressure in the pilot cell is monitored with a transducer amplified signal that gives an electronic output of the charge and discharge curves of the pilot cell. These curves are used to monitor the state of charge of the main battery and to control the amount of overcharge returned to the main battery after discharge. By setting the 100% or fully charged level of the main battery in the asymptotic portion of the charge curve, we control the amount of overcharge to the battery based on a straight line discharge curve. This is accomplished by adding a reference voltage to the transducer output to set the 100 - percent point, then amplifying the signals for zero to 100 - percent output.

The output has a dual purpose; it is displayed as a 0 to 100 - percent reading on a digital display and is also used to turn off the charge current when the main battery is fully charged. This prevents excessive overcharging and resulting water loss and reduced battery life since only the necessary and sufficient amount of charge is put back in following a discharge.

The test unit consists essentially of

1. A remotely controlled constant current power supply equipped with independent charge and discharge controls.

2. A reversing module capable of changing the polarity of the main battery in relation to the power supply, control currents and provide the load bank during discharge.

3. An adjustable timing unit capable of operating either in a manual or automatic mode with a range of 1 minute to 24 hours.

The integrated system is designed to give maximum versatility while using a relatively simple circuit with standard components. Two test systems were built, the first a laboratory unit without constraints in size. The second unit is a smaller version in which the pilot cell-transducer assembly is packaged separately. This permits mounting this and the battery away from the cycler to facilitate environmental tests.

The basic schematics of the test system are shown in Figures 5.1 and 5.2.

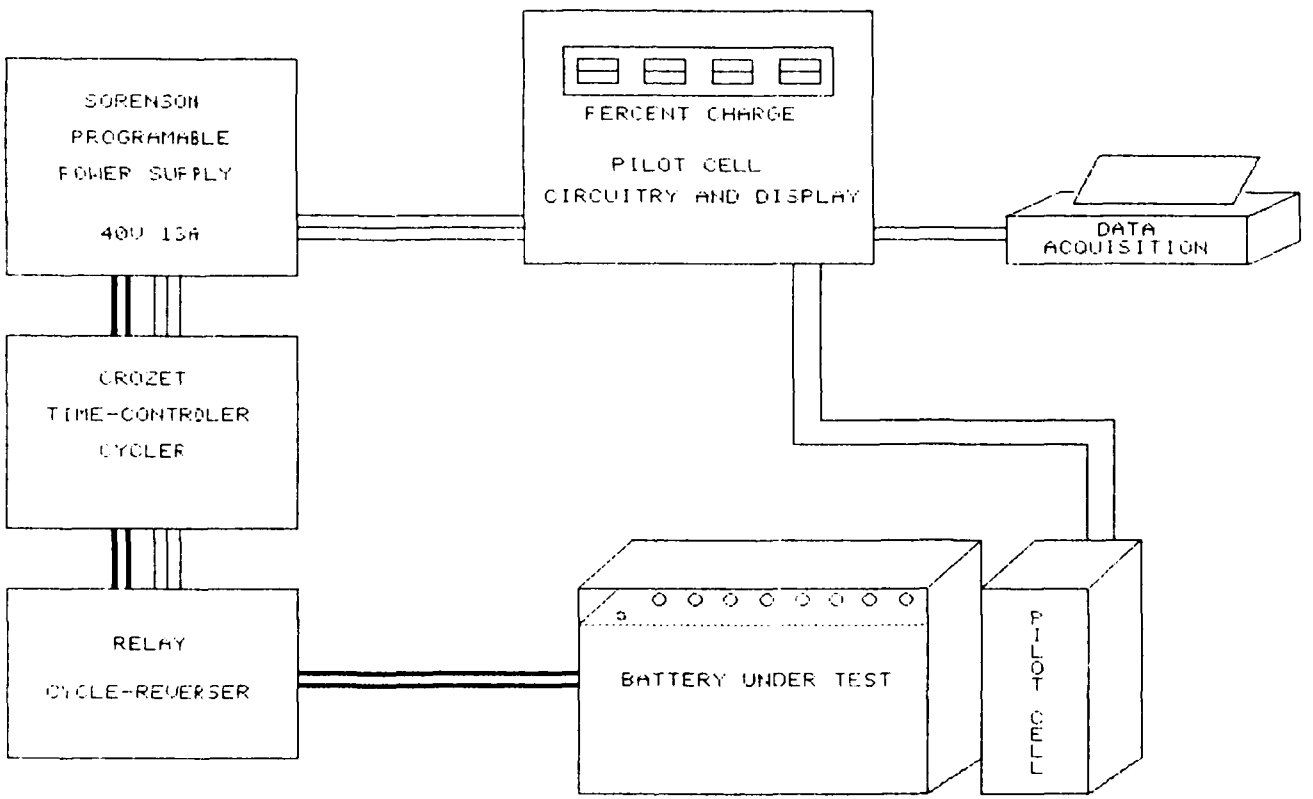

FIGURE 5.1. AIRCRAFT BATTERY STATE OF CHARGE INDICATOR

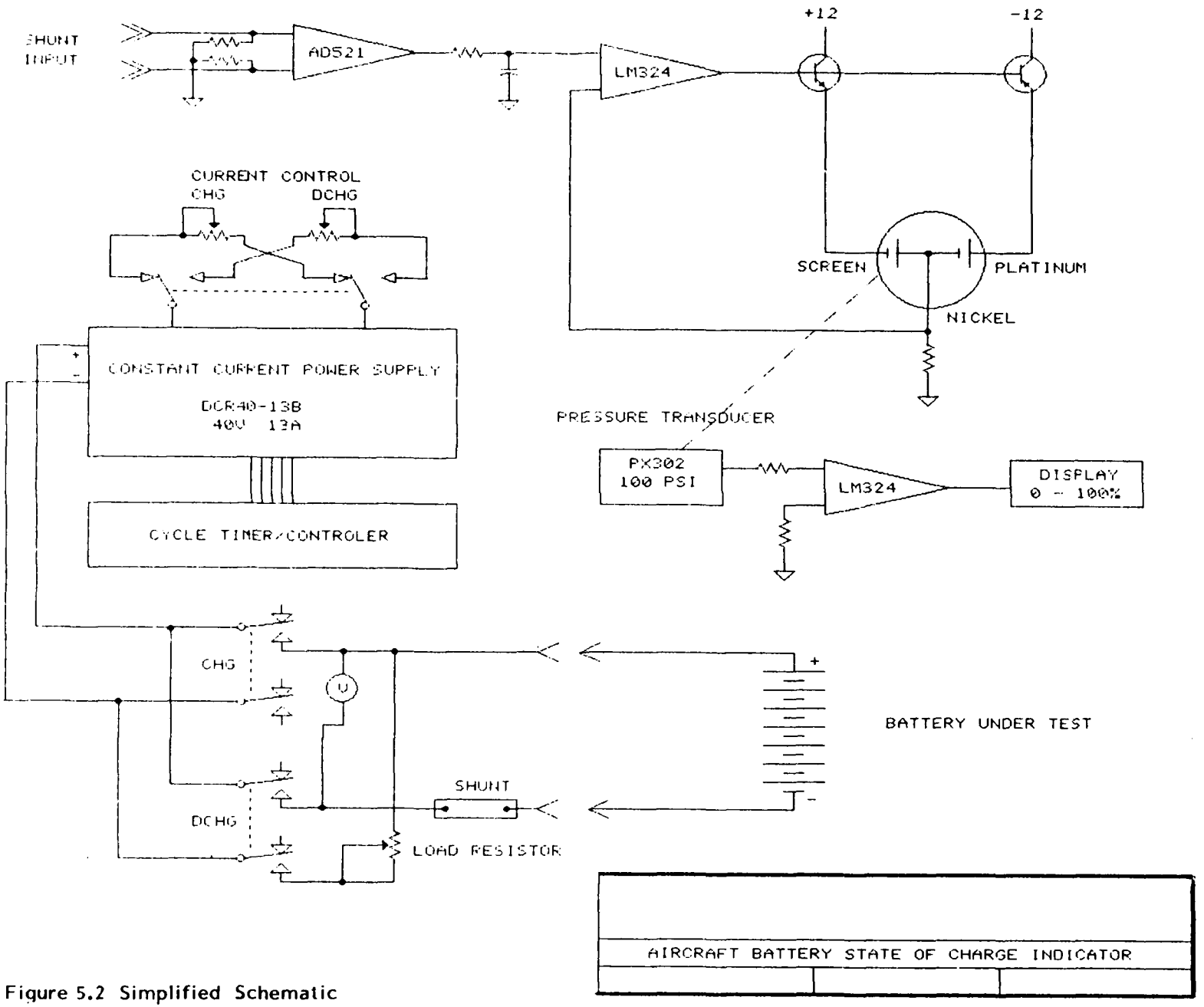

Figure 5.2 Simplified Schematic

SECTION 6

INTEGRATED AIRCRAFT BATTERY TRACKING SYSTEM

6.1 SYSTEM DESIGN AND CALIBRATION

After evaluating baseline characteristics and optimizing the design of electronic unit, the last phase of the research efforts commenced to determine the tracking characteristics of the Ni-0_2 cell when operated in tandem with the main battery.

The test unit consists essentially of a constant-current power supply to provide the power source, a cycling unit with provisions to vary cycling times and current and a fuel gauge which converts the pressure of the Ni-0_2 cell into present state of charge (Section 5).

Cell 27 was housed in the fuel gauge for the first series of evaluation tests. The cycling equipment was first calibrated with one Saft aircraft cell, and the calibration curve is shown in Figure 6.1. Next, a battery stack of 16 Saft aircraft cells connected in series was cycled in conjunction with the same Ni-0_2 Cell 27 and a typical profile of current, voltage and state of charge is shown in Figure 6.2. After about 10 cycles, the experiment had to be discontinued because

- Three of the Saft cells had shorted out.
- Capacity obtained by discharging one cell did not truly represent capacity of stack possibly because of variations between cells.
- Preset parameters of cycler were out of phase with characteristics of the pilot cell.

In view of these factors, we decided to repeat the experiment. Another pilot cell, 28, was built, again using a section of nickel electrode cut out from a Saft cell. This cell and the Saft

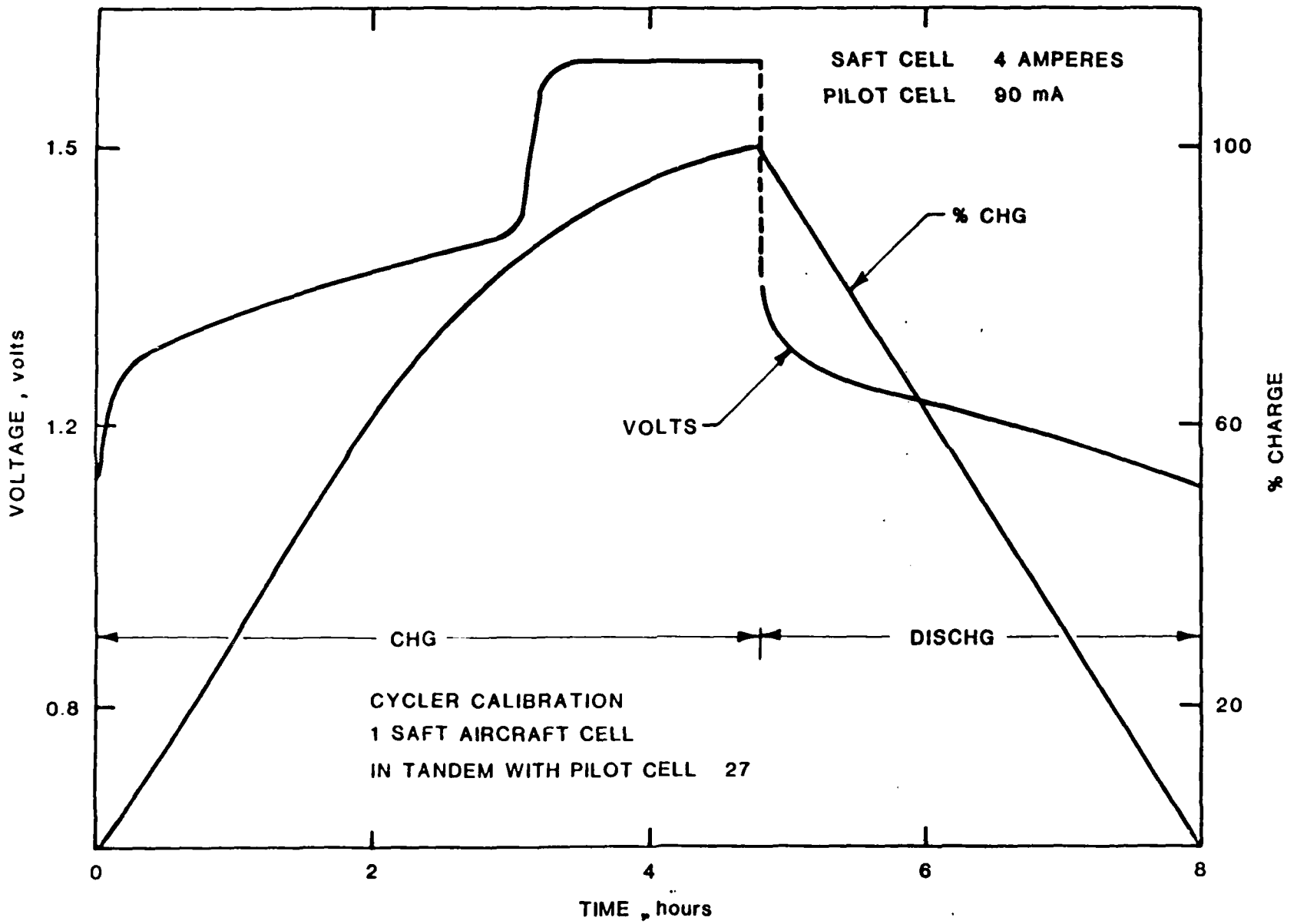

FIGURE 6.1 CALIBRATION OF TRACKING CYCLER

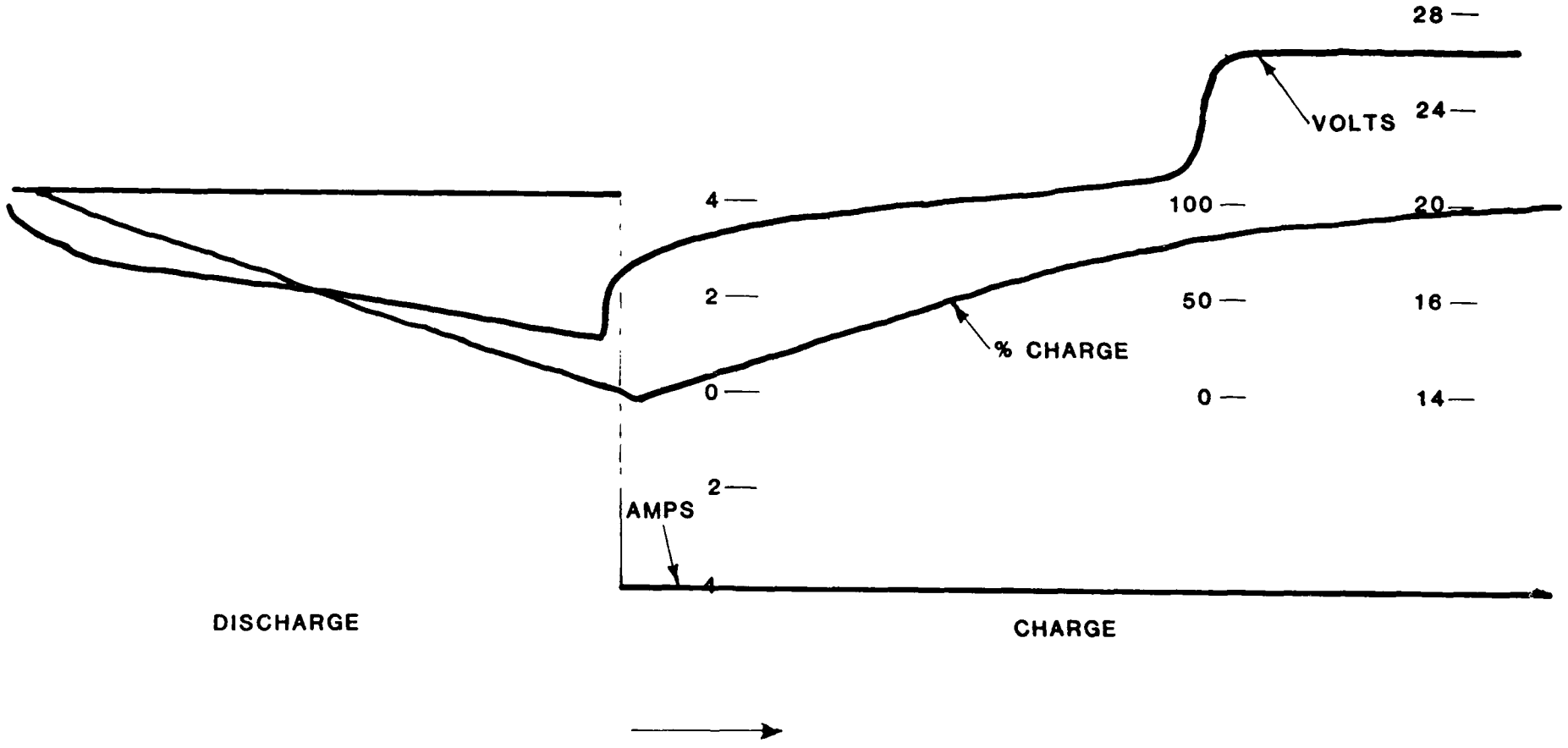

FIGURE 6.2 PERFORMANCE OF 16-CELL SAFT BATTERY

battery stack of 13 cells were first tested separately to identify their characteristics and the following capacities were obtained.

SAFT		PILOT CELL	
End V	Ah	End V	Ah
13.0	16.9	- 0.8	0.221
12.0	17.4	- 0.9	0.237
11.0	17.6	- 1.0	0.258

The performance characteristics of the two are shown in Figure 6.3. Based on these data, operating parameters of the tracking cycler were modified. The design specifications are given in Table 6.1.

The battery and pilot cell were connected to the tracking cycler such that operation of the pilot cell was in tandem with the battery. The cycler was also equipped with a provision to cut off the charge current when the fuel gauge reading (% charge) exceeded 100%.

Cycling of the system was started and the first 5 cycles were utilized to fine-tune system parameters after which cycling was continued in the automatic operating mode. A typical charge-discharge cycle is shown in Figure 6.4.

6.2 SYSTEM OPERATION AND PROOF OF CONCEPT

The next step in proving the system concept was to evaluate the relationship between the actual capacity of the battery to be monitored and the displayed value of its state of charge between 0 and 100%.

Since an excessive overcharge could be more detrimental to

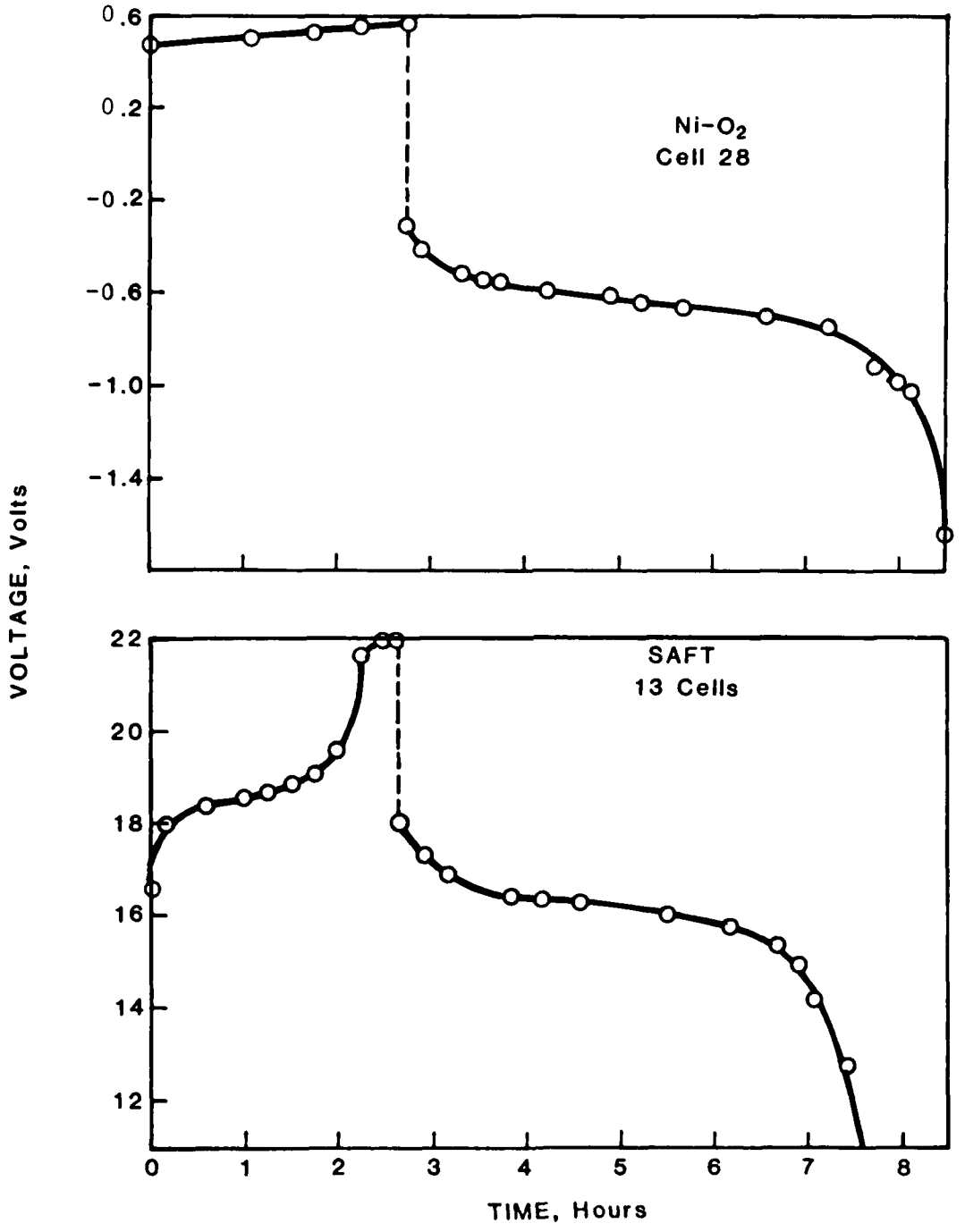

FIGURE 6.3 PERFORMANCE CHARACTERISTICS OF BATTERY AND PILOT CELL

TABLE 6.1

TRACKING CYCLER SPECIFICATIONS

	SAFT	$Ni-O_2$
From graph, total time to end of discharge	7.45 hrs	7.55 hrs
Charge time	2.65	2.75
Discharge time	4.80	4.80
Discharge current	3.6A	46 mA
Actual delivered capacity	17.28 Ah	0.221 Ah
Discharge		
DOD	75%	75%
Capacity to be removed	12.95 Ah	0.166 Ah
I	3.6 A	46 mA
t	3.6 hrs	3.6 hrs
Charge		
Overcharge	11%	11%
Capacity to be put in	14.39 Ah	0.184 Ah
I	3.6 A	46 mA
t	4.0 hrs	4.0 hrs
i.e. cycler to be calibrated to,		
Charge	4.0 hrs @ 3.6 A	4.0 hrs @ 46 mA
Discharge	3.6 hrs @ 3.6 A	3.6 hrs @ 46 mA

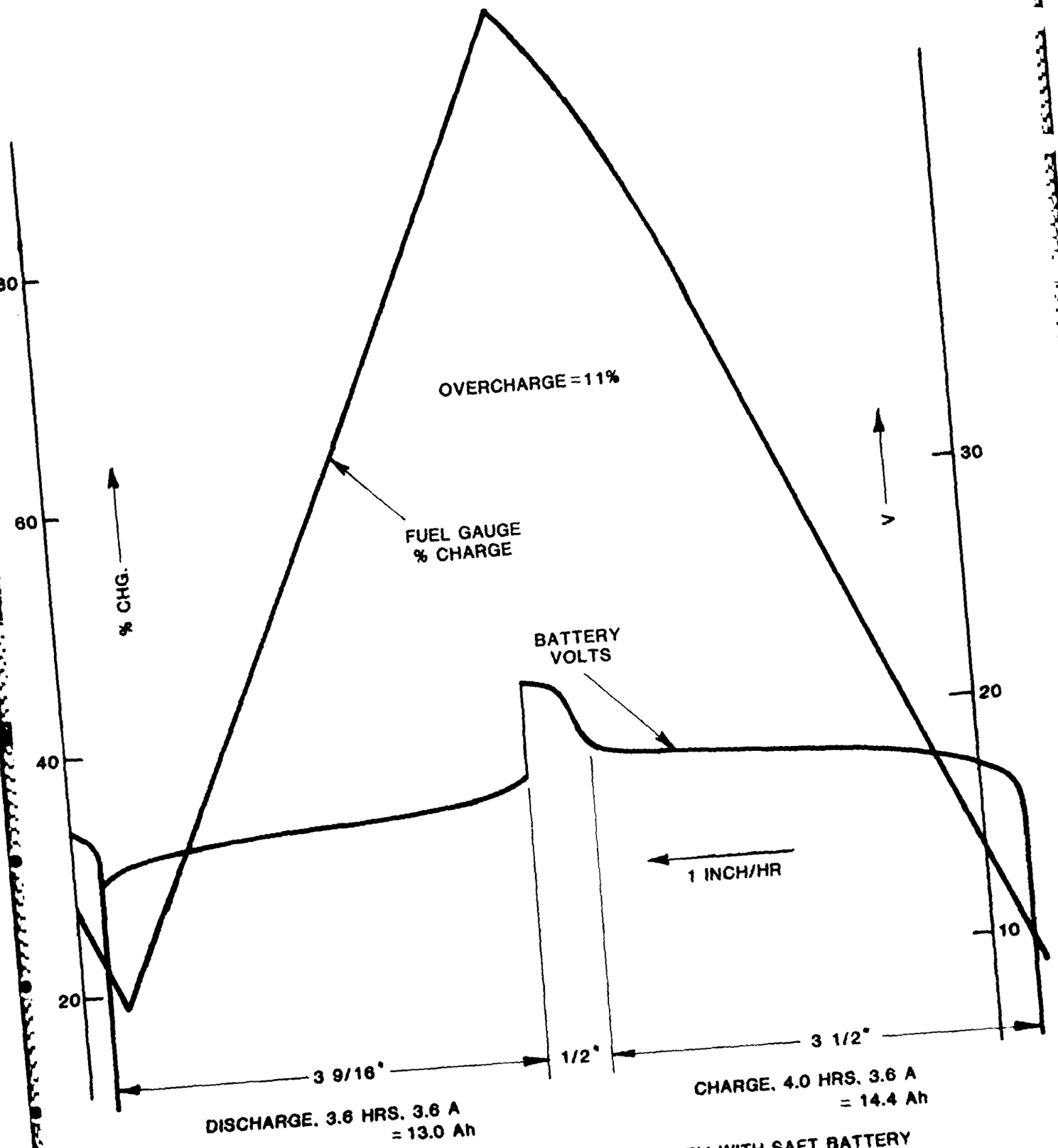

FIGURE 6.4 OPERATION OF PILOT CELL IN TANDEM WITH SAFT BATTERY

oxygen cell, runaway conditions could upset the equilibrium tandem operation. To eliminate this factor, the tracking cycler was equipped with provisions to terminate the current when the battery was fully charged.

A 13-cell stack of Saft aircraft battery was run in tandem with a nickel oxygen cell containing an identical nickel electrode. After initial calibration, the system was operated in the automatic cycling mode to the specifications in Table 6.1. After ensuring that the system was functioning properly as per designed specifications, tests were started to investigate the relationship between state-of-charge and delivered capacity. The procedure employed for the tests is as follows:

1. Set cycler to "manual" operation.
2. Charge until fuel gauge reaches the desired state-of-charge.
3. Discharge to end battery voltage of 11.0 V.
4. Repeat steps 2 and 3 for a different state-of-charge.

The series of tests were performed in both directions with the state of charge values going down in steps from 100% and going up in steps from 15%. The test data are summarized in Table 6.2 and a plot of delivered capacity vs. state-of-charge is shown in Figure 6.5.

During each discharge, (starting from a particular state of charge), the fuel gauge reading was monitored continually. As shown in Figures 6.6 and 6.7, the state-of-charge was linear with the capacity removed and the slope of the line was independent of the state-of-charge. A typical profile of percent charge and battery voltage is shown in Figure 6.8.

TABLE 6.2

STATE OF CHARGE VS. DELIVERED CAPACITY

CYCLE NO.	CHARGE		DISCHARGE		Ah out/Ah in
	% CHG.	Ah	% CHG.	Ah	%
29	100	15.84	0	15.30	97
30	90	14.40	0	13.75	95
31	80	12.78	0	12.38	97
32	60	8.78	4	8.60	98
33	40	5.29	8	4.79	91
34	30	3.54	7	3.48	98
35	22	2.41	7	2.28	95
36	10	0.54	6	0.54	100
37	15	0.58	11	0.54	93
38	20	1.62	9	1.50	93
39	30	3.42	8	3.42	100
40	40	5.40	2	5.69	105
41	50	7.06	4	6.88	97
42	60	9.47	0	9.04	95
43	70	10.80	2	10.51	97
44	80	12.42	3	11.95	96
45	90	14.40	1	13.68	95
46	100	18.58	-5	16.20	87

Saft 13 cell stack: I = 3.6A End V = 11.0 V

NiO_2 cell 28: I = 46 mA

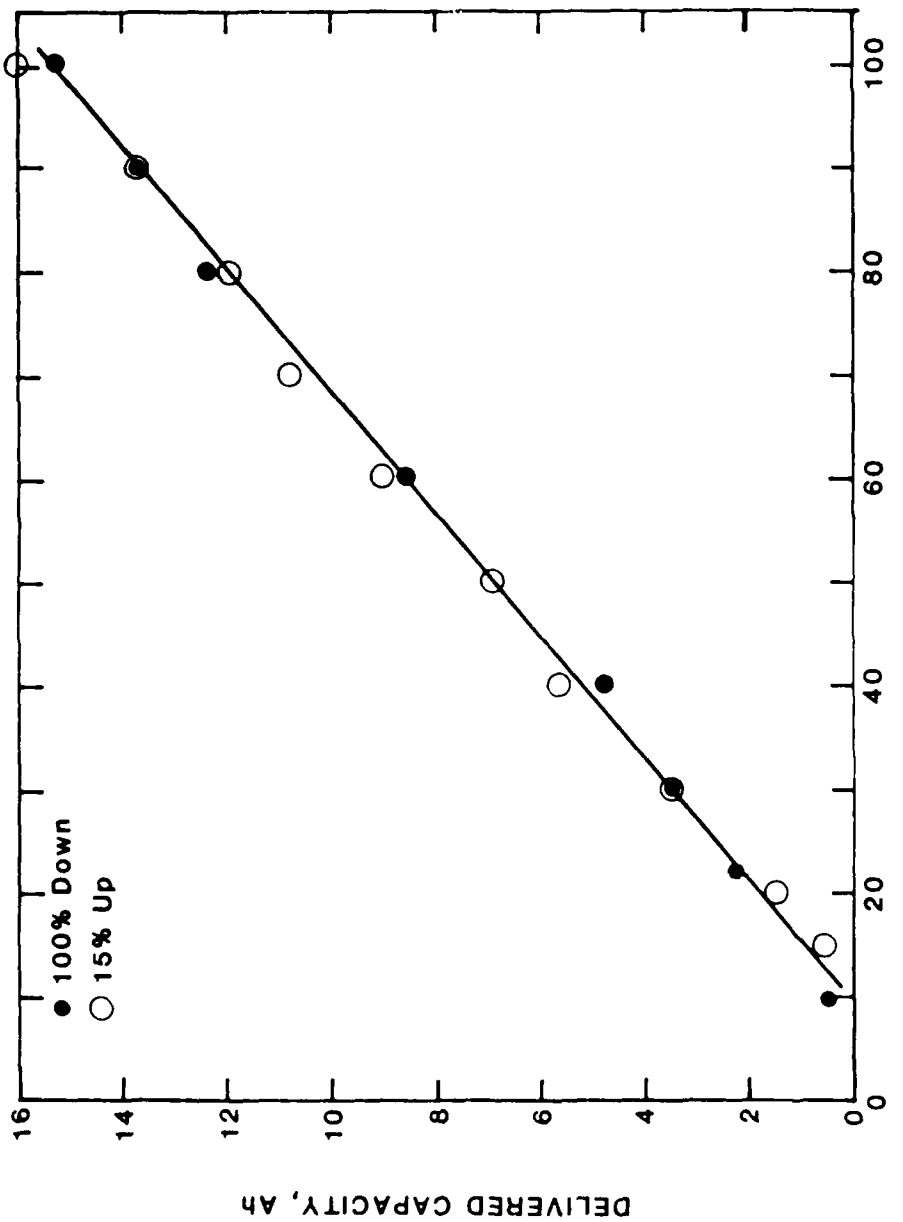

FIGURE 6.5 STATE OF CHARGE vs. DELIVERED CAPACITY

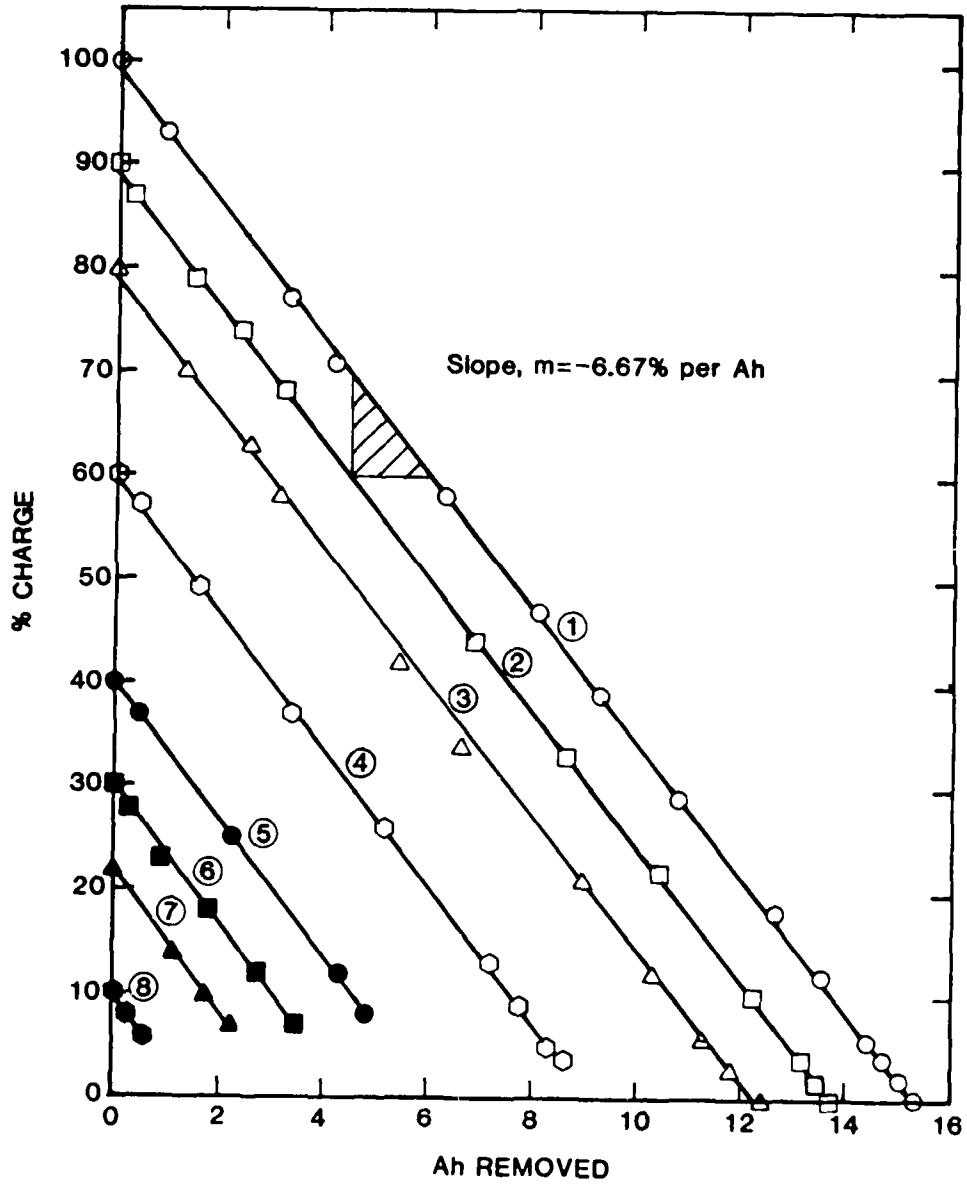

FIGURE 6.6 CAPACITY vs. STATE OF CHARGE a 100 TO 10%

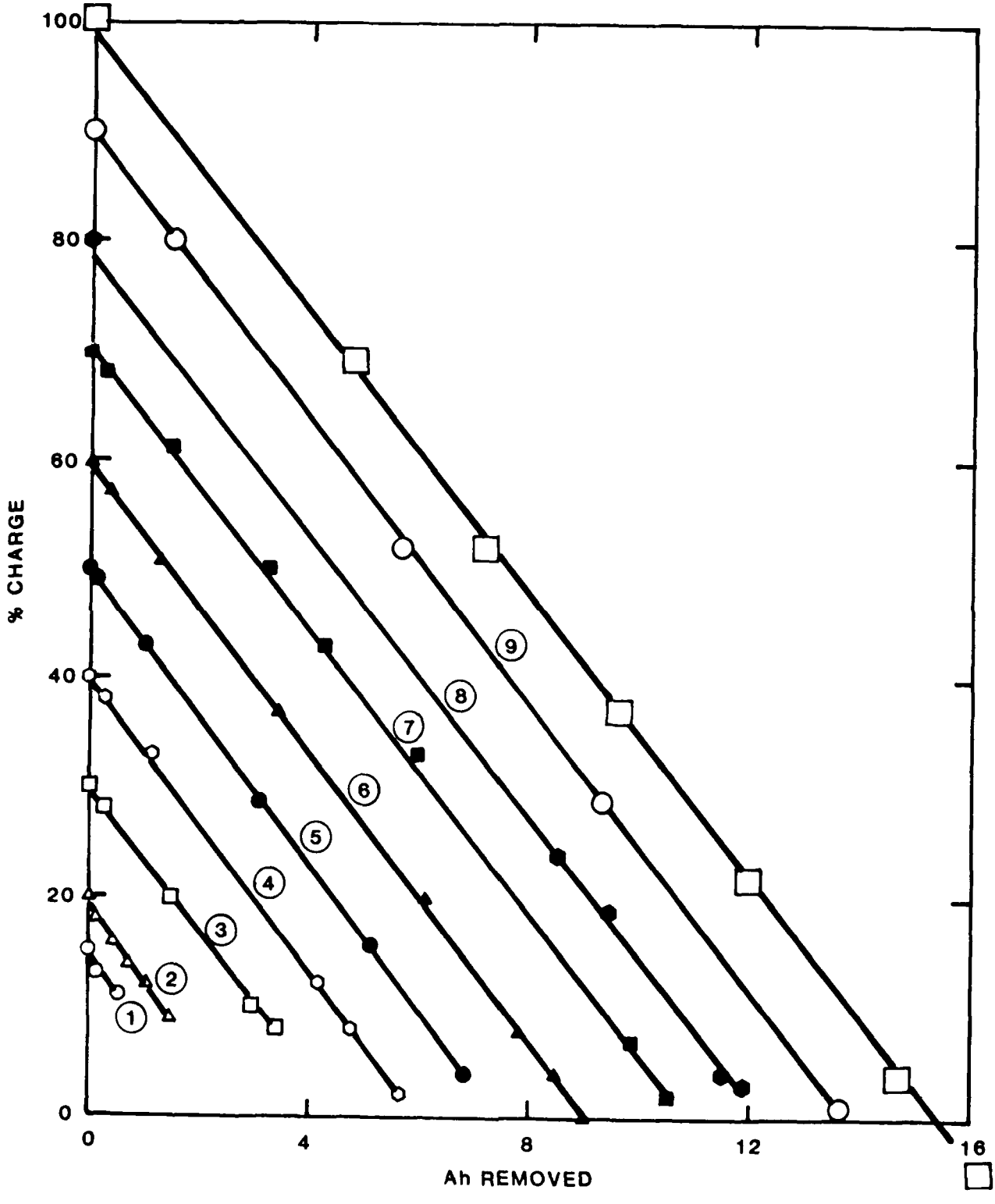

FIGURE 6.7 CAPACITY vs. STATE OF CHARGE AT 15 TO 100%

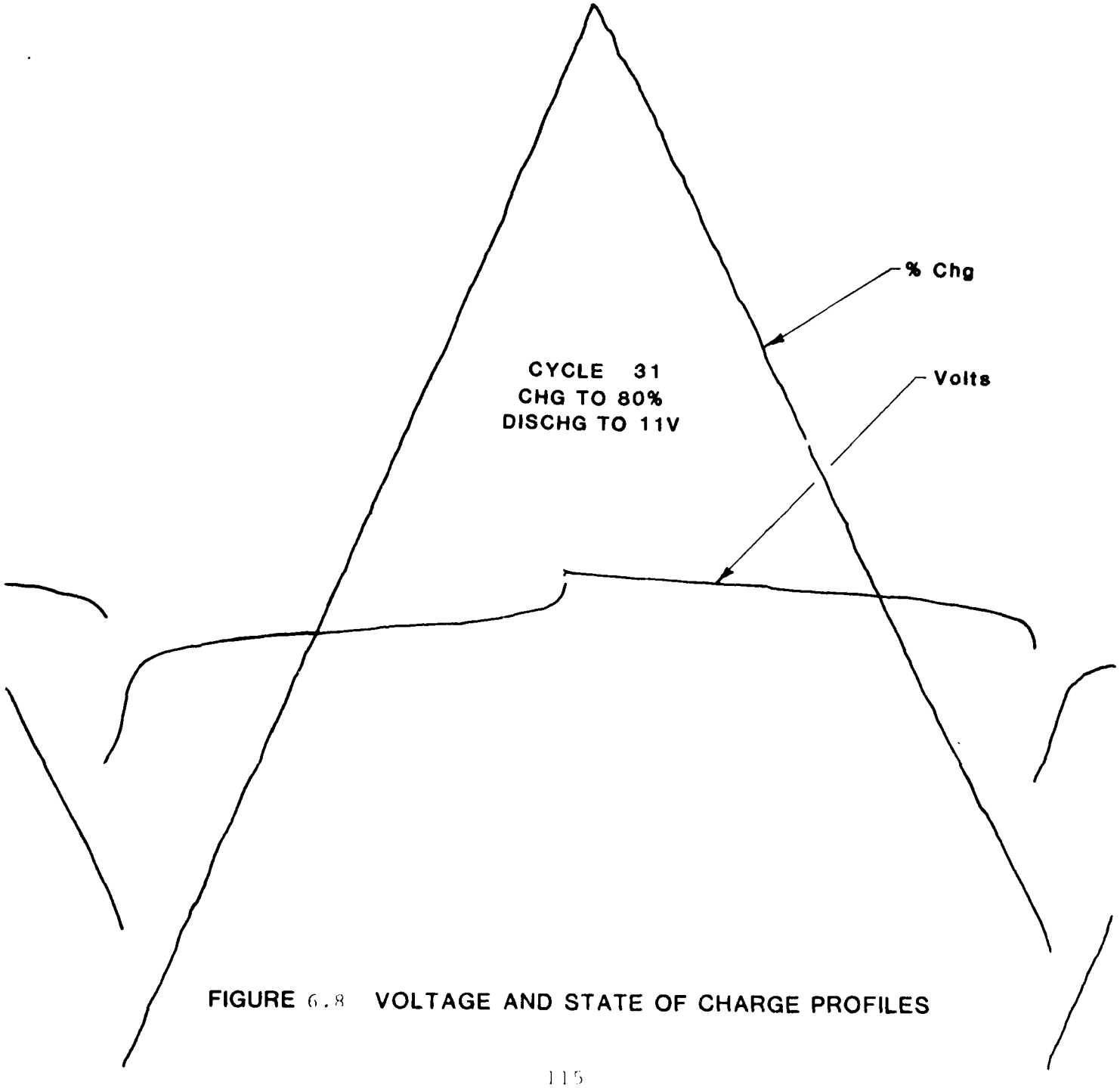

FIGURE 6.8 VOLTAGE AND STATE OF CHARGE PROFILES

The results obtained from this series of tests indicate

1. Excellent capability of the pilot cell to track the state of charge of the main battery.
2. Linearity of state of charge and capacity (Figure 6.5).
3. Constant slope of state of charge vs. capacity curves, (Figures 6.6 and 6.7).
4. Reproducible data.

The test results also identify one parameter which required further study. Since the battery is discharged fully to the same potential each time, under ideal conditions, the fuel gauge should indicate the same value of state of charge. However, the fuel gauge reading at the end of discharge did not remain constant.

The system was thoroughly checked and the problem was traced to a defective electronic component which had compounded the normal fluctuations caused by changes in ambient temperature. One more shorted aircraft cell was removed and system calibrated. The current to the battery was kept the same at 3.5 A and current to the Ni-O_2 cell was increased from 46 to 48 mA. Performance characteristics for cycle 63 are shown in Figure 6.9.

As scheduled, after 100 cycles, cycling was interrupted and the test matrix state of charge versus delivered capacity was repeated. The test procedure was as follows: Discharge regime of cycle 102 was continued for a longer period until the state of charge of the battery reached 0%. This gives the capacity remaining when the battery's state of charge is 10%.

The procedure was repeated increasing the state of charge in steps to 100%, followed by decreasing in steps to 5%. The experimental data are summarized in Table 6.3.

The test data confirm that the tracking characteristics are both linear and reproducible. Figure 6.10 shows the amount of

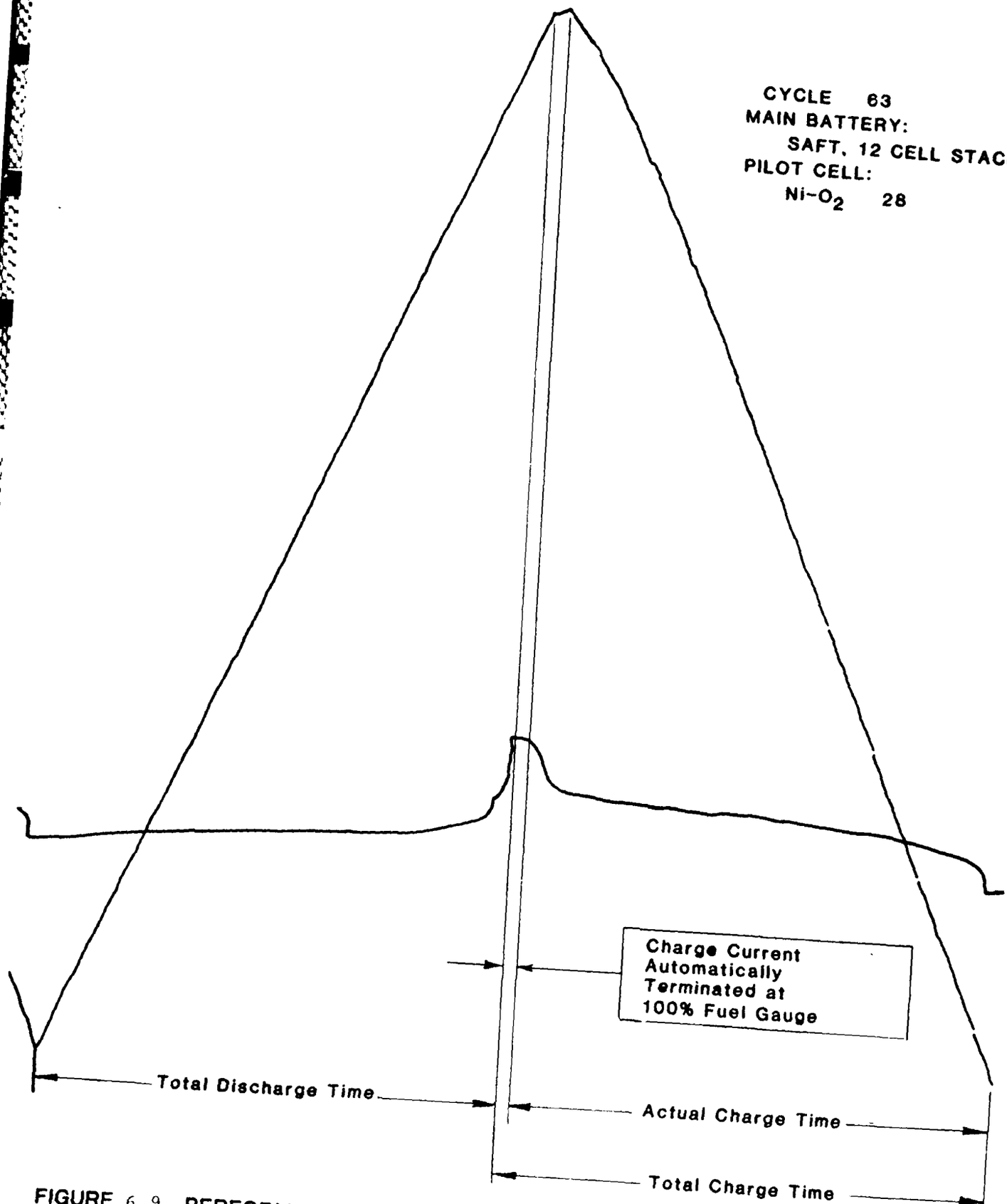

FIGURE 6.9 PERFORMANCE CHARACTERISTICS OF TRACKING CYCLER-CYCLE 63

TABLE 6.3

STATE OF CHARGE VS. DELIVERED CAPACITY

CYCLE NO.	CHARGE				DISCHARGE TO 0%		
	END V	HOURS	Ah	%	END V	HOURS	Ah
103	15.94	0.42	1.46	10	12.64	0.42	1.46
104	15.92	0.83	2.92	20	12.50	0.88	3.09
105	16.84	1.47	5.15	40	9.70	1.65	5.78
106	17.02	2.67	9.35	60	12.75	2.52	8.82
107	17.30	3.33	11.66	80	10.00	3.42	11.97
108	19.75	4.67	16.35	100	12.80	4.25	14.88
109	19.95	4.50	15.75	100	13.60	4.25	14.88
110	17.93	4.08	14.28	92	13.93	3.83	13.41
111	17.17	2.83	9.91	70	12.46	3.16	11.06
112	17.04	1.92	6.72	50	6.10	2.16	7.56
113	16.83	1.33	4.66	33	12.00	1.62	5.67
114	16.15	0.43	1.52	10	13.40	0.40	1.40
115	15.80	0.20	0.70	5	13.65	0.20	0.70

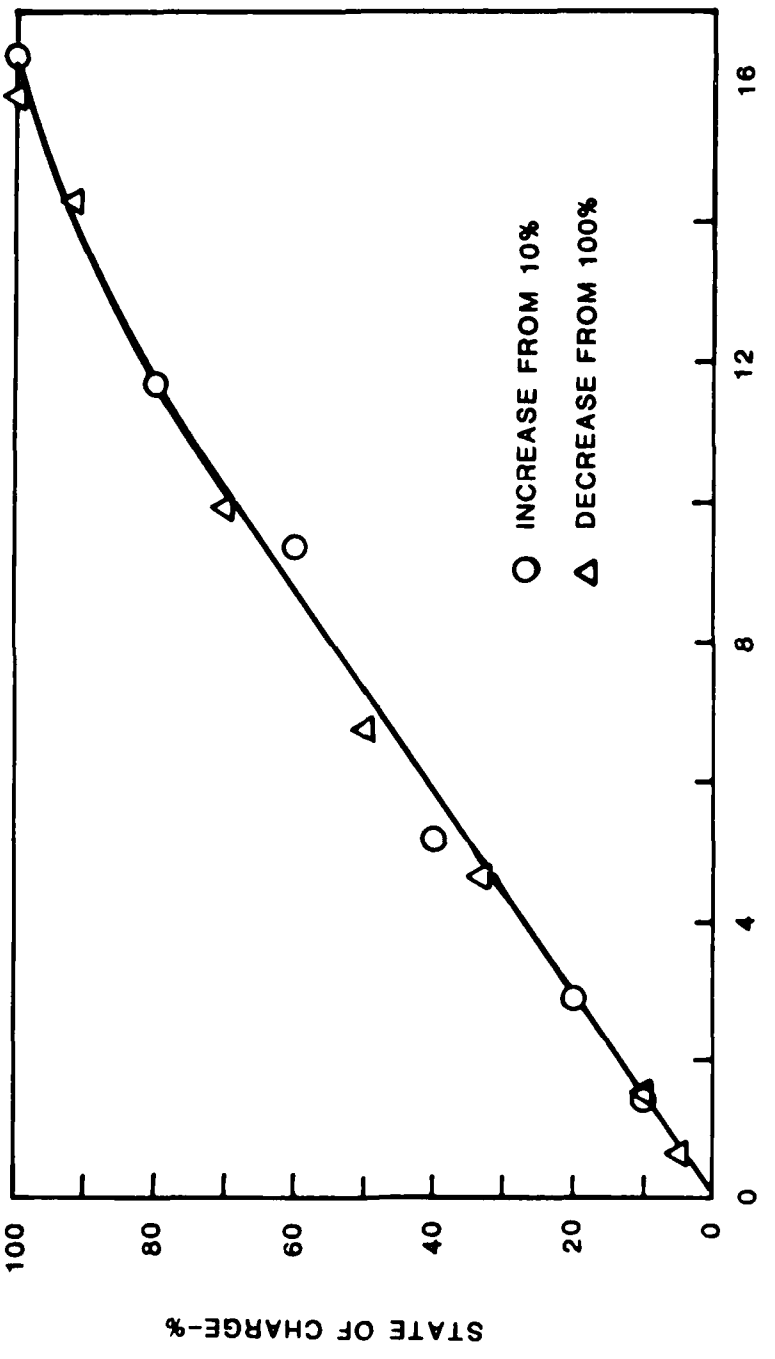

FIGURE 6.10 CHARGE INPUT vs. STATE OF CHARGE

ampere hour input required to bring the battery's state-of-charge up from 0%. After a state-of-charge of about 85% was reached, the linear relationship changed, indicating a leveling off in pressure of the $Ni-O_2$ cell. The linearity of delivered capacity and state-of-charge is shown in Figure 6.11.

After completing this series of tests, tandem operation was resumed on the automatic cycling regimen. After the system was cycled over 400 times, the voltages at the end of discharge were lower, indicating loss in capacity. It was decided to continue cycling with increased overcharge and terminate the testing if improved capacity did not result.

The performance characteristics for cycle 407 are shown in Figure 6.12, and for cycle 360 in Figure 6.13. Obviously, the major variation is the drop in the end of discharge voltage from 11.7 to 4.0 volts.

6.3 SYSTEM LIFE AND STABILITY

The results of the efforts expended described in Sections 6.1 and 6.2 indicate that the concept of using a nickel oxygen pilot cell to track the state-of-charge of the main battery is certainly viable and functional; accordingly, work on investigating system life and stability was started.

Four different nickel cadmium aircraft batteries - three commercially available and one furnished by the Air Force - were tested. The batteries investigated are

1. Saft Part No. VP120KHB
2. Marathon Part No. 12M220
3. General Electric Part No. 11AC-20

Purchased from Aeroquality Sales Lyndhurst, N. J.

4. Marathon- Government furnished equipment Type MA-5

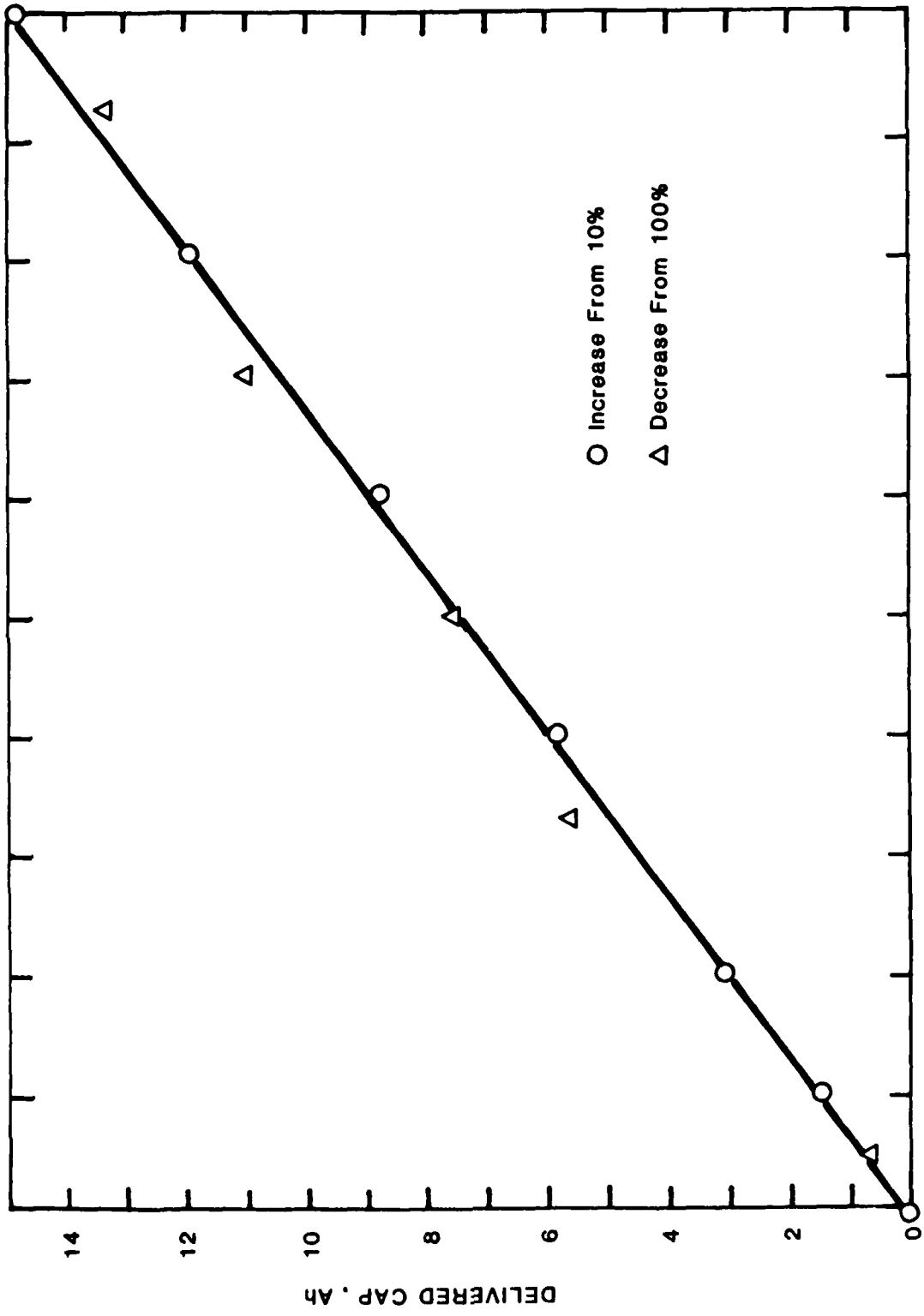

FIGURE 6.11 STATE OF CHARGE vs. DELIVERED CAPACITY

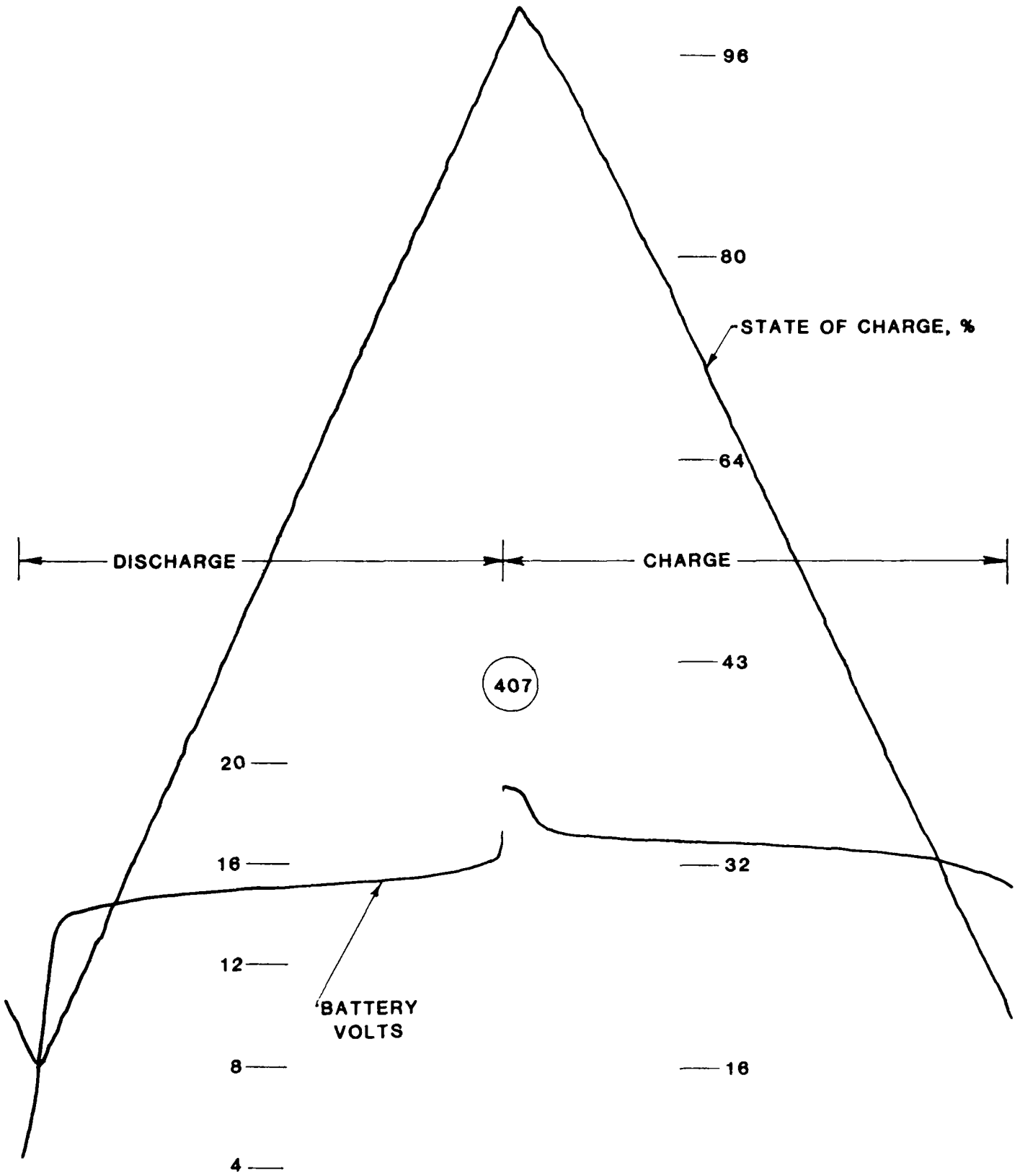

FIGURE 6.12 TANDEM OPERATION TRACKING CYCLER 1, CYCLE 407

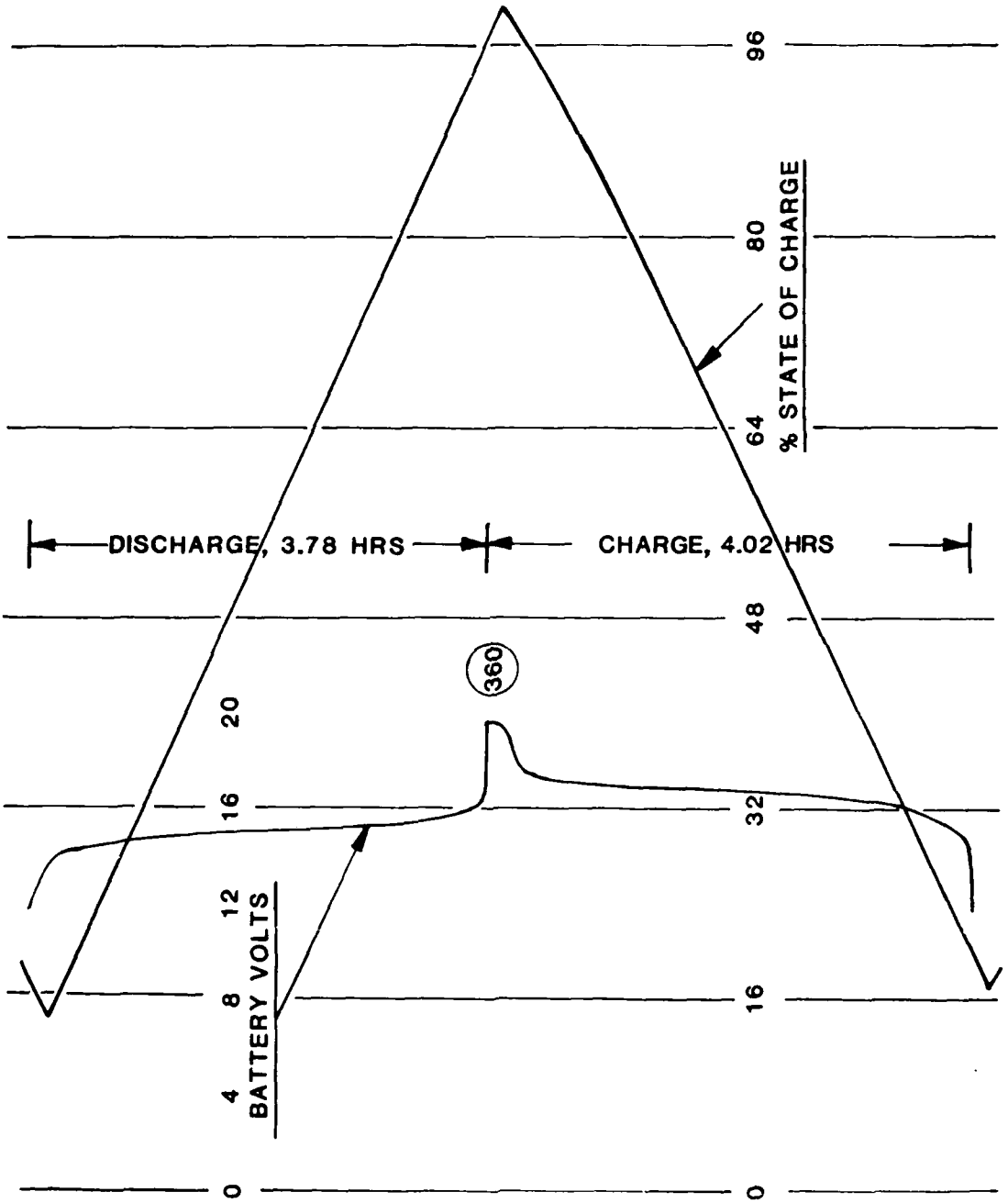

FIGURE 6.13 TANDEM OPERATION–TRACKING CYCLER 1, CYCLE 360

The test schedule was staggered such that all the four batteries could be tested using the two tracking cyclers. Within the range to which it is designed for, the cycler can be used with any battery as long as the currents to the battery and pilot cell are maintained proportional to their respective capacities. In addition, it is emphasized again that it is imperative that the positive electrode of the nickel oxygen cell should be identical to that in the battery for the system to be compatible.

6.3.1 Saft Aircraft Battery

The Saft battery was used for preliminary evaluation and the results were discussed in paragraphs 6.1 and 6.2. Despite the lower voltage at the end of discharge, as scheduled, tests were continued to identify the reasons for the lower potential.

The 12-cell battery stack was removed from the cycler and tested for capacity. First, the battery was charged at 6 amps to 19.0 volts (1.58 v/cell) followed by a charge of 2 amps for 3 hours. It was then discharged at 6 amps and the delivered capacity was 14.0 Ah to an end voltage of 9.6 volts (0.8V/cell). The test was repeated and identical results were obtained. The discharge curve is shown in Figure 6.14.

Fresh cells at the commencement of tests for tracking accuracy delivered a capacity of 16.0 Ah. The loss in capacity after 500 cycles is 12.5%. The tests were stopped and the tracking characteristics during Cycle 495 are shown in Figure 6.15.

6.3.2 Marathon Aircraft Battery

A second cycler, similar to the first, was built to evaluate the tracking characteristics using the aircraft battery made by a second manufacturer (Marathon). As before, a nickel oxygen cell was

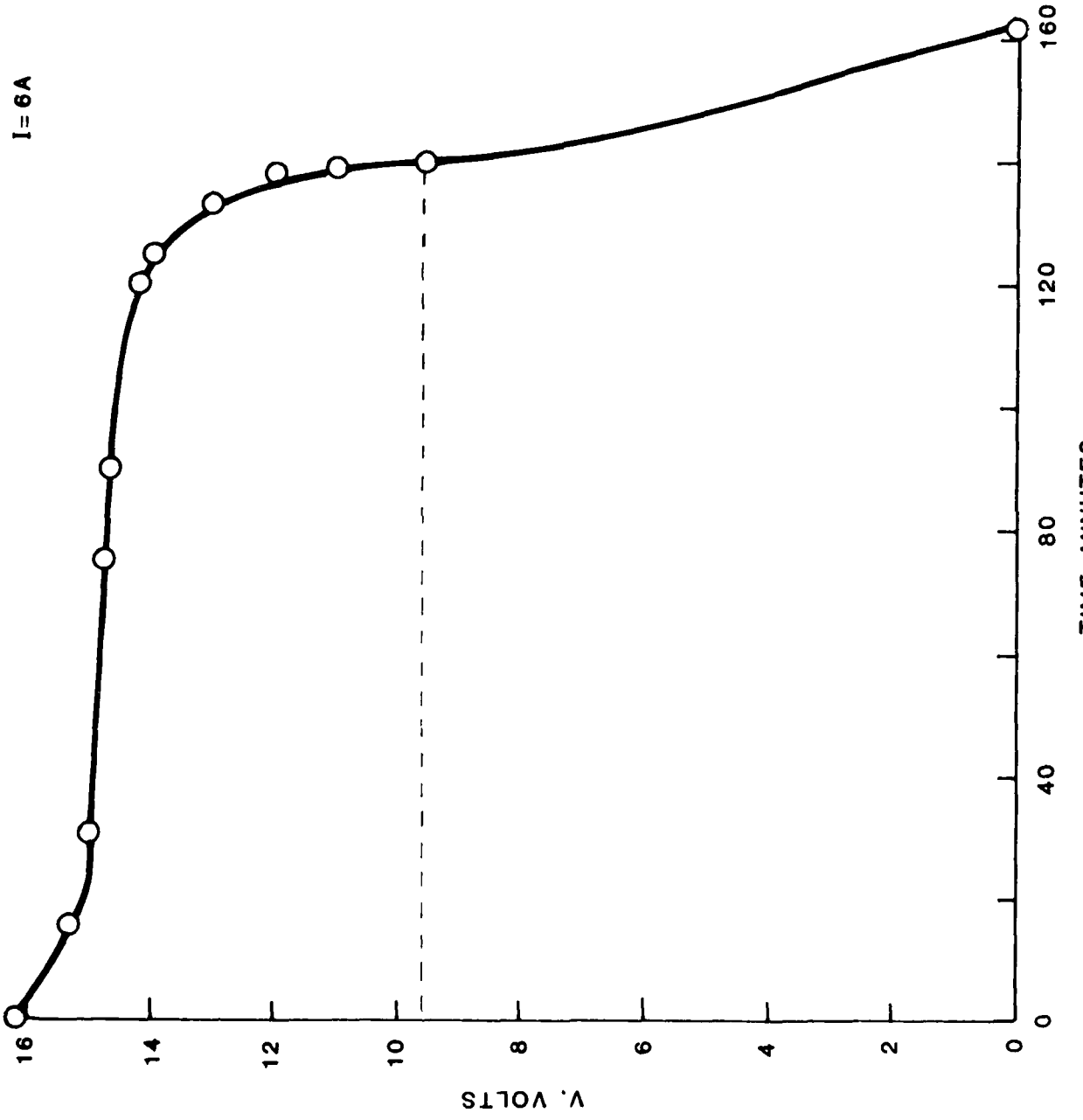

FIGURE 6.14 DISCHARGE PERFORMANCE OF SAFT AIRCRAFT 12-CELL STACK

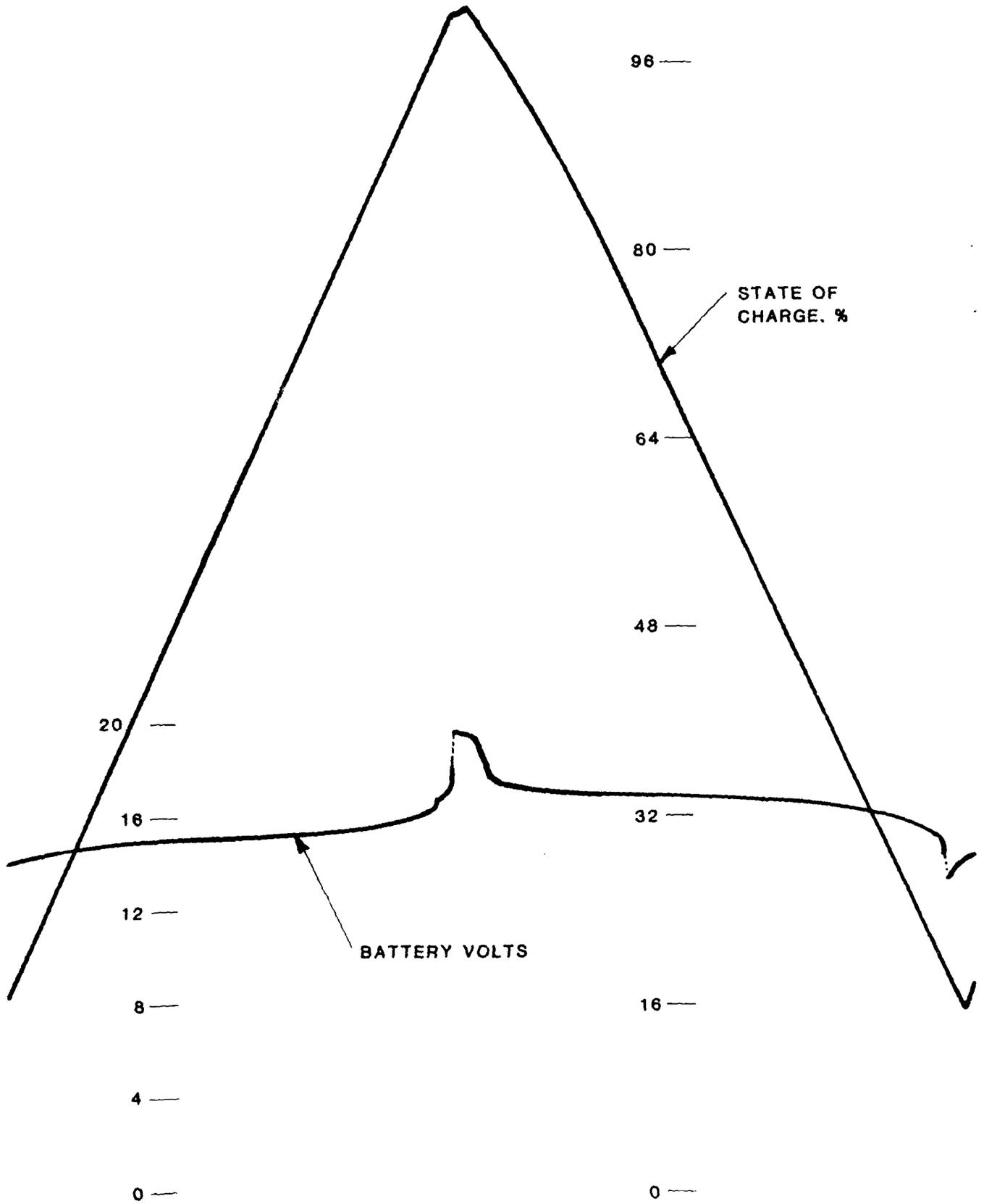

FIGURE 6.15 TANDEM OPERATION - TRACKING CYCLER 1, CYCLE 495

built with an identical nickel electrode used in Marathon cells. Cycling currents and times were adjusted and the battery was fully charged, followed by a deep discharge and the performance characteristics are shown in Figure 6.16. Based on the results, further fine tuning of Ni-0_2 cell current was made and cycling was started at ambient conditions. State of charge and voltage profiles for cycle 18 are shown in Figure 6.17.

Tandem cycling was continued at room temperature to ensure satisfactory operation. We decided to run the cycling tests at constant temperature to improve accuracy even more by eliminating ambient temperature excursions. The pilot cell was kept in an oven and the battery in a water bath, both maintained at 31°C. Problems were encountered in keeping the battery and pilot cell in phase. The temperature was dropped to 25°C and the operation was normal. The data for cycles 121 and 195 are shown in Figures 6.18 and 6.19.

Life tests were interrupted to evaluate the capacity delivered against the state of charge. The test procedure was similar to that used for Saft battery, the only difference being that the Saft battery was tested at ambient temperature while tests with the Marathon battery were carried out at a constant temperature of 25°C.

The battery was charged to various levels between 10 percent and 100 percent in each case discharged fully and the delivered capacities were calculated. The tests were repeated in the opposite direction, lowering the state of charge in steps between 100 percent and 10 percent. In all cases, the battery was discharged until the state of charge was 0 percent. The results are summarized in table 6.4 and Figure 6.20.

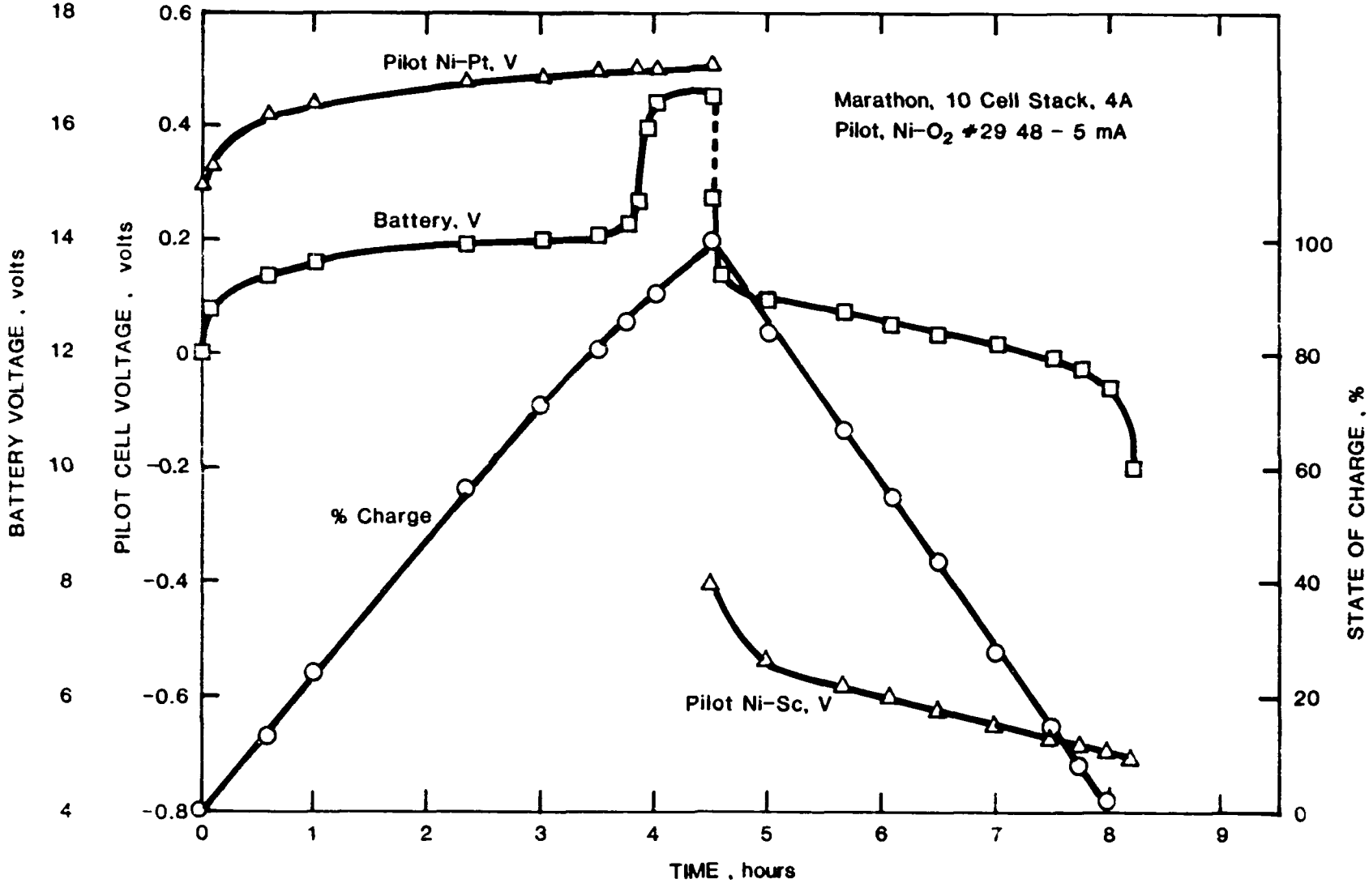

FIGURE 6.16 TRACKING CYCLER 2 - 100% D.O.D.

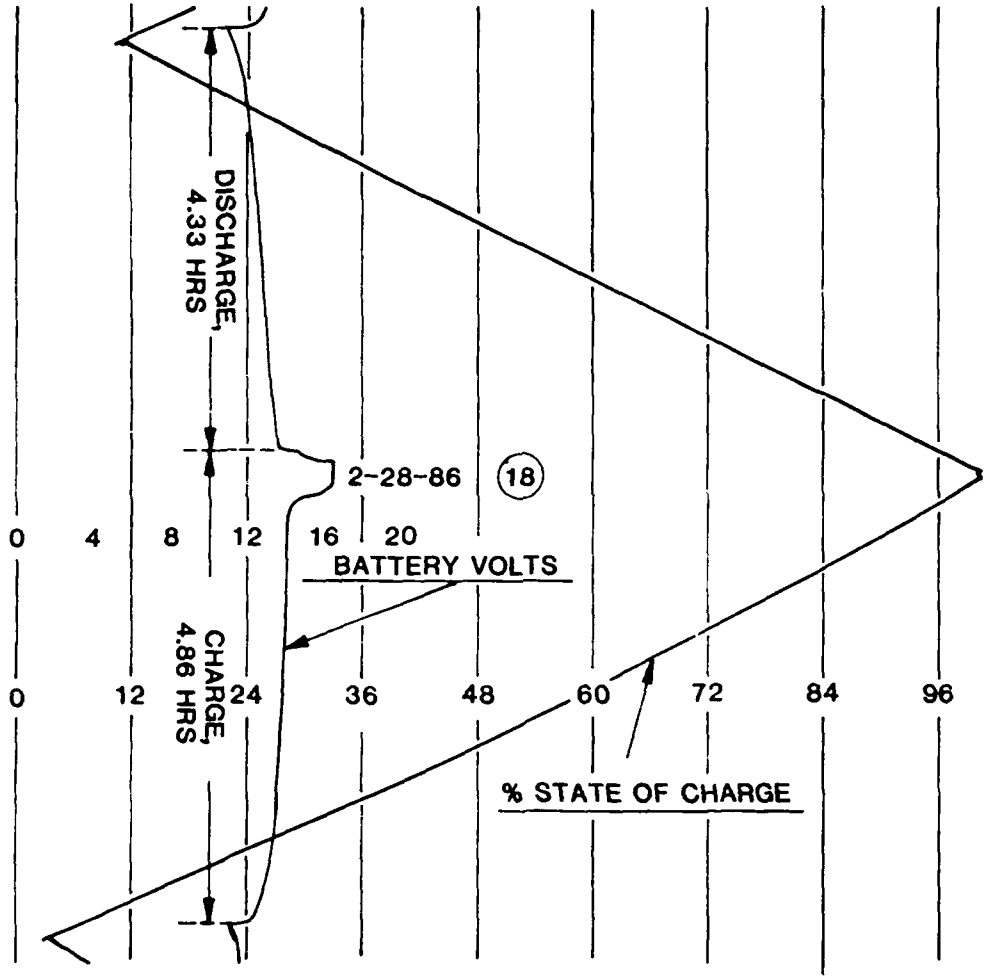

FIGURE 6.17 PERFORMANCE CHARACTERISTICS-TRACKING CYCLER 2, CYCLE 18

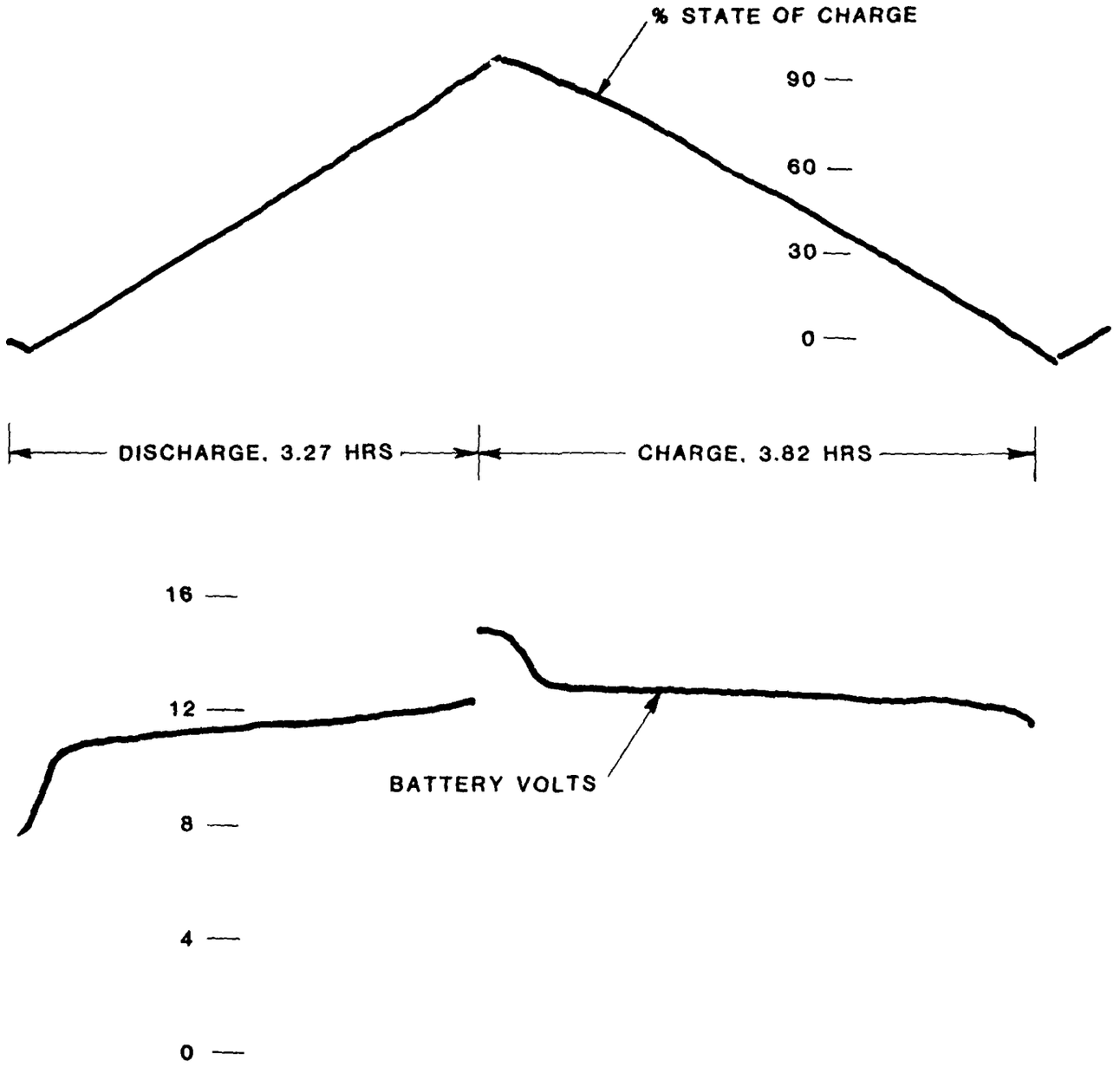

FIGURE 6.18 TANDEM OPERATION, TRACKING CYCLER 2, CYCLE 121

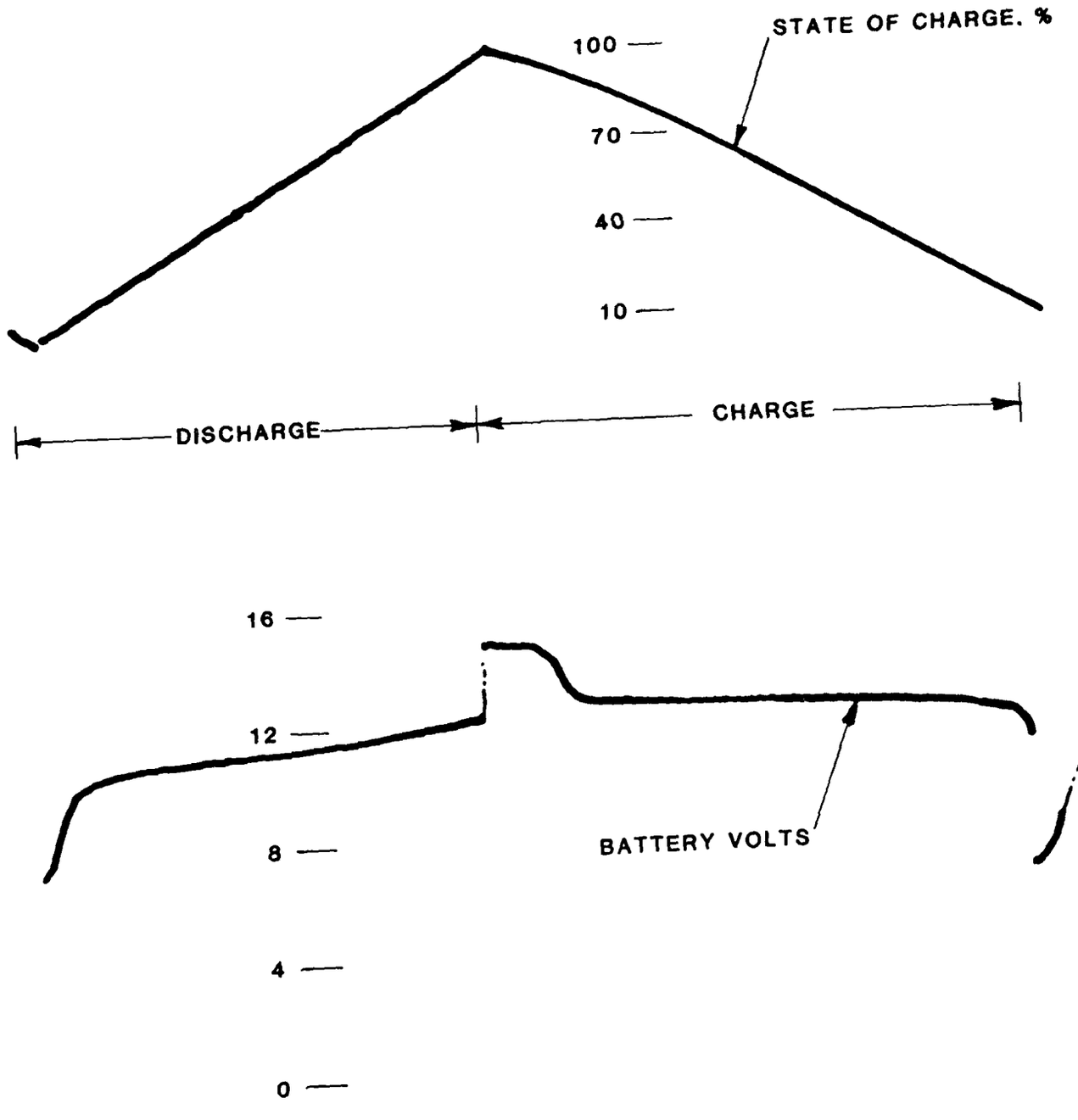

FIGURE 6.19 TANDEM OPERATION - TRACKING CYCLER 2, CYCLE 195

TABLE 6.4

STATE OF CHARGE VS. DELIVERED CAPACITY

TRACKING CYCLER 2 MARATHON 9 CELLS @ 4.0 A

CHARGE TO X %; DISCHARGE TO 0 % CONSTANT T = 25°C

Cycle	CHARGE				DISCHARGE					% over	Ah out
No.	Hrs.	Ah	end V	%	Hrs.	Ah	end V	%	Δ %	Charge	Ah in.
204	0.37	1.48	12.32	10	0.42	1.68	5.14	0	10	-	1.14
205	0.67	2.68	12.48	20	0.63	2.53	5.23	0	20	60	0.79
206	1.93	7.72	12.69	60	1.88	7.53	5.95	0	60	264	1.01
207	1.22	4.88	12.64	40	1.25	5.00	5.80	0	40	-37	1.03
208	2.55	10.20	12.84	80	2.53	10.12	5.95	0	80	104	0.99
209	3.27	13.08	14.61	100	3.15	12.60	4.12	0	100	29	0.96
210	3.32	13.28	14.76	100	3.10	12.40	2.36	0	100	5	0.93
211	2.92	11.68	13.00	90	2.78	11.12	5.20	0	90	-6	0.95
212	2.25	9.00	12.78	70	2.16	8.64	3.33	0	70	-19	0.96
213	1.60	6.40	12.69	50	1.57	6.28	5.70	0	50	-26	0.98
214	0.97	3,87	12.60	30	0.95	3.80	5.47	0	30	-38	0.98
215	0.33	1.32	12.47	10	0.35	1.40	3.37	0	10	-65	1.06

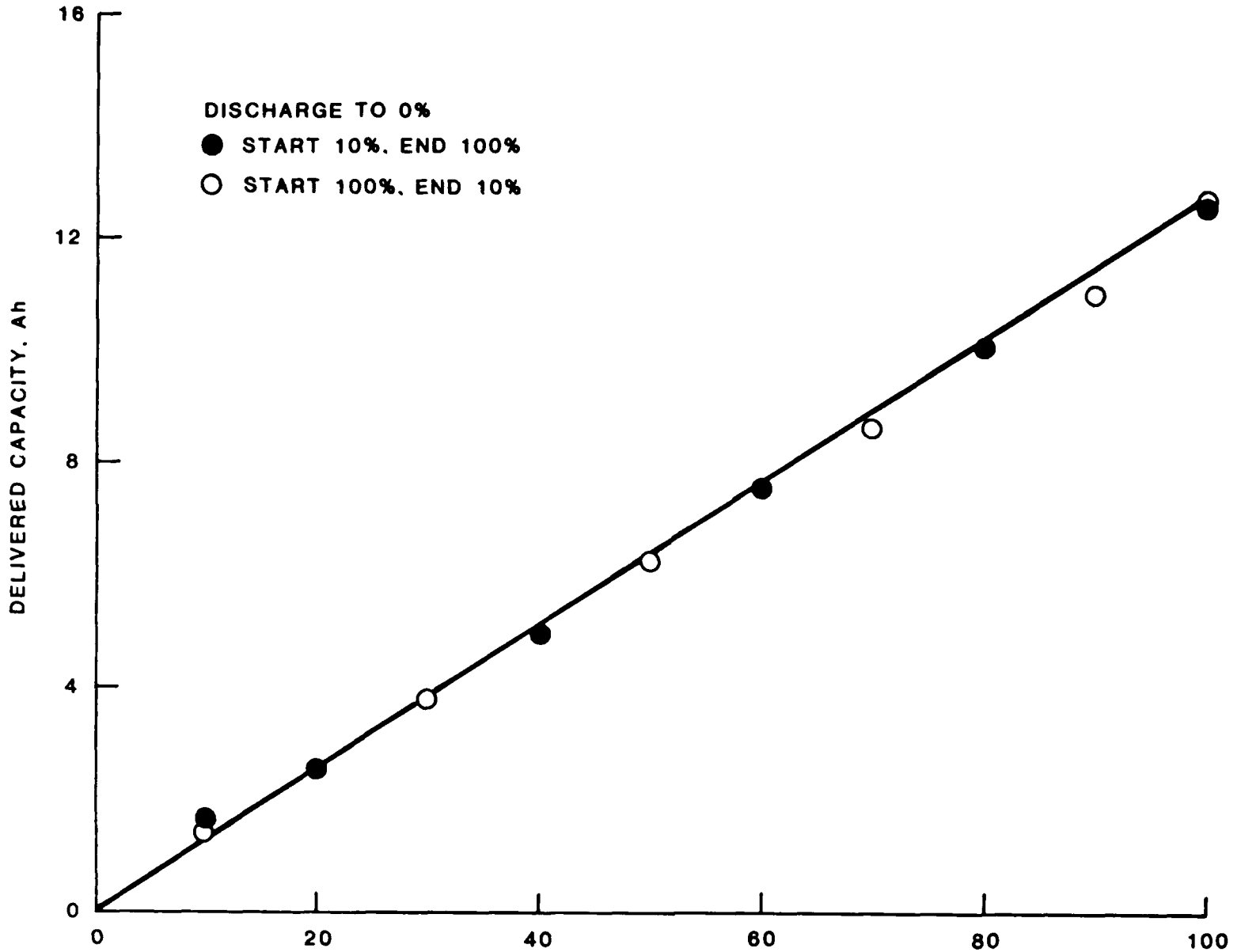

FIGURE 6.20 STATE OF CHARGE VS. DELIVERED CAPACITY - TRACKING CYCLER 2, MARATHON

A similar series of tests were done terminating discharge when the battery voltage reached 6.0V (0.67 V per cell). The data are given in Table 6.5 and illustrated in Figure 6.21.

Having completed over 200 cycles at a constant temperature of 25°C, the same setup was used to evaluate the performance at cold temperature. First attempts were made to reduce the temperature using dry ice. This resulted in the temperature going down much lower than desired (-40°C) and the system did not function at so low a temperature. The delivered capacities of both the aircraft battery and the pilot cell were lower but not to the same extent. In addition, some of the components in the electronics circuitry were not rated for operation at such a low temperature. This approach was therefore abandoned and an auxiliary refrigeration chilling unit was purchased. Pending receipt of the unit, life cycle tests on tandem operation were resumed at ambient temperature and the tracking characteristics (cycle 343) are shown in Figure 6.22.

The refrigerator-chiller unit was commissioned to operation and test runs for calibration were started. Temperature of the battery and NiO_2 cell were maintained at 6-7°C and 10-11°C respectively. Currents and gain were adjusted for tandem operation and the state of charge readings at full charge and full discharge are given below.

Discharge was considered complete when the battery voltage reached 8.0 V (0.8V/c

TABLE 6.5

% CHARGE REMOVED VS. DELIVERED CAPACITY

TRACKING CYCLER 2 MARATHON, 9 CELLS @ 4.0 A

CHARGE TO X %, DISCHARGE TO 6.0V (0.67V/CELL); CONSTANT TEMPERATURE, 25°C

Cycle No.	CHARGE				DISCHARGE				Δ %	% Over Charge	Ah out / Ah in.
	Hrs.	Ah	end V	%	Hrs.	Ah	end V	%			
216	0.25	1.00	12.52	10	0.12	0.48	6.00	8	2	-	0.48
217	0.47	1.87	12.58	20	0.40	1.60	6.00	8	12	289	0.86
218	1.05	4.20	12.66	40	1.16	4.64	6.00	4	36	163	1.10
219	1.82	7.28	12.75	60	1.78	7.13	6.00	3	57	57	0.98
220	2.50	10.00	12.88	80	2.35	9.40	6.00	6	74	40	0.94
221	3.33	13.32	14.30	100	2.67	10.68	6.00	15	85	42	0.80
222	3.00	12.00	14.76	100	2.70	10.80	6.00	14	86	12	0.90
223	2.72	10.88	12.98	90	2.45	9.80	6.00	12	78	1	0.90
224	1.90	7.60	12.74	70	1.77	7.08	6.00	14	56	-22	0.93
225	1.16	4.64	12.64	50	1.20	4.80	6.00	13	37	-35	1.03
226	0.58	2.33	12.53	30	0.55	2.20	6.00	14	16	-51	0.94
227	0.27	1.07	12.40	20	0.22	0.88	6.00	15	5	-51	0.62

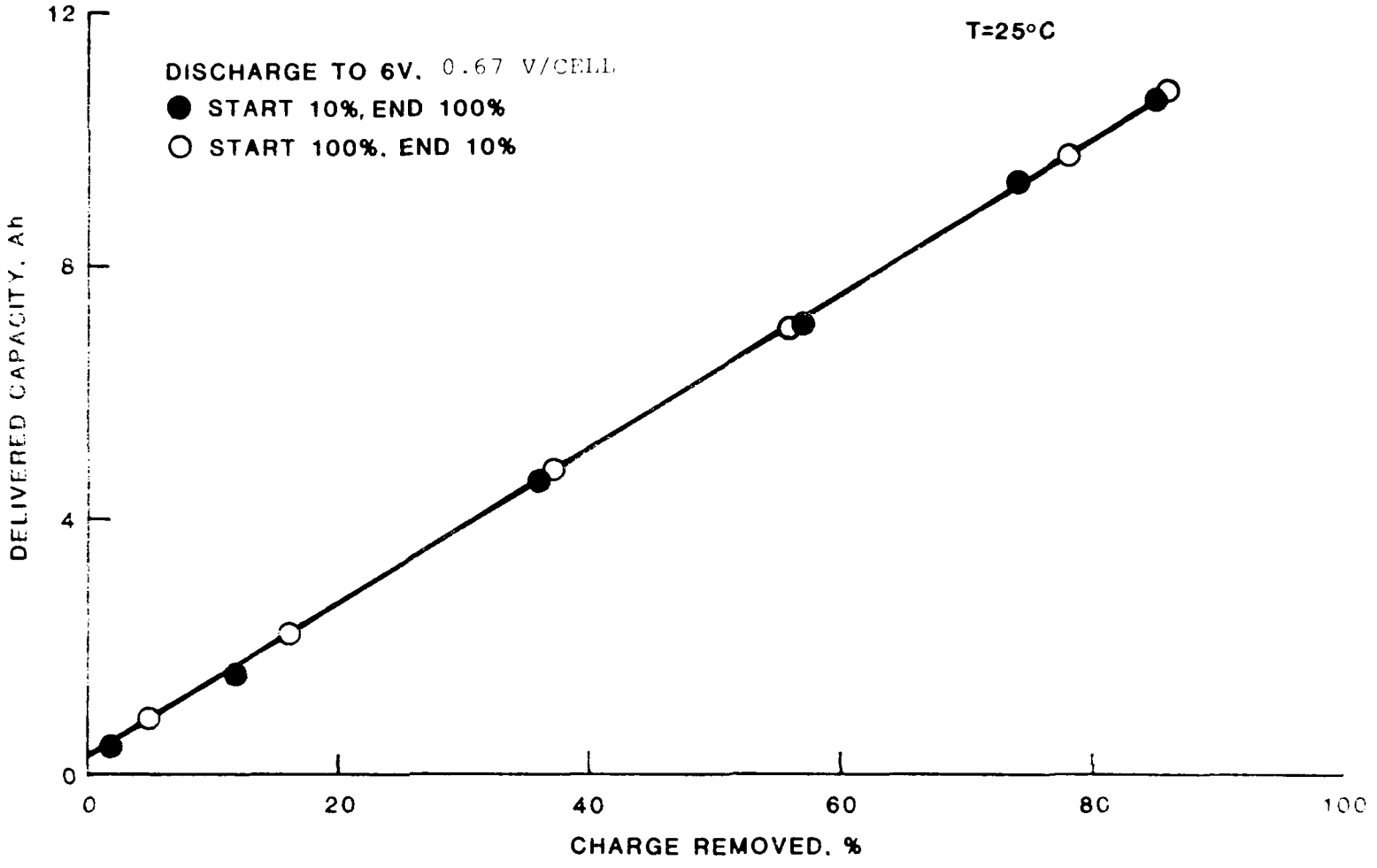

FIGURE 4.21 PERCENT CHARGE REMOVED VS. DELIVERED CAPACITY - TRACKING CYCLER 2, MARATHON

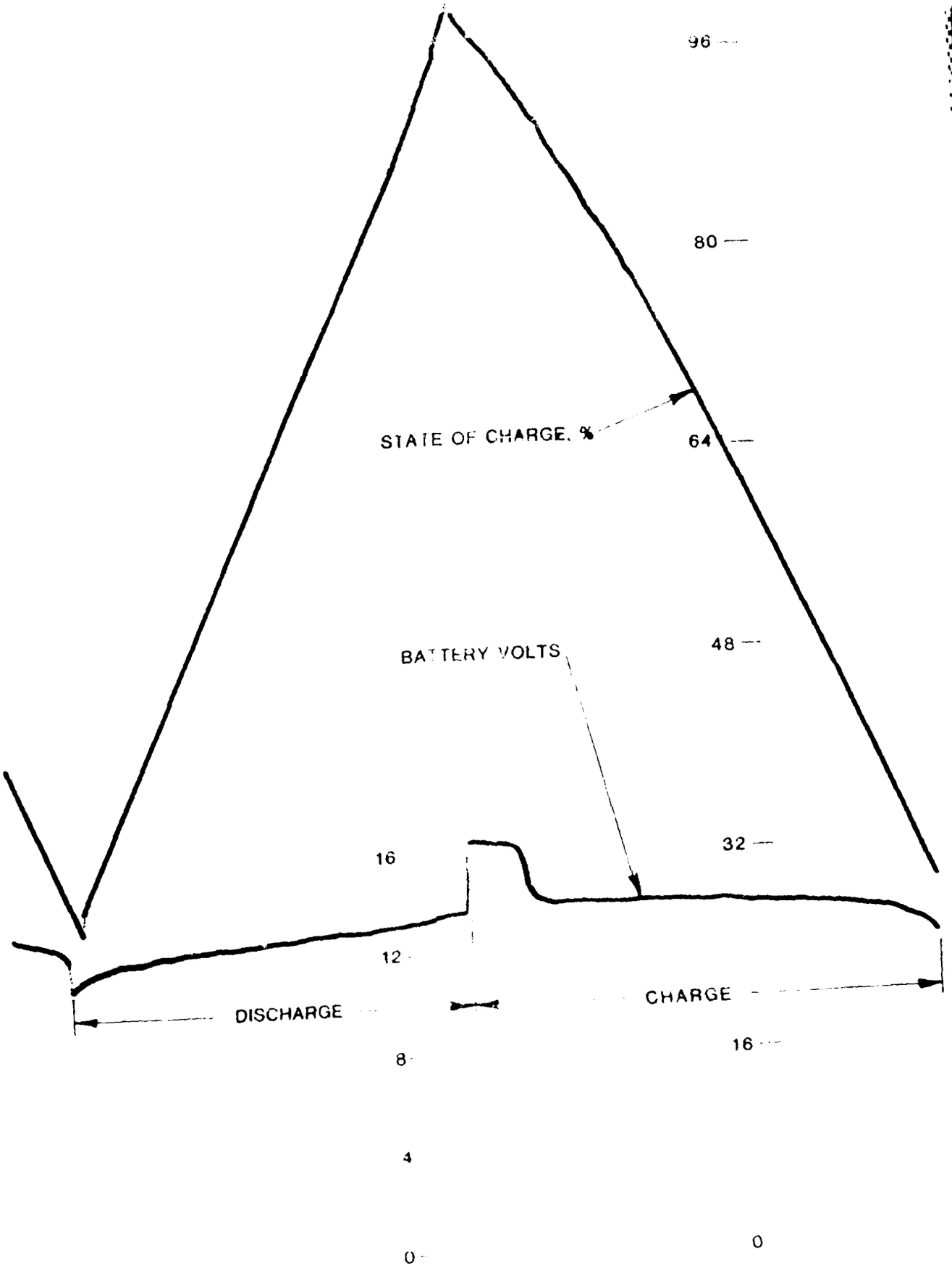

FIGURE 6.22 TANDEM OPERATION, TRACKING CYCLER 2, CYCLE 343

Cycle No.	Volts/State of Charge - %	
	Fully Charged	Fully Discharged
398	14.4/100	0.5/43
399	16.7/100	8.0/38
400	16.8/100	8.0/37
401	16.8/100	8.0/33
402	16.8/100	8.0/28
403	16.8/100	8.0/28
404	16.8/100	7.6/9
405	16.8/100	8.0/9
406	16.8/100	8.0/11
407	16.8/100	8.0/2
408	16.8/100	8.0/3

After adjusting currents to the battery and pilot cell for tandem operation, the system was subjected to the standard state of charge vs. delivered capacity test matrix.

Tests were carried out in both directions - going up in steps to 100% and vice versa. The experimental data are summarized in Table 6.6 and the linear relationship is shown in Figure 6.23. Figure 6.24 shows the dependency of delivered capacity on percent of charge removed.

The changes in the state of charge with capacity are shown in Figure 6.25. Cycling in the "auto" regimen was resumed and data for cycle 530 are shown in Figure 6.26.

Tests were stopped after 670 cycles due to expiration of contract and the system was still performing well. This is the longest number of cycles achieved on tandem operation. Prior to termination of tests, a manual cycle - full charge/100% discharge - was performed, results of which are shown in Figure 6.27.

6.3.3 General Electric Aircraft Battery

After testing of Saft battery was completed, the same tracking cycler (1) was used to evaluate the tracking characteristics with G.E. aircraft battery. Pilot Cell 50 was built with a

TABLE 6.6

State of Charge vs. Delivered Capacity

10 Cell Marathon @ 3.5A/Ni-O_2 29 @ 59 mA

Date	Cycle #	Mode	T°c	Hrs	Ah	End V	End %	% over-charge	% Ah Eff.	▲%
1 26/87	412	Chg.	6	0.37	1.28	13.6	10	-		
		Dischg.	8	0.25	0.88	8.0	5		69	5
	413	Chg.	6	0.57	1.98	13.9	20	125		
		Dischg.	6	0.58	2.04	8.0	4		100	16
1 27/87	414	Chg.	6	1.22	4.27	14.1	40	100		
		Dischg.	6	1.33	4.62	8.0	5		100	33
	415	Chg.	6	1.97	6.88	14.2	56	40		
		Dischg.	7	2.03	7.12	8.0	5		100	55
1 28/76	416	Chg.	7	2.75	9.63	14.5	80	35		
		Dischg.	7	2.83	9.91	8.0	6		100	74
1 29/87	417	Chg.	5	3.50	12.25	16.6	100	24		
		Dischg.	7	3.43	12.01	8.0	6		98	91
	*	Dischg.	7	3.67	12.85	2.2	0		100	100
1 30/87	418	Chg.	5	3.70	12.95	16.6	100	0		
		Dischg.	7	3.55	12.43	8.0	4		96	83
	*	Dischg.	7	3.70	12.95	4.0	0		100	100
2 2/87	419	Chg.	5	3.16	11.06	14.7	90	-15		
		Dischg.	7	3.22	11.27	8.0	5		100	85
2 4/87	420	Chg.	6	2.22	7.77	14.3	70	-31		
		Dischg.	7	2.37	8.30	8.0	7		100	63
	421	Chg.	6	1.47	5.15	14.2	50	-38		
		Dischg.	7	1.65	5.78	8.0	7		100	43

TABLE 6.6 (continued)

State of Charge vs. Delivered Capacity

10 Cell Marathon @ 3.5A/Ni-O_2 29 @ 59 mA

Date	Cycle No.	Mode	T°c	Hrs	Ah	End V	End %	% over-charge	% Ah Eff.	▲%
2 5/87	422	Chg.	6	0.77	2.68	14.0	30	-53		
		Dischg.	6	0.68	3.09	8.0	7		100	23
	423	Chg.	7	0.28	0.99	13.7	10	-81		
		Dischg.	7	0.13	0.47	7.7	7		47	3
		Dischg.	7	0.25	0.88	1.4	4		88	6
	424	Pilot cell current offset adjusted and auto cycle started.								

* Discharge continued beyond 8V to 0%

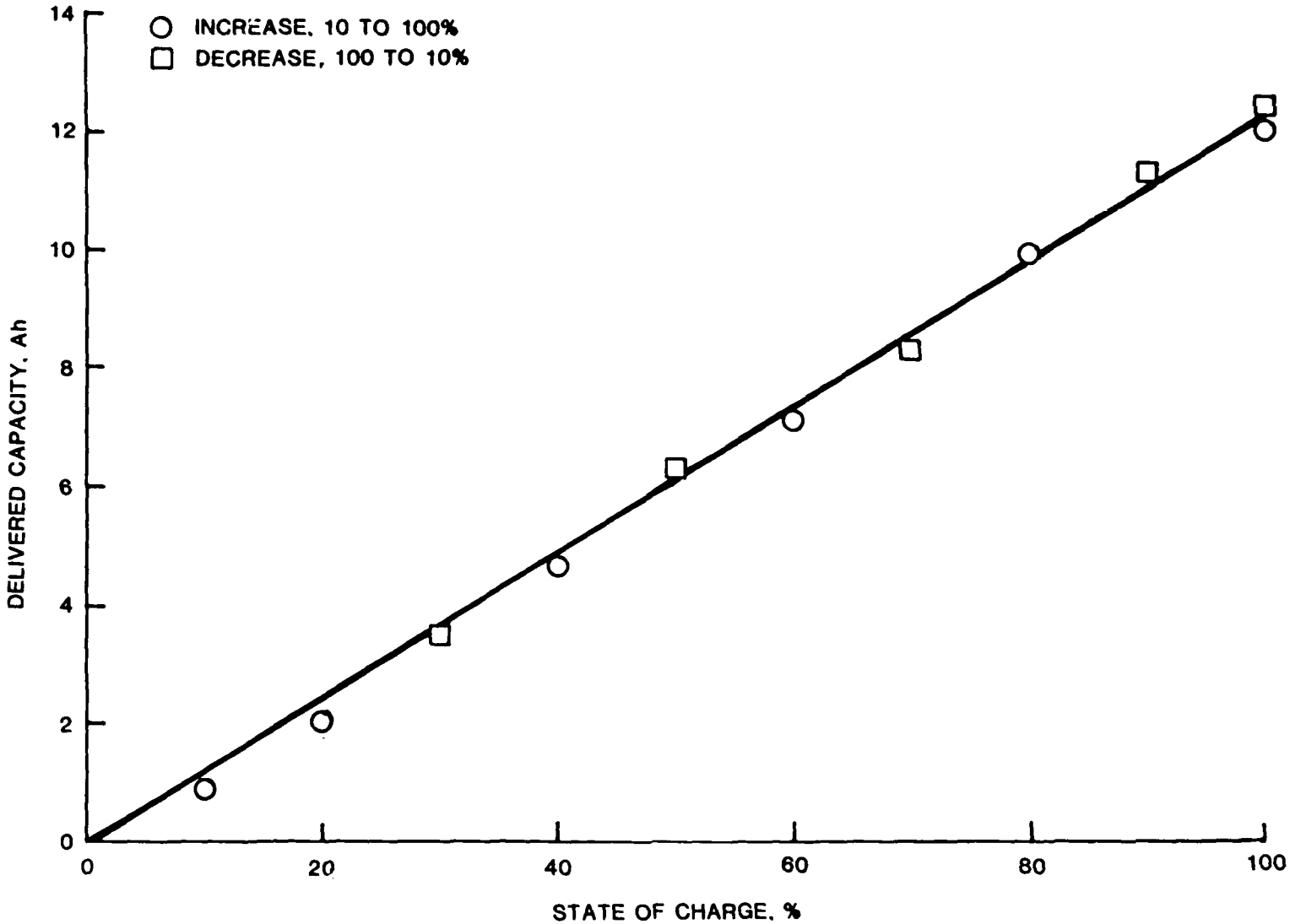

FIGURE 6.23 STATE OF CHARGE VS. DELIVERED CAPACITY – TANDEM OPERATION AT 6°C

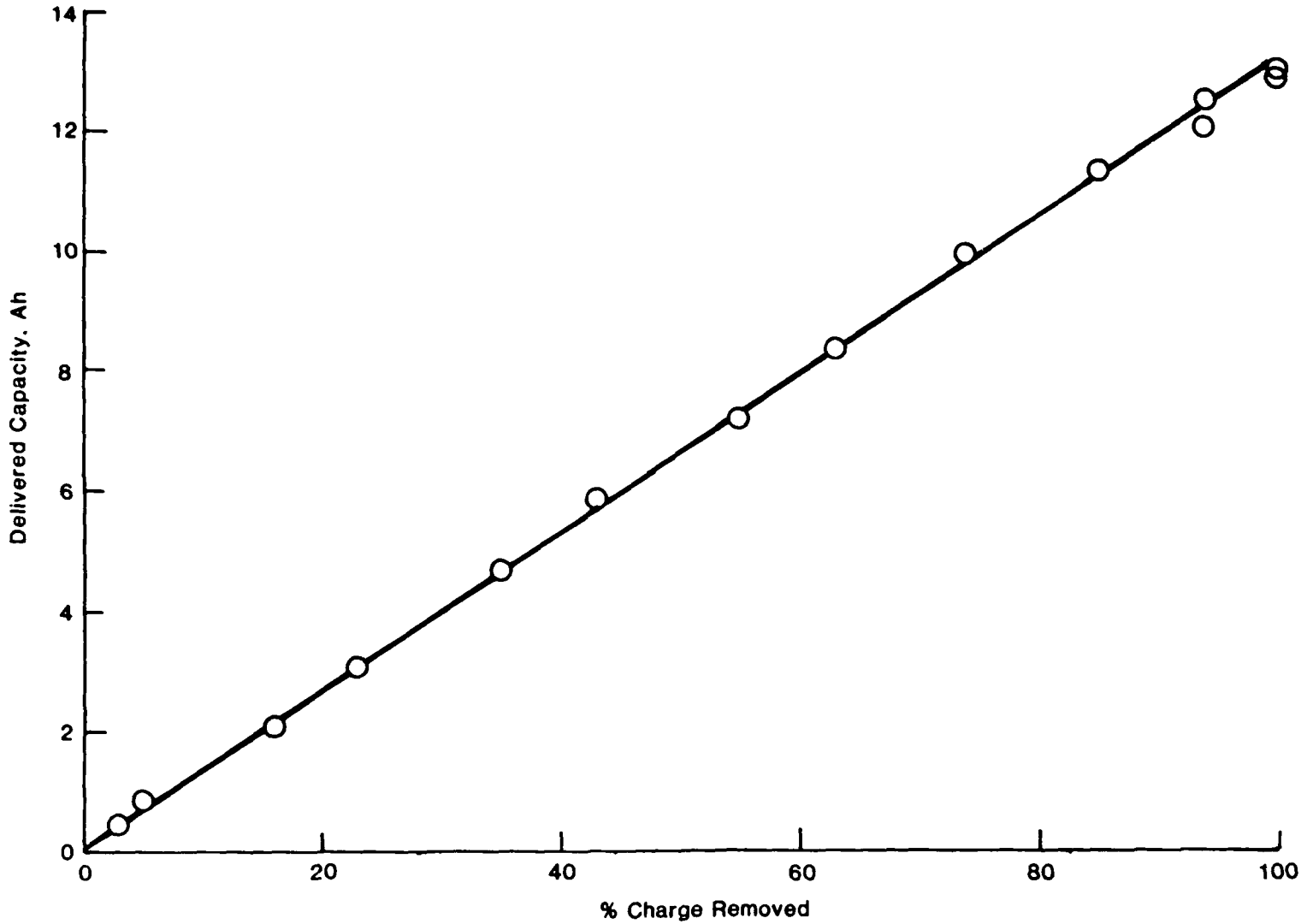

FIGURE 6.24 % CHARGE REMOVED VS. DELIVERED CAPACITY - TANDEM OPERATION AT 6°C

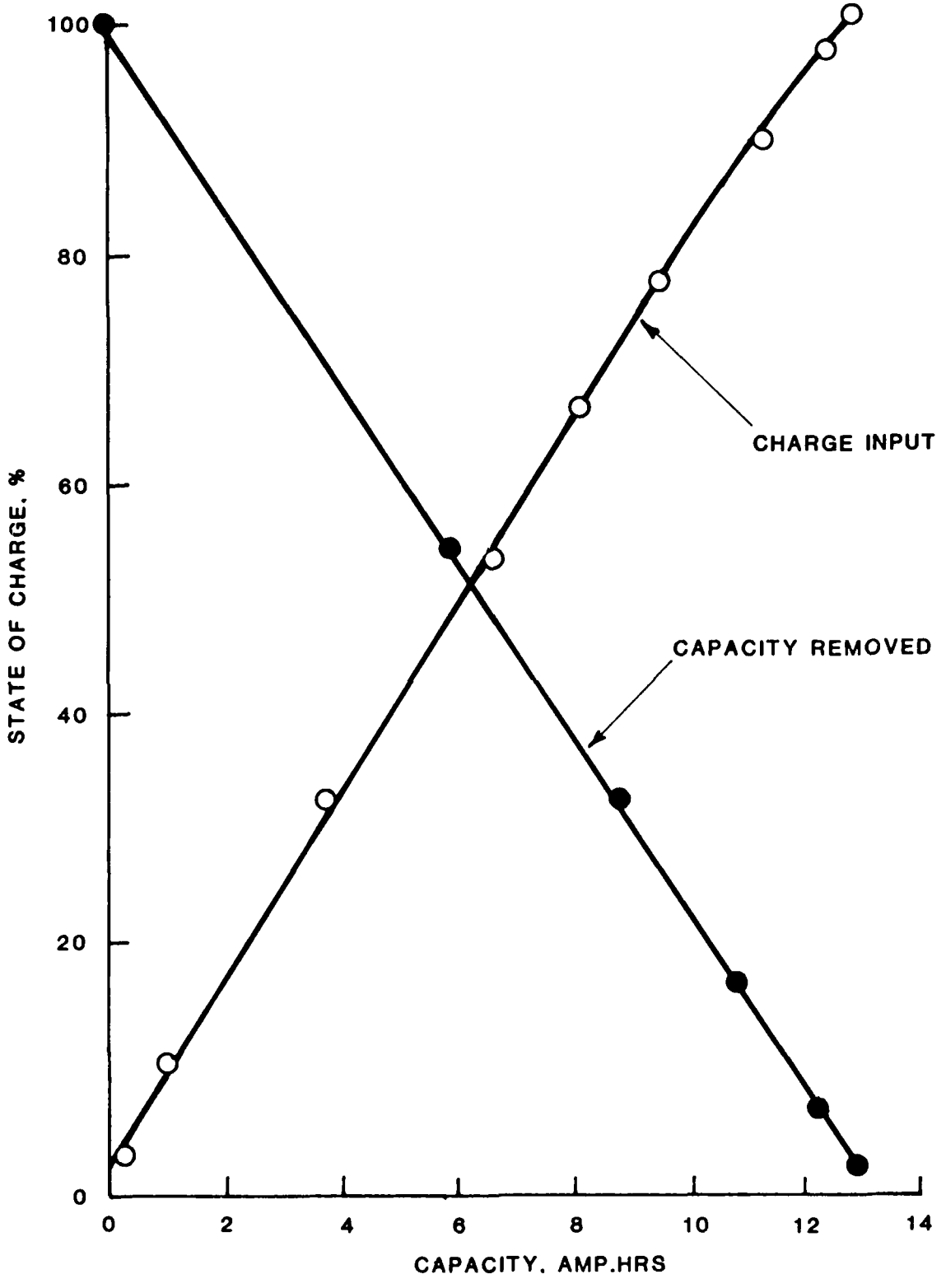

FIGURE 6.25 CAPACITY VS. STATE OF CHARGE - TANDEM OPERATION AT 6°C

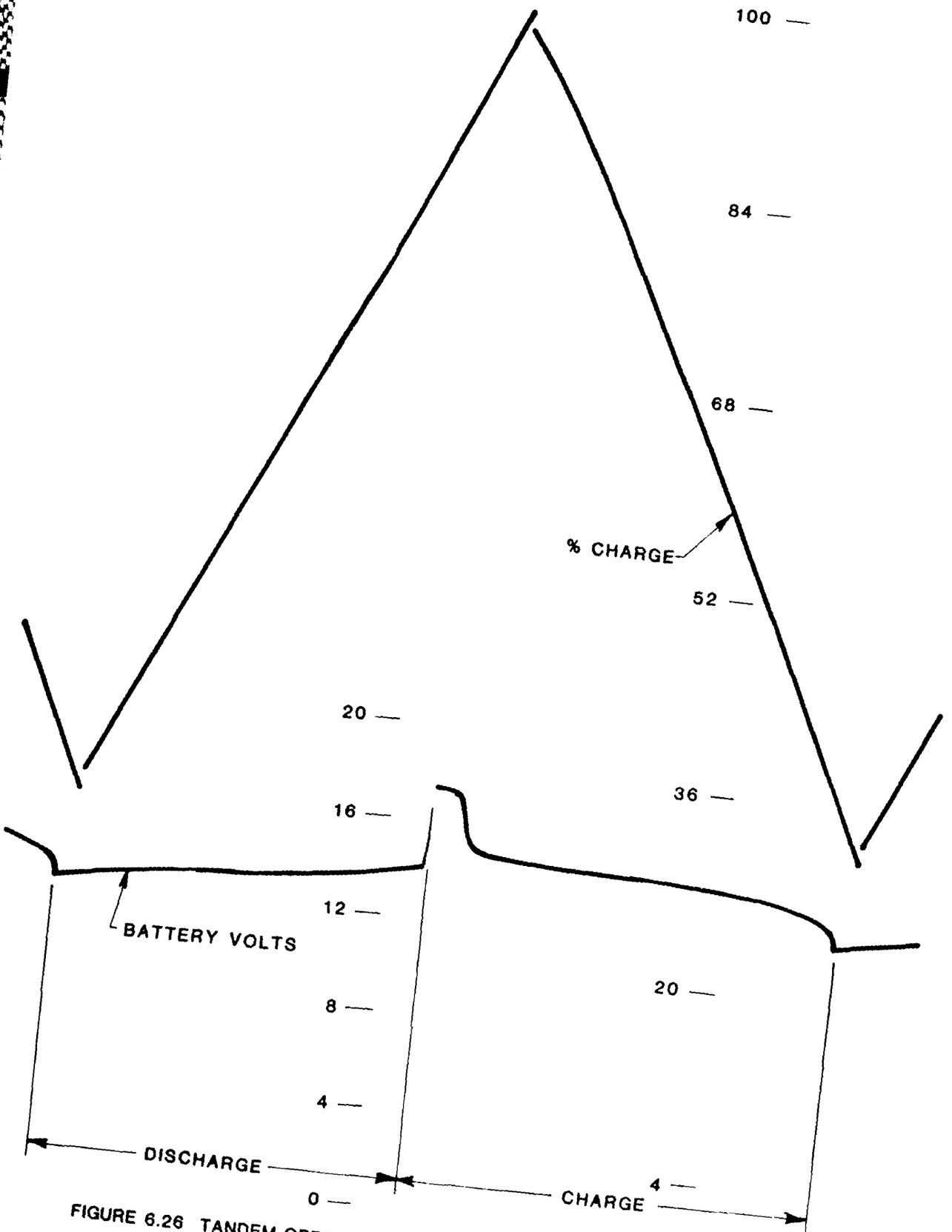

FIGURE 6.26 TANDEM OPERATION. TRACKING CYCLER 2. CYCLE 530

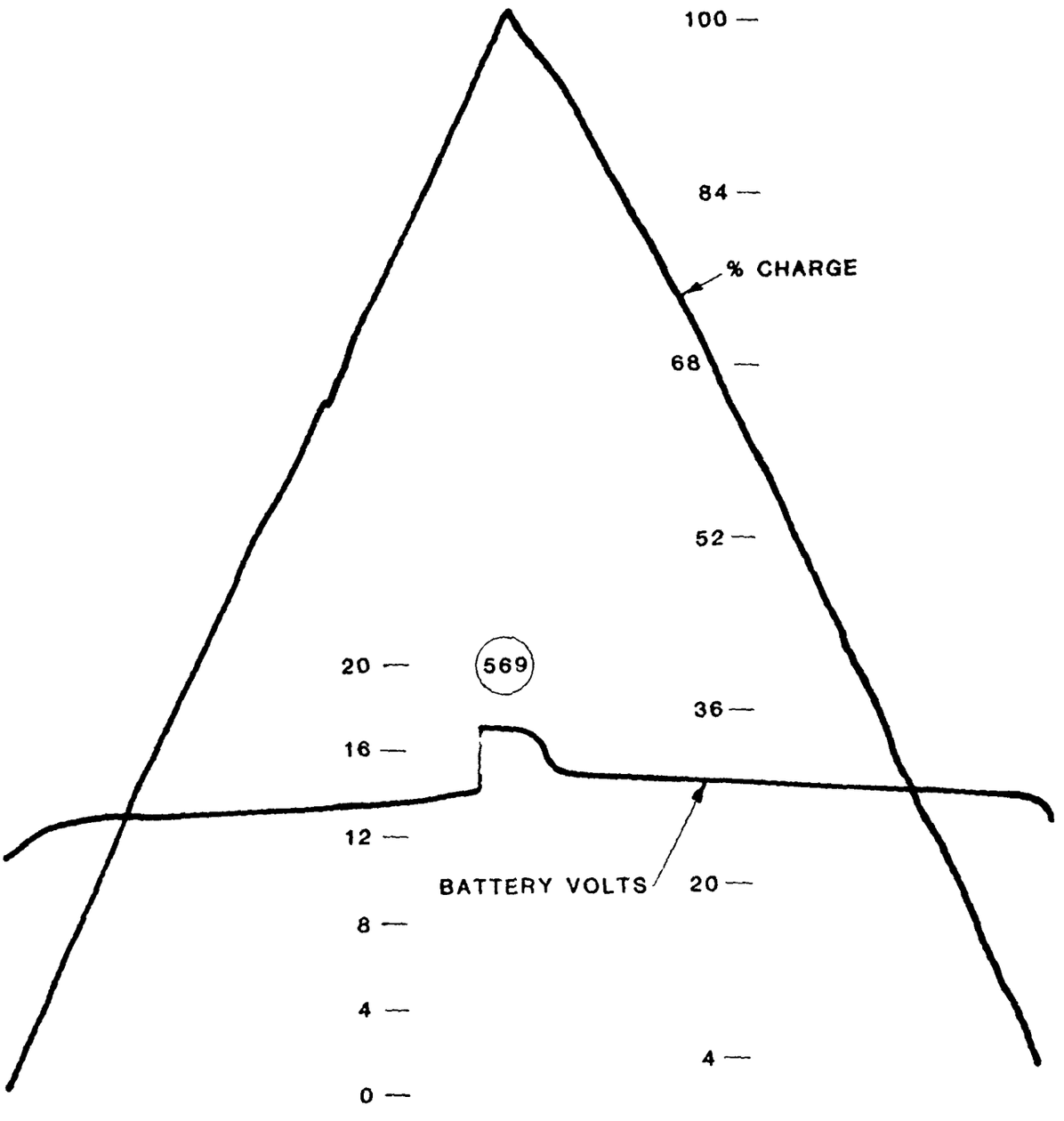

FIGURE 6.27 TRACKING CYCLER 2 - MANUAL CYCLE. 100% D.O.D.

nickel electrode cut out of the one from the battery. The pilot cell and a GE 16-cell aircraft battery were connected to the tracking cycler. The system was calibrated for tandem operation and the calibration data are presented in Table 6.7.

Life cycle tests were started and Figure 6.28 shows for cycle 21, that the battery did not reach full charge. Cycling was interrupted and system was recalibrated as per data in Table 6.8.

Following same procedure used with Saft and Marathon batteries, tests to evaluate the relationship between state-of-charge and delivered capacity were carried out. Currents to the 16-cell-GE aircraft battery and the Ni-O_2 cell were kept constant at 3.5 amps and 67 mA respectively.

Starting with the battery in a fully discharged state, the battery was charged to 10% followed by discharging until the state-of-charge reached 0%. The battery voltage and charge % were monitored and their variations with time are shown in Figure 6.29. The same procedure was repeated in steps to full charge of 100% and the experimental data are shown in Figures 6.30 through 6.34. The variations in state of charge for the different steps are shown in Figure 6.35.

The series of tests were repeated in the other direction, starting from full charge, and the results are shown in Figure 6.36. Figure 6.37 shows the relationship between capacity and state-of-charge during charge and discharge. The results are summarized in Table 6.9 and Figure 6.38.

After 85 cycles, tests were stopped to make the tracking cycler available to test the battery furnished by the Air Force.

TABLE 6.7

CALIBRATION DATA, GE-16 CELL STACK AND PILOT 50

Cell No.	Mode	BATTERY				PILOT				% Chg End	BATTERY		Adjust	mA I Pilot Calculated
		Hrs	I avg Amps	Ah	End V	Hrs	I avg mA	Ah	End V C-Ni vs Pt D-Ni vs Sc		% over Charge	Ah eff %		
1	Charge	5.92	3.5	20.72	26.39	4.92	85.0	0.418	0.565	73	-	-	73-99%	71
	Discharge	5.08	3.5	17.78	0	4.00	84.8	0.339	-1.131	21	-	86		67
2	Charge	5.83	3.5	20.41	26.65	4.67	85.0	0.397	0.550	93	15	-	93-98%	68
	Discharge	4.92	3.5	17.22	2.00	3.75	84.9	0.318	-1.100	25	-	84	85-70 mA	65
3	Charge	5.67	3.5	19.85	26.66	5.42	69.7	0.378	0.547	100	15	-		67
	Discharge	4.75	3.5	16.63	0.80	4.33	70.0	0.303	-1.050	29	-	84	29-15%	64
4	Charge	5.58	3.5	19.53	26.55	5.58	69.3	0.387	0.534	97	17	-	97-100%	69
	Discharge	4.58	3.5	16.03	12.80	4.58	70.0	0.321	-1.107	8	-	82	8-3%	70
5	Charge	5.56	3.5	19.46	26.72	5.56	69.1	0.384	0.531	96	21	-	96-100%	69
	Discharge	4.77	3.5	16.70	12.80	4.77	70.1	0.334	-1.885	0	-	86		70
6	Charge	5.16	3.5	18.06	26.78	5.16	69.1	0.357	0.536	100	8	-		69
	Discharge	4.97	3.5	17.40	12.80	4.97	69.8	0.347	-1.976	6	-	96	70-69%	70
7	Charge	5.50	3.5	19.25	26.63	5.50	69.0	0.380	0.532	99	11	-		69
	Discharge	4.58	3.5	16.03	12.80	4.58	69.0	0.316	-1.150	1	-	83		69
8	Charge	5.87	3.5	20.53	26.75	5.87	68.9	0.404	0.539	100	25	-		69
	Discharge	4.75	3.5	16.63	12.80	4.75	69.0	0.328	-2.032	0	-	81		69
9	Charge	5.20	3.5	18.20	0	5.20	69.0	0.359	-2.032	-19	-	89		60
	Discharge	5.83	3.5	20.41	26.45	5.37	68.9	0.370	0.514	100	12	-		69

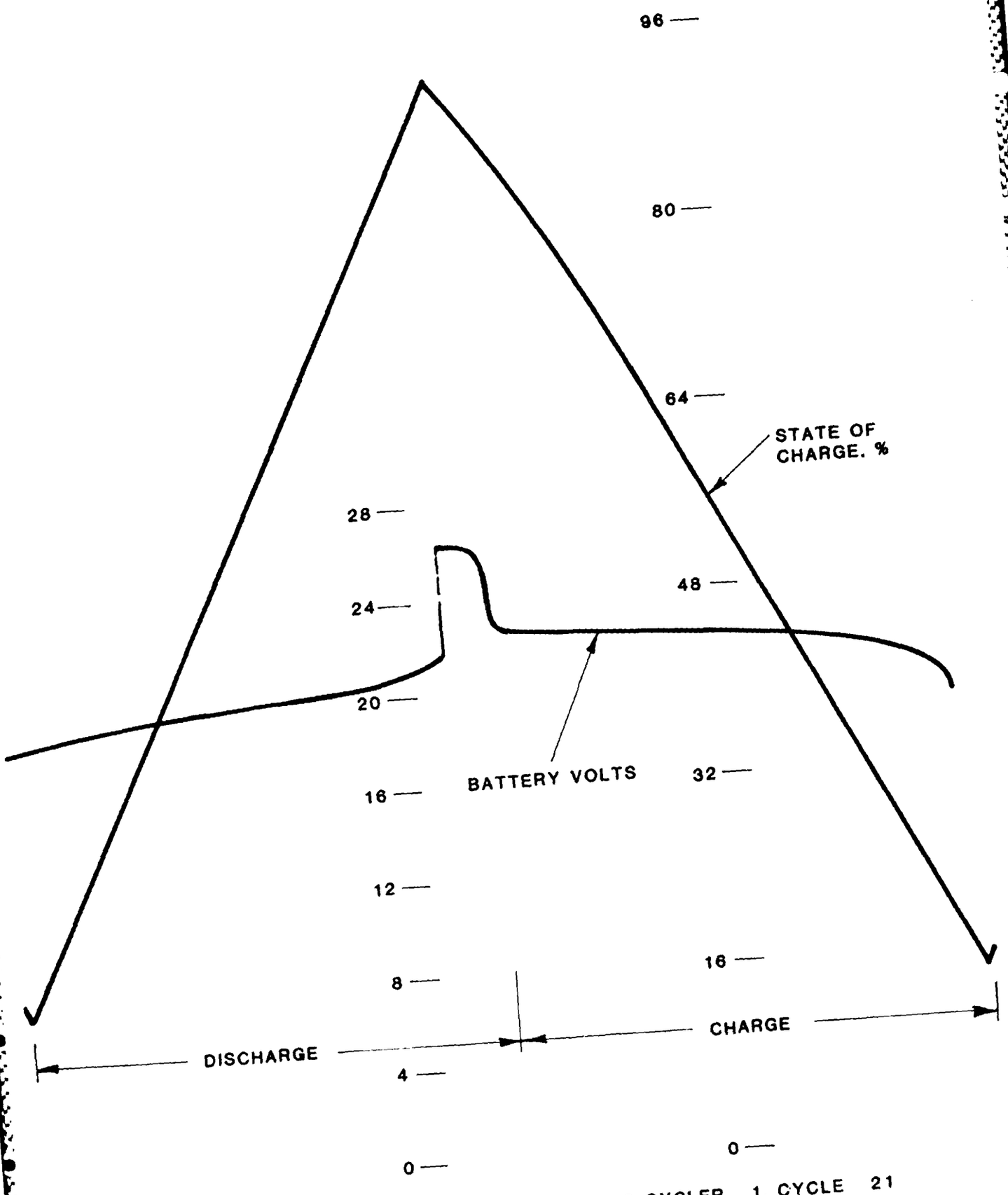

FIGURE 6.28 TANDEM OPERATION, TRACKING CYCLER 1, CYCLE 21

TABLE 6.8

TRACKING CYCLER 1 - CALIBRATION

GE: 16-CELL STACK, 3.5A AND NI-0 50, 67 mA

Cycle No.	Mode	t Hrs.	Battery end V	Battery Ah	Pilot * end V	Pilot Ah	State of Charge %	% Overcharge	% Ah Eff.
40	Chg	-	26.7	-	0.538	-	100	-	-
	Dischg	4.08	11.0	14.28	-1.259	0.273	0	-	-
41	C	4.28	26.6	14.98	0.533	0.287	100	5	-
	D	4.08	8.8	14.28	-2.000	0.273	0		95
42	C	4.58	26.6	16.03	0.530	0.307	100	12	-
	D	4.03	10.7	14.11	-1.400	0.269	0	-	88
43	C	4.75	26.3	16.63	0.525	0.318	100	18	-
	D	4.05	11.5	14.28	-1.230	0.273	0	-	86
44	C	4.25	24.6	14.88	0.527	0.288	100	4	-
	D	3.92	0	13.72	-1.400	0.261	6	-	9-
45	Adjusted full charge 100%; Full discharge ,								
46	12.8V (o.8V/cell) to 0%								
47	C	4.38	26.6	15.33	0.534	0.293	100	-	-
	D	4.06	10.0	14.28	-1.500	0.272	-4	-	93
48	C	4.33	26.6	15.16	0.534	0.290	100	6	-
	D	4.95	1.0	14.18	-1.700	0.270	0	-	94
49	C	4.38	26.3	16.03	0.526	0.306	100	13	-
	D ⊛	3.83	12.8	13.41	-1.095	0.255	0	-	84
50	C	4.35	26.4	15.23	0.531	0.291	100	14	-
	D ⊡	3.89	11.0	13.62	-1.100	0.259	0	-	89

⊛ Discharged immediately after full charge

⊡ Fully charged on stand, then discharged

* Ni vs Pt on charge, Ni vs screen on discharge

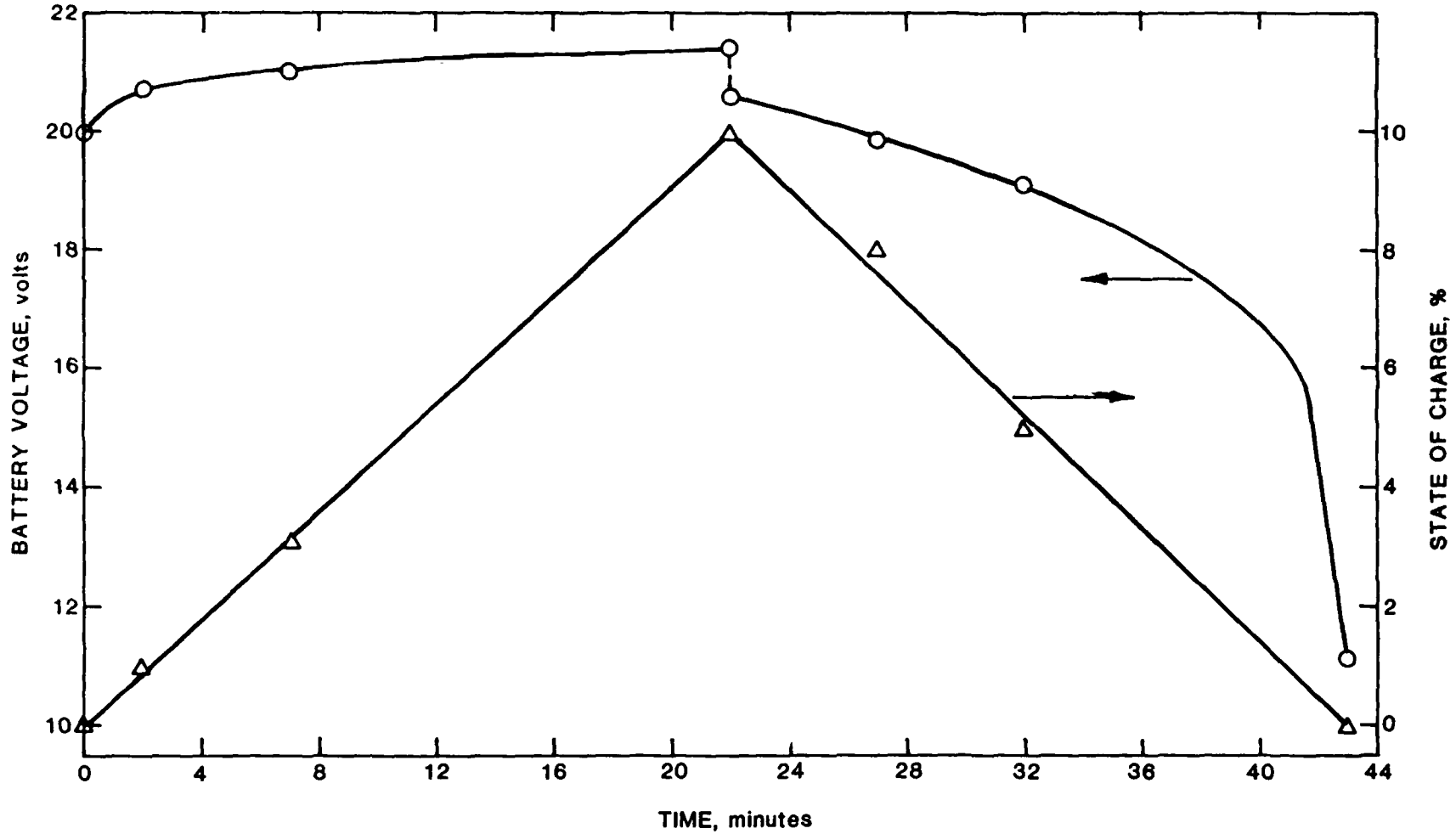

FIGURE 6.29 - BATTERY VOLTAGE AND STATE OF CHARGE-CHARGE TO 10%

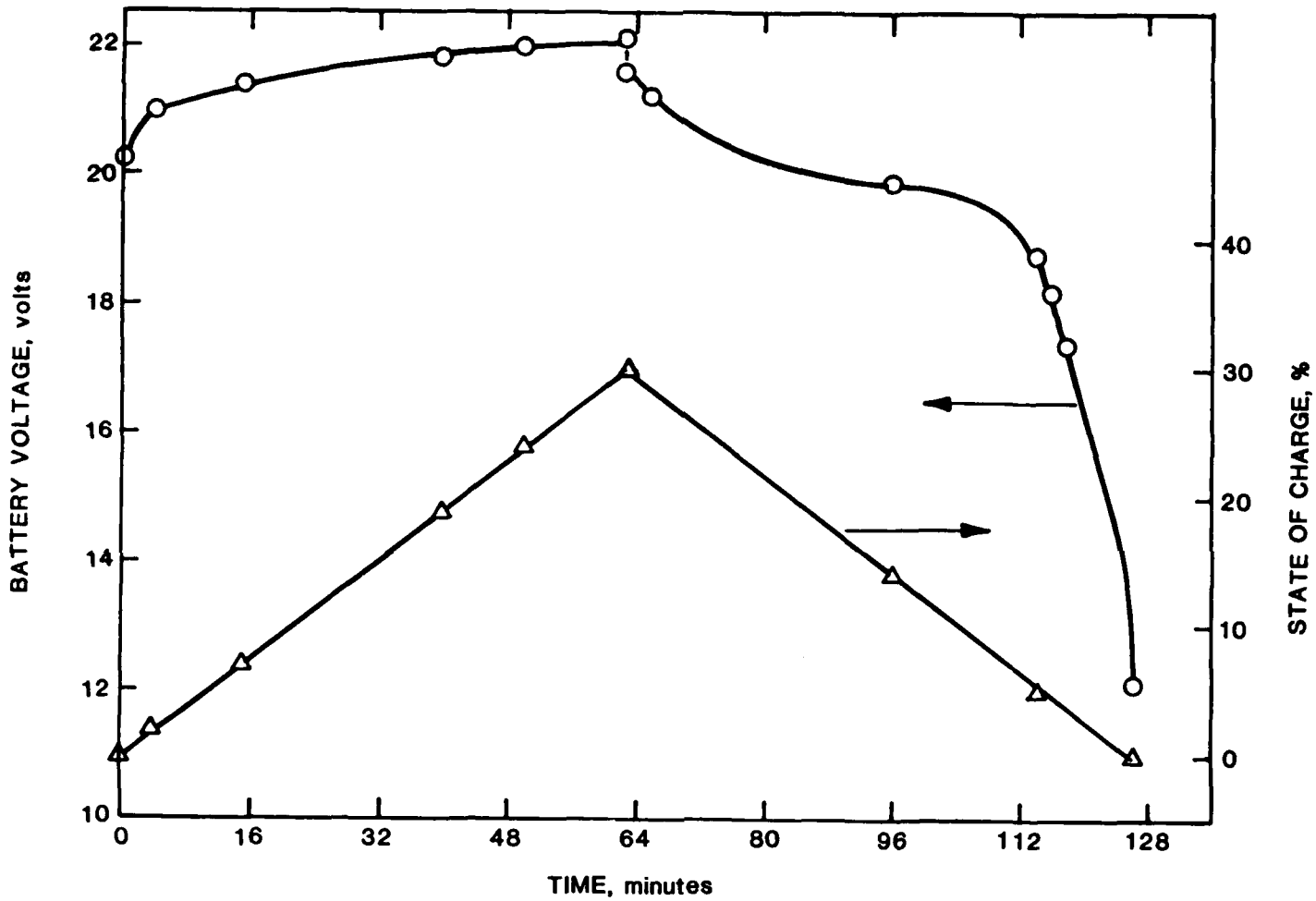

FIGURE 6.30 - BATTERY VOLTAGE AND STATE OF CHARGE-CHARGE TO 30%

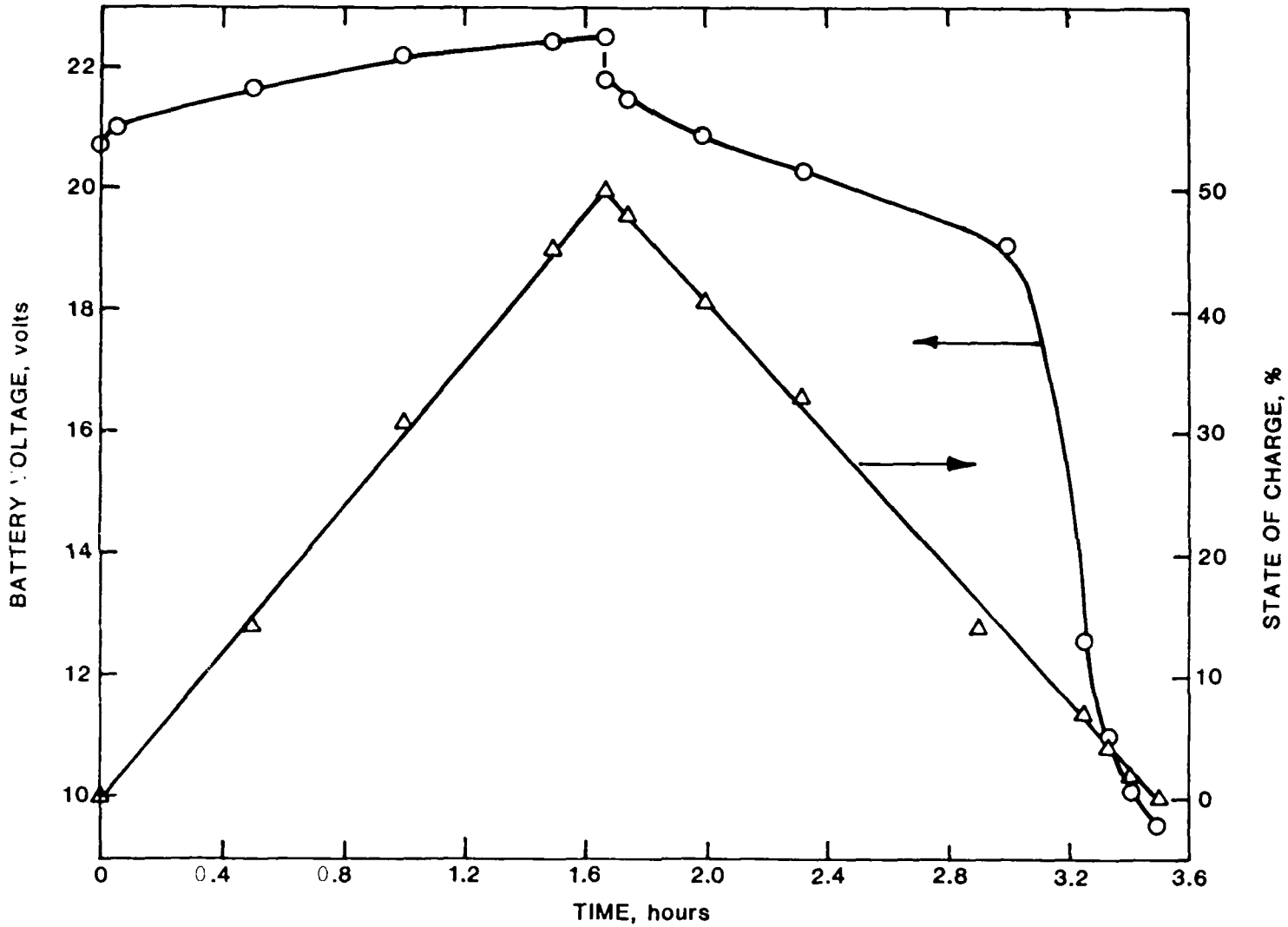

FIGURE6.31 - BATTERY VOLTAGE AND STACK OF CHARGE-CHARGE TO 50%

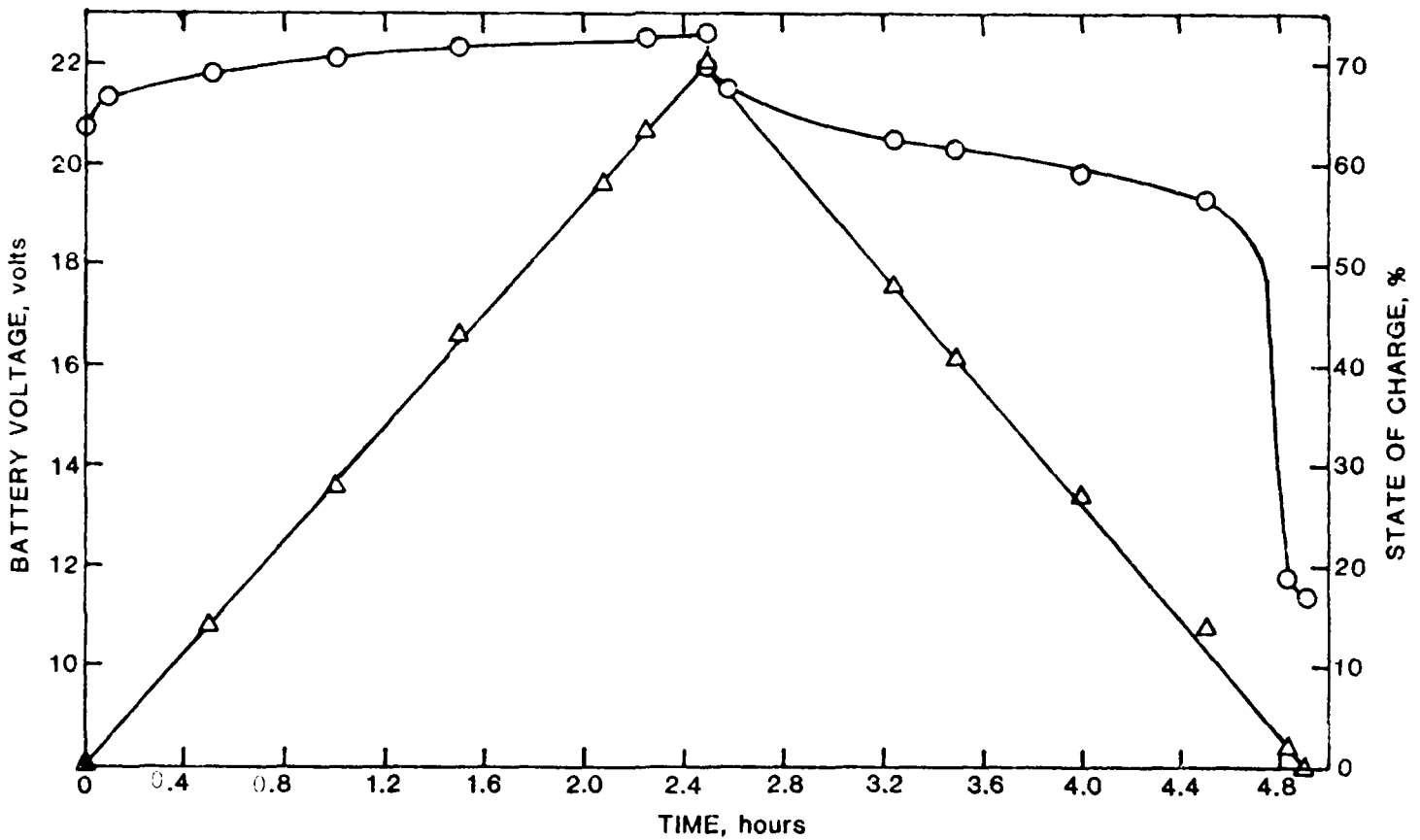

FIGURE 6.32 - BATTERY VOLTAGE AND STACK OF CHARGE-CHARGE TO 70%

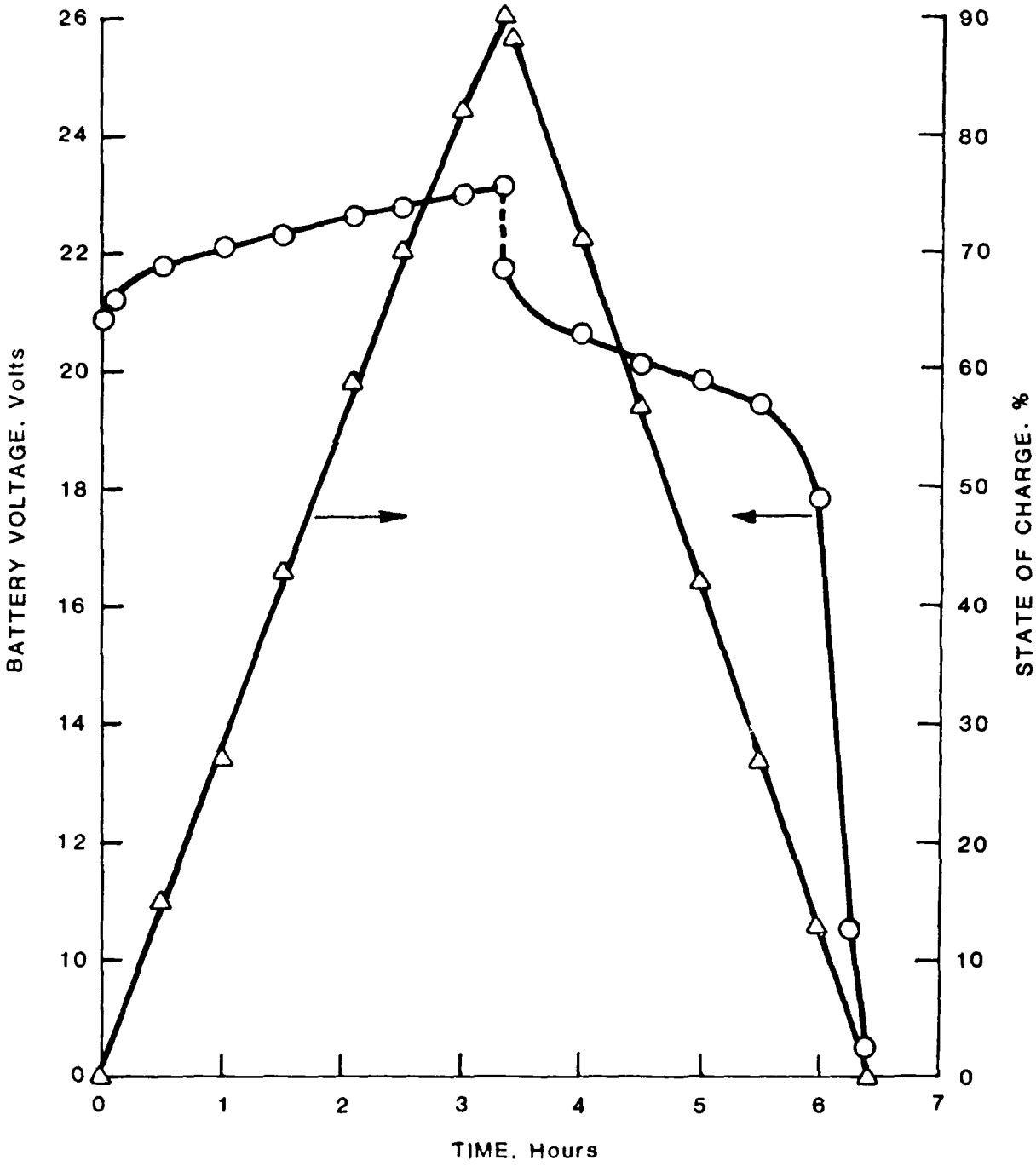

FIGURE 6.33 BATTERY VOLTAGE AND STATE OF CHARGE CHARGE TO 90%

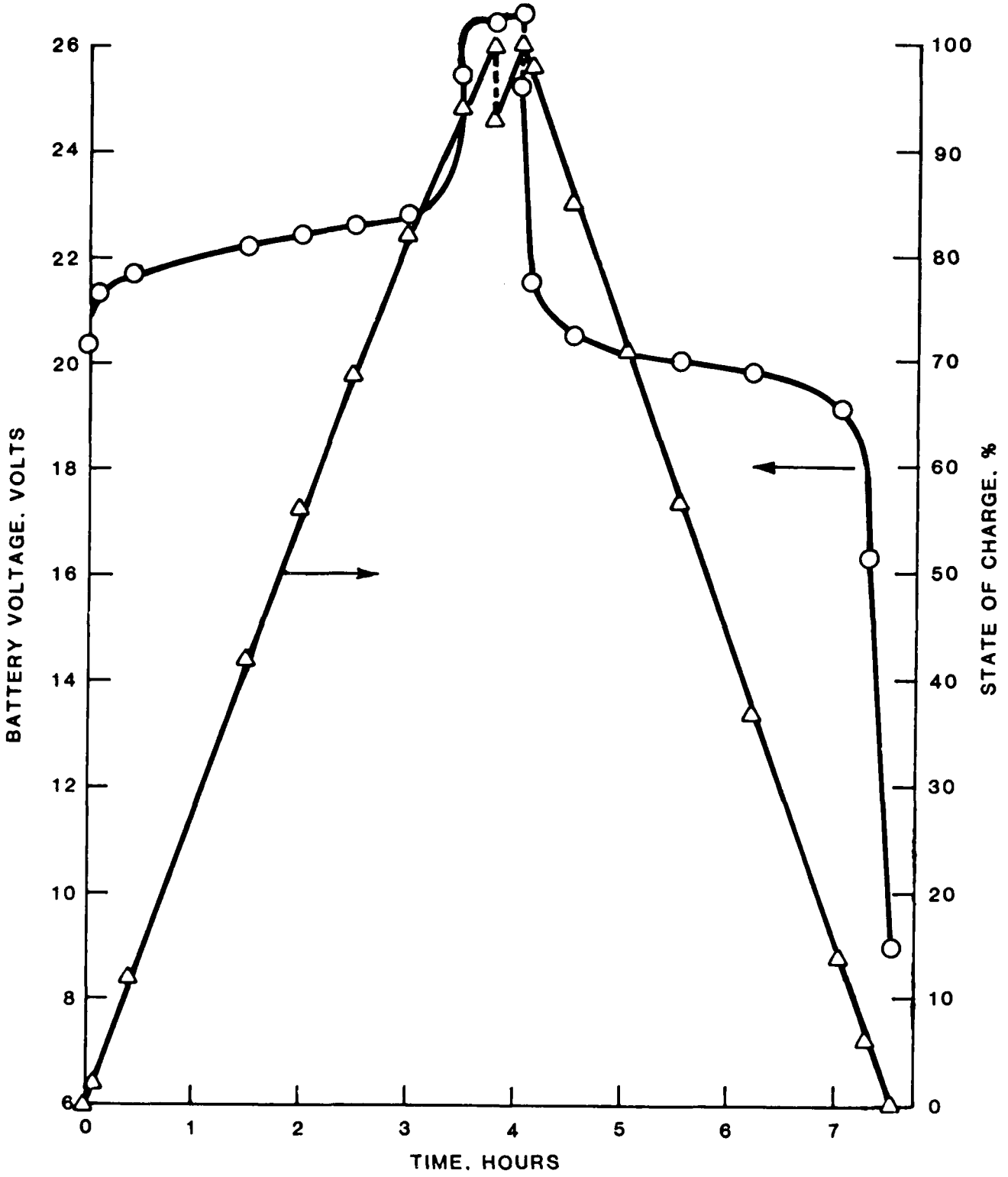

FIGURE 6.34 BATTERY VOLTAGE AND STATE OF CHARGE - CHARGE TO 100%

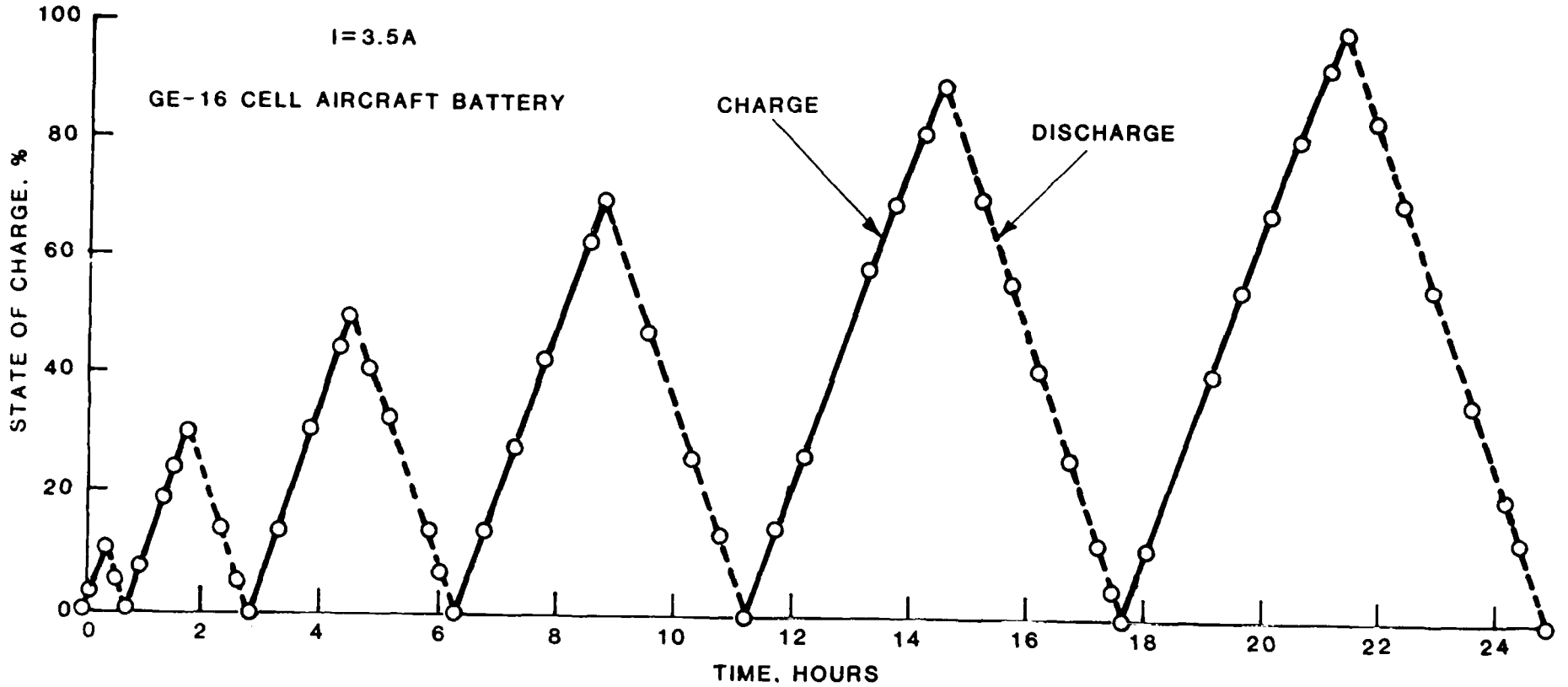

FIGURE 6.35 VARIATIONS IN STATE OF CHARGE

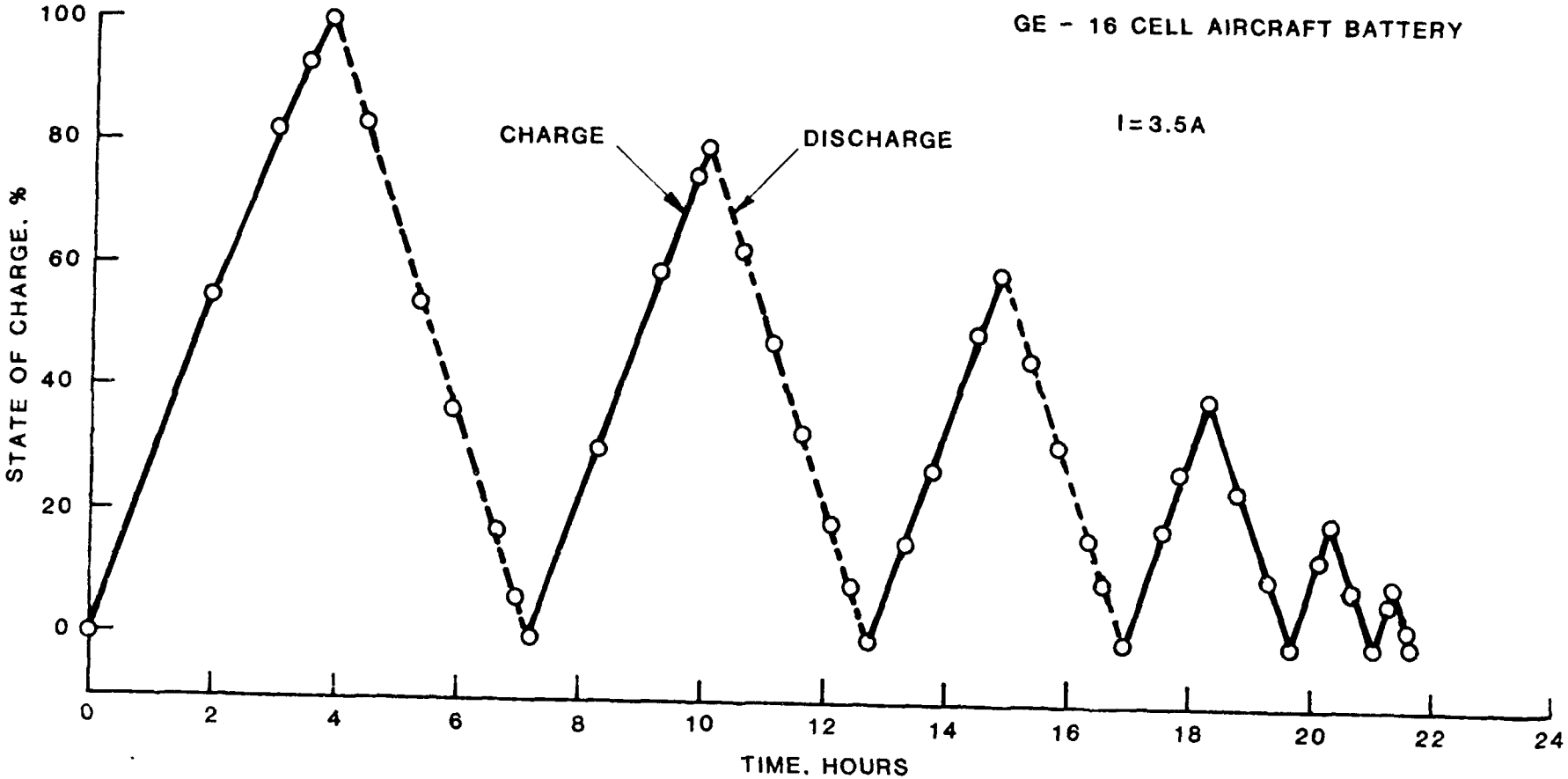

FIGURE 6.36 VARIATIONS IN STATE OF CHARGE

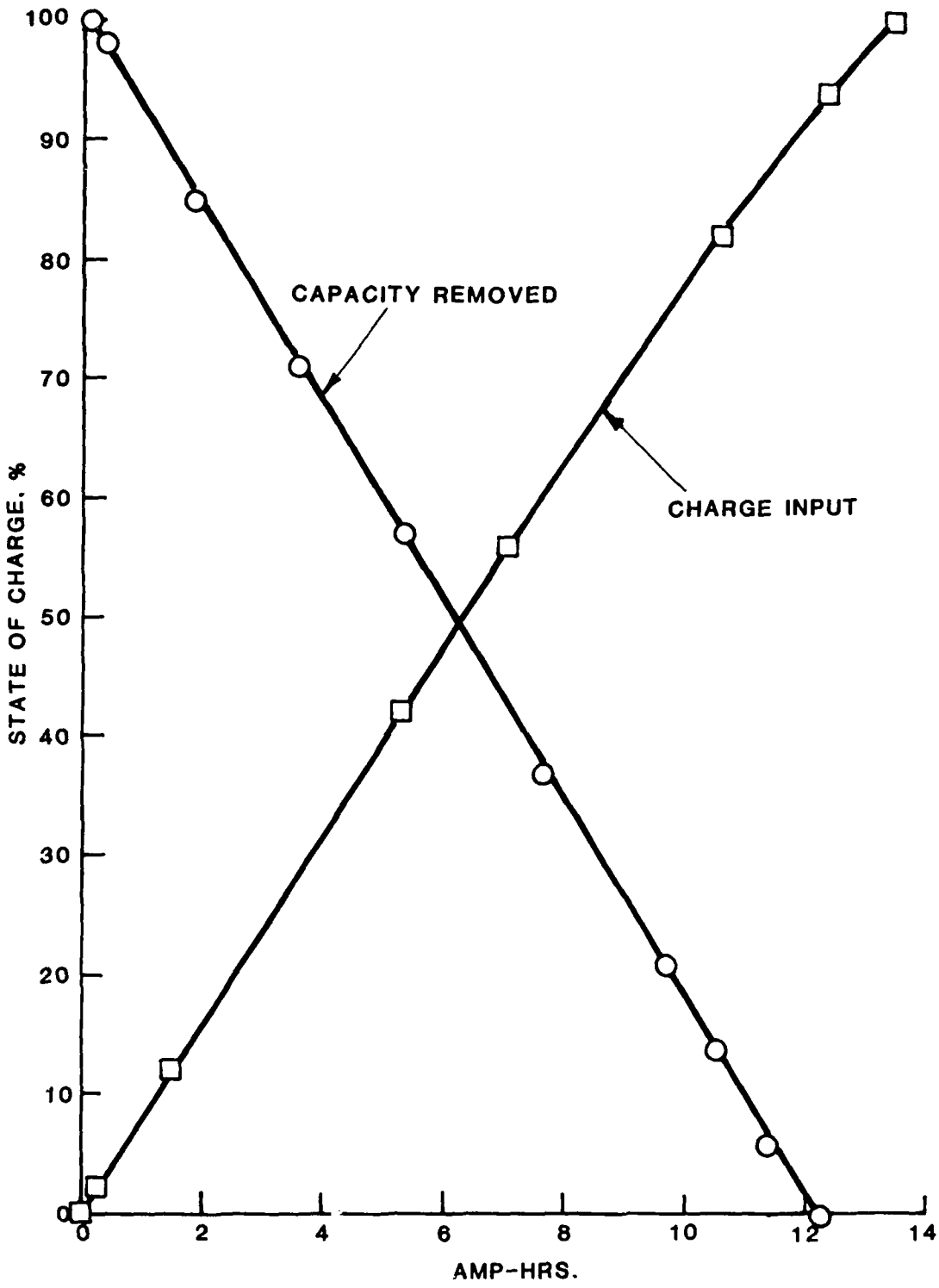

FIGURE 6.37 CAPACITY VS. STATE OF CHARGE

TABLE 6.9: STATE OF CHARGE VS. DELIVERED CAPACITY

TRACKING CYCLER 1: GE, AIRCRAFT 16-CELL at 3.5A/PILOT 50 at 67 mA

DATE	CYCLE NO.	CHARGE				DISCHARGE				%	% OVER CHARGE	% Ah EFF
		HRS.	AH	END V	%	HRS	AH	END V	%			
11-17-86	72	0.37	1.28	21.4	10	0.35	1.23	11.1	0	10	-	96
	*		0.028	0.429			0.023	-1.040				
"	73	1.05	3.68	22.1	30	0.105	3.68	12.1	0	30	199	100
	*		0.070	0.453			0.070	-1.040				
11-18-86	74	1.67	5.85	22.5	50	1.83	6.41	9.6	0	50	59	109
	*		0.112	0.483			0.123	-1.075				
"	75	2.50	8.75	22.6	70	2.41	0.844	11.4	0	70	37	96
	*		0.168	0.501			0.161	-1.060				
11-19-86	76	3.33	11.66	23.1	90	3.08	10.78	8.5	0	90	38	92
	*		0.223	0.521			0.206	-1.105				
11-20-86	77	3.80	13.30	26.6	100	3.50	12.25	9.0	0	100	23	92
	*		0.255	0.530			0.235	-1.046				
11-24-86	78	3.80	13.30	26.6	100	3.63	12.71	9.9	0	100	9	96
	*		0.255	0.528			0.243	-1.060				
11-25-86	79	2.83	9.91	22.7	80	2.73	9.56	8.3	0	80	-22	96
	*		0.190	0.501			0.183	-1.100				
11-25-86	80	2.08	7.28	22.4	60	2.08	7.28	10.8	0	60	-24	100
	*		0.139	0.484			0.139	-1.070				
11-25-86	81	1.38	4.83	22.3	40	1.37	4.80	6.0	0	40	-34	99
	*		0.092	0.474			0.092	-1.112				
11-26-86	82	0.68	2.39	22.1	20	0.67	2.35	1.5	0	20	-50	98
	*		0.046	0.457			0.045	-1.072				
11-26-86	83	.35	1.23	21.9	10	0.32	1.11	0.9	0	10	-48	90
	*		0.023	0.447			0.021	-1.048				

* Ni-O_2 Cell data: V = Ni vs Pt on chg & Ni vs sercon on discharge

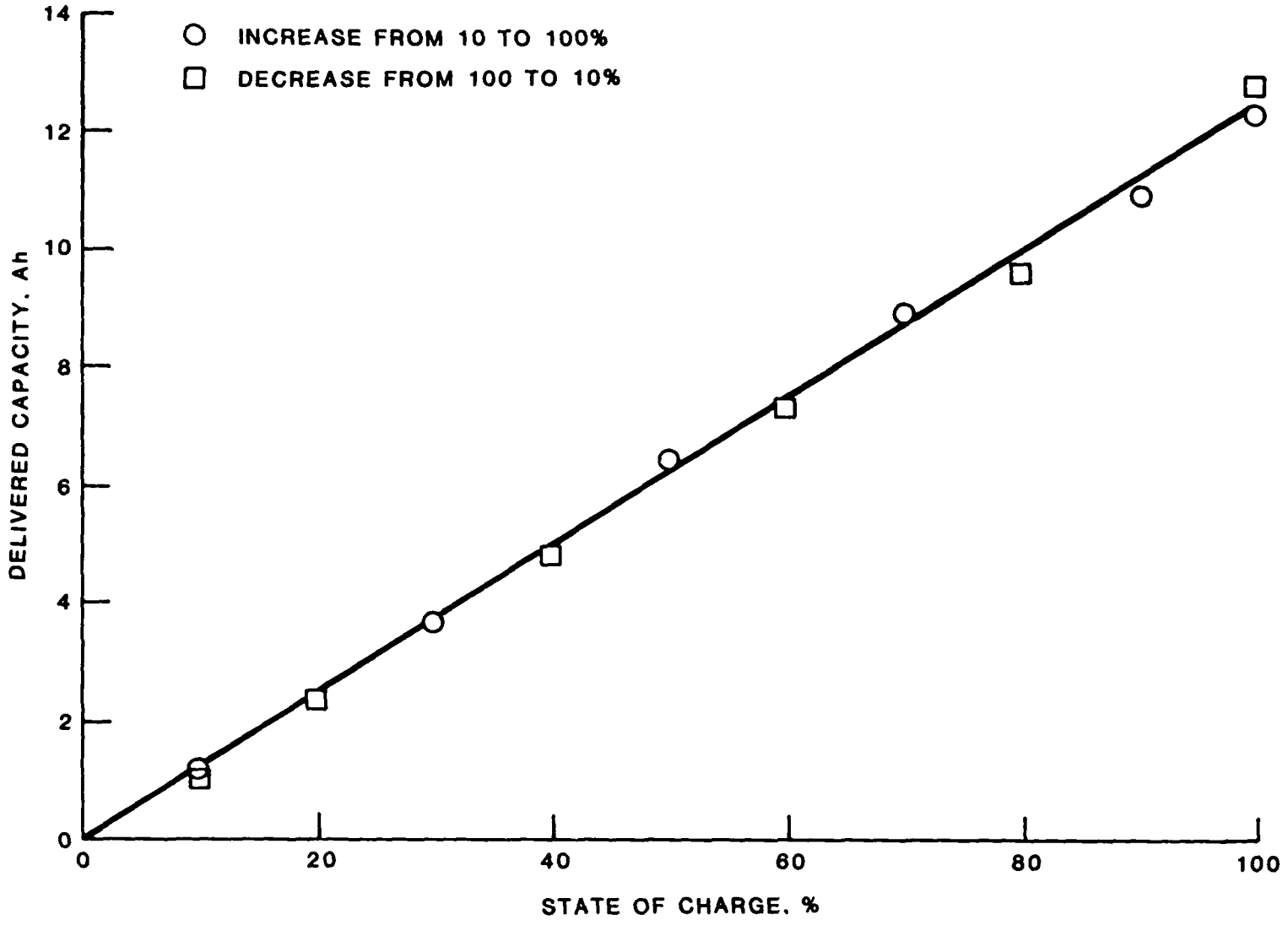

FIGURE 6.38 STATE OF CHARGE VS. DELIVERED CAPACITY

6.3.4 Marathon Aircraft Battery, Type MA-5 GFE

The 19-cell Marathon aircraft battery furnished by the Air Force was first tested separately as follows:

Charge: to 29.0 volts (1.55V/Cell) at 13.5 amps plus 1 hour at 3.0 amps.

Discharge: to 15.2 volts (0.80V/Cell) at 9.0 amps.

The test was repeated and the delivered capacities were 34.0 and 34.5 Ah as shown in Figures 6.39 and 6.40.

Tracking cycler 1 was used to evaluate tandem operation of Marathon, GFE battery with a compatible Ni-0_2 cell 59. Calibration was started on a manual mode charging and discharging to 100%. Currents and gain control were adjusted and state of charge displays were set to read 100% on full charge and 0% when completely discharged. The voltage of the battery when fully discharged was arbitrarily set to 19.0 volts (1.0V per cell). Initial calibration data are given in Table 6.10.

Tests to evaluate the relationship between state of charge and delivered capacity were started. Battery was charged in steps to 10, 20, 40, 60, 80, and 100%; after each charge, it was discharged to an end voltage of 19.0 V (1.0V per cell) and the delivered capacity was calculated. From the results summarized in Table 6.11, the system exhibited good tandem operation up to 80%. When 100% charge was attempted, the state of charge (and hence pressure of Ni-0_2 cell) started leveling off at 88%, this indicates that the Ni-0_2 cell was fully charged prior to battery getting the full charge. The system was checked thoroughly and the trouble was traced to a faulty control resistor. The resistor was replaced, system recalibrated and life cycle tests were started. Performance during cycle 102 is shown in Figure 6.41.

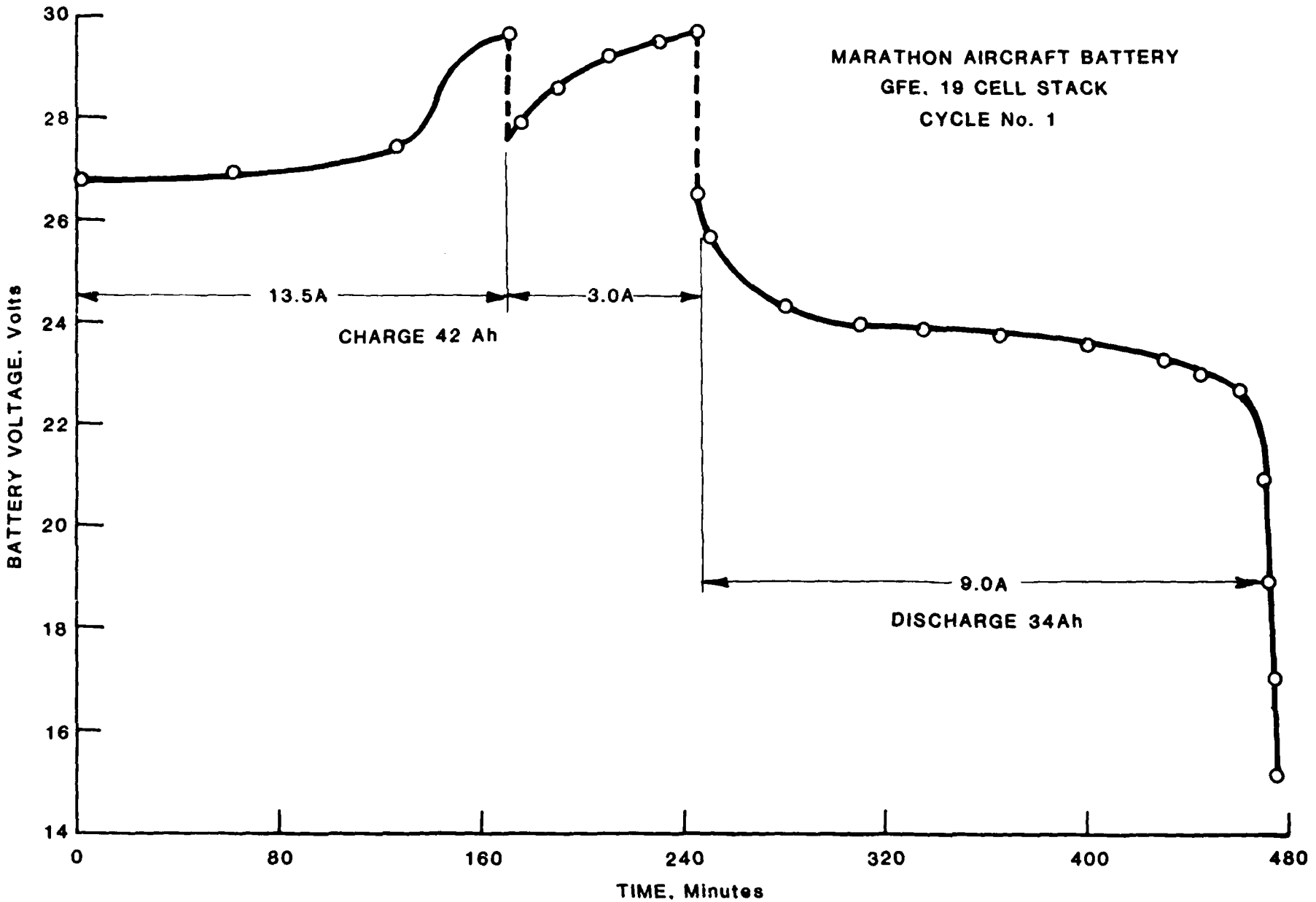

FIGURE 6.39 PERFORMANCE CHARACTERISTICS- GFE MARATHON AIRCRAFT BATTERY. CYCLE 1

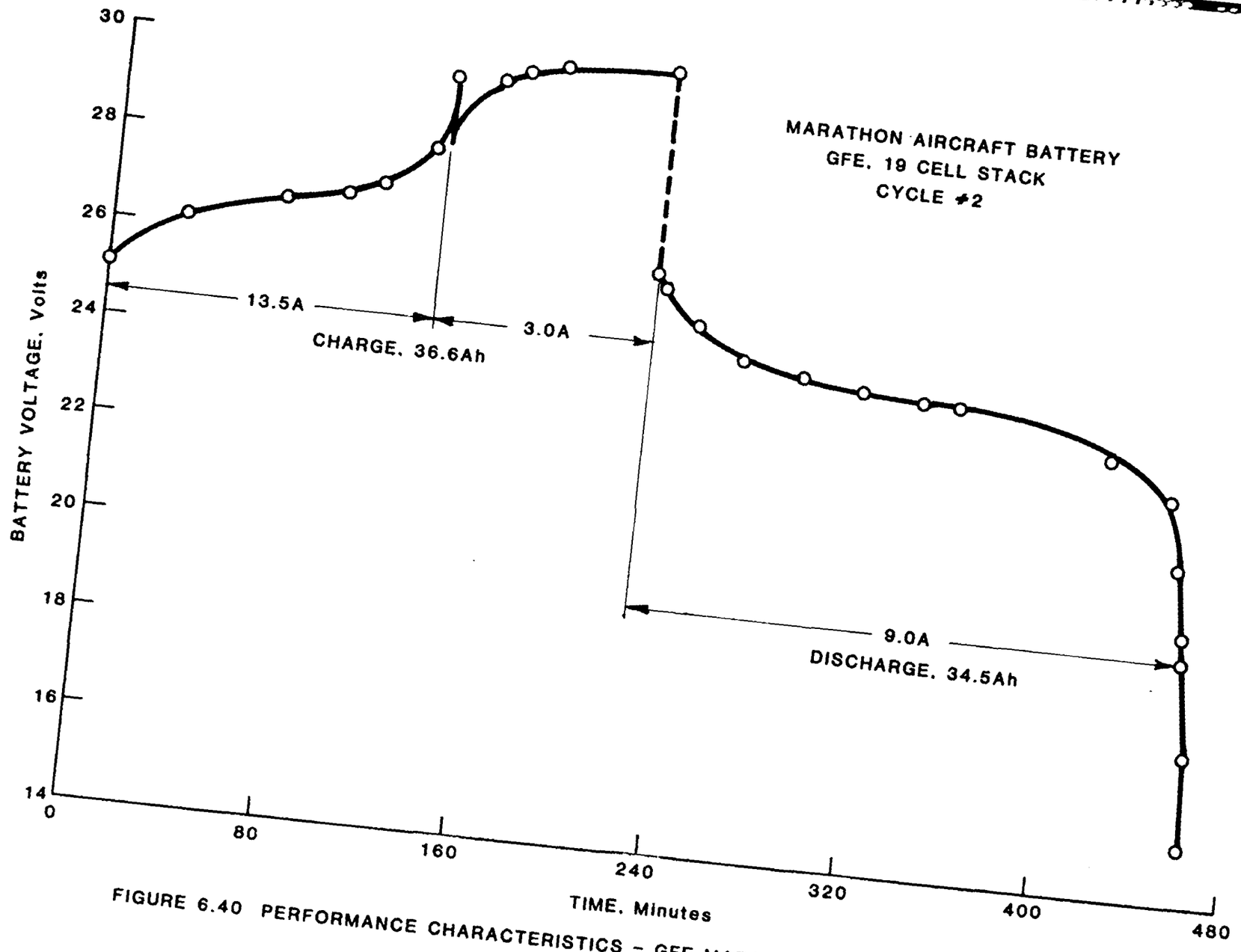

FIGURE 6.40 PERFORMANCE CHARACTERISTICS - GFE MARATHON AIRCRAFT BATTERY, CYCLE 2

TABLE 6.10

INITIAL CALIBRATION FOR TANDEM OPERATION

TRACKING CYCLER 1

MARATHON MA-5, 19 CELL BATTERY/NiO_2 CELL 59

CYCLE NO.	MODE	AMPS.	END V	HRS.	AH.	NiO_2 CELL mA	STATE OF CHG. %
3	Charge	8.0	31.35	4.75	38.00	101.4	100
	Discharge	"	19.00	4.34	34.72	103.2	-
4	Charge	"	31.78	4.92	39.36	101.0	100
	Discharge	"	19.00	4.45	35.60	102.4	-8
5	Charge	"	31.82	4.83	38.64	101.5	100
	Discharge	"	19.00	4.38	35.04	103.4	-2
6	Charge	"	31.77	4.95	39.60	101.9	100
	Discharge	"	19.00	4.55	36.40	102.3	0
7	Charge	"	31.57	5.05	40.40	102.2	100
	Discharge	"	19.00	4.62	36.96	102.0	-9
8	Charge	8.0	30.77	4.63	37.04	100.2	100
	Discharge	"	15.00	4.17	33.36	100.3	4
9	Charge	"	31.12	4.92	39.36	99.7	100
	Discharge	"	16.00	4.50	36.00	99.7	-4
10	Charge	"	31.65	4.83	38.64	99.6	100
	Discharge	"	15.90	4.50	36.00	99.5	0

TABLE 6.11

TRACKING CYCLER 1

State of Charge vs. Delivered Capacity

59 Cell, GFE, Marathon MA-5 at 8.0A/Ni-O_2 59 at 101 mA

Date	Cycle #	Mode	Hours	Ah	End V	End %	% over-charge	% Ah Eff.	▲%
2 3/87	13	Chg.	0.62	4.93	26.09	10	-		-
		Dischg.	0.43	3.47	18.77	0		70	10
	14	Chg.	0.95	7.60	26.31	20	119		20
		Dischg.	0.97	7.73	19.00	0		100	40
	15	Chg.	1.92	15.36	26.61	40	99		40
		Dischg.	1.87	14.96	19.00	-2		97	42
2 4/87	16	Chg.	2.88	23.04	26.90	60	54		62
		Dischg.	2.78	22.24	19.00	-1		97	61
2 5/87	17	Chg.	3.92	31.36	27.70	80	41		
		Dischg.	3.75	30.00	19.00	-3		96	83
2 6/87	18*	Chg.	4.95	39.60	31.92	100*	32		-
		Dischg.	4.47	35.76	19.00	0		90	100

* Started levelling off at 88%, adjusted to 100%

We observed that during discharge, battery temperature showed a higher increase than normal. Each of the 19 cells was checked individually and two showed deterioration. The depth of discharge was reduced to 80% from 100% and characteristics during cycle 140 are shown in Figure 6.42.

Cycling was continued and the two weak cells failed completely and went into reverse. They were isolated and tests were stopped after 270 cycles due to contract expiration. Prior to stopping tests, two deep discharges were done, results of which are given in Figures 6.43 and 6.44. This confirms that the system continues to operate effectively in tandem.

With the completion of this final subtask, technical efforts of the contract were terminated.

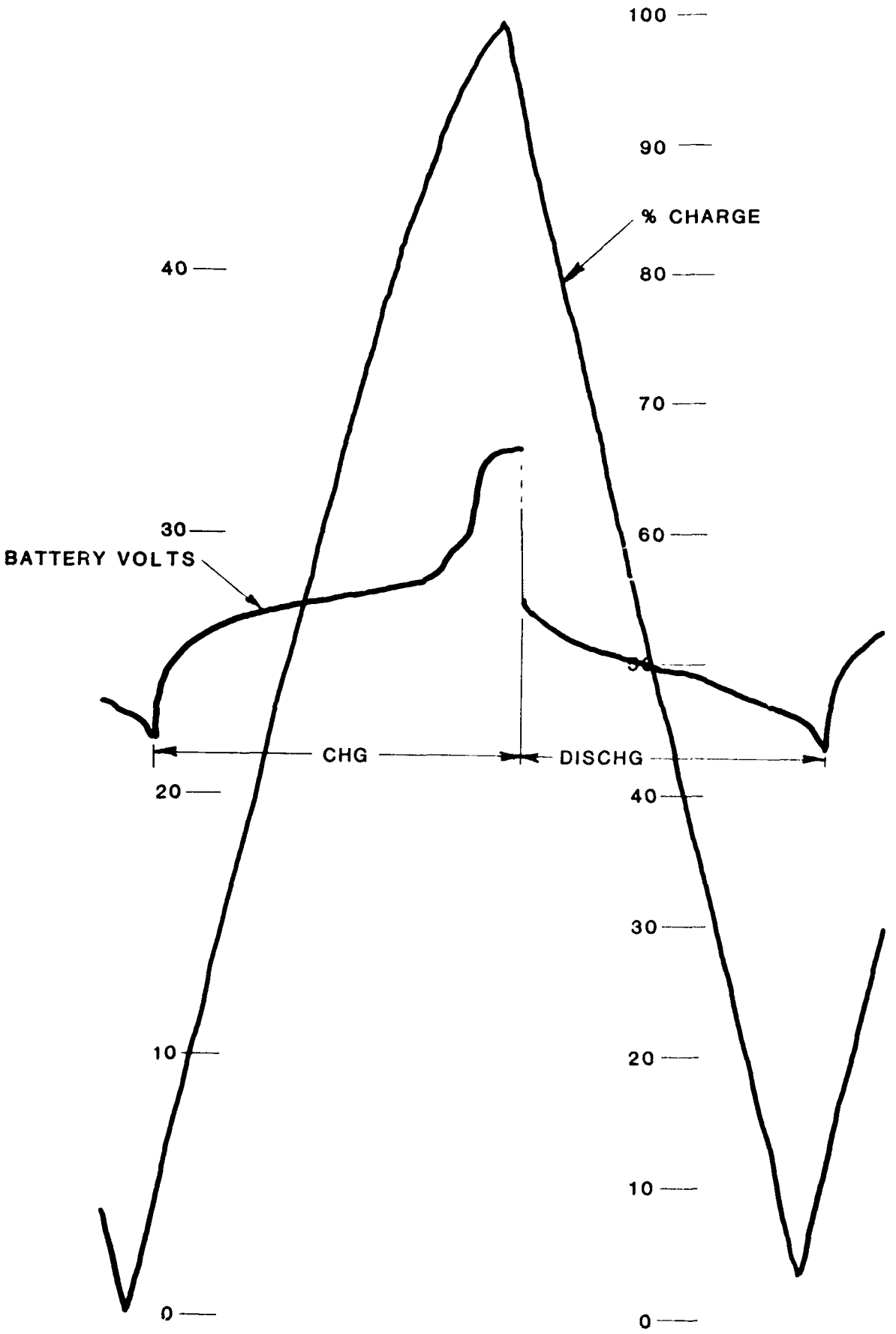

% CHARGE FIGURE 6.41 TANDEM OPERATION. TRACKING CYCLER 1. CYCLE 102

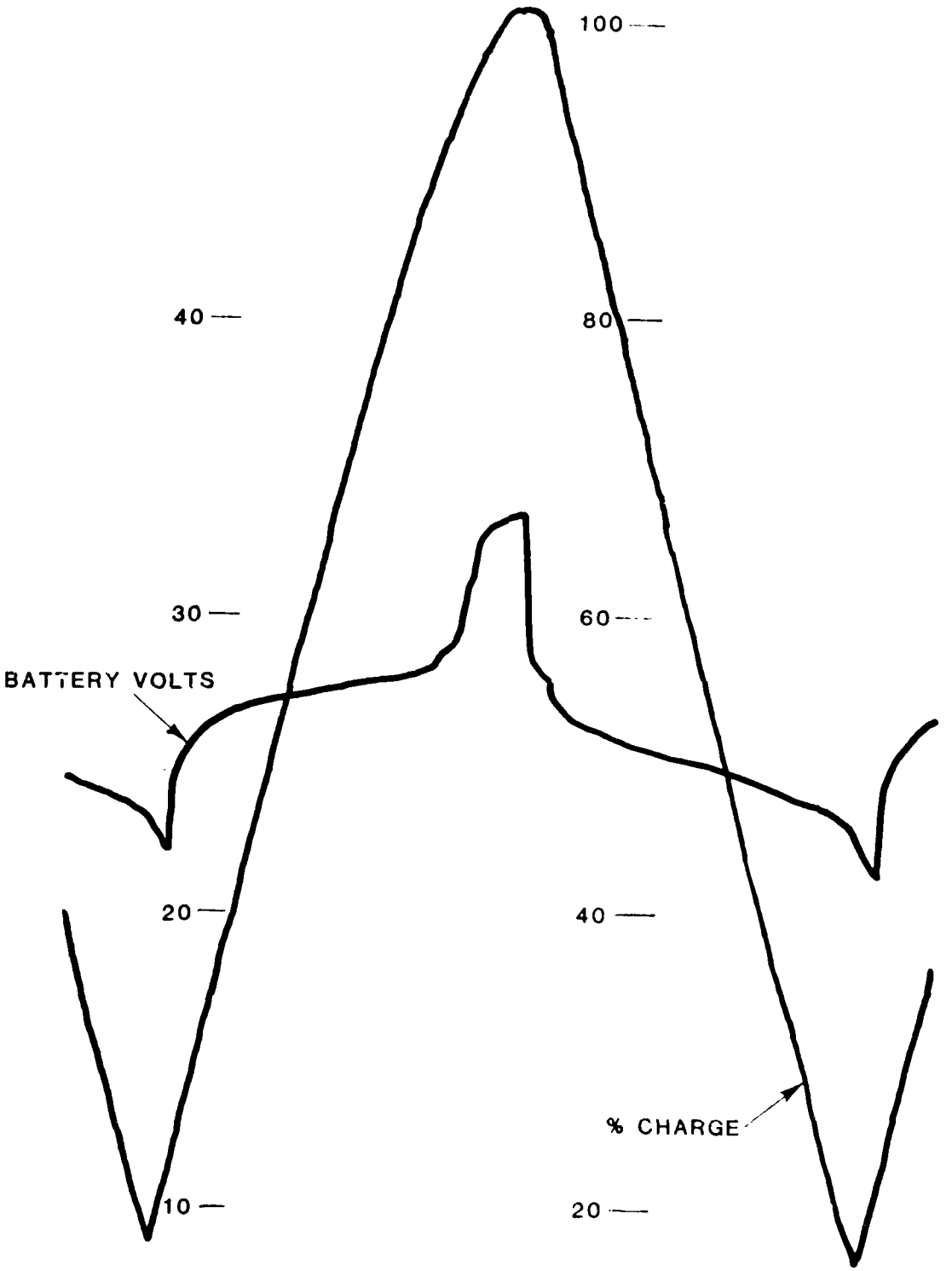

FIGURE 6.42 TANDEM OPERATION, TRACKING CYCLER 1, CYCLE 140

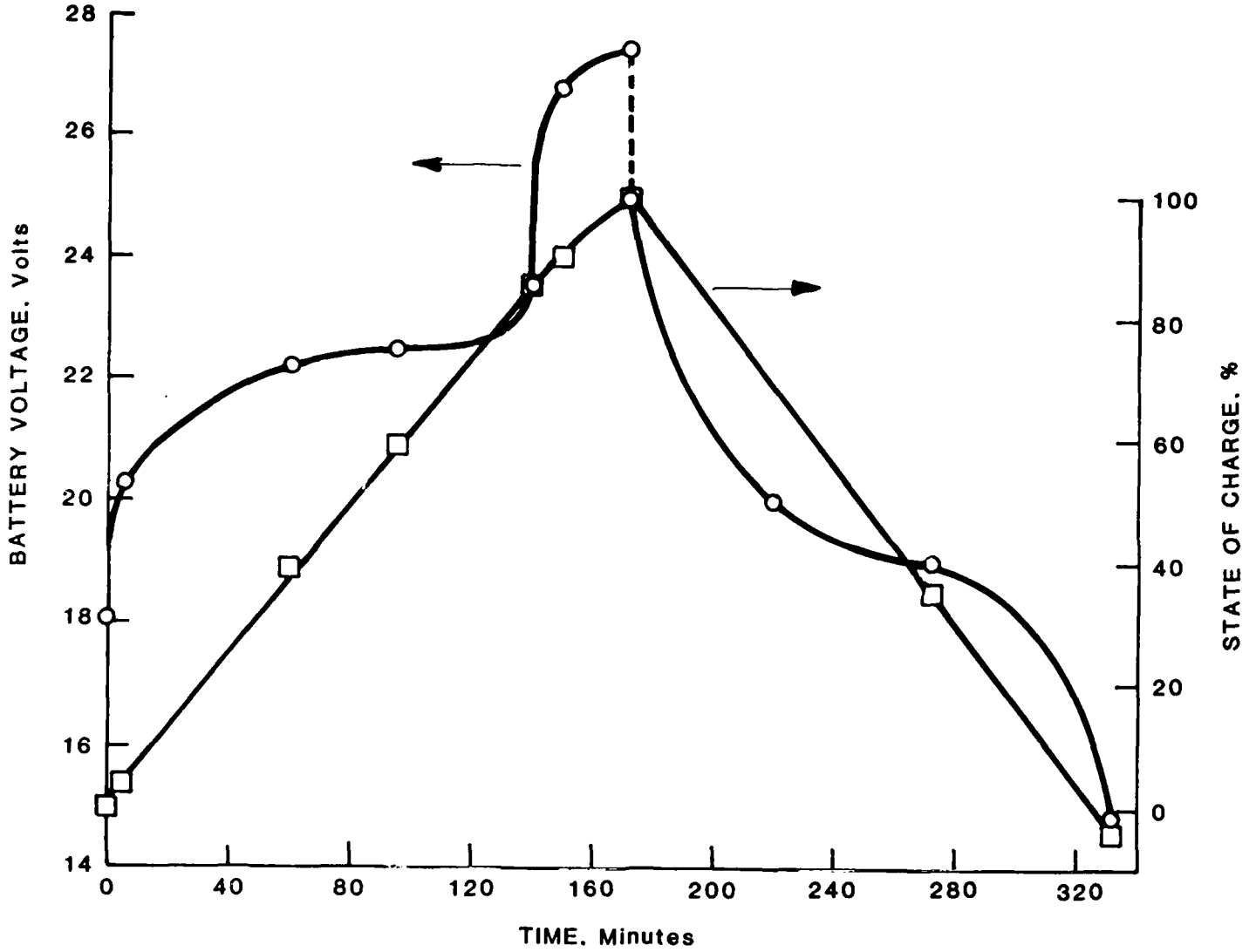

FIGURE 6.43 TRACKING CYCLER No. 1 - 100% DOD

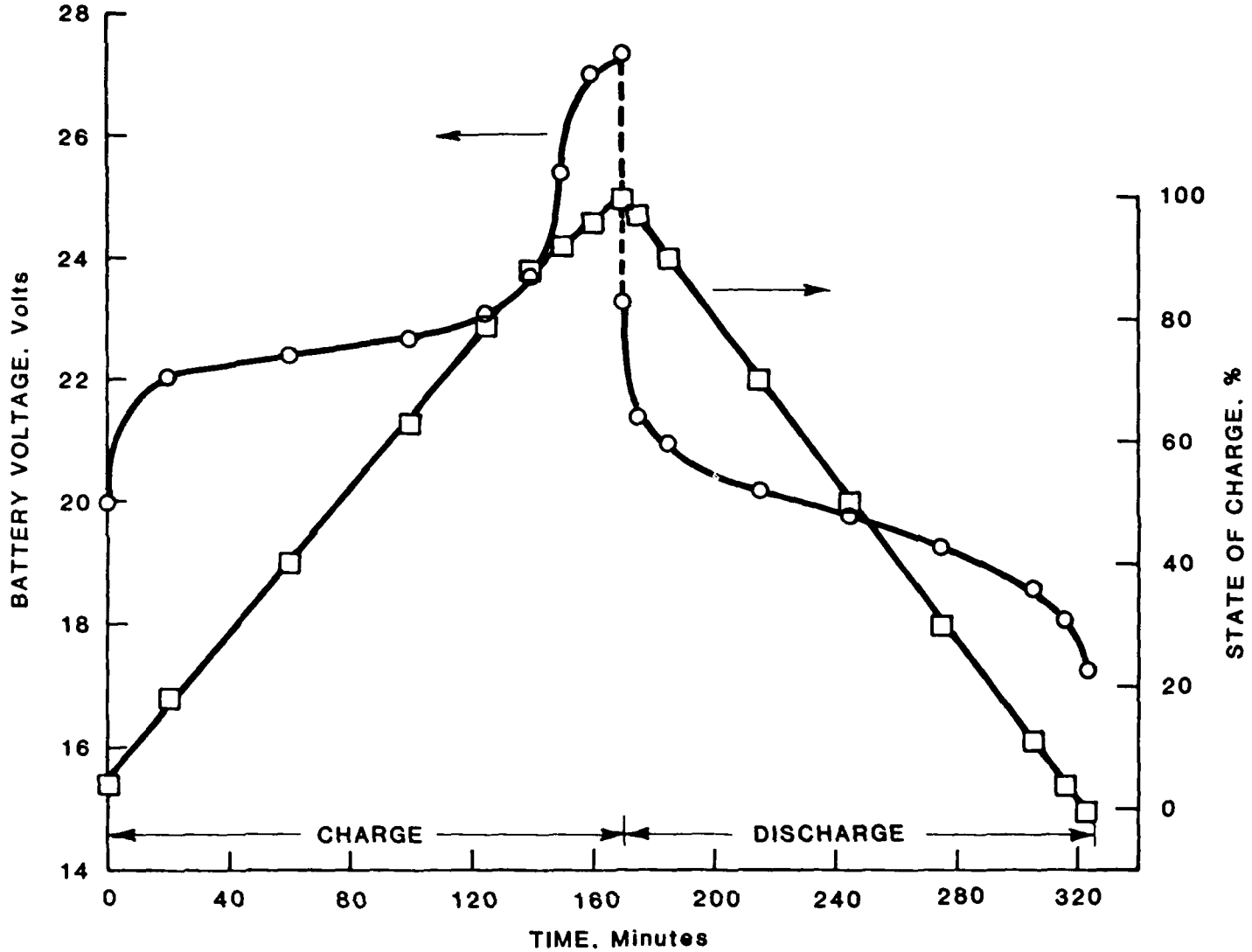

FIGURE 6.44 TRACKING CYCLER No.1 - 100% DOD

SECTION 7

SUMMARY AND CONCLUSIONS

$Ni-O_2$ Cells made with nickel electrodes of different types were first characterized. Nickel electrodes of the roll-bonded (ERC) and sintered (Saft and Marathon) types were tested for charge/discharge rates effects, effects of over-charge/over discharge, and linearity of pressure. The test results proved that the performance characteristics of the nickel-oxygen cells are more than adequate and will be capable of tracking the state of charge of the main battery.

Special tests were also conducted to monitor the potentials of each working electrode separately both during charge and discharge. This enabled a better understanding of the performance of each individual electrode and identify which electrode deteriorated first and causes cell failure. This information is valuable in predicting estimates of life and improving performance of the nickel-oxygen cell. Tests to monitor the performance of each working electrode separately proved that eventual cell failure was caused by deterioration of the nickel electrode. Long term life tests have shown that the life of $Ni-O_2$ cells is well in excess of that of aircraft batteries. In addition, increased polarization of the nickel electrode does not affect the relationship between the state of charge of the nickel electrode and cell pressure.

Having established this, selected representative cells were subjected to continuous cycling tests on alternate charge-discharge regimes to obtain data on cell life. The results indicate that the cells can sustain continuous cycling for extended time periods and retain their stability to give the required, reliable and

reproducible parameters.

Commercial aircraft cells (Saft and Marathon) were purchased and their characteristics were also evaluated.

The aircraft cells and nickel-oxygen cells fabricated with electrodes used in aircraft cells were thus qualified and found to be acceptable.

An electronic cycling system was designed and built and tests were started. Initial experiments were designed to understand the electrical interfaces that would be required, tracking capabilities of the pilot cell and critical areas that need more detailed investigation.

During the second year, efforts were continued in characterizing the performance of Ni-O_2 cells. The test results confirmed that the performance characteristics of the cells surpass the requirements for tracking the state of charge of commercial aircraft batteries.

Efforts during this phase were also directed at proving the system concept. Using an electronics system designed and built in house, feasibility of tandem operation was demonstrated. A Saft aircraft battery was operated in tandem and over 500 cycles were obtained during a 7-month period. The Ni-O_2 cell was still functioning well and tests were terminated due to loss in capacity of the battery.

A second tracking cycler was built and a Marathon aircraft battery was tested both at ambient and at constant temperatures. Fluctuations in cell pressure and hence, the percent state of charge caused by variations in temperature were eliminated by keeping the Ni-O_2 cell at constant temperature; accordingly, this

resulted in an improved tracking accuracy.

During the final year of the contract the major thrust was towards evaluating life and stability of full integrated systems on tandem operation. Four different batteries were evaluated as integrated systems and all four performed satisfactorily.

To summarize, efforts expended under this concept have demonstrated that

1. The concept is viable
2. System has been developed from conceptual to laboratory stage
3. Extensive testing has demonstrated that the system is reliable and reproducible with a satisfactory level of accuracy.
4. Real-time data show an acceptable level of performance over extended periods of time.
5. Life of the pilot cell is well in excess of the life of the battery.

The research efforts have also identified critical areas that need to be investigated further to take the development to prototype and then to product. Under another contract, ERC has successfully developed a bifunctional O_2 electrode. Since this does not require a third electrode for charging, the electronic circuiting will be simpler.

Another area for future investigations is to compensate for temperature excursions, thereby preventing system errors due to pilot cell and battery becoming out of phase due to temperature effects. It is conceivable that compensation can be done electronically.

Finally, system operation can be simplified. Currently, the system has to be monitored closely and readjusted and/or recalibrated to compensate for slow decay of the battery. Efforts need to be directed at eliminating this problem.

In conclusion, continued efforts to fine tune the system is strongly recommended to develop the unit further from proven laboratory to reliable product stage.

☆ U.S. GOVERNMENT PRINTING OFFICE: 1988 — 548-054 80816

END

DATE

FILMED

8-88

DTIC